

January 1977

## Estimation Theory Applied to River Water Quality Modeling

David S. Bowles

William J. Grenney

J. Paul Riley

Follow this and additional works at: [https://digitalcommons.usu.edu/water\\_rep](https://digitalcommons.usu.edu/water_rep)



Part of the [Civil and Environmental Engineering Commons](#), and the [Water Resource Management Commons](#)

---

### Recommended Citation

Bowles, David S.; Grenney, William J.; and Riley, J. Paul, "Estimation Theory Applied to River Water Quality Modeling" (1977). *Reports*. Paper 588.

[https://digitalcommons.usu.edu/water\\_rep/588](https://digitalcommons.usu.edu/water_rep/588)

This Report is brought to you for free and open access by the Utah Water Research Laboratory at DigitalCommons@USU. It has been accepted for inclusion in Reports by an authorized administrator of DigitalCommons@USU. For more information, please contact [digitalcommons@usu.edu](mailto:digitalcommons@usu.edu).



ESTIMATION THEORY APPLIED TO RIVER  
WATER QUALITY MODELING

by

David S. Bowles  
William J. Grenney  
and  
J. Paul Riley

Utah Water Research Laboratory  
College of Engineering  
Utah State University  
Logan, Utah 84322

Final Report for

Project Number ES-1-G  
Engineering Experiment Station  
College of Engineering  
Utah State University  
Logan, Utah 84322

April 1977

99008

ESTIMATION THEORY APPLIED TO RIVER  
WATER QUALITY MODELING

by

David S. Bowles  
William J. Grenney  
and  
J. Paul Riley

Utah Water Research Laboratory  
College of Engineering  
Utah State University  
Logan, Utah 84322

Final Report for

Project Number ES-1-G  
Engineering Experiment Station  
College of Engineering  
Utah State University  
Logan, Utah 84322

April 1977

## ACKNOWLEDGMENTS

The work on which this dissertation is based was made possible with a developmental research grant from the Engineering Experiment Station, College of Engineering, Utah State University. I am sincerely grateful to Dr. E. Joe Middlebrooks, Dean, College of Engineering, for making these funds available through Experiment Station project number ES-1-g, entitled "River water quality modeling: A combined deterministic-stochastic approach." Also, I wish to thank Dr. L. Douglas James, Director, Utah Water Research Laboratory, and Dr. Garry Z. Watters, Associate Dean, College of Engineering, for providing the additional computer funds needed to complete this research.

I am deeply indebted to my dissertation director, Dr. William J. Grenney, and my major professor, Dr. J. Paul Riley, for their guidance, encouragement, and financial support throughout my studies and research at Utah State University. In addition, I would like to thank Drs. Calvin G. Clyde, A. Leon Huber, and Bartell C. Jensen for serving on my supervisory committee and for their review of the dissertation. In particular, I wish to acknowledge Dr. Huber for making available some graph plotting software and for assisting in its application to this study.

Gratitude is also expressed to Mr. Karl Fugal of the Utah State University Computer Center for his help in resolving problems associated with the use of the Burroughs B6700 computer. Also, I wish to acknowledge Becky Jo Hansen, Nancy Goodman, Barbara South, Vicki Westover, and Jenny Demakos for their careful typing of the dissertation manuscript, and Mr. Richard Goacher for drafting the figures.

Special thanks goes to my wife, Valerie, for her love, prayers, encouragement, and wonderful understanding throughout my graduate career. Without her this dissertation would not have been possible. In addition, I wish to acknowledge the inspiration that our daughter, Penny-Anne, has provided during the latter months of this study. Next, I would like to recognize the role of my parents, Stanley and Elsie Bowles. Their continued encouragement and support at all stages of my education have been a strong motivating force.

For my final acknowledgment I shall borrow the words of Dr. Otto J. Helweg (Helweg, 1975): "I now wish to acknowledge the Source behind all I am and hope to be, the Triune God who is Creative Father, Saving Son, and Indwelling Spirit. This may be trite to some, naive to others, but to those of like heart , an important confession."

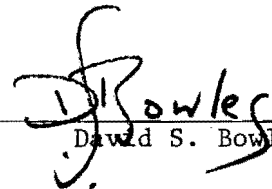
  
David S. Bowles

TABLE OF CONTENTS

	Page
ACKNOWLEDGMENTS . . . . .	ii
LIST OF TABLES . . . . .	vii
LIST OF FIGURES. . . . .	viii
ABSTRACT . . . . .	xiii
 Chapter	
I. INTRODUCTION . . . . .	1
Background . . . . .	2
Objective . . . . .	5
Summary of Contents . . . . .	5
II. LITERATURE REVIEW . . . . .	7
Introduction . . . . .	7
Review of Estimation Theory . . . . .	7
Review of the Applications of Estimation Theory to Water Resources . . . . .	12
Model identification . . . . .	12
Model calibration . . . . .	13
River forecasting . . . . .	18
Sampling program design . . . . .	20
Missing data fill-in . . . . .	20
Control. . . . .	23
III. DESCRIPTION OF THE ESTIMATION THEORY TECHNIQUES APPLIED. . . . .	24
Introduction . . . . .	24
Simplified Derivation of the Linear Kalman Filter. . . . .	24
Extended Kalman Filter. . . . .	28
Linearized Kalman Filter . . . . .	32
Smoothing Algorithm . . . . .	35
Sequential Kalman Filters . . . . .	37
Numerical Aspects . . . . .	41
Computational Aspects . . . . .	42
IV. APPLICATION TO THE JORDAN RIVER. . . . .	44
Introduction . . . . .	44
Description of the Lower Jordan River Basin. . . . .	44

TABLE OF CONTENTS (Continued)

Chapter	Page
Process Model . . . . .	47
Biochemical oxygen demand . . . . .	54
Ammonia-nitrogen . . . . .	54
Nitrate-nitrogen . . . . .	55
Algae . . . . .	55
Organic nitrogen . . . . .	59
Dissolved oxygen . . . . .	59
Stream temperature . . . . .	60
Streamflow . . . . .	60
Limitations of the process model. . . . .	61
Measurement Model . . . . .	62
Point Loads and Lateral Inflows. . . . .	63
Initial Conditions . . . . .	65
V. RESULTS . . . . .	67
Introduction . . . . .	67
Calibration of the Deterministic Process Model. . . . .	67
Determination of Process Model Noise Variances. . . . .	73
Trial-and-error approach . . . . .	74
Adaptive filtering approach . . . . .	77
Results from the Extended Kalman Filter . . . . .	78
Results from the Smoothing Algorithm . . . . .	89
Sensitivity Studies . . . . .	96
Sensitivity study on process model noise variance . . . . .	98
Sensitivity study on measurement noise variance. . . . .	98
Sensitivity study on the initial estimation error variance . . . . .	102
Sensitivity study on point load estimation error variance . . . . .	103
Coefficient Estimation . . . . .	107
K <sub>23</sub> estimation . . . . .	109
K <sub>45</sub> estimation . . . . .	114
Estimation of the nitrogen cycle coefficients . . . . .	117
NO <sub>3</sub> -N lateral inflow estimation . . . . .	124
NH <sub>3</sub> -N lateral inflow estimation . . . . .	126
Computational Requirements . . . . .	126

TABLE OF CONTENTS (Continued)

Chapter	Page
VI. SUMMARY, CONCLUSIONS, AND RECOMMENDATIONS . . . . .	134
Summary . . . . .	134
Conclusions . . . . .	136
Recommendations . . . . .	139
LITERATURE CITED . . . . .	142
APPENDIX A. USERS MANUAL FOR COMPUTER PROGRAMS . . . . .	147
I. Filter Model (EKFLKF) . . . . .	149
II. Data Sorting Program (PRSORT) . . . . .	187
III. Plotting Program (P). . . . .	193
VITA . . . . .	205



LIST OF TABLES

Table	Page
2.1 Summary of applications of estimation theory to water resources . . . . .	14
4.1 Measurement noise variances (R) and initial estimation ( $P(\xi_0)$ and $P^b(\epsilon)$ ) in $(\text{mg}/1)^2$ . . . . .	64
4.2 Concentration of the parameters in point loads and tributaries in $\text{mg}/1$ . . . . .	66
4.3 Concentration of the parameters in the lateral inflow and bottom deposits . . . . .	66
5.1 Key to the computer runs . . . . .	68
5.2 Reaction rates and model coefficients from the calibration of the deterministic process model. . . . .	70
5.3 Process model noise variances (Q) in $(\text{mg}/1\text{-day})^2$ . . . . .	79
5.4 Mean square error of the difference between the filter estimates and the measured values in $(\text{mg}/1)^2$ . . . . .	80
5.5 Values of the statistics used in the sensitivity runs . . . . .	97
5.6 Estimation error variances (Y) for the point load located at river mile 31.70 (51.0 km). . . . .	105
5.7 Process model noise variances (Q) and initial estimation error variances ( $P(\xi_0)$ ) for the coefficients and lateral inflow concentrations estimated in runs 15 through 18 and 21 . . . . .	110
A-1 Input data and decision parameters for filter model (EKFLKF) . . . . .	154
A-2 Definition of state vector, measurement vector, input vector, and model coefficient vector . . . . .	162
A-3 Input data and decision parameters for data sorting program (PRSORT). . . . .	190
A-4 Input data and decision parameters for plotting program (P) . . . . .	195

## LIST OF FIGURES

Figure	Page
1.1 A schematic representation of the state estimation procedure . . . . .	4
2.1 A schematic representation of the filtering procedure (adapted from Moore, 1973) . . . . .	10
3.1 Flow diagram for the extended Kalman filter algorithm . . . . .	33
3.2 Flow diagram for the backward linearized Kalman filter algorithm . . . . .	36
3.3 Sequential application of extended Kalman filters to a hypothetical river system . . . . .	39
3.4 Relationships between the computer programs developed for this study . . . . .	43
4.1 Map of the Lower Jordan River Basin (adapted from Harr et al., 1971) (1 mile = 1.61 km) . . . . .	45
4.2 Schematic diagram of the water quality parameters, biochemical transformations, and non-point loads represented by the process model . . . . .	49
4.3 Process model equations, $\dot{\underline{X}} = \underline{f} [\underline{X}(\xi), \underline{U}(\xi); \xi] + \underline{w}(\xi)$ . . . . .	52
4.4 Jacobian matrix, $F[\underline{X}(\xi), \underline{U}(\xi); \xi]$ , for the process model . . . . .	53
4.5 Graphic representation of Equations 4.11 and 4.14 describing the preferential uptake of nitrogen by algae. . . . .	58
5.1 Measured and predicted values of BOD - deterministic process model calibration (1 mile = 1.61 km) . . . . .	71
5.2 Measured and predicted values of DO - deterministic process model calibration (1 mile = 1.61 km) . . . . .	71
5.3 Measured and predicted values of NH <sub>3</sub> -N - deterministic process model calibration (1 mile = 1.61 km) . . . . .	71
5.4 Measured and predicted values of NO <sub>3</sub> -N - deterministic process model calibration (1 mile = 1.61 km) . . . . .	71
5.5 Measured and predicted values of (ORG-N + ALG-N) - deterministic process model calibration (1 mile = 1.61 km) . . . . .	72

LIST OF FIGURES (Continued)

Figure	Page
5.6 Measured and predicted values of ALG-N - deterministic process model calibration (1 mile = 1.61 km). . . . .	72
5.7 Measured and predicted values of ORG-N - deterministic process model calibration (1 mile = 1.61 km). . . . .	72
5.8 The trial-and-error approach for establishing the process model variances (Q) . . . . .	76
5.9 Basic EKF results for BOD (run 8) (1 mile = 1.61 km) . . . . .	82
5.10 Basic EKF results for DO (run 8) (1 mile = 1.61 km) . . . . .	82
5.11 Basic EKF results for NH <sub>3</sub> -N (run 8) (1 mile = 1.61 km) . . . . .	83
5.12 Basic EKF results for NO <sub>3</sub> -N (run 8) (1 mile = 1.61 km) . . . . .	83
5.13 Basic EKF results for (ALG-N + ORG-N) (run 8) (1 mile = 1.61 km) . . . . .	84
5.14 Basic EKF results for ALG-N (run 8) (1 mile = 1.61 km) . . . . .	84
5.15 Basic EKF results for ORG-N (run 8) (1 mile = 1.61 km) . . . . .	85
5.16 Smoothing algorithm results for BOD (XS and PS) (1 mile = 1.61 km) . . . . .	91
5.17 Smoothing algorithm results for DO (XS and PS) (1 mile = 1.61 km) . . . . .	91
5.18 Smoothing algorithm results for NH <sub>3</sub> -N (XS and PS) (1 mile = 1.61 km) . . . . .	92
5.19 Smoothing algorithm results for NO <sub>3</sub> -N (XS and PS) (1 mile = 1.61 km) . . . . .	92
5.20 Smoothing algorithm results for (ALG-N + ORG-N) (XS and PS) (1 mile = 1.61 km) . . . . .	93
5.21 Smoothing algorithm results for ALG-N (XS and PS) (1 mile = 1.61 km) . . . . .	93
5.22 Smoothing algorithm results for ORG-N (XS and PS) (1 mile = 1.61 km) . . . . .	94
5.23 Sensitivity study on process model noise variance for NH <sub>3</sub> -N (1 mile = 1.61 km) . . . . .	94

LIST OF FIGURES (Continued)

Figure	Page
5.24 Sensitivity study on measurement noise variance for NH <sub>3</sub> -N - NH <sub>3</sub> -N results (1 mile = 1.61 km) . . . . .	.101
5.25 Sensitivity study on measurement noise variance for (ALG-N + ORG-N) - (ALG-N + ORG-N) results (1 mile = 1.61 km) . . . . .	.101
5.26 Sensitivity study on the initial estimation error variance for NO <sub>3</sub> -N (1 mile = 1.61 km) . . . . .	.104
5.27 Sensitivity study on the estimation error variances associated with the point load at river mile 31.70 - NO <sub>3</sub> -N results (1 mile = 1.61 km). . . . .	.106
5.28 Sensitivity study on the point load estimation error variances associated with the point load at river mile 31.70 - ALG-N results (1 mile = 1.61 km) . . . . .	.106
5.29 Coefficient estimation for K <sub>23</sub> - K <sub>23</sub> results (run 15) (1 mile = 1.61 km) . . . . .	.111
5.30 Coefficient estimation for K <sub>23</sub> - DO results (run 15) (1 mile = 1.61 km) . . . . .	.111
5.31 Coefficient estimation for K <sub>23</sub> - NH <sub>3</sub> -N results (run 15) (1 mile = 1.61 km) . . . . .	.112
5.32 Coefficient estimation for K <sub>23</sub> - NO <sub>3</sub> -N (run 15) (1 mile = 1.61 km) . . . . .	.112
5.33 Coefficient estimation for K <sub>23</sub> - ALG-N results (run 15) (1 mile = 1.61 km) . . . . .	.113
5.34 Coefficient estimation for K <sub>45</sub> - K <sub>45</sub> results (run 16) (1 mile = 1.61 km) . . . . .	.115
5.35 Coefficient estimation for K <sub>45</sub> - ALG-N results (run 16) (1 mile = 1.61 km) . . . . .	.115
5.36 Coefficient estimation for K <sub>45</sub> - ORG-N results (run 16) (1 mile = 1.61 km) . . . . .	.116
5.37 Estimation of the nitrogen cycle coefficients - K <sub>23</sub> results (run 21) (1 mile = 1.61 km) . . . . .	.118
5.38 Estimation of the nitrogen cycle coefficients - K <sub>45</sub> results (run 21) (1 mile = 1.61 km) . . . . .	.118

LIST OF FIGURES (Continued)

Figure	Page
5.39 Estimation of the nitrogen cycle coefficients - $K_{52}$ results (run 21) (1 mile = 1.61 km). . . . .	119
5.40 Estimation of the nitrogen cycle coefficients - $\hat{\mu}$ results (run 21) (1 mile = 1.61 km) . . . . .	119
5.41 Estimation of the nitrogen cycle coefficients - $K_{S3}$ results (run 21) (1 mile = 1.61 km) . . . . .	120
5.42 Estimation of the nitrogen cycle coefficients - BOD results (run 21) (1 mile = 1.61 km) . . . . .	120
5.43 Estimation of the nitrogen cycle coefficients - DO results (run 21) (1 mile = 1.61 km) . . . . .	121
5.44 Estimation of the nitrogen cycle coefficients - $NH_3$ -N results (run 21) (1 mile = 1.61 km) . . . . .	121
5.45 Estimation of the nitrogen cycle coefficients - $NO_3$ -N results (run 21) (1 mile = 1.61 km) . . . . .	122
5.46 Estimation of the nitrogen cycle coefficients - ALG-N results (run 21) (1 mile = 1.61 km) . . . . .	122
5.47 Estimation of the nitrogen cycle coefficients - ORG-N results (run 21) (1 mile = 1.61 km) . . . . .	123
5.48 Lateral inflow concentration estimation for $NO_3$ -N - $NO_3$ -N lateral inflow results (run 17) (1 mile = 1.61 km). . . . .	125
5.49 Lateral inflow concentration estimation estimation for $NO_3$ -N - $NH_3$ -N results (run 17) (1 mile = 1.61 km) . . . . .	125
5.50 Lateral inflow concentration estimation for $NO_3$ -N - $NO_3$ -N results (run 17) (1 mile = 1.61 km). . . . .	128
5.51 Lateral inflow concentration estimation for $NO_3$ -N - ALG-N results (run 17) (1 mile = 1.61 km). . . . .	128
5.52 Lateral inflow concentration estimation for $NO_3$ -N - ORG-N results (run 17) (1 mile = 1.61 km). . . . .	129
5.53 Lateral inflow concentration estimation for $NH_3$ -N - $NH_3$ -N lateral inflow results (run 8) (1 mile = 1.61 km) . . . . .	130
5.54 Lateral inflow concentration estimation for $NH_3$ -N - $NH_3$ -N results (run 18) (1 mile = 1.61 km). . . . .	130

LIST OF FIGURES (Continued)

Figure	Page
5.55 Lateral inflow concentration estimation for $\text{NH}_3\text{-N}$ - $\text{NO}_3\text{-N}$ results (run 18) (1 mile = 1.61 km). . . . .	131
5.56 Lateral inflow concentration estimation for $\text{NH}_3\text{-N}$ - ALG-N results (run 18) (1 mile = 1.61 km). . . . .	131
5.57 Lateral inflow concentration estimation for $\text{NH}_3\text{-N}$ - ORG-N results (run 18) (1 mile = 1.61 km). . . . .	132
5.58 Comparison of the costs of computer runs . . . . .	133
A-1. Overall flow diagram of filter model . . . . .	150
A-2. Overall flow diagram of data sorting program . . . . .	188
A-3. Overall flow diagram of plotting program . . . . .	194

ABSTRACT

Estimation Theory Applied to River

Water Quality Modeling

by

David S. Bowles, Doctor of Philosophy

Utah State University, 1977

Major Professor: Dr. J. Paul Riley  
Dissertation Director: Dr. William J. Grenney  
Department: Civil and Environmental Engineering

The extended Kalman filter (EKF) is used to represent BOD, DO, and nitrogen cycling in a 36.4 mile (58.6 km) stretch in the Jordan River, Utah, under the assumption of steady-state conditions. Approximate minimum variance estimates of the water quality parameters are provided by the EKF filter. These estimates are obtained through a combination of two independent estimates of the state of the river water quality system: (1) predictions of the system state from a "phenomenologically meaningful" process model of the biochemical and stream transport processes; and (2) measurements of the water quality parameters. These two estimates are combined by a weighting procedure based on the uncertainties associated with the process model predictions and the measurements. The EKF also yields an estimation error covariance matrix from which confidence limits for the accuracy of the parameter estimates are obtained.

A sequential arrangement of extended Kalman filters is utilized. Each EKF in the sequence represents a river reach for which hydraulic and water quality characteristics are fairly uniform. Initial conditions for each EKF are based on the final conditions of the previous EKF adjusted to

represent the effect of point loads or tributaries discharging into the main river between the two reaches.

A trial-and-error calibration procedure is used to obtain values for the model coefficients in the process model operated as a deterministic model independent of the filter. Determination of values for the Q matrix by a trial-and-error procedure is described. The approach is based on the requirement that the mean square error of the differences between the filter estimates and the measurements be not less than the measurement noise variance.

A property of the EKF is that information contained in the measurements is used only in subsequent estimates of the system state. Therefore, information in the measurements is used only downstream of the sampling point at which the measurement was taken. To make use of the measurements in both the up- and downstream directions a fixed-interval smoothing algorithm (FIS) is implemented. This technique combines state estimates from filter passes in the up- and downstream directions. Sequential linearized Kalman filters are used for the pass in the upstream, or backward direction. Unlike the forward and backward estimates of the estimation error (P), the smoothed values are not characterized by discrete jumps at sampling points. Instead, the estimation error rises to a peak approximately midway between sampling locations. This characteristic indicates that when information from all the measurements is used confidence in the estimates decreases with distance from the adjacent sampling points. Smoothed values of P are less than the values obtained from applying the forward EKF alone; thus indicating that the estimates obtained from the FIS are better, in a minimum variance sense, than the estimates obtained from the forward EKF.



To assist in gaining familiarity with the filtering technique, several sensitivity studies are performed. The sensitivity of filter estimates to changes in the following statistics was investigated: the process model noise variance, the measurement noise variance, the initial estimation error variance, and the point load estimation error variance. A large value for the process model noise variance has the effect of: (1) increasing the rate of growth of the estimation error, and (2) placing additional weighting on the measurements because the larger estimation error implies less confidence in the process model predictions. At sampling points the measurement update procedure always results in an estimation error less than the measurement noise regardless of the values used for the process model noise variances. Changing the values of the measurement noise affects (1) the level of the estimation error after measurement updates, and (2) the weighting given to measurements. A larger initial estimation error variance gives relatively more weighting to the measurements but this effect decreases with distance from the upstream boundary. The sensitivity study on the point load estimation error variances indicates a small, but noticeable, effect on the estimation errors, and therefore, a slight effect on the state estimates via the weighting procedure.

The capability of estimating model coefficients and lateral inflow concentrations simultaneously with the water quality parameters is demonstrated. In one run five coefficients in the equations describing nitrogen cycling are estimated. This run also provides an example of filter divergence.

(220 pages)

CHAPTER 1  
INTRODUCTION

Background

River water quality models can be used for many different purposes including prediction of the effects of management strategies, and forecasting future levels of pollution over the short-term or the long-term. Water quality models are also used in stream assessment studies to assist in understanding the important physical processes controlling stream water quality. This task is approached by identifying diffuse and point sources of water quality parameters,<sup>1</sup> collecting hydraulic and stream quality data, and proposing a model of the biochemical and stream transport processes. Typically the model is deterministic and will facilitate physical interpretation of the processes occurring in the prototype system. However, stochastic considerations of the uncertainties associated with the stream system, the data, the model, or the model responses are not usually explicitly considered.

Aquatic or hydrologic process are inherently random in nature. Yevjevich (1971) has explored the sources of stochasticity in geophysical and hydrologic processes. He concluded that 'the atmosphere is the major source of stochasticity' while 'the main influence of the oceans and the continental surfaces as well as the underground water is, however, to attenuate the high stochasticity produced by the atmosphere.' According to Yevjevich (1974) it is common misconception that the need for stochastic

---

<sup>1</sup>Throughout this dissertation the term "parameter" denotes water quality constituents. To avoid confusion with the constants in the mathematical model these constants are referred to as "coefficients."

considerations is only 'temporary,' and will be replaced when the underlying physical mechanisms are better understood. The sequence of true states of a natural system is a stochastic process, that is, it depends not only on the system inputs but also on random environmental disturbances.

Available water quality and hydraulic data are always subject to uncertainties associated with sampling procedures and analytical techniques. Other limitations of data are that they are never continuous in time or space, and that it is seldom possible to measure all the pertinent state variables due to financial and technological limitations.

Mathematical models are never completely accurate representations of the prototype system. A minimum level of prediction uncertainty will result due to the inherent randomness of nature, even with a "perfect" model. Riley (1970) also attributes this lack of accuracy to losses of information about the real world system during the development of the model. In the first place information is lost when we conceptualize what the prototype system is like. This is because the real system must be "viewed" through various kinds of noisy and incomplete data gathered about the system. Another significant loss of information occurs during the conversion of the conceptual model into a mathematical model. This loss of information is caused by such factors as simplifications or omissions that are necessary to make the solution of the problem mathematically tractable or consistent with the available computing facilities. Common examples of these factors are linearization, and the omission of a dispersion term in the stream transport equation. The uncertainties associated with mathematical models are in the variables, the model coefficients, the form of the model, and the numerical solution technique.

Since the real stream system, the data collected from that system, and the stream model are each thwart with uncertainties, and since incompleteness characterizes the data and the stream model, it is inevitable that the model predictions will also be uncertain. The results from estimation theory that are applied in this study, provide a means for modeling these uncertainties. Figure 1.1 is a schematic representation of the occurrence of environmental disturbances in the prototype system and noise in the measurement process. It also shows the estimation theory technique for explicitly treating these uncertainties. The crux of the estimation technique is the weighting procedure for combining two independent estimates of the state of the stream system based on: (1) the measurements, and (2) predictions from a model of the stream processes. These two independent estimates are weighted according to the levels of uncertainty associated with each estimate. Measurement uncertainty is specified as a white Gaussian noise process,  $N(\underline{0}, R)$ <sup>1</sup>. Uncertainty in the process model predictions is partially dependent on the process model uncertainty which is specified by another white Gaussian noise process,  $N(\underline{0}, Q)$ . By combining the measurements and the process model predictions the estimation procedure used in this study provides approximate minimum variance estimates of the true state of the stream water quality parameters, and confidence limits representing the reliability or accuracy of these estimates. The technique uses all available information, in the form of: (1) "a phenomenologically meaningful" process model of the stream processes; (2) measurements of the water quality parameters; and (3) prior estimates of the system state (water quality parameters) and the uncertainty with which these prior estimates are known.

---

<sup>1</sup>The underbar notation indicates a vector.

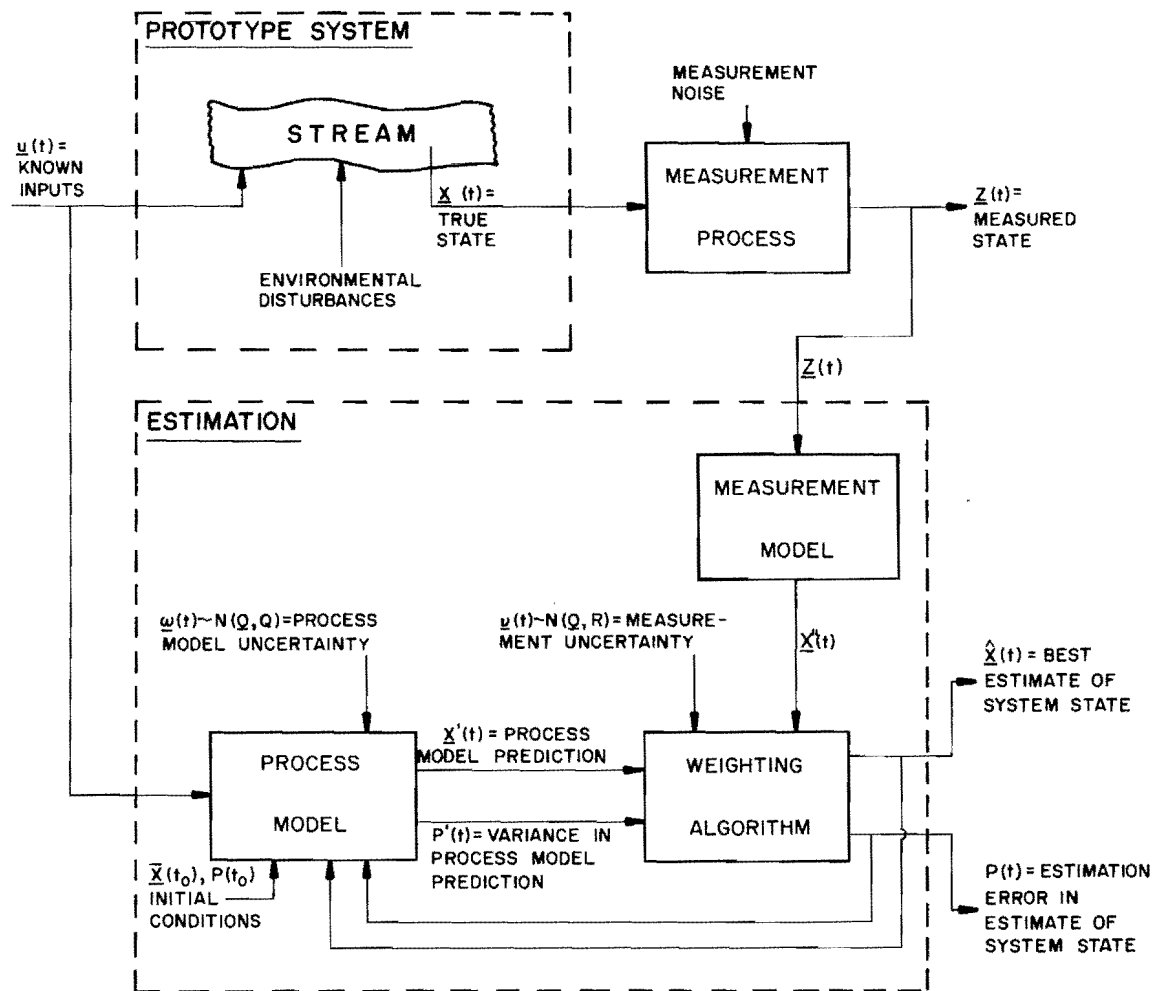


Figure 1.1. A schematic representation of the state estimation procedure.

### Objective

The overall objective of this study is:

To investigate and evaluate the application of estimation theory to river water quality modeling.

To achieve this objective a filter model is developed to represent several water quality parameters in a real river system. The process model is based on established deterministic techniques for representing river water quality. Model and data uncertainty are handled through a state estimation procedure with the result that uncertainty associated with the final estimates is less than the individual uncertainties associated with either the process model predictions, or the measurements individually. This is referred to as the "filtering result" and is proven in Chapter 3. The limited availability of suitable data and computer funds have restricted the study to a steady-state model.

### Summary of Contents

Chapter 2 contains a literature review. The review is divided into two parts: (1) a review of estimation theory, and (2) a review of the applications of estimation theory to water resources.

The main result from estimation theory utilized in this study is the extended Kalman filter. This and other estimation theory techniques are described in Chapter 3. The sequential mode of application of the Kalman filter to a river under the assumption of steady-state conditions is explained. Also numerical and other computational aspects of the study are briefly described.

Chapter 4 contains descriptions of the study river, the process model and the measurement model. Details of other aspects of the problem set-up such as point load concentrations, lateral inflow loadings, and initial conditions also are included.

In Chapter 5 the results are presented. After a section in which calibration of the deterministic process model is described, the technique used to obtain suitable values for the variances in the process model noise covariance matrix,  $Q$ , is explained. The subsequent sections contain the results and discussion of results for: the filter run, the smoothing algorithm run, several sensitivity studies, and some coefficient estimation runs. An example of filter divergence is included in one of the coefficient estimation runs. In the final section of Chapter 5 the computational requirements of the estimation theory techniques applied are summarized.

A summary of the research accomplished in this study is contained in Chapter 6. In addition, several conclusions and recommendations for further work are made.

Appendix A is a users manual for the computer programs written for this project. It includes input instructions, program listings, and flow charts.

## Chapter 2

### LITERATURE REVIEW

#### Introduction

The review of literature is divided into two parts: (1) a review of estimation theory, and (2) a review of the application of estimation theory to water resources. The applications reviewed in the second section are also summarized in tabular form for easy reference.

#### Review of Estimation Theory

During the mid-1960's modern estimation theory techniques were extensively applied to the real-time problems of space and missile guidance and navigation including the Apollo mission (Leondes, 1970). Gelb (1974) defines estimation as:

The process of extracting information from data -- data which may only infer the desired information and which may contain errors. Modern estimation methods use known relationships to compute the desired information from the measurements, taking account of measurement errors, the effects of disturbances, and control actions on the system, and prior knowledge of the information. Diverse measurements can be blended to form "best" estimates, and information which is unavailable for measurement can be approximated in an optimal fashion.

Estimation problems can be classified by the relationship between times of measurements and times at which estimation is required:

- 1) Filtering: Estimate the state vector,  $\underline{X}$ , at time  $t$  based on measurements up to and including time  $t$
- 2) Prediction: Estimate  $\underline{X}$  at time  $t' > t$  based on measurements up to time  $t$
- 3) Smoothing: Estimate  $\underline{X}$  at time  $t' < t$  based on measurements up to time  $t$



The idea of obtaining approximations or estimates of unknown quantities can be traced to the development of least squares estimation. According to Young (1974) both Gauss (1821) and Legendre (1806) appear to have used least squares analysis at the beginning of the nineteenth century. The mathematical theory of probability did not exist at this time and, therefore, least squares estimation was formulated as a deterministic approach. (See for example Kreider et al., 1966).

In the early 1940's Wiener (1949) solved the continuous-time problem of linear least-squares estimation for stochastic processes. Wiener's work was prompted by the problem of designing anti-aircraft fire-control systems. His solution involved reducing the problem to that of solving certain integral equations such as the Wiener-Hopf equations. However, the frequency-domain Wiener filter did not gain much practical acceptance. The main reasons for this were difficulties in synthesizing a suitable data processing scheme; and, the incompatibility with practical problems of the assumptions of stationarity and knowledge of the entire past of the observable processes. With the advent of the high speed digital computer the effort was diverted from attempts at trying to solve the Wiener-Hopf equation for particular problems, to a search for a time-domain algorithm which would produce numerical estimates from numerical measurements. The search was further stimulated by the real-time problems of space and missile guidance and navigation.

The breakthrough came with the work of Kalman and Bucy in the early 1960's (Kalman, 1960; Kalman and Bucy, 1961; Kalman, 1963). Essentially the Kalman-Bucy or Kalman filter is no more than a "recipe" for combining two independent estimates of a state vector (Lettenmaier and Burges, 1976) to provide a "best" (minimum variance) estimate of the system state

(Figure 2.1). The two independent estimates of system state are given by (1) a "process model" based on a prior understanding of the physical system, and (2) measurements on part or all of the state vector. These two estimates contain levels of uncertainty. The filter combines the model and data estimates by weighting them according to the uncertainties associated with each one. Output from the filter comprises a new improved estimate of the system state and the variance associated with that estimate (Moore, 1973). In contrast to the Wiener filter, the Kalman filter utilizes the relatively flexible state-space structure and is a recursive algorithm. Because of its recursive nature only the most recent measurements are stored by the computer. This feature saves computer memory and permits real-time estimation. Although the theory of filtering is quite complex the result is basically a pair of differential or difference equations for propagation of the mean and covariance of the probability distribution function of the state variables conditioned on processed past measurements.

A linear model is assumed in the basic Kalman filter. In the case of a nonlinear model the computational requirements for an exact solution to equations describing the evolution of the conditional probability density function become impractical for most problems and, therefore, approximations are used (Schmidt, 1976). The three most common approximations are: the linearized Kalman filter, the extended Kalman filter, and the iterated extended Kalman filter. The linearized Kalman filter is linearized about an a priori trajectory for the state vector. The extended Kalman filter is linearized about the latest estimate of state, and the iterated extended Kalman filter includes iterations on the estimate at each measurement until there is little change in the estimate.

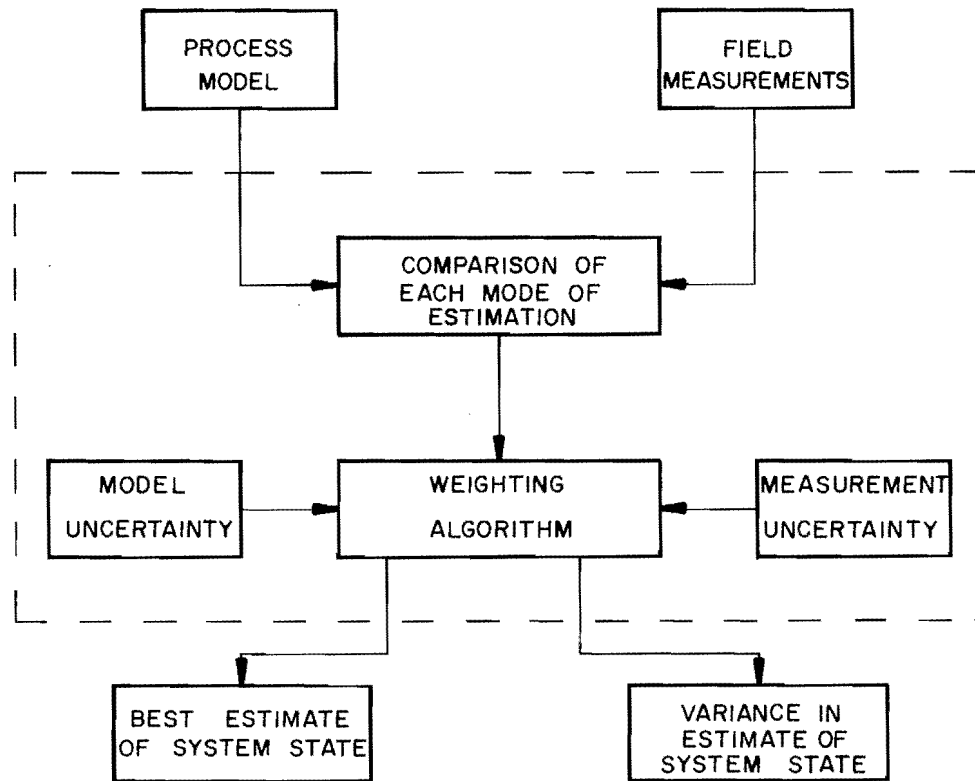


Figure 2.1. A schematic representation of the filtering procedure (adapted from Moore, 1973).

Each of the Kalman-type filters referred to above involves minimum variance estimation albeit approximate for the case of a nonlinear model.

Other criteria for estimation are:

- 1) Joint maximum likelihood (Bayesian)
- 2) Maximum likelihood (non-Bayesian)
- 3) Least squares (dynamic programming, invariant imbedding)

Because nonlinear filters differ in both the criterion of optimality and the approximations used it is not possible to compare the different filters except through computational studies (Schwartz and Stear, 1968). Since computational studies are based on specific problems the comparisons made using the results of these studies may apply only to the problem considered. Lee (1972) compared nine approximate nonlinear filters for a hypothetical BOD-DO river water quality problem. He concluded that for his problem the dynamic programming least squares and the first-order minimum variance filter were far superior to the other filters on the basis of performance and computational time. However, Lee did not consider the extended Kalman filter.

Young et al. (1971) proposed an instrumental variable-approximate maximum likelihood (IV-AML) technique as an alternative to the extended Kalman filter. The IV-AML approach is a recursive time series analysis procedure and is less flexible but computationally more efficient than the extended Kalman filter.

The reader is referred to Lee (1972) for a fairly comprehensive historical review of estimation theory. Also of interest is a tutorial paper by Young (1974) in which the parallelism between recursive least squares estimation and Kalman filtering is discussed. Young (1974) and Moore (1971)

also point out that the state estimation problem may be viewed as an extension of Bayesian analysis applied to dynamic systems.

### Review of the Applications of Estimation Theory to Water Resources

In the past five years the literature has contained several examples of applications of estimation theory to water quality and hydrologic problems. A summary of each study is contained in Table 2.1. Several differences in uses for estimation techniques in water resources problems have been identified and form the framework for synthesizing previous work in the following discussion.

#### Model identification

The process model is an essential part of the procedure for estimating the state of a system. This model is described in the state-space form and comprises a set of first-order, deterministic, linear or nonlinear, differential or difference equations with an additive white Gaussian noise term. The initial process model may be an empirical transfer function, or it may be based on some heuristic feeling or physio-chemical understanding of the system (Whitehead and Young, 1975). Graupe, Isailovic, and Yevjevich (1975) argue for the mathematical statistical model on the grounds of such statistical advantages as unbiasedness, convergence, and optimality in estimating model coefficients; whereas, Young (1974) claims that "internally descriptive" models tend to make better use of a priori information on the physical nature of the system and thus are more attractive from the "information theoretic" standpoint. In either case estimation techniques provide a means of assessing the adequacy of particular model structures by careful analysis of the process model noise covariance matrix ( $Q$ ). Also the desirability of adding or deleting state variables

may be assessed by studying changes in the estimation error covariance matrix (P) (Lettenmaier and Burges, 1976). Beck (1973, 1975) and Beck and Young (1976) developed a process model for BOD-DO-algae interaction in the River Cam, England, through repeated use of the extended Kalman filter together with statistical and other tests. In a related study (Whitehead and Young, 1975; Young and Whitehead, 1975) a rainfall-runoff model was identified by repeated application of the instrumental variable-maximum likelihood technique.

#### Model calibration

Estimation techniques are potentially useful in model calibration. Coefficients in the process model can be estimated at the same time as state variables are estimated. Coefficient estimation is achieved by augmenting the state vector with the coefficients to be estimated after a satisfactory model structure is obtained. Usually the process model adopted for these coefficients is based on the assumption that the coefficients are constant except for model uncertainty. Lettenmaier and Burges (1976) point out that in the context of estimation theory model calibration is viewed in an essentially Bayesian sense in which the actual process is well identified but calibration coefficients must be determined. Many of the studies referred to in Table 2.1 include coefficient estimation (e.g., Beck, 1973; Koivo and Phillips, 1976). Graupe, Isailovic, and Yevjevich (1975) handle non-stationarity in the model coefficients by estimating different sets of coefficients for different seasons. An alternative would be to identify a model to represent coefficient non-stationarity and include this as part of the process model. Nonlinear filtering techniques are usually necessary for coefficient

Table 2.1. Summary of applications of estimation theory to water resources.

Reference	Type of Application	Estimation Technique
Lee and Hwang (1971)	Dynamic stream model for BOD-DO using synthetic data. Coefficient estimation and sensitivity studies on initial state vector and a weighting matrix.	Invariant Imbedding Least Squares Filter
Lee (1972)	A computational comparison of 9 approximate non-linear filter algorithms for a dynamic stream model of BOD-DO using synthetic data. Coefficient estimation and sensitivity studies. Application of minimum variance filter to activated sludge process and nonlinear hydrologic process model including coefficient estimation. Comprehensive historical review of estimation theory.	Linearized Kalman Filter Invariant Imbedding Least Squares Filter Minimum Variance Filter and others
Moore (1971) Moore and Brewer (1972) Moore (1973) Brewer and Moore (1974)	Development of an approach for designing river water quality monitoring systems that maximizes predictive accuracy subject to a cost constraint. Application of the technique to a simulated river with twelve reaches for temperature, zooplankton, phytoplankton, and nitrate. Illustrations of filter characteristics and divergence control.	Extended Kalman Filter
Beck (1973) Beck (1975) Beck and Young (1976)	Dynamic stream model for BOD-DO-algae using field data collected over a 2.9 mile (4.7 km) reach of the River Cam in eastern England. Process model was the outcome of a thorough model identification procedure. Coefficient estimation.	Extended Kalman Filter

Table 2.1. Continued

Reference	Type of Application	Estimation Technique
Pearce, DeGuida, Dandy, and Moore (1975)	Evaluation of estimation theory as a technique for design of sampling networks for dispersion experiments in Massachusetts Bay. Filter handles temporal propagation of the system states while spatial relationships are handled separately by a finite element method.	Linear Kalman Filter
Whitehead and Young (1975) Young and Whitehead (1975)	Dynamic stream model for flow-BOD-DO using field data collected on a 34 mile (55 km) stretch of the Bedford-Ouse River System, England. BOD-DO model identification was achieved by Beck (1973). Identification of a rainfall-runoff model was based on autoregressive-moving average (AR-MA) methods.	Multivariable Instrumental Variable-Approximate Maximum Likelihood
Lettenmaier (1975) Lettenmaier and Burges (1976)	Dynamic stream model for BOD-DO using simulated data. Lucid introduction to state estimation techniques in water resource system modeling. Discussion of divergence in Kalman filter and potential uses of estimation theory.	Linear Kalman Filter Extended Kalman Filter
Bowles and Grenney (1976a) Bowles and Grenney (1976b)	Steady-state stream model for BOD-DO and nitrogen cycling using field data collected over a 36.4 mile (58.6 km) stretch of the Jordan River, Utah. Comparison of filter estimates and results from a deterministic solution of the process model. Coefficient estimation and sensitivity studies on several statistics. The final results from this study are presented in this dissertation.	Sequential Extended Kalman Filters Sequential Linearized Kalman Filters Fixed-Interval Smoothing Algorithm



Table 2.1. Continued

Reference	Type of Application	Estimation Technique
Özgören, Longman, and Cooper (1974)	Formulation of dynamic stream model for BOD-DO. A five-day delay in BOD measurements is handled through the use of a smoother. Artificial river aeration is controlled by a stochastic optimal feedback control. No application is described.	Linear Kalman Filter
Perlis and Okunseinde (1974)	Development of an approach for designing water quality monitoring schemes subject to cost and accuracy constraints. Application to a simulated TOC/BOD-DO system. Current measurement of TOC and five-day delayed BOD results combined by a scheme that employs the projection of the delayed measurement to the time of on-line estimation.	Multiple Linear Kalman Filters
Bras and Rodriguez-Iturbe (1975)	Development of an approach for "optimal" rain gage network design subject to cost and network accuracy constraints. Application to simulated storms. Extension of the method to enable accuracy constraints to be placed on basin discharge estimated from rain gage data via a rainfall-runoff filter model.	Linear Kalman Filter
Graupe, Isailovic, and Yevjevich (1975)	Rainfall-runoff, input-output, model applied to Karst catchment of the Trebišnjica River, Yugoslavia. Identification of a linear-optimal process model based on autoregressive-moving average (ARMA) methods. Measurement errors are filtered out by linear Kalman filter.	Linear Kalman Filter

Table 2.1. Continued

Reference	Type of Application	Estimation Technique
Koivo and Phillips (1976)	Dynamic stream model for BOD-DO using synthetic data. Sinusoidally varying point source of BOD and photo-synthetic source. Coefficient estimation.	Linear Kalman Filter
Moore, Dandy, and deLucia (1976)	Development of an approach for designing sampling programs in a completely mixed impoundment. Application to nutrients and algal biomass in top two meters of Lake Washington using field data and synthetic data.	Linearized Kalman Filter

estimation because a linear process model often becomes nonlinear when model coefficients are treated as state variables. In addition, computer costs increase as the order of the state vector is incremented. Therefore, the amount of computational effort required for filter models that include coefficient estimation can increase very rapidly.

### River forecasting

The river forecasting problem is a "natural" application for estimation theory. A filter algorithm is used to determine "best" estimates of the system state from noisy measurements as they become available, and from the process model conditioned on previous measurements. Most of the river quality forecasting studies reported in the literature have been based on a one-dimensional dynamic stream model (e.g., Lee and Hwang, 1971; Moore, 1971; Koivo and Phillips, 1976). Due to the scarcity of data suitable for verifying dynamic river water quality models, noisy data often have been generated on a digital computer using a pseudo-random number generator to introduce normally distributed process model noise and measurement noise. With the exception of Moore's work (Moore, 1971; Moore and Brewer, 1972; Moore, 1973; Brewer and Moore, 1974) synthetic stream data were obtained using a model identical to the process model. Under these conditions the filter problem is merely the inverse of the data generation exercise. Noise effects are normally distributed and the process model and coefficients are known exactly. Although results from studies utilizing synthetic data have demonstrated the application of estimation theory to river quality forecasting the approach circumvents the vagaries of real data. Moore attempted to generate data

that were more realistic and which, therefore, presented a more challenging filtering problem. He did this by adding several variables to the simulation model that were not in the process model and by adding noise to certain model coefficients and model inputs. Thus, the filter problem was not the inverse of the data generation problem.

Two techniques have been proposed for incorporating delayed measurements into the filter procedure for river forecasting. In a theoretical paper, Özgören, Longman, and Cooper (1974), formulated an approach that makes use of a smoothing procedure to utilize the five-day delayed BOD data. In another paper, Perlis and Okunseinde (1974) proposed the use of TOC data in lieu of delayed BOD measurements. When BOD data become available, a multiple Kalman filter model is used to combine current measurements of TOC and five-day delayed BOD results by a scheme that employs the projection of the delayed measurements to the time of on-line estimation.

Estimation techniques also have been applied to the problem of hydrologic forecasting. Lee (1972) formulated a rainfall-runoff process model of the hydrologic system from the nonlinear Prasad (1967) model and tested the approximate minimum variance filter model using generated data. Bras and Rodríguez-Iturbe (1975) developed a hydrologic process model for storms with separate stream and overland flow segments but ignoring infiltration. Their model is based on solutions to the kinematic wave equations and was tested using synthetic data. Whitehead and Young (1975) used ad hoc and time series empirical relationships in a rainfall-runoff process model to represent the Bedford-Ouse River System in Eastern England. Time series transfer function techniques (Box and Jenkins, 1970) were also used by Graupe, Isailovic, and Yevjevich (1975) to identify rainfall-runoff re-

relationships for a process model of the hydrology of the catchment of the Trebišnjica River in Yugoslavia. For cases where measurement errors cannot be considered negligible the autoregressive-moving average transfer function model is no longer linear-optimal with respect to true runoff although it is linear-optimal with respect to runoff measurements. Therefore, in these cases, measurement errors are filtered out using a linear Kalman filter.

Recently, the National Weather Service, which is the Federal Agency responsible for river and flood forecasting in the United States, has become interested in applying estimation theory techniques to operational hydrologic forecasting (Hydrologic Research Laboratory, 1976). Estimation theory techniques should improve both the accuracy and reliability of forecasts. Accuracy will be enhanced through the objective procedure for updating forecast model performance based on observations of river stages and other variables that become available during real-time simulation. Reliability will be improved as a result of reducing the uncertainty associated with river forecasts by filtering out measurement noise. In addition the application of estimation techniques to real-time hydrologic forecasting will yield confidence intervals on forecasts of the mean.

#### Sampling program design

Use of filtering techniques for the design of sampling programs is facilitated by the fact that the equations for the propagation of the estimation error covariance matrix are independent of the values of the actual measurements. Therefore, knowledge of the accuracy of a proposed sampling network can be obtained a priori without measurement data. Only the statistics of the measurement error ( $R$ ) are required and these can be determined by analysis of the sampling procedures and analytical tech-

niques. Different measurement coefficient matrices (H) (described in Chapter 3) can be formulated to represent different configurations of sampling locations and different combinations of the variables to be measured. A cost constraint may be placed on the sampling schemes represented by the H matrices. The optimal sampling network is selected as the network that provides for estimates of the variables with maximum time between samples, while meeting a constraint on the maximum attainable estimation error (P). A global optimum design cannot be guaranteed since only those measurement coefficient matrices that are formulated by the designer are evaluated. This technique for sampling program design bases the selection of an "optimal" design on the use to which the data are to be put, that is making estimates of the state of the system with the aid of a priori knowledge contained in the process model. Costs associated with different degrees of estimation uncertainty could be introduced into the objective function. A disadvantage of the procedure is the rapid growth in size of the state vector, and therefore, computer costs, as the number of space points or system variables is increased.

Moore and Brewer pioneered the use of filtering techniques for the design of water quality monitoring schemes. The approach was first applied (Moore 1971, 1973) to four water quality variables on a river that was divided into twelve reaches. A temporal and spatial distribution of the measurements, and the measurement techniques to be used were determined by the procedure.

Perlis and Okunseinde (1974) based the decision to make a measurement on the relative savings from improved estimation compared with the cost of measurements. Their technique yields the location of a single sampling point and the temporal spacing of samples.

Pearce, DeGuida, Dandy, and Moore (1975) evaluated estimation theory as a technique for the design of sampling networks for dispersion experiments. A two-dimensional finite element model is used to simulate spatial aspects of dispersion in Massachusetts Bay. It is proposed that temporal aspects be handled by the linear Kalman filter, thus facilitating selection of an "optimal" sampling network.

As part of the National Eutrophication Survey, Moore, Dandy, and deLucia (1976) used a linearized Kalman filter to evaluate sampling frequencies in a completely mixed impoundment. In addition to model and data uncertainty, phenomological uncertainty in the system inputs was considered. The approach was applied to nutrients and algal biomass in the top 7 feet (2 m) of Lake Washington using both field and synthetic data.

Linear Kalman filter techniques are utilized in a method for "optimal" rain gage network design developed by Bras and Rodriguez-Iturbe (1975) with cooperation from Moore and others. The design procedure includes constraints on costs and the accuracy of mean aerial rainfall estimates. An application was made using synthetic storm data. The design procedure is extended via a rainfall-runoff filter model, so that the accuracy constraint may be placed on estimates of basin discharge which are obtained from the precipitation measurements.

#### Missing data fill-in

Lettenmaier and Burges (1976) propose that estimation techniques are applicable in situations where a cause-effect model could be employed to fill in missing observations in otherwise reasonably complete data time series. In this way understanding of the physical system is utilized instead of being largely ignored as it is in regression methods.

### Control

Moore and Brewer (1972) propose that filter models be used to obtain "best" estimates of the state variables in an environmental system, such as a river, and that these estimates be used to control the system via a feedback control procedure. A theoretical example of artificial river aeration operated by a stochastic optimal feedback control law is given by Özgören, Longman, and Cooper (1974). Bras and Rodriguez-Iturbe (1975) propose the use of estimation and control theory to determine reservoir operating rules with the purpose of satisfying a given objective. They point out that some difficulty might be expected because of the assymmetric nature of the loss functions in this problem.



## CHAPTER 3

## DESCRIPTION OF THE ESTIMATION THEORY

## TECHNIQUES APPLIED

Introduction

In the previous two chapters the development and basic philosophy of estimation theory are outlined. In this chapter the techniques of estimation theory applied in this study are described in detail. These techniques are:

- (1) extended Kalman filter (EKF),
- (2) linearized Kalman filter (LKF),
- (3) smoothing algorithm.

In addition the sequential mode of application of the Kalman filter to a river under the assumption of steady-state conditions is presented. Numerical and other computational aspects of the study are briefly described at the end of the chapter. Firstly, a simplified derivation of the linear Kalman filter is given to provide an intuitive feeling for the technique.

Simplified Derivation of the Linear Kalman Filter

A mathematical rigorous derivation of the Kalman filter requires familiarity with advanced statistical theory. Barnham and Humphries (1970) have presented a less rigorous but intuitively appealing derivation which is reproduced as follows.

Firstly, the case of a single state variable,  $X$ , is considered. Let  $X'$  and  $X''$  be two independent estimates of  $X$  with variances of  $\sigma'^2$  and  $\sigma''^2$  respectively. The goal is to combine these estimates to form a weighted mean that has the property of being the minimum variance estimate,  $\hat{X}$ , of  $X$ . A linear combination of  $X'$  and  $X''$  using a weighting factor  $W$  is formed as follows:

$$\hat{X} = (1 - W) X' + WX'' \quad \dots \dots \dots (3.1)$$

The expected or mean value of  $\hat{X}$  is given by:

$$E(\hat{X}) = (1 - W) E(X') + WE(X'') \quad \dots \dots \dots (3.2)$$

By definition the variance,  $\sigma^2$ , of  $\hat{X}$  is given by:

$$\begin{aligned} \sigma^2 &= E \{ [\hat{X} - E(\hat{X})]^2 \} \\ &= E \{ [(1 - W)X' + WX'' - (1 - W)E(X') - WE(X'')]^2 \} \\ &= (1 - W)^2 \sigma'^2 + W^2 \sigma''^2 \quad \dots \dots \dots (3.3) \end{aligned}$$

To find the minimum variance estimate of  $W$  we minimize  $\sigma^2$  with respect to  $W$ , as follows:

$$\frac{\partial \sigma^2}{\partial W} = -2(1 - W) \sigma'^2 + 2W \sigma''^2 = 0 \quad \dots \dots \dots (3.4a)$$

and

$$\frac{\partial^2 \sigma^2}{\partial W^2} = 2\sigma'^2 + 2\sigma''^2 \geq 0 \quad \dots \dots \dots (3.4b)$$

From Equation 3.4a  $W^*$ , the minimum variance estimate of  $W$  is:

$$W^* = \frac{\sigma'^2}{\sigma'^2 + \sigma''^2} \quad \dots \dots \dots (3.5)$$

Substituting  $W^*$  into Equations 3.1 and 3.3 yields:

$$\hat{X} = X' - W^* (X' - X'') \quad \dots \dots \dots (3.6)$$

$$\sigma^2 = \sigma'^2 (1 - W^*) \quad \dots \dots \dots (3.7)$$

In the Kalman filter the estimate  $X'$  is obtained from a model of the process  $X$ , and the estimate  $X''$  is the measured value of  $X$  which is represented by  $Z$ . Now  $Z$  is considered to update  $X'$  to produce the minimum variance estimate  $\hat{X}$ .

The "filtering result" referred to in Chapter 1 states that the variance ( $\sigma^2$ ) of  $\hat{X}$  is always less than or equal to the variance ( $\sigma'^2$ ) of  $X'$  or the variance ( $\sigma''^2$ ) of  $X''$  individually. Therefore, according to the minimum variance criterion, the estimate  $\hat{X}$  is a better estimate of  $X$  than either  $X'$  or  $X''$ . The "filtering result" for the one-dimensional case is proven below. It can be expressed by the following pair of inequalities:

$$\sigma^2 \leq \sigma'^2 \quad . . . . . (3.8a)$$

$$\sigma^2 \leq \sigma''^2 \quad . . . . . (3.8b)$$

The first inequality is proven by inspection of Equation 3.7 since from Equation 3.5  $W^* \leq 1$ . Proof of the second inequality proceeds by substituting Equation 3.5 into Equation 3.7 and rearranging to obtain the following equation for  $\sigma''^2$ :

$$\sigma''^2 = \frac{(\sigma'^2)^2}{\sigma'^2 - \sigma^2} - \sigma'^2 \quad . . . . . (3.9)$$

Now the first inequality (Equation 3.8a) may be written as the following equality in which  $\Delta\sigma^2$  is a slack variable:

$$\sigma'^2 = \sigma^2 + \Delta\sigma^2 \quad . . . . . (3.10)$$

Substituting Equation 3.10 into Equation 3.9 yields the following expression:

$$\sigma''^2 = \sigma^2 + \frac{\sigma^4}{\Delta\sigma^2} \quad . . . . . (3.11)$$

and since  $\frac{\sigma^4}{\Delta\sigma^2} \geq 0$  we have:

$$\sigma^2 \leq \sigma'^2$$

(QED)

Barnham and Humphries (1970) also present the multidimensional extension to their simplified derivation of the Kalman filter. This case requires some matrix algebra and allows for the situation in which  $\underline{X}'$  and  $\underline{Z}$  ( $=\underline{X}''$ ) may, in general, be vectors of different orders which are related by the coefficient matrix H as follows:

$$\underline{Z} \sim \underline{HX}' \dots \dots \dots (3.12)$$

The result for the multidimensional case is:

$$\hat{\underline{X}} = \underline{X}' - K (\underline{HX}' - \underline{Z}) \dots \dots \dots (3.13)$$

$$P = (I - KH)P' \dots \dots \dots (3.14)$$

in which

K = Kalman gain matrix (multidimensional  $W^*$ )

$$K = P'H^T (HP'H^T + R)^{-1} \dots \dots \dots (3.15)$$

P = estimation error covariance matrix associated with the minimum variance filter estimates after the measurement update (multidimensional  $\sigma^2$ )

$$P = E[(\underline{X} - \hat{\underline{X}}) (\underline{X} - \hat{\underline{X}})^T] \dots \dots \dots (3.16)$$

P' = estimation error covariance matrix associated with the process model prediction before the measurement update (multidimensional  $\sigma'^2$ )

$$P' = E[(\underline{X} - \underline{X}') (\underline{X} - \underline{X}')^T] \dots \dots \dots (3.17)$$

R = measurement noise covariance matrix (multidimensional  $\sigma''^2$ )

$$R = E[(\underline{X} - \underline{Z}) (\underline{X} - \underline{Z})^T] \dots \dots \dots (3.18)$$

T = superscript denoting matrix transpose





$$\begin{aligned} \underline{u}_k &= m\text{-vector of measurement noise at time } t_k \\ E[\underline{u}(t)\underline{u}^T(s)] &= 0, \text{ for all } t \text{ and } s \dots \dots \dots (3.22) \end{aligned}$$

$$\begin{aligned} R_k &= \text{measurement noise covariance matrix at time } t_k \\ R_k &= E[\underline{u}_k \underline{u}_k^T] \dots \dots \dots (3.23) \end{aligned}$$

Equation 3.21 is referred to as the measurement model. Alternative formulations of the EKF are available in which the measurement model is nonlinear and continuous. However, for the river water quality problem under consideration a linear discrete measurement model is appropriate.

The continuous-discrete EKF algorithm is given by the following vector-matrix recursion equations:

At time  $t_{k+1}$  prior to a measurement at  $t_{k+1}$

$$\begin{aligned} \underline{X}(t_{k+1}|t_k) &= \underline{X}(t_k|t_k) + \int_{t_k}^{t_{k+1}} \underline{f}[\underline{X}(t|t_k), \underline{U}(t);t] dt \\ &\dots \dots \dots (3.24) \end{aligned}$$

$$\begin{aligned} P(t_{k+1}|t_k) &= P(t_k|t_k) + \int_{t_k}^{t_{k+1}} \{F[\underline{X}(t|t_k), \underline{U}(t);t] P(t|t_k) \\ &+ P(t|t_k) F^T[\underline{X}(t|t_k), \underline{U}(t);t] + Q(t)\} dt \dots \dots (3.25) \end{aligned}$$

At time  $t_{k+1}$  after a measurement at  $t_{k+1}$

$$\begin{aligned} \underline{X}(t_{k+1}|t_{k+1}) &= \underline{X}(t_{k+1}|t_k) + K_{k+1} \{Z_{k+1} - H \underline{X}(t_{k+1}|t_k)\} \\ &\dots \dots \dots (3.26) \end{aligned}$$

$$\begin{aligned} P(t_{k+1}|t_{k+1}) &= \{I - K_{k+1} H\} P(t_{k+1}|t_k) \{I - K_{k+1} H\}^T + K_{k+1} R_{k+1} K_{k+1}^T \\ &\dots \dots \dots (3.27) \end{aligned}$$

in which

$\Delta(t_a | t_b) = \Delta$  at time  $t_a$  conditioned on measurements up to, and including, those at time  $t_b$  where  $\Delta$  is  $\underline{X}$  or  $P$

$I = nxn$  identity matrix

$F[\cdot] =$  Jacobian of  $f[\cdot]$  defined by:

$$F_{ij}[\cdot] = \frac{\partial f_i[\cdot]}{\partial X_j}, \text{ for } i, j = 1, 2, \dots, n \quad \dots \quad (3.28)$$

$F_{ij}[\cdot] =$  element of  $F[\cdot]$  in  $i$ th row and  $j$ th column

$f_i[\cdot] =$   $i$ th row of  $f[\cdot]$

$X_j =$   $j$ th state variable in  $\underline{X}(t)$

$K_{k+1} =$  Kalman gain matrix at time  $t_{k+1}$  given by:

$$K_{k+1} = P(t_{k+1} | t_k) H^T \{HP(t_{k+1} | t_k) H^T + R_{k+1}\}^{-1} \quad \dots \quad (3.29)$$

Gelb (1974) derives Equation 3.25 which is used for propagating the estimation error covariance matrix ( $P(t_{k+1} | t_k)$ ) associated with the process model predictions between measurement updates. Beck and Young (1976) describe the function of the Kalman gain matrix as that of filtering the error  $\{\underline{z}_{k+1} - H\underline{x}(t_{k+1} | t_k)\}$  in Equation 3.26, to minimize the effects of the measurement noise on the state and coefficient estimates. At the same time the filtering action should have a minimal effect on those random effects not attributable to measurement noise, such as those resulting from environmental disturbances to the prototype system.

It should be noted that Equation 3.27 is equivalent to Equation 3.14. However, according to Jazwinski (1970) Equation 3.27 is better conditioned for numerical computations and will tend to retain more faithfully the





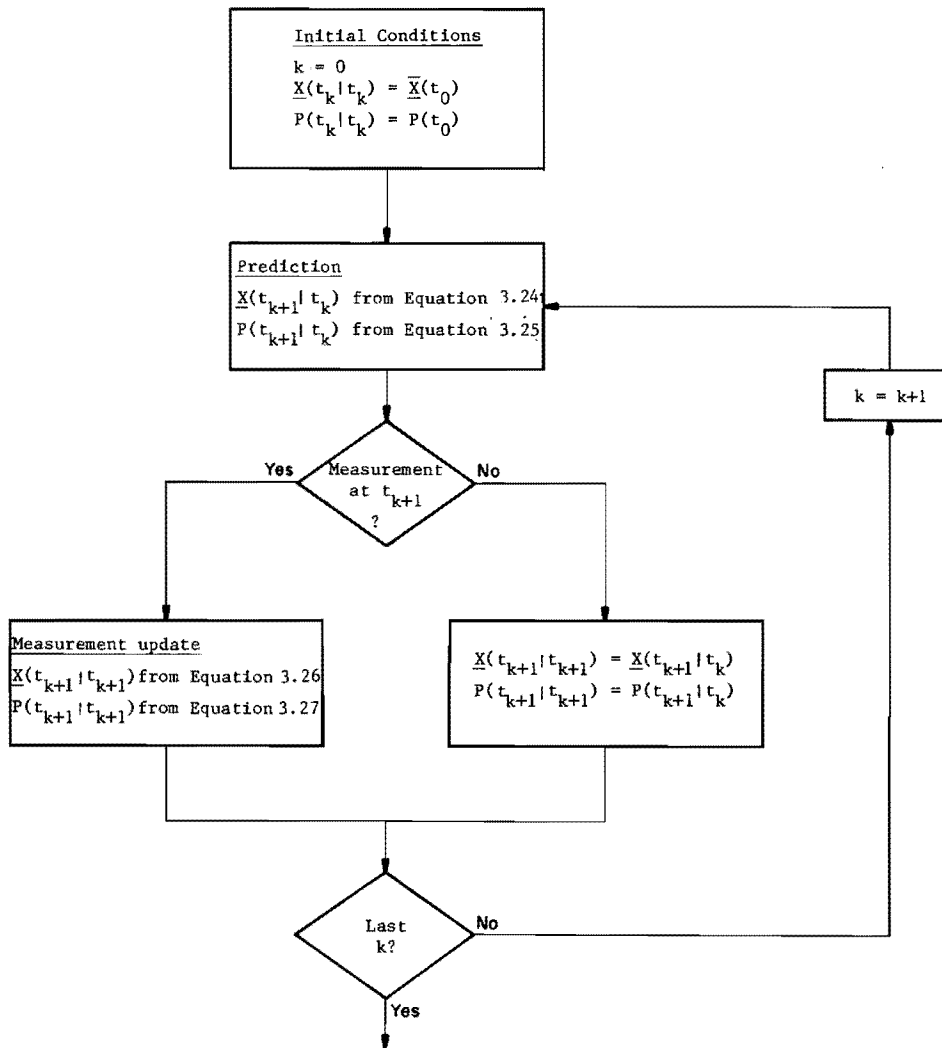


Figure 3.1. Flow diagram for the extended Kalman filter algorithm.

in which

T = value of t at the end of the forward pass

N = value of k at the end of the forward pass

The continuous-discrete LKF algorithm is given by the following vector-matrix recursion equations:

At time  $\tau_{k+1}$  "after" a measurement at  $\tau_{k+1}$

$$\begin{aligned} \underline{X}^b(T-\tau_{k+1} | T-\tau_k) &= \underline{X}^b(T-\tau_k | T-\tau_k) + \int_{\tau_k}^{\tau_{k+1}} \\ &\quad \{-f[\underline{X}(T-\tau | T-\tau_k), \underline{U}(T-\tau); T-\tau] \\ &\quad -F[\underline{X}(T-\tau | T-\tau_k), \underline{U}(T-\tau); T-\tau] [\underline{X}^b(T-\tau_k | T-\tau_k) \\ &\quad -\underline{X}(T-\tau | T-\tau_k)]\} d\tau \dots \dots \dots (3.32) \end{aligned}$$

$$\begin{aligned} P^b(T-\tau_{k+1} | T-\tau_k) &= P^b(T-\tau_k | T-\tau_k) + \int_{\tau_k}^{\tau_{k+1}} \\ &\quad \{-F[\underline{X}(T-\tau | T-\tau_k), \underline{U}(T-\tau); T-\tau] P^b(T-\tau | T-\tau_k) - P^b(T-\tau | T-\tau_k) \\ &\quad F^T[\underline{X}(T-\tau | T-\tau_k), \underline{U}(T-\tau); T-\tau] + Q(T-\tau)\} d\tau \dots \dots (3.33) \end{aligned}$$

At time  $\tau_{k+1}$  "prior to" a measurement at  $\tau_{k+1}$

$$\begin{aligned} \underline{X}^b(T-\tau_{k+1} | T-\tau_{k+1}) &= \underline{X}^b(T-\tau_{k+1} | T-\tau_k) \\ &\quad + K_{k+1}^b \{Z_{N-k-1} - H \underline{X}^b(T-\tau_{k+1} | T-\tau_k)\} \dots \dots (3.34) \end{aligned}$$

$$\begin{aligned} P^b(T-\tau_{k+1} | T-\tau_{k+1}) &= \{I - K_{k+1}^b H\} P^b(T-\tau_{k+1} | T-\tau_k) \\ &\quad \{I - K_{k+1}^b H\}^T + K_{k+1}^b R_{N-k-1} K_{k+1}^{bT} \dots \dots (3.35) \end{aligned}$$

in which

b = superscript denoting values of  $\underline{X}$ , P, and K associated with the backward (LKF) filter

$\tau_k$  = backward time variable defined by:



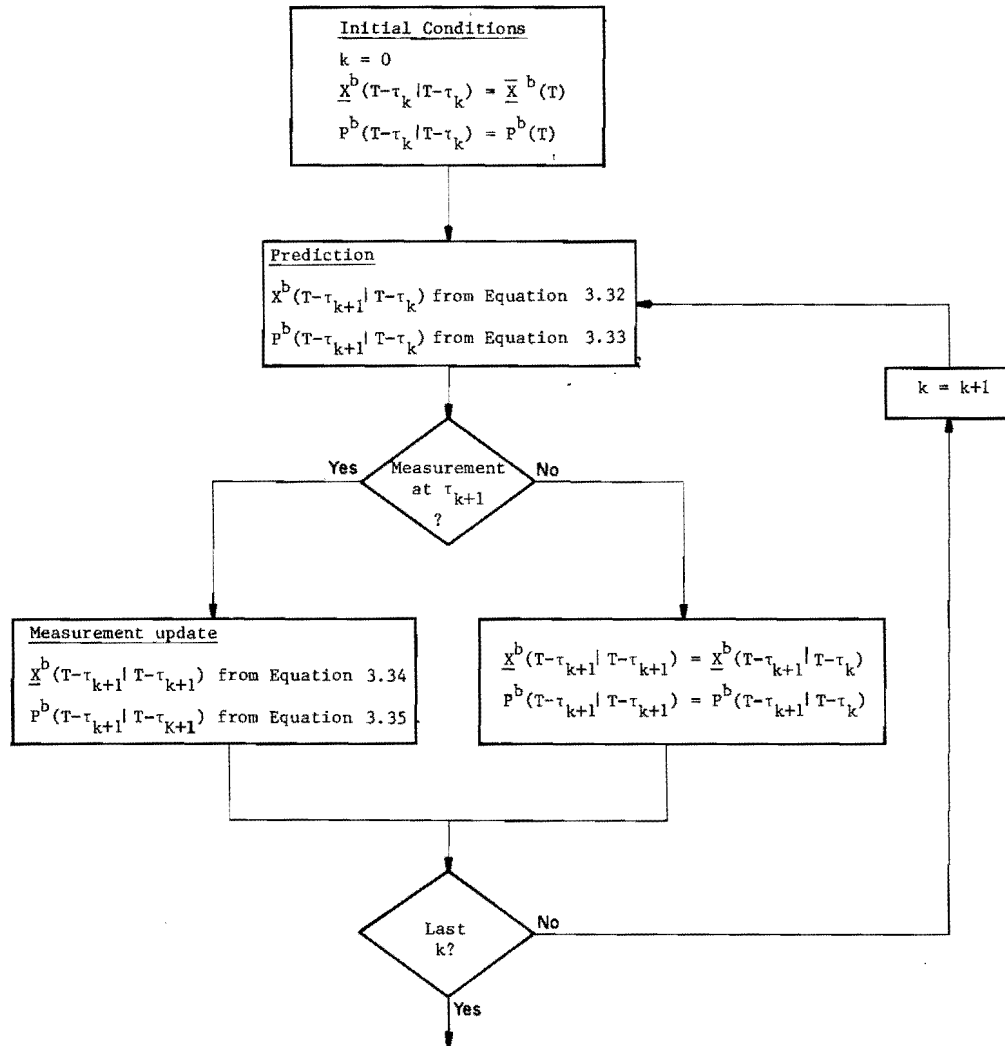


Figure 3.2. Flow diagram for the backward linearized Kalman filter algorithm.

### Sequential Kalman Filters

Several previous applications of the Kalman filter to river water quality have incorporated dynamic process models. Conventional dynamic river water quality models are formulated in terms of two independent variables, space and time. However, estimation theory techniques are developed for only a single independent variable. To circumvent this problem it is necessary to define a new state vector component of order  $n$  for each of the  $r$  reaches of the river. Thus, a dynamic filter model of  $n$  water quality parameters applied to a river divided into  $r$  reaches would result in a total state vector of order  $nr$ . As the spatial resolution is improved, or in the case of large river systems dynamic filter models can have large state vectors and therefore, very high computer costs (Moore, 1973).

In Chapter 2 it was observed that many of the previous applications of estimation theory to river water quality problems have been demonstrated using synthetic, rather than real data. The reason for this is the dearth of water quality data suitable for verifying dynamic water quality models. It may also be due, in part, to the desire of researchers to determine how close filter estimates come to the true state of the system. This may be readily shown using synthetic data since the true system states are known before they are imbedded in the generated noise.

In this study, real data from the Jordan River, Utah were used. The water quality data were collected for use in a steady-state deterministic river water quality simulation model. Therefore, these data were collected at a time when flow conditions in the Jordan River were approximately steady-state. It was decided to use a steady-state process model



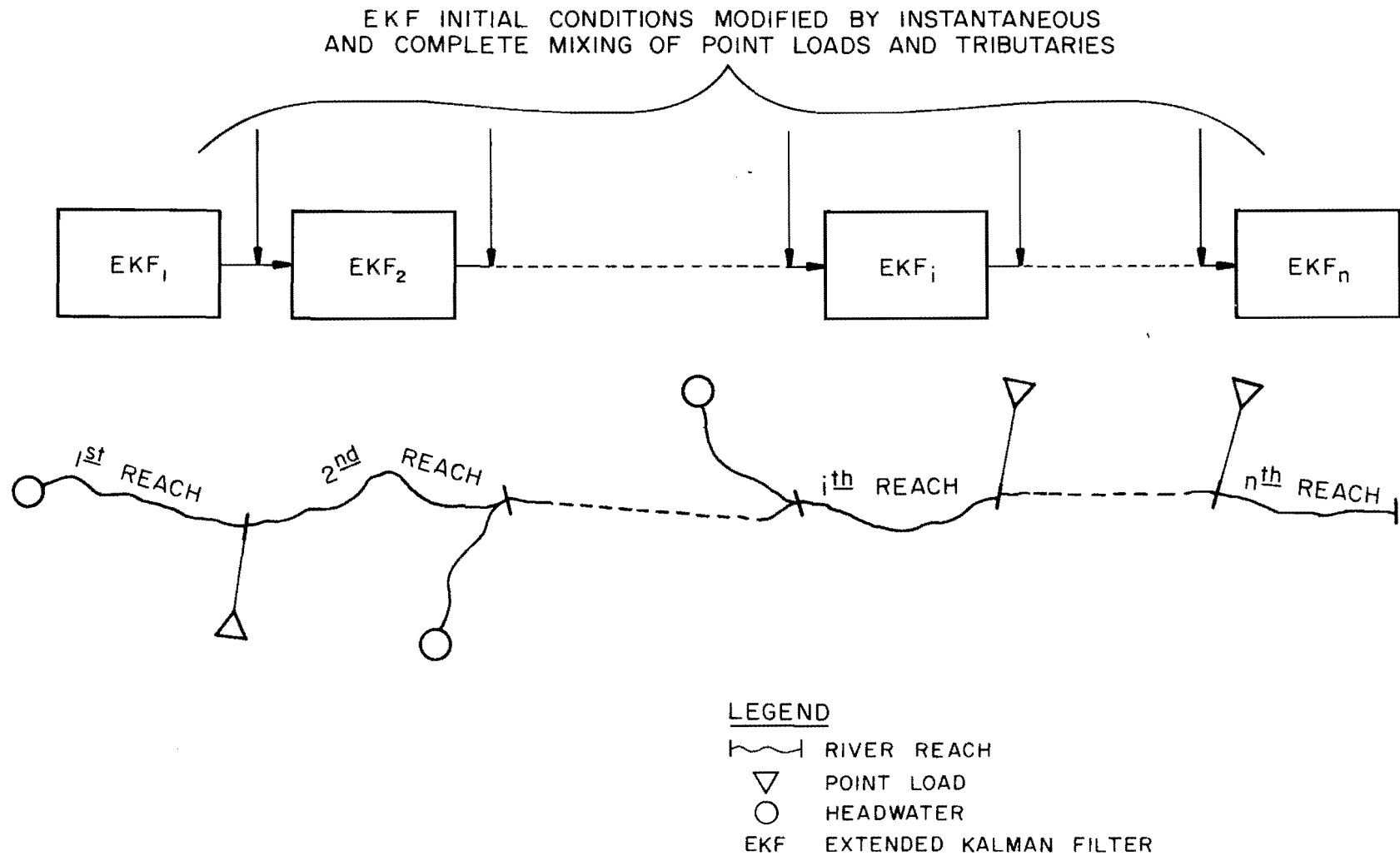


Figure 3.3. Sequential application of extended Kalman filters to a hypothetical river system.



- $k_2$  = dilution factor for the point load =  $s_p / (S_u + s_p)$   
(dimensionless)
- $\underline{X}_d$  = state estimate immediately downstream of the reach junction  
(mg/l)
- $\underline{X}_u$  = state estimate immediately upstream of the reach junction  
(mg/l)
- $S_u$  = streamflow immediately upstream of the reach junction (cfs)
- $s_p$  = flowrate of the point load or tributary (cfs)
- $\underline{1}_p$  = n-vector of concentrations of the parameters in the point  
load or tributary (mg/l)

To modify the estimation error covariance matrix (P) it was assumed that the steady-state concentrations of the parameters in the point load or tributary are normally distributed random variables, that is:

$$\underline{1}_p \sim N(\bar{\underline{1}}_p, Y) \quad \dots \dots \dots (3.41)$$

in which

- $\bar{\underline{1}}_p$  = mean value of  $\underline{1}_p$  (mg/l)
- $Y$  = nxn estimation error covariance matrix of the water quality  
parameter concentrations in point load (mg/l)<sup>2</sup>

Noting that  $\underline{X}_d$  is a linear function of  $\underline{X}_u$  and  $\underline{1}_p$ , and assuming that  $\underline{X}_u$  and  $\underline{1}_p$  are stochastically independent, the estimation error covariance matrix is modified using the following relationship which is based on a theorem in Hogg and Craig (1970):

$$P_d = k_1^2 P_u + k_2^2 Y \quad \dots \dots \dots (3.42)$$

in which

- $P_d$  = estimation error covariance matrix P immediately downstream  
of reach junction (mg/l)<sup>2</sup>



consistent with the objective of the study and resulted in a time step of 0.02 days (28.8 minutes). To improve the spatial resolution of the model a smaller value of  $\Delta t$  would be necessary.

#### Computational Aspects

The EKF, LKF, and FIS algorithms described above were programmed in FORTRAN computer language for the Burroughs B6700 computer located on the campus of Utah State University. In addition to tabular line printer output, the filter results were dumped onto punched cards via a data sort-int program, PRSORT. Results contained on these cards were plotted on a plotter which is linked to the EAI Pacer computer at the Utah Water Research Laboratory. The relationships between the computer programs developed for this study are illustrated in Figure 3.4. Appendix A contains a users manual for the programs and includes flow charts, input instructions, and program listings.

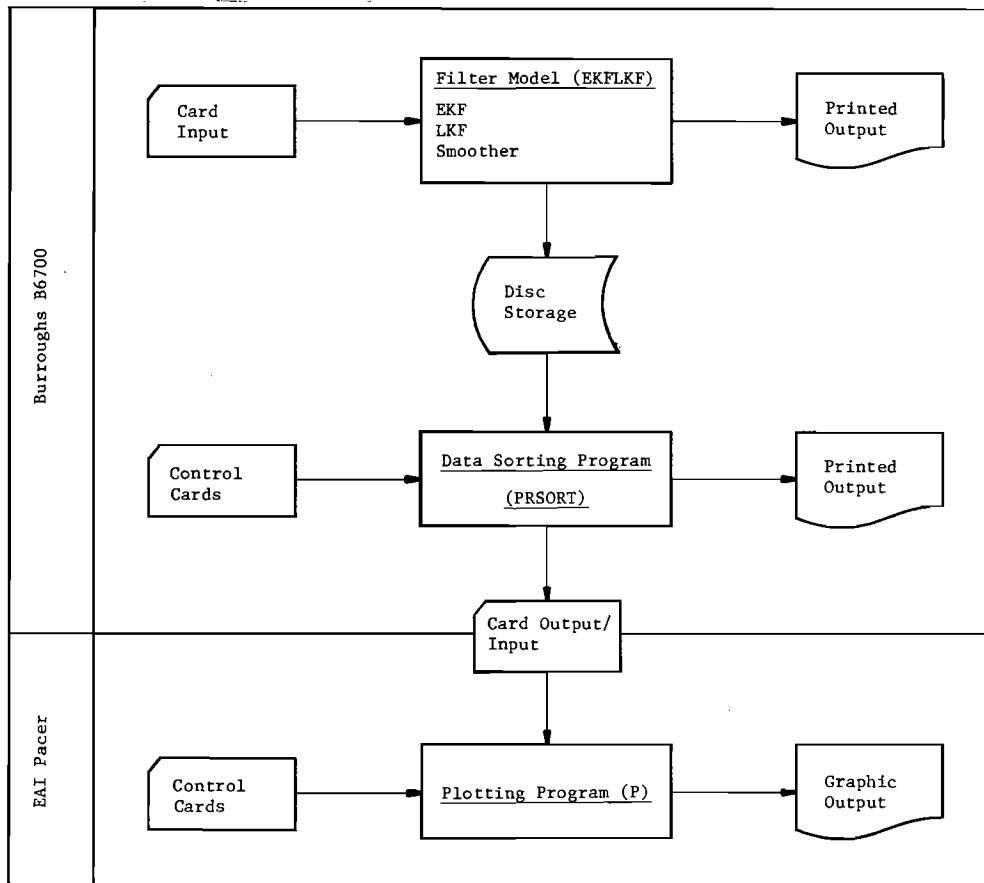


Figure 3.4. Relationships between the computer programs developed for this study.

## CHAPTER 4

## APPLICATION TO THE JORDAN RIVER

Introduction

One of the initial tasks in this study was to find a river for which sufficient water quality and hydraulic data are available to facilitate the application of estimation theory techniques to water quality simulation. Since BOD-DO models dominate the water quality modeling literature, including previous applications of estimation theory to water quality modeling (see Chapter 2), it was hoped that data for parameters other than, but possibly including BOD-DO, would be available. After an extensive search of published data the Jordan River in the north-central region of Utah was selected. Water quality data were derived from water samples collected by Hydrosience, Inc. (1976). Samples were obtained over a 24 hour period on September 24 and 25, 1975, and cover the lower 39.2 miles (63.1 km) of the river.

This chapter contains descriptions of the lower Jordan River Basin, the process model, and the measurement model. Also included are details of other aspects of the problem set-up such as point load concentrations, lateral inflow loadings, and initial conditions.

Description of the Lower Jordan River Basin

The Jordan River is a small but significant river originating as regulated outflow from Utah Lake shown in Figure 4.1. It flows for approximately 55 miles (88 km) through a variety of land use areas before discharging into the marshy zones at the southeastern end of the Great Salt Lake. The lower 40 miles (64 km) which are of interest in this study,

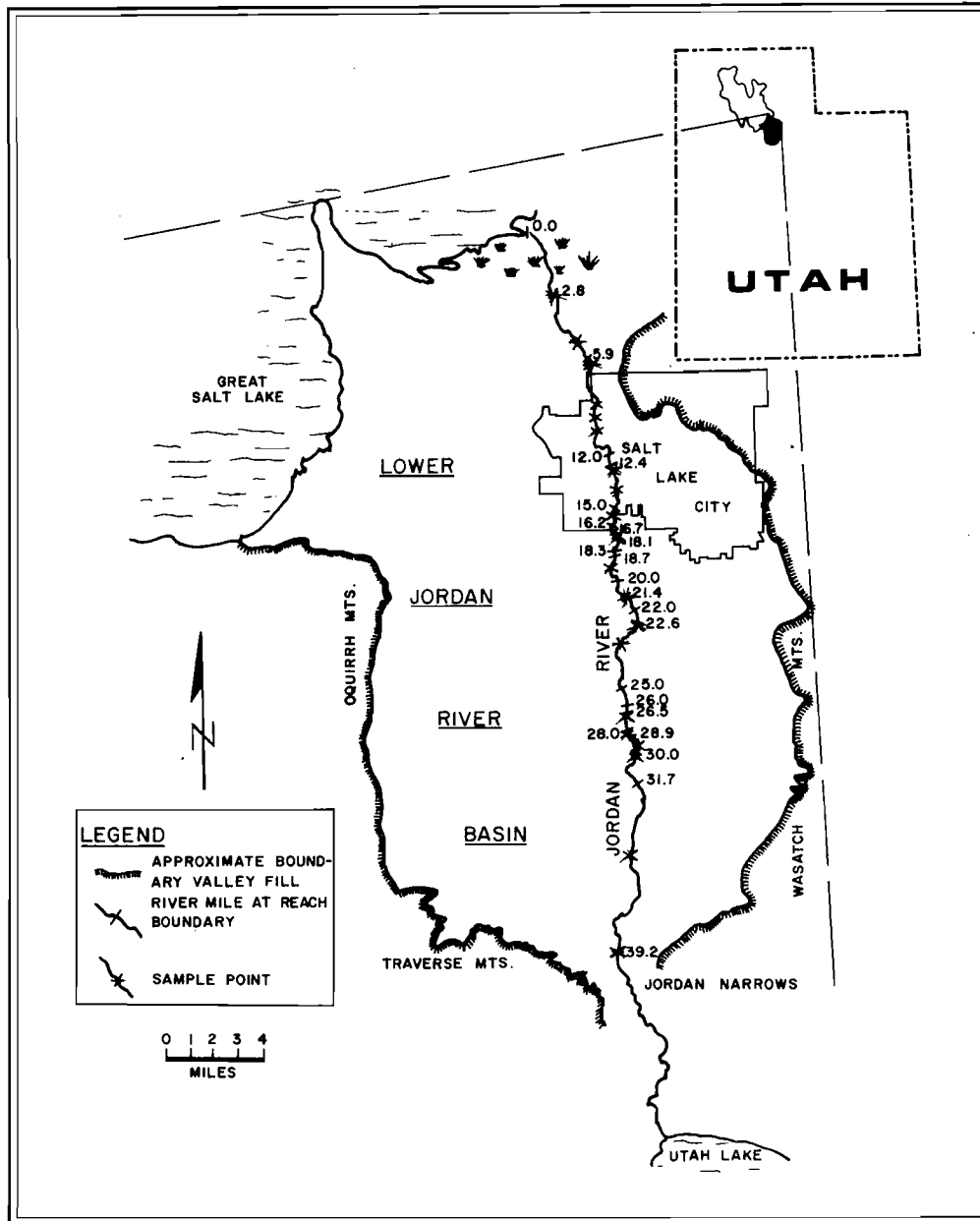


Figure 4.1. Map of the Lower Jordan River Basin (adapted from Harr et al., 1971) (1 mile = 1.61 km).

pass through a valley area which is flanked by the Wasatch Mountains to the east, the Oquirrh Range to the west, and the Traverse Mountains to the south. Elevations range from 4,200 feet (1,300 m) on the valley floor to more than 10,000 feet (3,000 m) in the surrounding mountains. The valley floor delineated in Figure 4.1 is approximately 500 square miles (1,300 km<sup>2</sup>) in area.

A number of irrigation canals divert water from the river at the Jordan Narrows for use in agricultural areas in the western and southwestern parts of the valley. Within the study area flow in the river is supplemented by several streams originating on the Wasatch Front.

Dixon et al. (1975) identified three major land use divisions along the river:

1. Upper agricultural reaches - mainly agricultural pasture land and small satellite communities south of Salt Lake City.
2. Industrial and urban areas - within and adjacent to Salt Lake City.
3. Lower agricultural reaches - north of Salt Lake County.

Associated with these land uses are a variety of economic activities. Salt Lake County is a major economic center with a number of important industries. The largest of these is Kennecott Copper Corporation located on the west side of the valley in the Oquirrh Mountains. Other major industries include several sand and gravel operations, refinery operations, dairies, several slaughter houses, and a smelter operation. Despite a trend toward residential development, agriculture is still a prominent activity in the area. Varieties of crops grown include wheat, vegetables, and fruits.

The river is important in that it provides: (1) water for municipal and industrial use, (2) irrigation water in a valley already importing water, (3) essential water for waterfowl management areas, (4) a convenient storm

and wastewater drainage system for the Jordan Valley, and (5) a potential recreational resource (Dixon et al., 1975). Eight municipal wastewater treatment plants and numerous urban stormwater drains, with perennial flow, discharge into the lower forty miles of the river. These loads, combined with diffuse inflow from agriculture and other sources, significantly degrade the water quality in this section of the river.

The Kalman filter model was applied to the lower 39.2 miles (63.1 km) of the Jordan River for which data were available. The river was divided into reaches with fairly uniform diffuse loading characteristics. Reach boundaries were partly determined by three major land use divisions along the river. Additional reach boundaries were necessary immediately downstream of point loads. Reach boundaries and sampling point locations are shown in Figure 4.1.

#### Process Model

A process model was formulated to describe biochemical oxygen demand, dissolved oxygen, and nitrogen cycling within the Jordan River. The six water quality parameters simulated by the model are listed below:

- $X_1$  = Carbonaceous biochemical oxygen demand (BOD) (mg/l)
- $X_2$  = Ammonia nitrogen ( $\text{NH}_3\text{-N}$ ) (mg/l)
- $X_3$  = Nitrate nitrogen ( $\text{NO}_3\text{-N}$ ) (mg/l)
- $X_4$  = Algae (ALG-N) (mg/l)
- $X_5$  = Organic nitrogen (ORG-N) (mg/l)
- $X_6$  = Dissolved oxygen (DO) (mg/l)

On the basis of data collected on the Jordan River nitrite-nitrogen ( $\text{NO}_2\text{-N}$ ) is negligible. Phosphorus measurements indicated that it was probably not the limiting nutrient in algal growth. It was, therefore, decided



that algal growth could be represented without including phosphorus in the model. ORG-N excludes viable algae which are represented by ALG-N.

Figure 4.2 shows the biochemical transformations and diffuse loads described by the process model equations. The nitrogen cycle is represented by four transformations: oxidation of  $\text{NH}_3\text{-N}$  to  $\text{NO}_3\text{-N}$ , uptake of  $\text{NH}_3\text{-N}$  and  $\text{NO}_3\text{-N}$  by algae, ALG-N becoming ORG-N as a result of the death of algae, and hydrolysis of ORG-N to  $\text{NH}_3\text{-N}$ . It is assumed that the production of  $\text{NH}_3\text{-N}$  during BOD decay is negligible.

Utilization of DO during nitrification and by the organic deposits on the stream bottom and during BOD decay are modeled. The impact on DO levels of photosynthesis and respiration by algae is not represented. This is justified because net  $\text{O}_2$  production is relatively small due to the highly turbid nature of the Jordan River which significantly increases the extinction of light entering the river. An additional reason for omitting the interaction of algae with DO is the dynamic nature of the photosynthetic and respiratory processes; they are diurnal processes, and thus could not be represented by the steady-state process model.

The one-dimensional transport equation given below forms the basis for the process model:

$$\frac{\partial AX}{\partial t} = - \frac{\partial SX}{\partial x} + \frac{\partial \left( DA \frac{\partial X}{\partial x} \right)}{\partial x} + 16.364q U + AJ - \frac{Bw}{28.317} \cdot \cdot \cdot \cdot (4.1)$$

in which

- X = concentration of the water quality parameter (mg/l)
- A = cross sectional area of the stream ( $\text{ft}^2$ )
- t = time (days)
- S = streamflow rate ( $\text{ft}^3/\text{day}$ )
- x = distance along the longitudinal stream axis (ft)

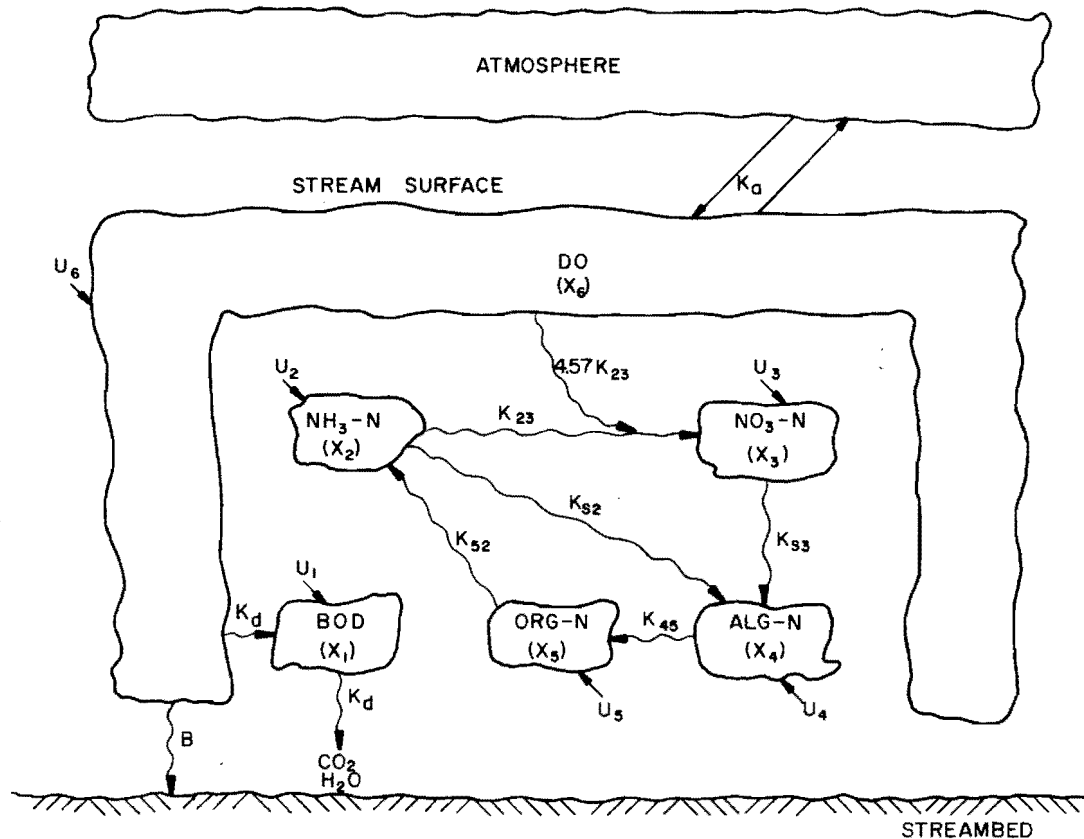


Figure 4.2. Schematic diagram of the water quality parameters, biochemical transformations, and non-point loads represented by the process model.



The final form of the basic process model equation is obtained by changing the independent variable in Equation 4.2 from distance downstream, to travel time, using the following relationship:

$$dx = v d\xi = \frac{S}{A} d\xi \quad \dots \quad (4.4)$$

in which

$$\xi = \text{travel time ranging from 0 to } E \text{ (days)}$$

and by assuming that:

$$h = \frac{A}{w} \quad \dots \quad (4.5)$$

in which

$$h = \text{stream depth averaged over the cross section (ft)}$$

Substituting Equations 4.4 and 4.5 into Equation 4.2 we obtain the following expression:

$$\frac{dX}{d\xi} = \frac{16.364q (U - X)}{A} - \frac{B}{28.317h} + J \quad \dots \quad (4.6)$$

The deterministic part of the process model is obtained by writing an equation in the form of Equation 4.6 for each of the six water quality parameters. These equations, modified by the addition of the process noise vector  $\omega$ , are contained in Figure 4.3, and are described in detail below. The matrix equation given in Figure 4.3 has the form of Equation 3.19. Linear first-order kinetics are assumed for all reactions except the uptake of  $\text{NH}_3\text{-N}$  and  $\text{NO}_3\text{-N}$  by algae which is represented by nonlinear saturation kinetics. It should be remembered that  $\underline{X}$  now represents the derivative of  $\underline{X}$  with respect to travel time ( $\xi$ ) and not standard time ( $t$ ). The Jacobian matrix,  $F(\cdot)$ , of  $\underline{f}(\cdot)$  in the process model is contained in Figure 4.4.

$$\begin{array}{l}
 \text{BOD} \\
 \text{NH}_3\text{-N} \\
 \text{NO}_3\text{-N} \\
 \text{ALG-N} \\
 \text{ORG-N} \\
 \text{DO}
 \end{array}
 \begin{array}{l}
 \dot{X}_1 \\
 \dot{X}_2 \\
 \dot{X}_3 \\
 \dot{X}_4 \\
 \dot{X}_5 \\
 \dot{X}_6
 \end{array}
 =
 \begin{array}{l}
 \left[ \frac{16.364 q (U_1 - X_1)}{A} - K_d X_1 \right. \\
 \left. \frac{16.364 q (U_2 - X_2)}{A} + K_{52} X_5 - K_{23} X_2 - \left( \frac{\gamma X_2}{\gamma X_2 + X_3} \right) \hat{\mu} \left( \frac{\beta X_2 + X_3}{K_{S3} + \beta X_2 + X_3} \right) X_4 \right. \\
 \left. \frac{16.364 q (U_3 - X_3)}{A} + K_{23} X_2 - \left( 1 - \frac{\gamma X_2}{\gamma X_2 + X_3} \right) \hat{\mu} \left( \frac{\beta X_2 + X_3}{K_{S3} + \beta X_2 + X_3} \right) X_4 \right. \\
 \left. \frac{16.364 q (U_4 - X_4)}{A} - K_{45} X_4 + \hat{\mu} \left( \frac{\beta X_2 + X_3}{K_{S3} + \beta X_2 + X_3} \right) X_4 \right. \\
 \left. \frac{16.364 q (U_5 - X_5)}{A} + K_{45} X_4 - K_{52} X_5 \right. \\
 \left. \frac{16.364 q (U_6 - X_6)}{A} + \frac{B_6}{28.317 \text{ h}} + K_a (X_{6\text{sat}} - X_6) - K_d X_1 - 4.57 K_{23} X_2 \right]
 \end{array}
 +
 \begin{array}{l}
 \omega_1 \\
 \omega_2 \\
 \omega_3 \\
 \omega_4 \\
 \omega_5 \\
 \omega_6
 \end{array}$$

Figure 4.3. Process model equations,  $\dot{\underline{X}} = \underline{f} [\underline{X}(\xi), \underline{U}(\xi); \xi] + \underline{\omega}(\xi)$ .

$-K_d - \frac{16.364 q}{A}$	0	0	0	0	0
0	$-\frac{K_{23} - \frac{16.364 q}{A}}{\hat{\mu} \gamma X_4}$ $\frac{(\gamma X_2 + X_3)^2 (K_{S3} + \beta X_2 + X_3)^2}{* [K_{S3} \beta X_2 (\gamma X_2 + X_3) + X_3 (K_{S3} + \beta X_2 + X_3) * (\beta X_2 + X_3)]}$	$\frac{\hat{\mu} \gamma X_2 X_4}{(\gamma X_2 + X_3)^2 (K_{S3} + \beta X_2 + X_3)^2}$ $* [K_{S3} (\gamma X_2 + X_3) + (K_{S3} + \beta X_2 + X_3) * (\beta X_2 + X_3)]$	$\left[ \frac{\gamma X_2}{\gamma X_2 + X_3} \right] \hat{\mu} \left[ \frac{\beta X_2 + X_3}{K_{S3} + \beta X_2 + X_3} \right]$	$K_{S2}$	0
0	$K_{23}$ $-\frac{\hat{\mu} X_3 X_4}{(\gamma X_2 + X_3)^2 (K_{S3} + \beta X_2 + X_3)^2}$ $* [K_{S3} \beta (\gamma X_2 + X_3) - \gamma (K_{S3} + \beta X_2 + X_3) * (\beta X_2 + X_3)]$	$-\frac{16.364 q}{A}$ $\frac{\hat{\mu} X_4}{(\gamma X_2 + X_3)^2 (K_{S3} + \beta X_2 + X_3)^2}$ $* [K_{S3} X_3 (\gamma X_2 + X_3) - \gamma X_2 (K_{S3} + \beta X_2 + X_3) * (\beta X_2 + X_3)]$	$\left[ \frac{X_3}{\gamma X_2 + X_3} \right] \hat{\mu} \left[ \frac{\beta X_2 + X_3}{K_{S3} + \beta X_2 + X_3} \right]$	0	0
0	$\frac{K_{S3} \hat{\mu} \beta X_4}{(K_{S3} + \beta X_2 + X_3)^2}$	$\frac{K_{S3} \hat{\mu}}{(K_{S3} + \beta X_2 + X_3)^2}$	$-\frac{K_{45} - \frac{16.364 q}{A}}{+ \hat{\mu} \left[ \frac{\beta X_2 + X_3}{K_{S3} + \beta X_2 + X_3} \right]}$	0	0
0	0	0	$K_{45}$	$-\frac{K_{52} - \frac{16.364 q}{A}}$	0
$-K_d$	$-4.57 K_{23}$	0	0	0	$-\frac{K_a - \frac{16.364 q}{A}}$

Figure 4.4. Jacobian matrix,  $F[\underline{X}(\xi), \underline{U}(\xi); \xi]$ , for the process model.

### Biochemical oxygen demand

The rate of change of BOD is represented by first-order biochemical oxidation and contributions from diffuse sources in the following equation:

$$\frac{dX}{d\xi} = \frac{16.364q (U_1 - X_1)}{A} - K_d X_1 \quad \dots \quad (4.7)$$

in which

$X_1$  = concentration of BOD (mg/l)

$U_1$  = concentration of BOD in the lateral inflow (mg/l)

$K_d$  = BOD decay rate (base e, per day)

### Ammonia-nitrogen

Uptake of  $\text{NH}_3\text{-N}$  by algae and oxidation to  $\text{NO}_3\text{-N}$  tend to reduce concentrations of ammonia while hydrolysis of organic nitrogen to  $\text{NH}_3\text{-N}$  and contributions from diffuse sources tend to increase  $\text{NH}_3\text{-N}$  levels. These processes are represented by the following equation:

$$\frac{dX_2}{d\xi} = \frac{16.364q (U_2 - X_2)}{A} - K_{52}X_5 - K_{23}X_2 - u_2 \quad \dots \quad (4.8)$$

in which

$X_2$  = concentration of  $\text{NH}_3\text{-N}$  (mg/l)

$X_5$  = concentration of ORG-N (mg/l)

$U_2$  = concentration of  $\text{NH}_3\text{-N}$  in the lateral inflow (mg/l)

$K_{52}$  = rate of decomposition of ORG-N to  $\text{NH}_3\text{-N}$  (base e, per day)

$K_{23}$  = nitrification rate ( $\text{NH}_3\text{-N}$  to  $\text{NO}_3\text{-N}$ ) (base e, per day)

$u_2$  = uptake rate of  $\text{NH}_3\text{-N}$  by algae (mg/l-day)

### Nitrate-nitrogen

The rate of change in concentration of  $\text{NO}_3\text{-N}$  is influenced by the accumulation of oxidized ammonia, uptake by algae, and contributions from diffuse sources. The following equation represents these processes:

$$\frac{dX_3}{d\xi} = \frac{16.364q (U_3 - X_3)}{A} + K_{23}X_2 - u_3 \quad \dots \quad (4.9)$$

in which

- $X_3$  = concentration of  $\text{NO}_3\text{-N}$  (mg/l)
- $U_3$  = concentration of  $\text{NO}_3\text{-N}$  in the lateral inflow (mg/l)
- $u_3$  = uptake rate of  $\text{NO}_3\text{-N}$  by algae (mg/l-day)

### Algae

The process model simulates the effects of phytoplankton on the other water quality parameters. These effects include the uptake of nitrogen, by algae, and the recycling of nitrogen contained in the algal cells to  $\text{NH}_3\text{-N}$  via the algae death process. Rate changes of concentrations of algae are represented by:

$$\frac{dX_4}{d\xi} = \frac{16.364q (U_4 - X_4)}{A} - K_{45}X_4 + u \quad \dots \quad (4.10)$$

in which

- $X_4$  = concentration of ALG-N (mg/l)
- $U_4$  = concentration of ALG-N in the lateral inflow (mg/l)
- $K_{45}$  = algal death rate (ALG-N to ORG-N) (base e, per day)
- $u$  = uptake rate of  $\text{NH}_3\text{-N}$  and  $\text{NO}_3\text{-N}$  by algae (mg/l-day)

Uptake of nutrients by phytoplankton is usually described by a Michaelis-Menton type hyperbola. A modified form of nonlinear saturation



kinetics, proposed herein, is used to represent the uptake of nitrogen by algae:

$$u = \hat{\mu} \frac{\beta X_2 + X_3}{K_{S3} + \beta X_2 + X_3} X_4 \dots \dots \dots (4.11)$$

in which

$\hat{\mu}$  = maximum specific growth rate of algae (base e, per day)

$K_{S3}$  = half-saturation coefficient for  $\text{NO}_3\text{-N}$  (mg/l)

$\beta$  = ratio of half-saturation coefficient for  $\text{NO}_3\text{-N}$  to half-saturation coefficient for  $\text{NH}_3\text{-N}$  (approximately 2 according to Caperon and Meyer, 1972) (dimensionless)

There is no yield coefficient in Equation 4.11 because all the parameters are expressed as nitrogen. Temperature and light factors are included in  $\hat{\mu}$ . Nitrogen uptake by algae is divided between the  $\text{NH}_3$  and  $\text{NO}_3$  forms by a coefficient  $\alpha$  as follows:

$$u_2 = \alpha u \dots \dots \dots (4.12)$$

$$u_3 = (1 - \alpha) u \dots \dots \dots (4.13)$$

$$\alpha = \frac{\gamma X_2}{\gamma X_2 + X_3} \dots \dots \dots (4.14)$$

in which

$\alpha$  = coefficient to divide  $u$  into  $u_2$  and  $u_3$  (dimensionless)

$\gamma$  = weighting coefficient to indicate the preference of algae for  $\text{NH}_3\text{-N}$  over  $\text{NO}_3\text{-N}$  (set equal to 2) (dimensionless)

The justification for Equation 4.11 is intuitive and should be tested experimentally. As more nitrogen in either the ammonia or nitrate forms becomes available, then the rate at which nitrogen is taken up by algae increases. This nonlinear characteristic is well recognized and is represented by the conventional Michaelis-Menton equation. However, the role of  $\beta$  in Equation 4.11 is to represent the preference of algae for the

ammonia form of nitrogen over the nitrate form. This preference phenomenon results in the half-saturation coefficient for  $\text{NO}_3\text{-N}$ ,  $K_{S3}$ , being approximately double the half-saturation coefficient for  $\text{NH}_3\text{-N}$ ,  $K_{S2}$ . Equations 4.12 through 4.14 are merely a way of partitioning the total algal uptake of nitrogen into uptake of ammonia, and uptake of nitrate.

When  $\text{NH}_3\text{-N}$  ( $X_2$ ) is zero Equations 4.11 and 4.14 become:

$$u = \hat{u} \frac{X_3}{K_{S3} + X_3} X_4 \dots \dots \dots (4.11a)$$

$$\gamma = 0 \dots \dots \dots (4.14a)$$

When  $\text{NO}_3\text{-N}$  ( $X_3$ ) is zero Equations 4.11 and 4.14 become:

$$u = \hat{u} \frac{X_2}{K_{S2} + X_2} X_4 \dots \dots \dots (4.11b)$$

$$\gamma = 1 \dots \dots \dots (4.14b)$$

Thus in each of these limiting cases the proposed model reduces to the conventional Michaelis-Menton model. As  $X_2$  and  $X_3$  simultaneously approach zero,  $u$  approaches zero but  $\gamma$  is undefined. Therefore, care must be taken not to attain this situation during the simulation. In practice, it is unlikely to occur except when the initial conditions for  $X_2$  and  $X_3$  are both set equal to zero.

Equations 4.11 and 4.14 are illustrated in Figure 4.5 for different levels of  $\text{NH}_3\text{-N}$  and  $\text{NO}_3\text{-N}$ . Reference to Figure 4.5 shows that the proposed model yields the same values for total nitrogen uptake ( $u$ ) for each of the following different situations: (1)  $\text{NH}_3\text{-N} = 0.75$  mg/l,  $\text{NO}_3\text{-N} = 0.0$  mg/l; (2)  $\text{NH}_3\text{-N} = 0.0$  mg/l,  $\text{NO}_2\text{-N} = 1.5$  mg/l; and (3)  $\text{NH}_3\text{-N} = 0.62$  mg/l,  $\text{NO}_3\text{-N} = 0.25$  mg/l. The proportion ( $\alpha$ ) of  $\text{NH}_3\text{-N}$  uptake ( $u_2$ ) to total nitrogen uptake ( $u$ ) is different for each situation, as follows: (1)  $\alpha=1.0$ , (2)  $\alpha=0.0$ , and (3)  $\alpha=0.8$ .

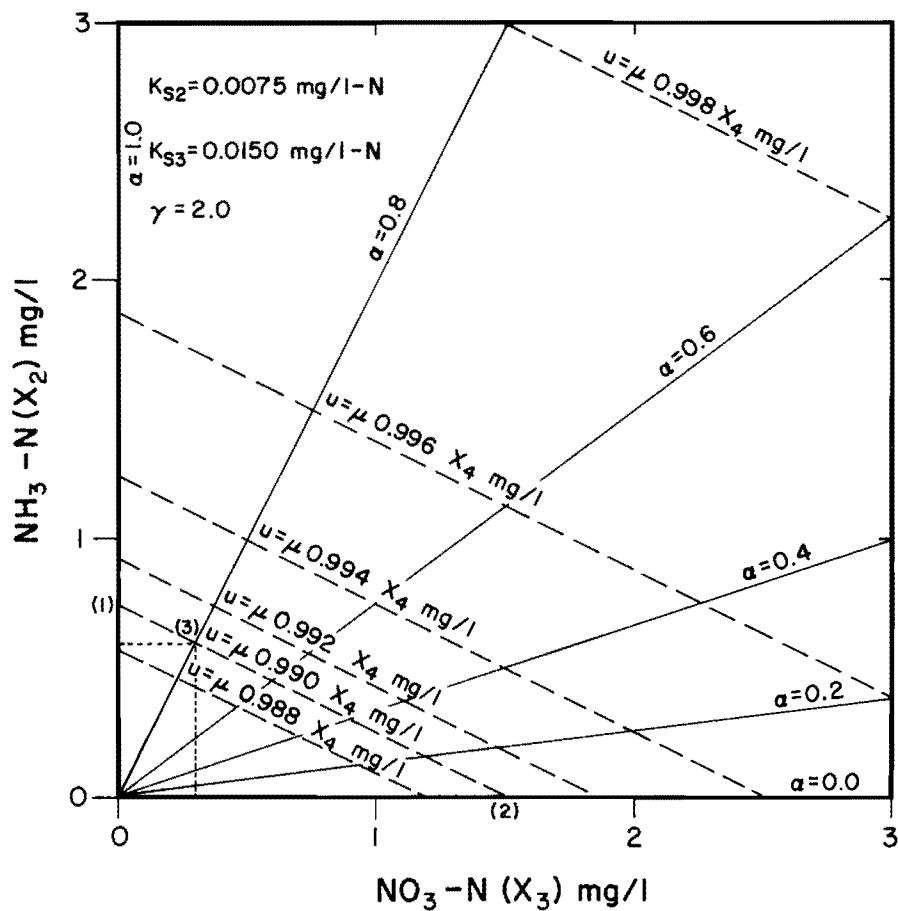


Figure 4.5. Graphic representation of Equations 4.11 and 4.14 describing the preferential uptake of nitrogen by algae.

### Organic nitrogen

The pool of organic nitrogen is fed by the death of algae and reduced by hydrolysis of ORG-N to  $\text{NH}_3\text{-N}$ . The rate of change of ORG-N with respect to travel time is simulated by the following equation:

$$\frac{dX_5}{d\xi} = \frac{16.364q (U_5 - X_5)}{A} + K_{45}X_4 - K_{52}X_5 \quad \dots \quad (4.15)$$

in which

$X_5$  = concentration of ORG-N (mg/l)

$U_5$  = concentration of ORG-N in the lateral inflow (mg/l)

### Dissolved oxygen

The dissolved oxygen content of a river is one of the most important water quality characteristics. It has minimum standards defined by law, is understood by the public, and is essential for oxygen consuming aquatic organisms. Concentrations of DO are affected by reaeration across the stream surface, carbonaceous oxygen demand, nitrogenous oxygen demand, uptake by the bottom deposits, and contributions from lateral inflow. The following expression is used to describe the rate change of DO in the Jordan River:

$$\frac{dX_6}{d\xi} = \frac{16.364q (U_6 - X_6)}{A} + \frac{B}{28.317h} + K_a(X_{6 \text{ sat}} - X_6) - K_d X_1 - 4.75K_{23}X_2 \quad \dots \quad (4.16)$$

in which

$X_6$  = concentration of DO (mg/l)

$U_6$  = concentration of DO in the lateral inflow (mg/l)



Simple flow budget calculations are used to calculate the change of streamflow in each  $\Delta x$  interval:

$$S_{out} = S_{in} + q v \Delta t \quad . . . . . (4.19)$$

in which

$$S_{out} = \text{streamflow out of the reach (cfs)}$$

$$S_{in} = \text{streamflow into the reach (cfs)}$$

At point loads or diversions streamflow is adjusted by the flow in the point load or diversion as follows:

$$S_d = S_u + s_p - s_d \quad . . . . . (4.20)$$

in which

$$s_d = \text{flowrate of diversion (cfs)}$$

Stream velocity is calculated using the following equation:

$$v = \frac{S}{A} \quad . . . . . (4.21)$$

Stream cross sectional area (A) and depth of streamflow (h) are given as known inputs for each reach. An initial value of streamflow is given at the upstream headwater. A flow balance for the Jordan River at the time of sampling was provided by Hydrosience, Inc. (personal communication, 1976).

#### Limitations of the process model

Schweppe (1973) states that filter performance is more sensitive to errors in the structure of the process model (and measurement model) than to errors in the uncertainty specifications (R, Q, and initial P matrices). In addition, to compensate for limitations in the process model, the value of Q is expected to increase as the quality of the process model decreases. For these reasons, some limitations of the process model are given below:

1. Removal of BOD by absorption and settling, and leaching of BOD from the bottom deposits are neglected.
2. Since  $\text{NO}_3\text{-N}$  is omitted, it is assumed that  $\text{NH}_3\text{-N}$  is the limiting form of nitrogen. Because first-order kinetics are used, the delay associated with the development of a population of nitrifying organisms is neglected. Bed contributions and leaching of nitrogen also are neglected.
3. The algae submodel fails when population changes resulted in either nitrogen fixation or phosphorus becoming the limiting nutrient.
4. Because of the data collection procedures used, the dynamic interactions between algae and DO due to photosynthesis and respiration are not represented in the current steady-state model.

#### Measurement Model

Formulation of the measurement model is determined by the functional relationships between the state variables and the measurement variables. The five measurement variables available in the Jordan River data are listed below:

$$\begin{aligned}
 Z_1 &= \text{BOD (mg/l)} \\
 Z_2 &= \text{NH}_3\text{-N (mg/l)} \\
 Z_3 &= \text{NO}_3\text{-N (mg/l)} \\
 Z_4 &= \text{ALG-N + ORG-N (mg/l)} \\
 Z_5 &= \text{DO (mg/l)}
 \end{aligned}$$

The very small amounts of nitrite measured in the system are lumped into the nitrate data.  $Z_4$  is actually a measurement of organic nitrogen which represents the sum of  $X_4$  (ALG-N) and  $X_5$  (ORG-N). Thus, the measurement model is given by the following expression with the form of Equation 3.21:

$$\begin{bmatrix} Z_1 \\ Z_2 \\ Z_3 \\ Z_4 \\ Z_5 \end{bmatrix} = \begin{bmatrix} 1 & 0 & 0 & 0 & 0 & 0 \\ 0 & 1 & 0 & 0 & 0 & 0 \\ 0 & 0 & 1 & 0 & 0 & 0 \\ 0 & 0 & 0 & 1 & 1 & 0 \\ 0 & 0 & 0 & 0 & 0 & 1 \end{bmatrix} \begin{bmatrix} X_1 \\ X_2 \\ X_3 \\ X_4 \\ X_5 \end{bmatrix} + \begin{bmatrix} v_1 \\ v_2 \\ v_3 \\ v_4 \\ v_5 \end{bmatrix} \quad . . . . . (4.22)$$

Equation 4.22 is an example of an incomplete measurement system since there are six state variables but only five measurement variables.

The values of variances on the diagonal of the measurement noise covariance matrix (R) are contained in Table 4.1. These values are consistent with values used in similar studies by Moore (1973) and Lettenmaier (1975). The measurement noise variances are assumed to represent errors in the accuracy of the analytical laboratory procedures, and sampling errors due to samples being unrepresentative of either the steady-state conditions, or the mean concentrations of constituents across the stream cross section. All off-diagonal elements of the R matrix, are assumed to be zero since no knowledge of the correlation between measurement errors for different variables is available. Although program capabilities permit the use of different R matrices at each sampling point, the same R matrix is used for each measurement. This approach is justified because there is no available evidence to indicate that R should be different for each measurement vector.

#### Point Loads and Lateral Inflows

Concentrations of the parameters in wastewater treatment plant (WWTP) effluents are based on typical values observed in the Lower Jordan River Valley. Parameter concentrations for other point loads and for lateral inflows are based on concentrations used in previous simulation studies on the Jordan River by Dixon et al. (1975) and by Hydrosience, Inc. (1976).



Table 4.1. Measurement noise variances (R) and initial estimation error variances ( $P(\xi_0)$  and  $P^b(\Xi)$ ) in  $(\text{mg/l})^2$ .

Parameters	Measurement Noise Variance	Initial Estimation Error Variance
BOD	1.00	1.00
NH <sub>3</sub> -N	0.01	0.01
NO <sub>3</sub> -N	0.04	0.04
ALG-N + ORG-N	0.25	-
DO	0.25	0.25
ALG-N	-	0.125
ORG-N	-	0.125

Both types of data are treated as known inputs to the process model. Table 4.2 lists the parameter concentrations for each type of point load and Table 4.3 contains the concentration of lateral inflows.

If point load parameter concentrations had been measured at the time of sampling, then the variances in the estimation error covariance matrix of point load parameter concentrations ( $Y$ ) could be set equal to the measurement error variances in  $R$ . Since point load parameter concentrations were based on typical values, measurement errors are not appropriate and, therefore, all elements of the  $Y$  matrix are set equal to zero. However, the effects of point load uncertainty on filter estimates ( $\underline{X}$ ) and on the estimation error covariance ( $P$ ) are shown by a sensitivity study on the diagonal elements of  $Y$ . The results of this sensitivity study are reported in Chapter 5.

#### Initial Conditions

Prior estimates of initial conditions, consisting of  $\bar{X}(\xi_0)$  and  $P(\xi_0)$ , were made at the upstream boundary located at river mile 39.2 (63.1 km). Measured values of the water quality parameters at river mile 39.2 (63.1 km) are used for  $\bar{X}(\xi_0)$ . The measurement noise variances are used for  $P(\xi_0)$  (see Table 4.1) implying that the initial conditions,  $\bar{X}(\xi_0)$  are known with the accuracy of the measurements. As a first approximation, the measurement noise associated with ALG-N + ORG-N was divided equally between ALG-N and ORG-N in  $P(\xi_0)$ . The covariances were neglected and hence the off-diagonal elements of  $P(\xi_0)$  were set equal to zero.

Table 4.2. Concentration of the parameters in point loads and tributaries in mg/l.

	BOD	NH <sub>3</sub> -N	NO <sub>3</sub> -N	ALG-N	ORG-N	DO
Wastewater treatment plant	60.0	12.0	5.0	0.0	0.0	3.95-6.0
Tributary	5.0	0.5	2.0	0.0	0.0	7.0
Agricultural return	10.0	1.0	2.0	0.0	0.0	7.9

Table 4.3. Concentration of the parameters in the lateral inflow and bottom deposits.

Diffuse Source	Parameter	Concentration	River Miles <sup>a</sup>
U <sub>1</sub>	BOD	8.0 mg/l	39.2-30.0
		12.0 mg/l	30.0-16.7
		50.0 mg/l	16.7-12.0
		0.0 mg/l	12.0- 2.8
U <sub>2</sub>	NH <sub>3</sub> -N	0.2 mg/l	39.2-31.7
		0.4 mg/l	31.7-30.0
		0.5 mg/l	30.0-28.9
		0.75 mg/l	28.9-12.0
		0.0 mg/l	12.0- 2.8
U <sub>3</sub>	NO <sub>3</sub> -N	1.5 mg/l	39.2-12.0
		0.0 mg/l	12.0- 2.8
U <sub>4</sub>	ALG-N	0.0 mg/l	39.2- 2.8
U <sub>5</sub>	ORG-N	0.0 mg/l	39.2- 2.8
U <sub>6</sub>	DO	7.3 mg/l	39.2-25.0
		7.6 mg/l	25.0-16.7
		7.5 mg/l	16.7- 2.8
B	BOD <sup>b</sup>	0.0 mg/ft <sup>2</sup> -day	39.2-16.7
		121.0 mg/ft <sup>2</sup> -day	16.7- 2.8

<sup>a</sup>1 mile = 1.61 km

<sup>b</sup>1 mg/ft<sup>2</sup>-day = 0.092 mg/m<sup>2</sup>-day

## CHAPTER 5

## RESULTS

Introduction

In this chapter the results from the application of estimation theory to the Jordan River are presented and discussed. The computer runs are broken into three groups:

1. Basic runs.
2. Sensitivity runs.
3. Coefficient estimation runs.

Brief descriptions of the individual runs performed in each of these groups are contained in Table 5.1. After a section in which the calibration of the deterministic process model is presented, the technique adopted for obtaining suitable values for the variances in the process model noise covariance matrix ( $Q$ ) is described. The following sections contain the results and discussion of results for: the filter run, the smoothing algorithm run, several sensitivity studies, and some coefficient estimation runs. An example of filter divergence is included in one of the coefficient estimation runs. In the final section of this chapter the computational requirements of the estimation theory techniques applied are summarized.

Calibration of the Deterministic  
Process Model

Values for the reaction rates and coefficients in the process model were approximated from values reported in the literature. These values were refined through a trial-and-error calibration procedure in which the process model was run as a separate deterministic model without the measurement update

Table 5.1. Key to the computer runs.

Run Group	Run <sup>a</sup>	Description
Basic	2	Calibration of the deterministic process model
	8	Application of the extended Kalman filters
	10	Application of the smoothing algorithm
Sensitivity	11	Sensitivity on the process model noise variance for NH <sub>3</sub> -N
	12	Sensitivity on the initial estimation error variance for NO <sub>3</sub> -N
	13	Sensitivity on the measurement noise variance for (ALG-N + ORG-N)
	14	Sensitivity on the measurement noise variance for NH <sub>3</sub> -N
	19 } 20 }	Sensitivity on the estimation error variance for the point load at river mile 31.7 (51.0 km)
Coefficient Estimation	15	Coefficient estimation for K <sub>23</sub>
	16	Coefficient estimation for K <sub>45</sub>
	17	Lateral inflow concentration estimation for NO <sub>3</sub> -N
	18	Lateral inflow concentration estimation for NH <sub>3</sub> -N
	21	Coefficient estimation for the nitrogen cycle coefficients (K <sub>23</sub> , K <sub>45</sub> , K <sub>52</sub> , $\hat{\mu}$ , and K <sub>S3</sub> )

<sup>a</sup>Runs 1, 3-7, 9 and many other unidentified runs are not described in this report. These runs were performed during the course of finalizing the runs that are present herein.

and estimation error covariance propagation steps. Final values for each of the reaction rates and model coefficients are contained in Table 5.2. These values were used for the subsequent Kalman filter runs. A possible criticism of the use of the data for calibrating the process model is that the predictions from the process model are now dependent on the data, and hence are not independent estimates of the system state. However, there is no alternative since only one set of data are available.

The difference of the two orders of magnitude between the calibration value of the half-saturation coefficient for  $\text{NO}_3\text{-N}$ , ( $K_{S3}=0.015$  mg/l), and the combined level of  $\text{NH}_3\text{-N}$  ( $X_2$ ) and  $\text{NO}_3\text{-N}$  ( $X_3$ ) in the Jordan river (0.0 - 2.5 mg/l), indicates that saturation kinetics for algae ( $X_4$ ) are unnecessary in this application. This is clearly illustrated by reference to Equation 4.11 which tends toward a linear function in  $X_4$  when  $(X_2 + X_3) \gg K_{S3}$ . However, the algae submodel was left in the general nonlinear form for this study.

Results from the calibration of the deterministic process model (run 2) are given in Figures 5.1 through 5.7. The model was run between river mile 39.2 (63.1 km) and river mile 2.8 (4.5 km), the locations of the extreme upstream and downstream sampling sites. Below river mile 2.8 (4.5 km) the river enters a marshy area where the total flow divides into many channels. Abrupt changes in the concentration profiles are due to the complete and instantaneous mixing of point loads. Measured values are indicated by "x" symbols. A fairly good agreement between model predictions and measured values is indicated for each of the water quality parameters in Figures 5.1 through 5.7.

The BOD profile rises sharply just below river mile 30.0 (48.3 km). Thereafter high levels of BOD are maintained by wastewater treatment plant

Table 5.2. Reaction rates and model coefficients from the calibration of the deterministic process model.

Symbol	Units	Value	River miles <sup>a</sup>
$K_d$	base e, per day	0.7	39.2-2.8
$K_{23}$	base e, per day	0.3	
$K_{S3}$	mg/l-N	0.015	
$K_{45}$	base e, per day	0.04	
$K_{52}$	base e, per day	0.1	
$X_{6sat}$	mg/l- $O_2$	7.9	
$\beta$	dimensionless	2.0	39.2-16.7
$\gamma$	dimensionless	2.0	
$\hat{\mu}$	base e, per day	{ 3.0 1.5	16.7- 2.8

<sup>a</sup> 1 mile = 1.61 km

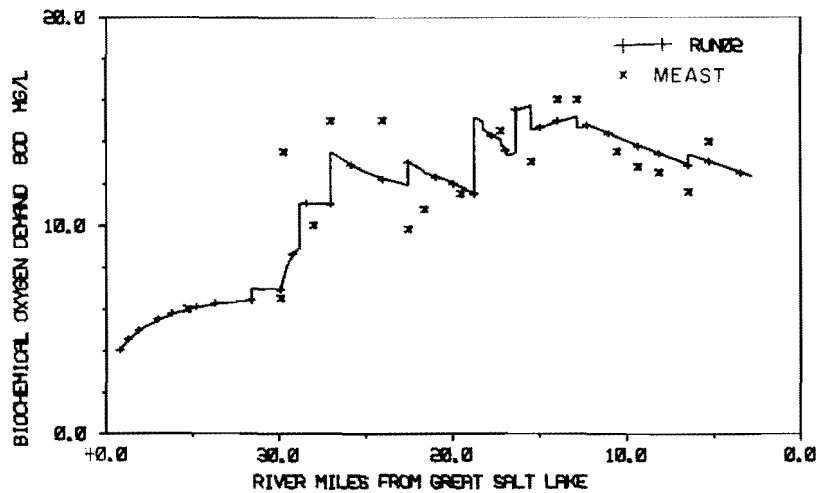


Figure 5.1. Measured and predicted values of BOD - deterministic process model calibration (1 mile = 1.61 km).

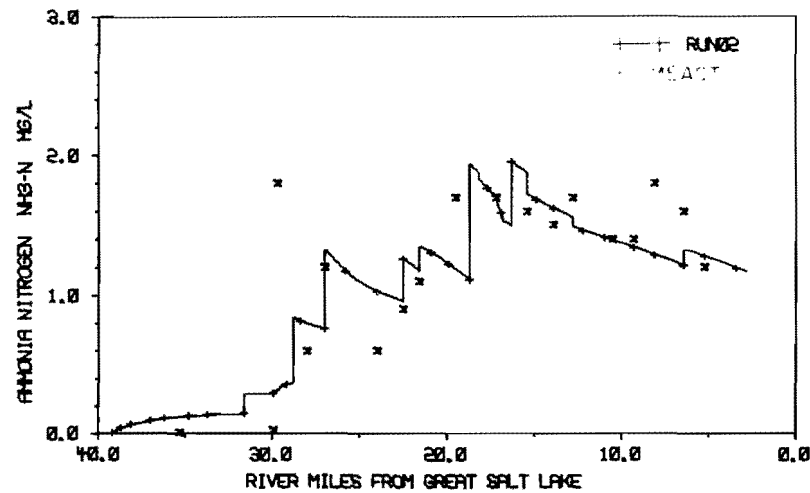


Figure 5.3. Measured and predicted values of  $\text{NH}_3\text{-N}$  - deterministic process model calibration (1 mile = 1.61 km).

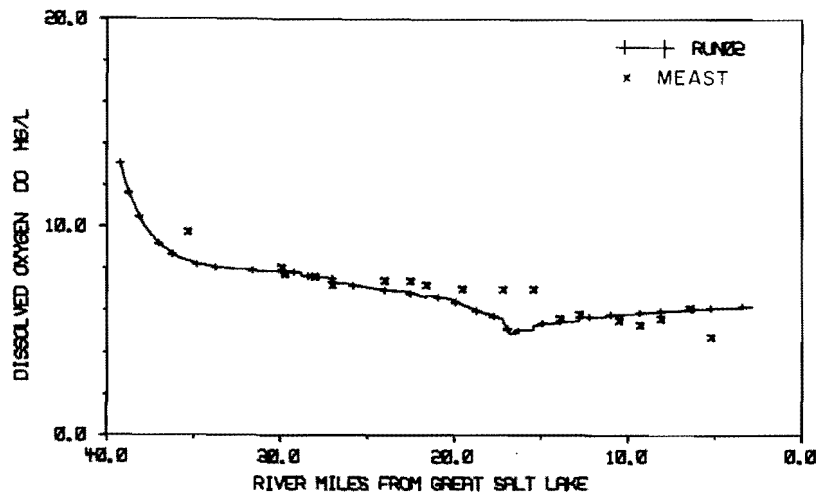


Figure 5.2. Measured and predicted values of DO - deterministic process model calibration (1 mile = 1.61 km).

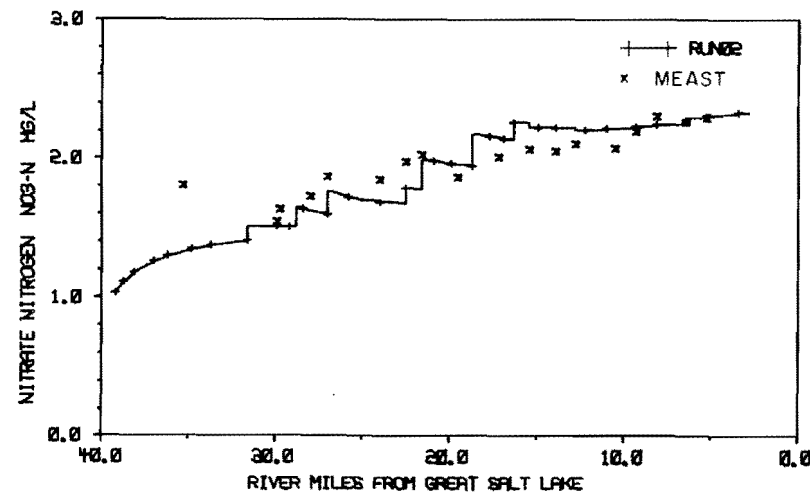


Figure 5.4. Measured and predicted values of  $\text{NO}_3\text{-N}$  - deterministic process model calibration (1 mile = 1.61 km).



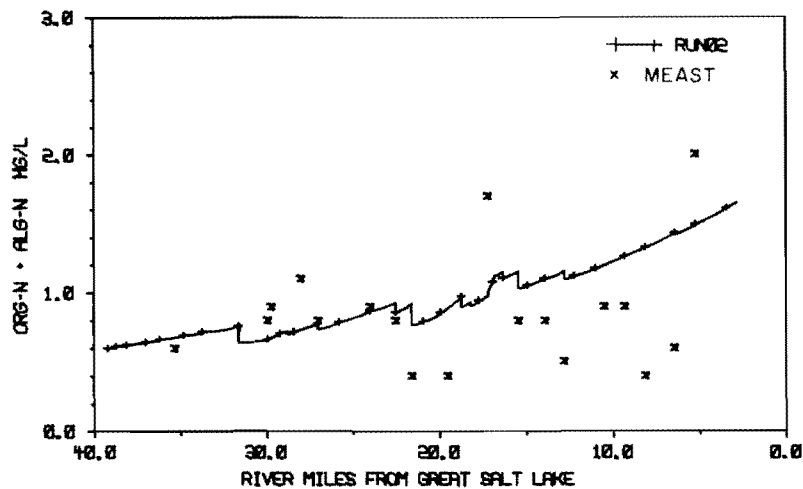


Figure 5.5. Measured and predicted values of (ORG-N + ALG-N) - deterministic process model calibration (1 mile = 1.61 km).

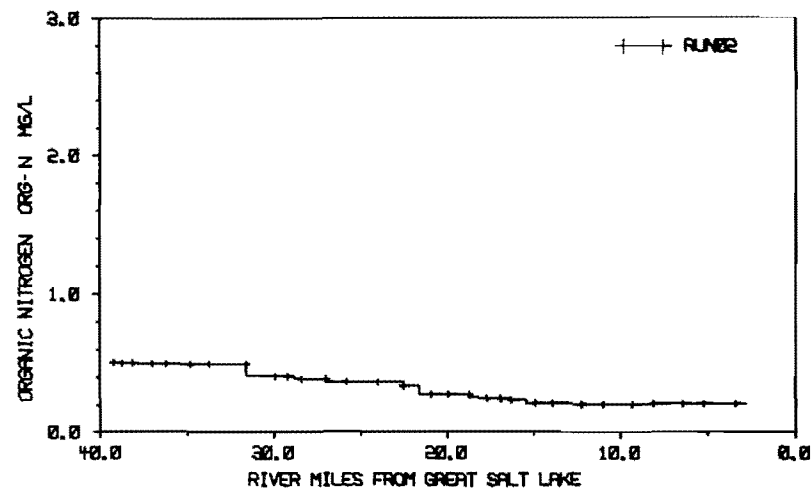


Figure 5.7. Measured and predicted values of ORG-N - deterministic process model calibration (1 mile = 1.61 km).

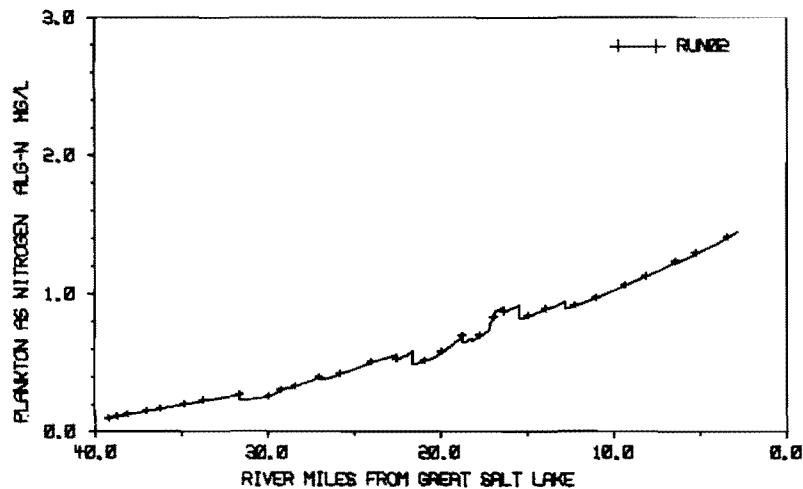


Figure 5.6. Measured and predicted values of ALG-N - deterministic process model calibration (1 mile = 1.61 km).

(WWTP) effluents and lateral loading. Upstream DO levels are supersaturated but quickly return to the DO saturation of 7.9 mg/l. Subsequent variations in DO concentration can be attributed mainly to BOD, nitrification, and benthic demands offset by reaeration. Predicted DO levels fall slightly below measured values around river mile 20.0 (32.2 km); this may be due to under-estimates of the assumed level of DO in the tributaries and lateral inflow.

Variation in the  $\text{NH}_3\text{-N}$  profile is similar to the variation in the BOD profile due to similar loading patterns.  $\text{NO}_3\text{-N}$  levels steadily increase along the study reaches. Both  $\text{NH}_3\text{-N}$  and  $\text{NO}_3\text{-N}$  are influenced by the algal uptake of nitrogen.

Figure 5.5 shows the deterministic process model predictions for (ALG-N + ORG-N) compared with the measured values. Along the lower half of the study section a reduced maximum specific growth rate for algae was indicated by the observed values of (ALG-N + ORG-N) and by the nitrogen uptake predictions. The river becomes relatively deep, and turbid in this section. On this basis the maximum specific growth rate,  $\hat{\mu}$ , was halved below river mile 16.7 (26.9 km) (see Table 5.2). Figures 5.6 and 5.7 show the deterministic process model predictions for ALG-N and ORG-N, respectively. ALG-N and ORG-N were separated by simulating the algal death process. These results indicate that an increasing concentration of algae is associated with a decreasing concentration of organic nitrogen.

#### Determination of Process Model Noise Variances

The process model noise covariance matrix (Q) contributes to the calculation of the estimation error covariance matrix (P), and thereby,

to the weighting procedure by which filter estimates are obtained from a combination of measurement values and the latest prediction of state from the process model. If  $Q$  is too large, implying a high degree of uncertainty in the process model, the filter estimates will follow the measurements too closely. On the other hand if  $Q$  is too small, unrealistically optimistic values for  $P$  will result (see Equation 3.25). This in turn results in the decay of the Kalman gain matrix ( $K$ ) and thus the measurements are almost entirely ignored (see Equation 3.26). Under these circumstances measurement updating is ineffective and the filter estimates can diverge from the true state of the system.

According to Jazwinski (1969) the process model noise "is a fiction designed to account for system (process) model errors which are non-stationary and generally of rather low frequency." This statement would appear to indicate that the task of determining a  $Q$  matrix is a formidable task, and indeed it is. It appears that unlike  $R$ ,  $Q$  can rarely be established from experience. There are basically two approaches to obtaining  $Q$ , neither of which has a strong theoretical basis:

1. Trial-and-error.
2. Adaptive filtering.

The trial-and-error approach is used in this study and is described first. For completeness a brief discussion of the philosophy of adaptive filtering follows.

#### Trial-and-error approach

The basis of this approach is that  $Q$  should be selected such that the mean square error of the differences between the filter estimates and the actual states of the system is consistent with the measurement noise variance in the  $R$  matrix for each measured variable. When synthetic data are

used it is possible to calculate the true mean square error because the actual state of the system is known. However, in applications to real systems the actual state of the system is the subject of estimation, and is therefore, unknown. In such cases the mean square error of the differences between the filter estimates and the actual system states is approximated by the mean square error of the differences between the filter estimates and the measurements, and is calculated as follows:

$$\text{MSE}_i = \frac{1}{N-1} \sum_{k=1}^N \left[ z_{k,i} - X_i(t_k | t_k) \right]^2 \quad . . . . . (5.1)$$

in which

$i$  = subscript denoting the  $i$ th measurement variable

$\text{MSE}_i$  = mean square error between the difference of the filter estimates and the measurements for the  $i$ th measurement variable  $(\text{mg/l})^2$

The trial-and-error process used for determining  $Q$  in this study is summarized in Figure 5.8.  $R$  is estimated from the literature. In this study  $P(\xi_0)$  is set equal to  $R$  since the extreme upstream measurement vector is used as the initial condition,  $X(\xi_0)$ , of the upstream Kalman filter. An arbitrary initial value of  $Q$  is used for the first run of the filter model. Then, for each measurement variable, the calculated values in MSE are compared with the measurement noise variances in  $R$ . If  $\text{MSE}_i$  is less than the measurement noise variance for the  $i$ th measurement variable, the corresponding variance in  $Q$  is decreased. A decrease in  $Q$  will reduce the estimation error covariance ( $P$ ), give more weighting to the process model estimates, and thus increase  $\text{MSE}_i$ . If  $\text{MSE}_i$  is much greater than the measurement noise variance for the  $i$ th measurement variable, the corresponding variance in  $Q$  is increased. Consequently,  $P$  is increased, less weighting is

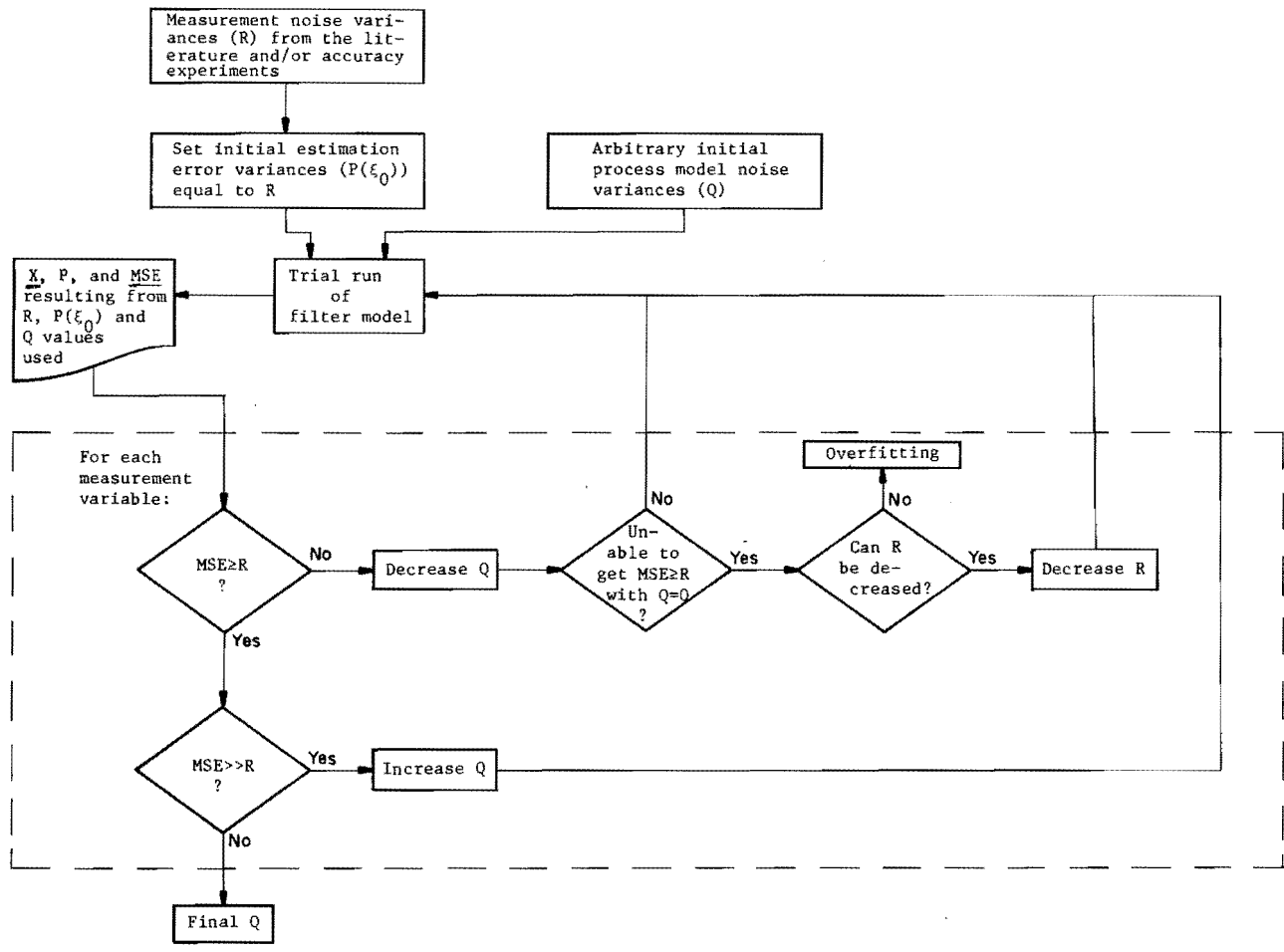


Figure 5.8 The trial-and-error approach for establishing the process model variances (Q).

given to the process model estimates, and hence  $MSE_i$  is reduced. The amount by which variances in  $Q$  must be changed is established by trial-and-error. Interaction between the variables complicates the procedure. For example, it will be shown later in this chapter that an increase in the process model noise variance for  $NH_3-N$  resulted in a decrease in the MSE for (ALG-N + ORG-N). No attempt was made to estimate values for the off-diagonal elements of the  $Q$  matrix.

If, by varying  $Q$ , it is not possible to increase  $MSE_i$  to the measurement noise variance for the  $i$ th measurement variable, then the value of the measurement noise variance should be reviewed. It may be that the measurement noise variance is too large for the data and, therefore, can be reduced. Another factor to consider is how good an estimate of the true MSE is the calculated MSE? It was observed that when the MSE was calculated for different sections of the river, the results varied by up to an order of magnitude.

A disadvantage of using the trial-and-error approach is that only a single value for  $Q$  is obtained. This value is used over the entire river system and may result in larger values of  $P$  in some reaches than would be obtained if  $Q$  were allowed to vary. The single value of  $Q$  is inevitably a compromise between different  $Q$  values that would be more satisfactory in particular reaches.

#### Adaptive filtering approach

Several different adaptive filtering procedures are described in the control and estimation theory literature. In contrast to the trial-and-error approach described above, adaptive filtering provides a mechanism for simultaneously estimating the  $Q$  matrix and the system states, based

on feedback from the residuals (Jazwinski, 1969; 1970). To give statistical significance to changes in  $Q$ , several measurements are processed, and the estimates smoothed, before  $Q$  is changed. The measurements are then reprocessed, thus introducing a lag time into real time estimation. To reduce the lag time short sequences of residuals are used. Therefore, the adaptive filter approach never "learns"  $Q$ . Jazwinski (1969) points out that this is a desirable feature because of the non-stationary and low frequency characteristics of process model noise.

A problem with adaptive filters is that a single large residual can result in a large value for  $Q$  which dies away slowly under the influence of smaller residuals. To avoid this problem Nahi and Schaeffer (1972) have designed a decision-directed adaptive filter. Their technique tests to determine the likelihood of a measurement coming from a distribution with the calculated estimation error covariance. On the basis of this test a decision is made as to whether or not to adjust  $Q$ .

Adaptive filtering is not used in this study because too few data are available on the Jordon River. In this situation the estimated values of  $Q$  would remain highly dependent on the initial values used for  $Q$  at the upstream boundary.

#### Results from the Extended Kalman Filter

Run 8 is the basic computer run using the final value of  $Q$  obtained from the trial-and-error procedure. Approximately twenty computer runs were necessary before an acceptable value for  $Q$  was found. Table 5.3 contains the final values of the variances in  $Q$ . Table 5.4 contains the mean square error of the differences between filter estimates and measurements for each measured parameter and for each computer run.

Table 5.3. Process model noise variances (Q) in  
(mg/l-day)<sup>2</sup>

Parameter	Variance
BOD	30.00
NH <sub>3</sub> -N	0.40
NO <sub>3</sub> -N	0.01
ALG-N	0.08
ORG-N	0.08
DO	0.10



Table 5.4. Mean square error of the difference between the filter estimates and the measured values in  $(\text{mg/l})^2$ .

Measurement Variable	Measurement Noise Variance	Mean Square Error (Filter ~ Measured) for Each Computer Run												
		Run 8	Run 10 <sup>a</sup>	Run 11	Run 12	Run 13	Run 14	Run 15	Run 16	Run 17	Run 18	Run 19	Run 20	Run 21 <sup>b</sup>
BOD	1.00	1.103	2.399 (0.536)	1.103	1.105	1.103	1.103	1.102	1.103	1.103	1.103	1.079	1.064	1.142
NH <sub>3</sub> -N	0.01	0.045	0.098 (0.022)	0.003	0.043	0.044	0.000 <sup>c</sup>	0.045	0.046	0.044	0.043	0.044	0.043	0.305
NO <sub>3</sub> -N	0.04	0.024	0.041 (0.009)	0.023	0.016	0.031	0.025	0.022	0.024	0.012	0.021	0.023	0.023	0.174
(ALG-N+ ORG-N)	0.25	0.258	0.222 (0.075)	0.225	0.018	0.038 <sup>d</sup>	0.189	0.304	0.256	0.125	0.218	0.219	0.208	7.524
DO	0.25	0.659	0.482 (0.063)	0.669	0.647	0.663	0.673	0.536	0.660	0.671	0.663	0.658	0.658	0.405

<sup>a</sup>These values were calculated over river miles 39.2 (63.1 km) to 19.4 (31.2 km). The values in parentheses are based on results from the smoothing algorithm which was applied over river miles 39.2 (63.1 km) to 19.4 (31.2 km).

<sup>b</sup>These values were calculated over river miles 39.2 (63.1 km) to 6.4 (10.3 km).

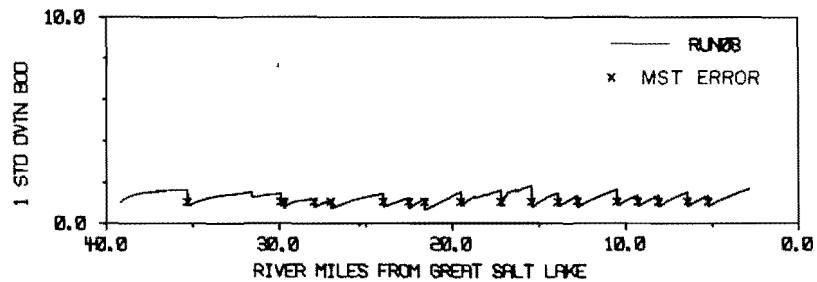
<sup>c</sup>MSE = 0.00000 and R for NH<sub>3</sub>-N in run 14 is 0.00001.

<sup>d</sup>R for (ALG-N + ORG-N) in run 13 is 0.01.

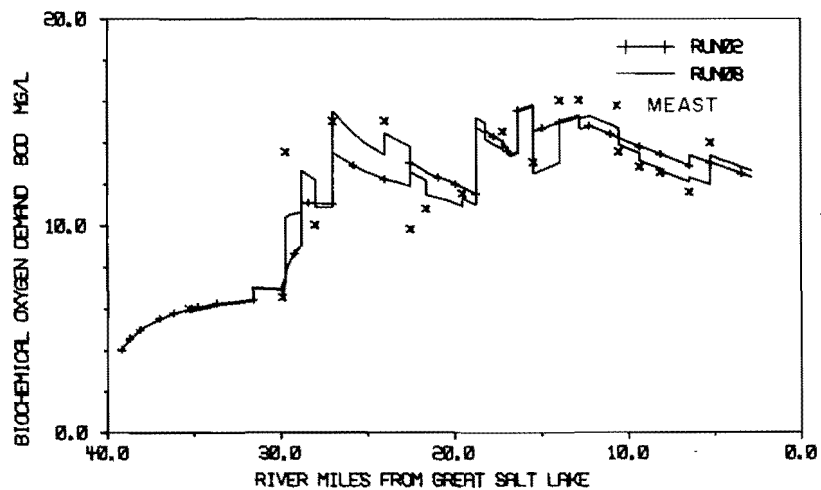
that, for run 8, the MSE is greater than the corresponding measurement variance for all the measured parameters except  $\text{NO}_3\text{-N}$ . Since all the available literature pointed to a measurement variance of about 0.04 for  $\text{NO}_3\text{-N}$ , it was not reduced below that value. When the process model variance for  $\text{NO}_3\text{-N}$  was reduced to zero the filter estimates of  $\text{ORG-N}$  became significantly negative. Therefore, as a compromise,  $Q$  for  $\text{NO}_3\text{-N}$  was set equal to 0.01, even though  $R$  remained greater than MSE for  $\text{NO}_3\text{-N}$ . This is an example of "over-fitting", in that the process model fits the data to within the accuracy of the data itself. The explanation for this case of over-fitting may be that the closeness of the filter estimates to the measurements is a chance occurrence that would not be expected if more sampling points were available.

Profiles representing one standard deviation of the estimation error variance are taken from the diagonal of the  $P$  matrix and are contained in the upper parts of Figures 5.9 through 5.15. Measurement noise variances are indicated by " $\chi$ " symbols at the one standard deviation level. Profiles representing the EKF estimate (conditional mean) of each of the state variables are contained in the lower parts of Figures 5.9 through 5.15. These figures also contain the results from run 2 to facilitate a comparison between the results from the purely deterministic process model and the results from the EKF. Measured values are indicated by " $\chi$ " symbols. (ALG-N + ORG-N) results in Figure 5.13 are obtained by adding the individual EKF estimates for ALG-N ( $X_4$ ) and ORG-N ( $X_5$ ). The following equation is used to calculate the estimation error of (ALG-N + ORG-N) (Hogg and Craig, 1970):

$$\sigma_{4+5} = (\sigma_4^2 + \sigma_5^2 + 2\gamma_{45})^{1/2} \quad . \quad . \quad . \quad . \quad . \quad . \quad . \quad . \quad (5.2)$$

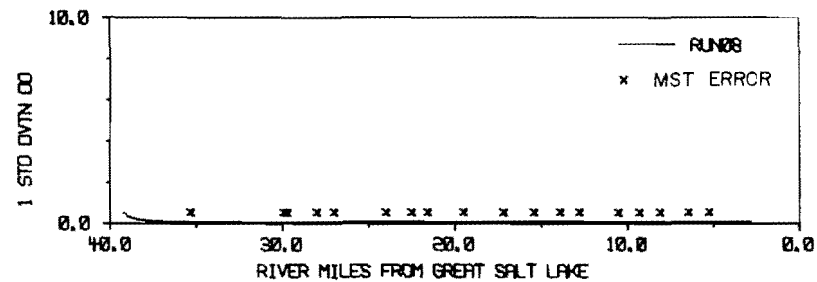


(a) Estimation and measurement errors

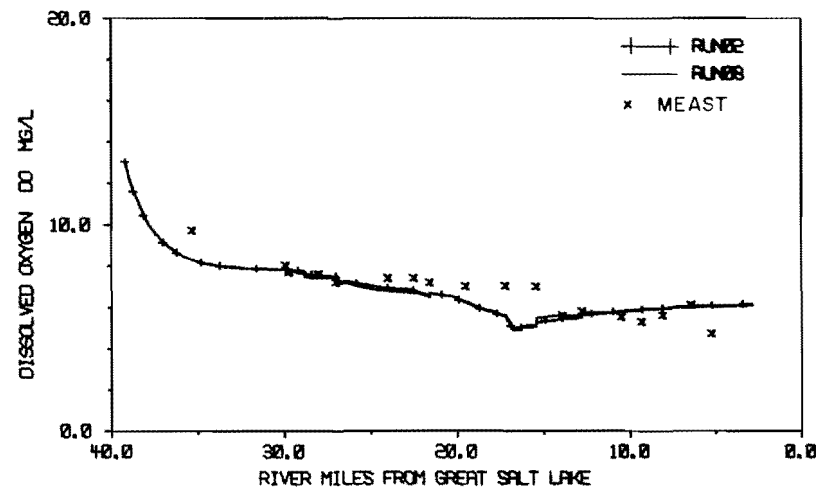


(b) Filter estimates and measured values

Figure 5.9. Basic EKF results for BOD (run 8) (1 mile = 1.61 km).

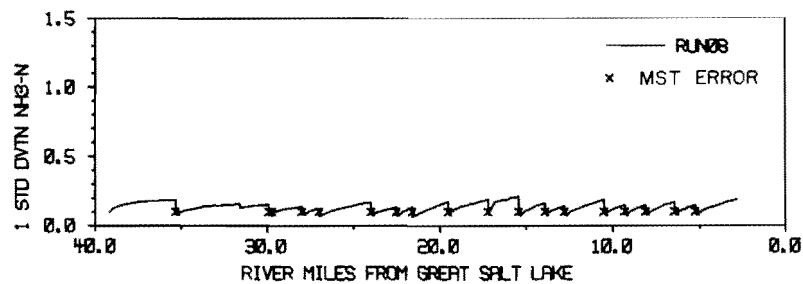


(a) Estimation and measurement errors

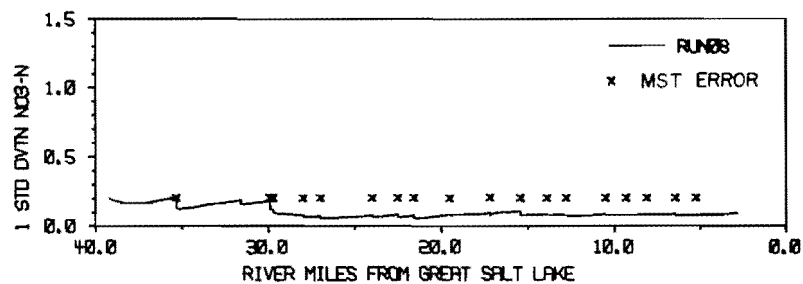


(b) Filter estimates and measured values

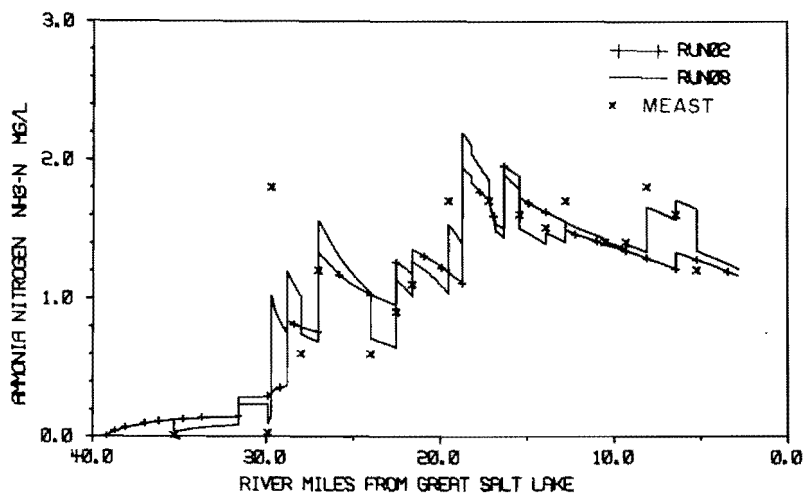
Figure 5.10. Basic EKF results for DO (run 8) (1 mile = 1.51 km).



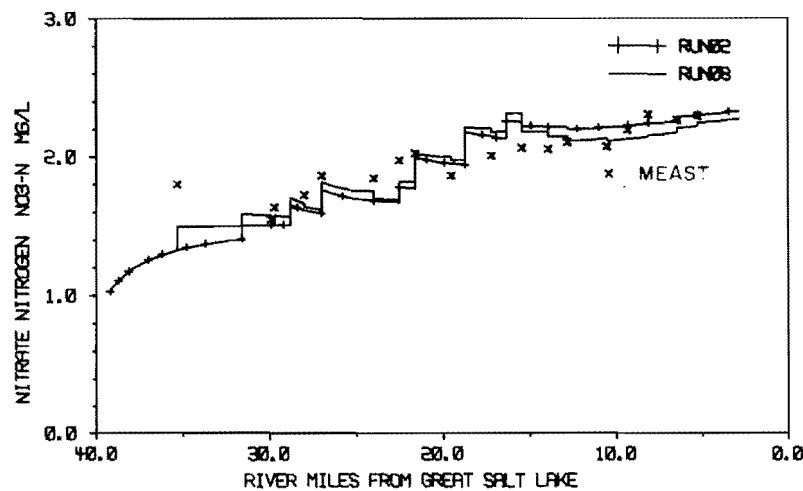
(a) Estimation and measurement errors



(a) Estimation and measurement errors



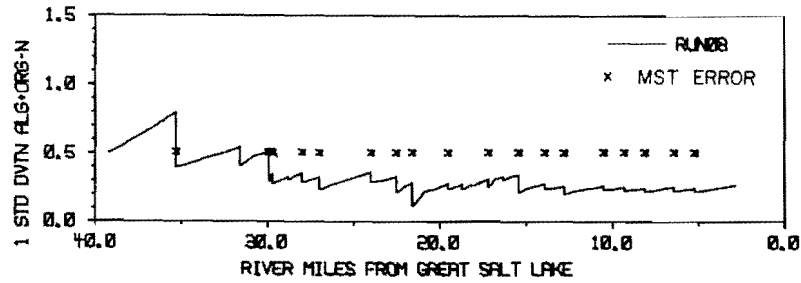
(b) Filter estimates and measured values



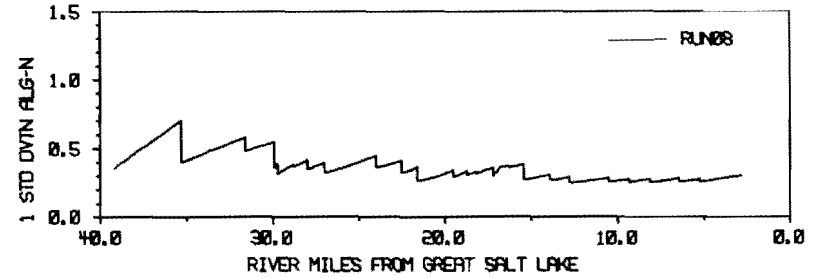
(b) Filter estimates and measured values

Figure 5.11. Basic EKF results for  $\text{NH}_3\text{-N}$  (run 8) (1 mile = 1.61 km).

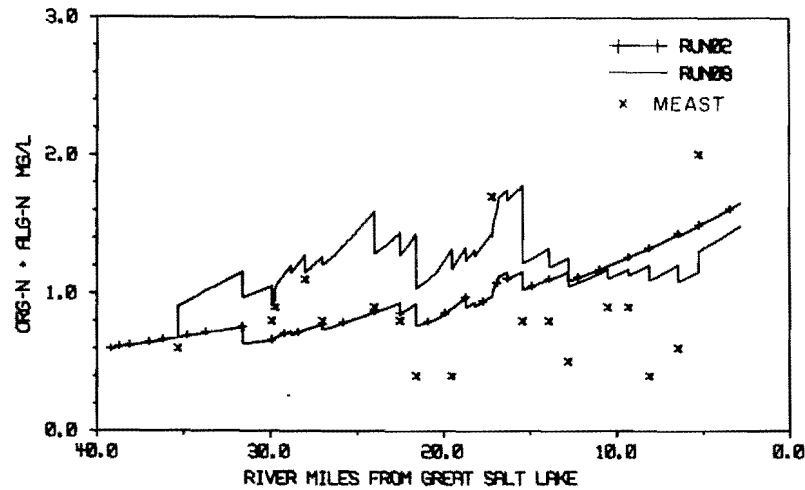
Figure 5.12. Basic EKF results for  $\text{NO}_3\text{-N}$  (run 8) (1 mile = 1.61 km).



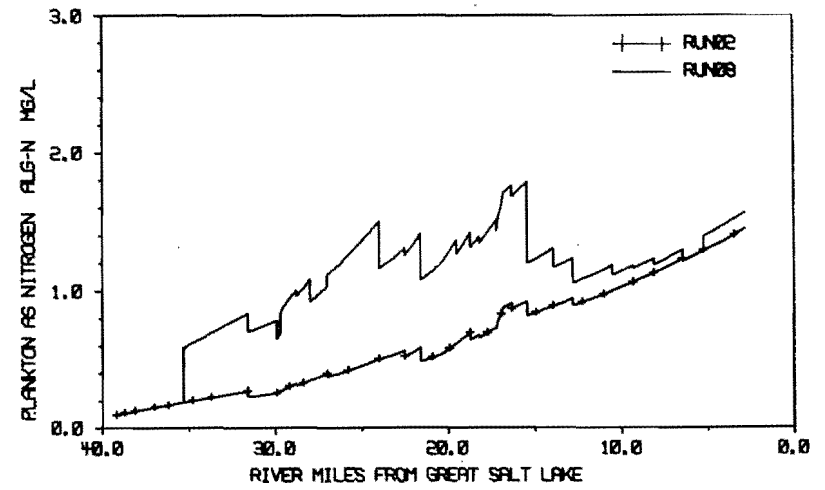
(a) Estimation and measurement errors



(a) Estimation and measurement errors



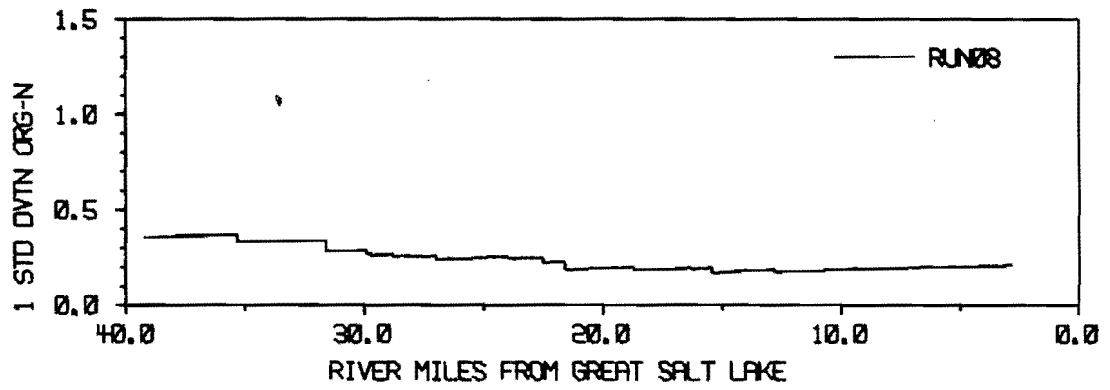
(b) Filter estimates and measured values



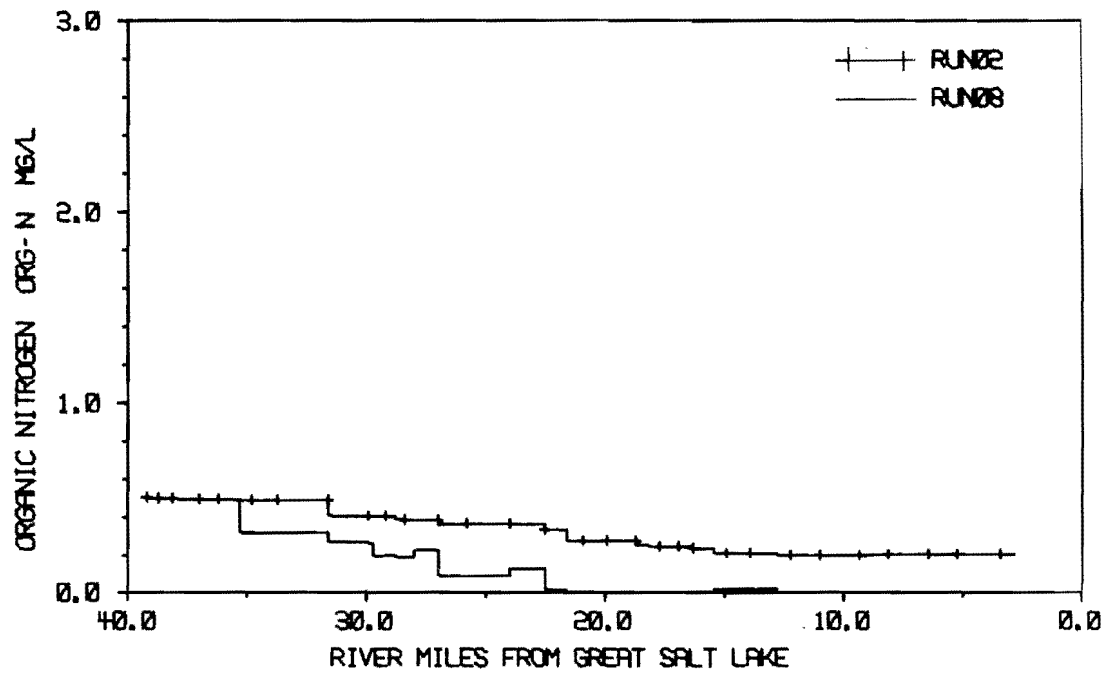
(b) Filter estimates and measured values

Figure 5.13. Basic EKF results for (ALG-N + ORG-N) (run 8) (1 mile = 1.61 km).

Figure 5.14. Basic EKF results for ALG-N (run 8) (1 mile = 1.61 km).



(a) Estimation and measurement errors



(b) Filter estimates and measured values

Figure 5.15. Basic EKF results for ORG-N  
(run 8) (1 mile = 1.61 km).

in which

$\sigma_{4+5}$  = one standard deviation for the estimation error variance of (ALG-N + ORG-N) (mg/l)

$\sigma_4^2$  = estimation error variance for ALG-N from the P matrix (mg/l)<sup>2</sup>

$\sigma_5^2$  = estimation error variance for ORG-N from the P matrix (mg/l)<sup>2</sup>

$\gamma_{45}$  = estimation error covariance for ALG-N and ORG-N from the P matrix (mg/l)<sup>2</sup>

The initial values of the estimation error shown in the upper plots are determined by the initial variances assigned to  $P(\xi_0)$ . Estimation errors then grow or decay in the downstream direction according to Equation 3.25. In the case of BOD (Figure 5.9), for example, the estimation grows, whereas for DO (Figure 5.10) the estimation error decays to almost zero. The growth or decay in P depends on the size of Q (see Table 5.3) and the signs on the elements of the Jacobian matrix, F (see Equation 3.25 and Figure 4.4). More specifically, an explanation for the decay of P for DO is that the reduction of DO concentrations is very well represented by the DO process model. Therefore, as estimation of DO proceeds downstream the confidence with which it can be said that DO approaches its saturation concentration, actually increases. In contrast the confidence associated with the estimates of other water quality parameters decrease with distance downstream from a measurement. This decrease in confidence, or increase in P, indicates that, for these parameters, the process model introduces uncertainty into the estimates as the distance downstream increases.

At river mile 35.1 (56.5 km), the location of the first sampling point, the estimation error drops abruptly to below the measurement error in accordance with Equation 3.27. This is an example of the "filtering result" whereby  $P(\xi_{k+1}|\xi_{k+1})$ , after the measurement update is less than either the measurement error, or the process model estimation error  $P(\xi_{k+1}|\xi_k)$  before the measurement update.

Between sampling points the estimation error grows or decays from the updated value of  $P$  at the nearest upstream sampling point. The evolution of  $P$  between sampling points is modified by the introduction of estimation error associated with point loads as described by Equation 3.42.

In this run the estimation error covariance matrix associated with point loads ( $Y$ ) is set equal to zero for each point load. An example of the impact of a point load on the estimation error is the small decrease in  $P$  at river mile 31.7 (51.0 km) between the first and second sampling points. In reality it is unreasonable to expect a decrease in  $P$  when a point load is added. A better representation would be for  $P$  to increase, which would require a non-zero  $Y$  matrix. If the point load parameter concentrations are measured at the time of sampling,  $Y$  could be set equal to the measurement noise variances ( $R$ ). In the absence of point load measurements  $Y$  may be determined by trial-and-error.  $Y$  should be varied until  $P$  is at least equal to, and preferably a little greater than its value immediately upstream of the point load. This approach would require several more computer runs after the  $Q$  matrix is established. The increase in  $P$  values brought about by the introduction of the point load estimation error will result in decreased values of MSE. There is a possibility that the new



MSE will be unacceptable and therefore necessitate further refinements of Q. Changes in Q may then require changes in Y and so the entire trial-and-error procedure for Q may be considerably lengthened by adding a trial-and-error determination of Y for each point load. To reduce computer costs in the present study it was decided not to estimate the Y matrices. Also it was decided that the assignment of arbitrary values to Y would be not better than having Y equal to zero. However, a sensitivity study described later in this chapter does illustrate the effect of a non-zero Y matrix.

A comparison of the deterministic process model predictions (run 2) and the EKF estimates (run 8) shows the effects of updating the process model predictions with information contained in the measurements. At sampling locations the EKF estimates change abruptly toward the measured value in accordance with Equation 3.26. The relative weight given to measurements and process model predictions to obtain the updated EKF estimate is determined by the relative values of R and  $P(\xi_{k+1} | \xi_k)$  respectively. It is interesting to note the effect on the size of measurement updating of the decreasing P value in the downstream direction for (ALG-N + ORG-N) (Figure 5.13). The residuals between measurements and filter predictions are greater downstream than upstream and yet the size of measurement updates of the filter estimate are approximately the same. This characteristic results because R remains constant while P decays, implying greater confidence in the process model predictions in the downstream reaches. At several locations a sampling point coincides with a point load with the result that the measurement update and instantaneous and complete mixing of the point load are superimposed on the profiles contained in the figures.

Because the filter estimates have been obtained to satisfy an approximate minimum variance criterion, an interpretation of every change in the profiles of EKF estimates in terms of the underlying physical processes or loading patterns, should be avoided. For example, one would not expect a discrete jump in the actual parameter concentration at a sampling location. This limitation will be somewhat modified by the application of a smoothing algorithm described in the next section.

In general, the differences between the filter estimates and deterministic predictions are relatively small. Greater differences between the deterministic and filter results would be expected if the filter had been run on a data set other than the one for which the process model was calibrated. However, the differences between the filter estimates and deterministic predictions for ALG-N and ORG-N do require some explanation (Figures 5.13 through 5.15). A relatively large measurement variance for (ALG-N + ORG-N) appears to be the underlying reason for the departure of EKF estimates from the measurements and the deterministic predictions. By considering the magnitude of the measurement noise, the deterministic predictions must be classed as a case of "over-fitting". ORG-N ( $X_5$ ) estimates became negative over several of the downstream reaches. Although this is clearly an undesirable feature in the case of constituent concentrations no effort was made to keep  $X_5$  non-negative since the worst negative estimate was quite small (about 0.1 mg/l).

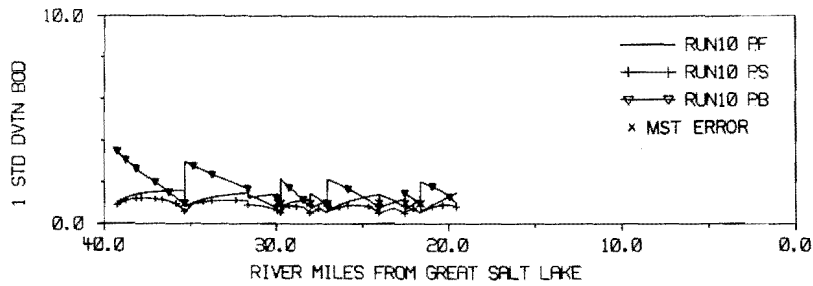
#### Results From the Smoothing Algorithm

By using the fixed-interval smoothing algorithm (FIS) all the measurements are used to estimate the state of the system at each location. In contrast only those measurements upstream of a location are used to estimate

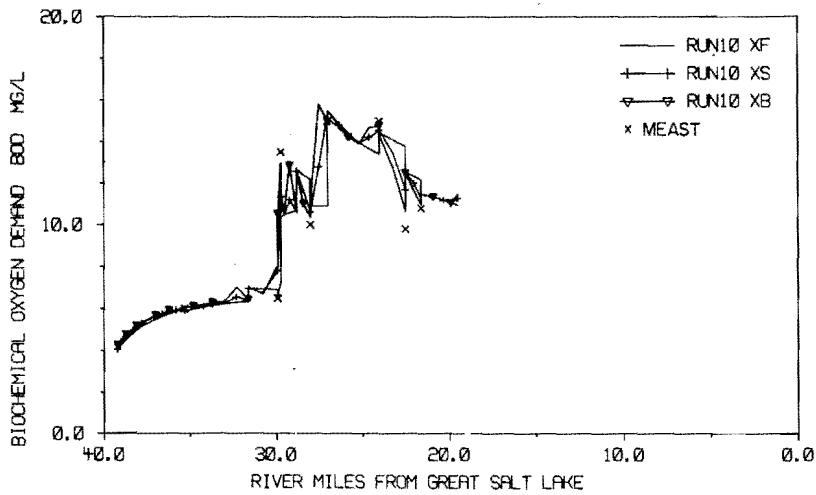
the state of the system when the forward EKF alone is used. The smoothed estimates are always equal to, or better than, the filtered estimates in the sense that the smoothed values for  $P$  are always equal to, or smaller than, the EKF values for  $P$ . A possible result of this reduction in  $P$  is that the positive-definite property of  $P$  will be lost during smoothing. This actually occurs during an attempt at smoothing the entire river system (river miles 39.2 (63.1 km) - 2.8 (4.5 km)) and led to severe divergence in the filter estimates. To avoid divergence a new value for the  $Q$  matrix should be established. Because of the prohibitive computer cost that would be associated with establishing a new  $Q$  matrix, the FIS was applied to only the first half of the river (river miles 39.2 (63.1 km) to 19.4 (31.2 km)), for which the  $Q$  matrix used in run 8 could be used without divergence occurring.

The initial conditions, the  $R$  and  $Q$  matrices, and the values for the coefficients in the process model are identical in basic EKF run (run 8) and in the forward EKF of the smoothing run (run 10). Thus, the results from the forward filter in run 10 are identical to those in run 8. The problem set-up for the backward LKF is the same as for the forward EKF with the exception that new initial conditions,  $\underline{X}^b(\Xi)$ , are specified at the downstream boundary. The initial state vector,  $\underline{X}^b(\Xi)$  is set equal to the measurement vector at river mile 19.4 (31.2 km), and  $P^b(\Xi)$  is based on  $R$  and is equal to  $P(\xi_0)$  (see Table 4.1).

Smoothed estimates and their associated estimation errors are contained in Figures 5.16 through 5.22. In addition, the forward EKF estimates and backward LKF estimates are included; although their inclusion results in three overlapping traces, it is felt that a careful comparison of the traces is informative.

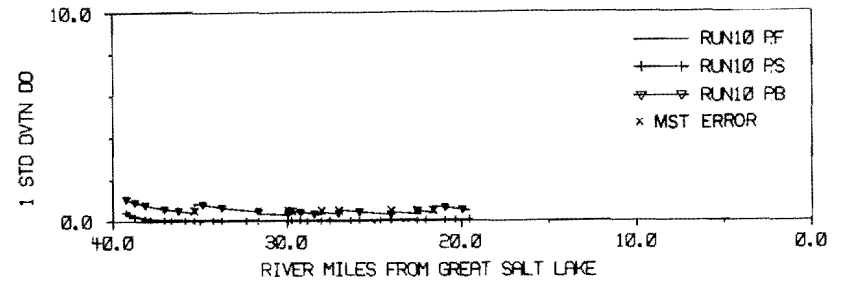


(a) Estimation and measurement errors

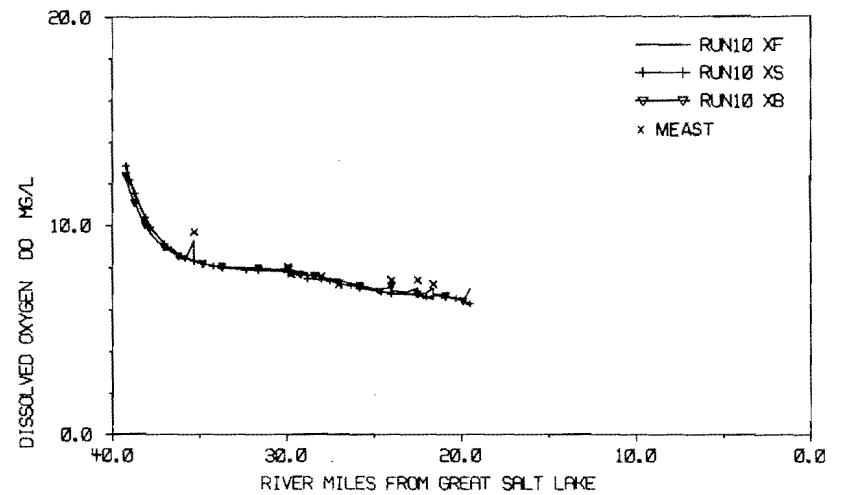


(b) Filter estimates and measured values

Figure 5.16. Smoothing algorithm results for BOD (XS and PS) (1 mile = 1.61 km)

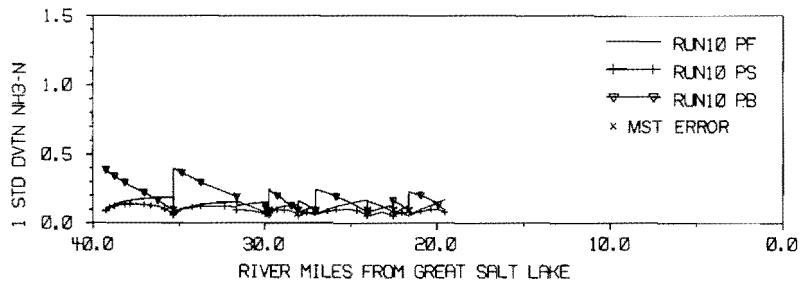


(a) Estimation and measurement errors

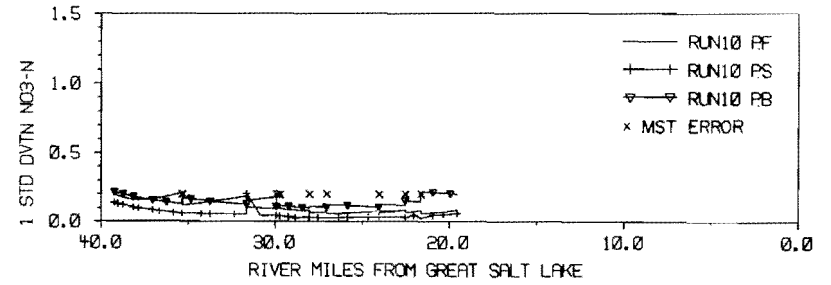


(b) Filter estimates and measured values

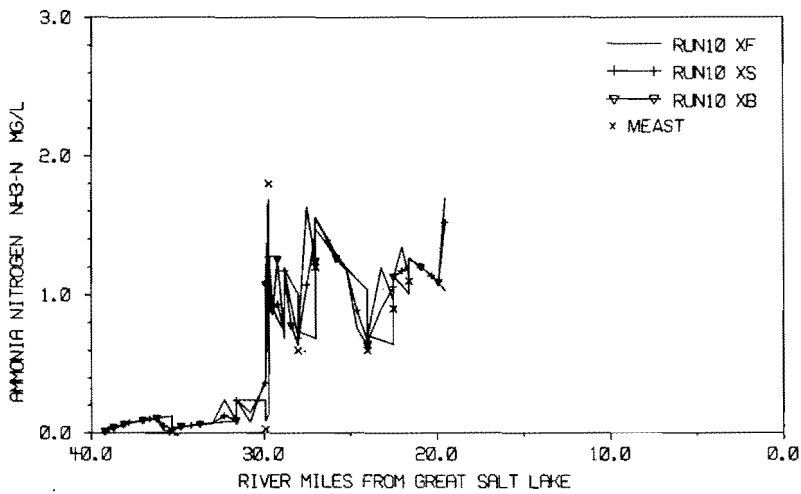
Figure 5.17. Smoothing algorithm results for DO (XS and PS) (1 mile = 1.61 km)



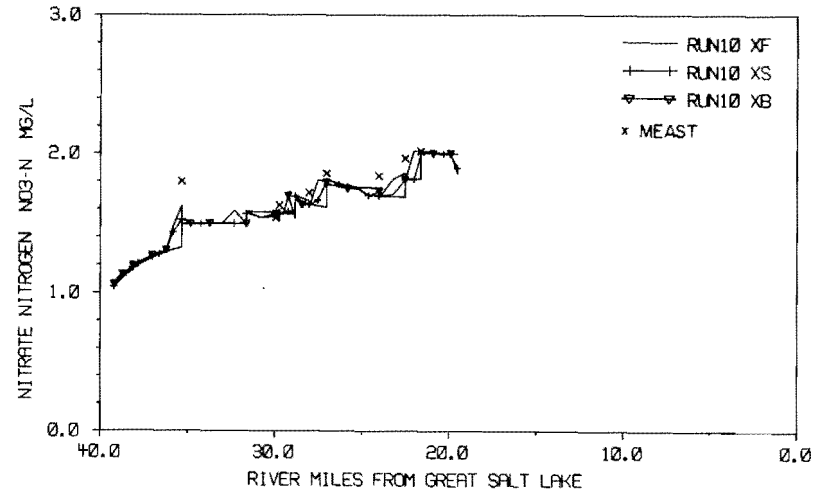
(a) Estimation and measurement errors



(a) Estimation and measurement errors



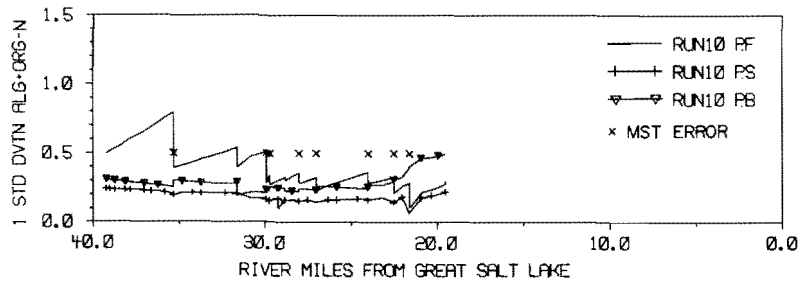
(b) Filter estimates and measured values



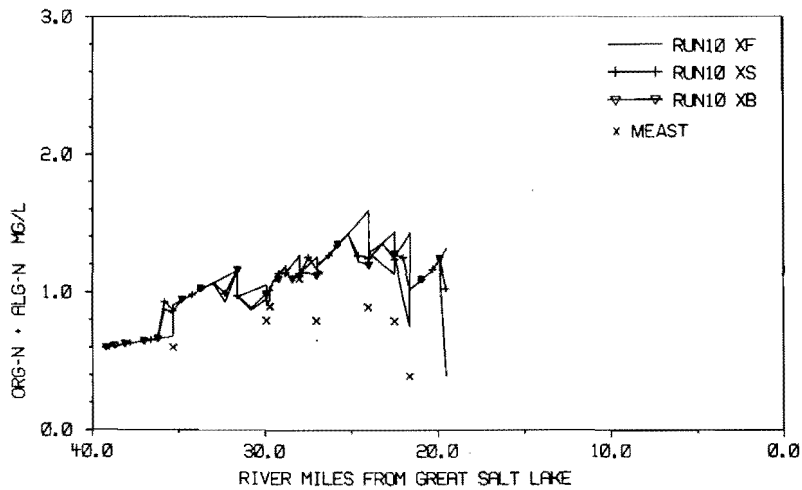
(b) Filter estimates and measured values

Figure 5.18. Smoothing algorithm results for NH<sub>3</sub>-N (XS and PS) (1 mile = 1.61 km)

Figure 5.19. Smoothing algorithm results for NO<sub>3</sub>-N (XS and PS) (1 mile = 1.61 km)

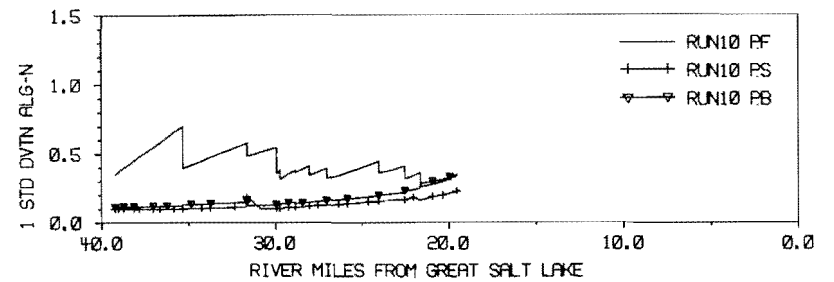


(a) Estimation and measurement errors

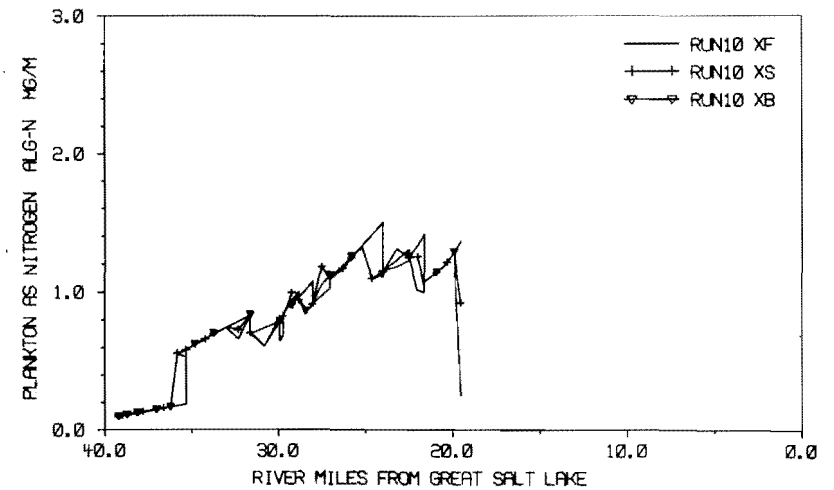


(b) Filter estimates and measured values

Figure 5.20. Smoothing algorithm results for (ALG-N + ORG-N) (XS and PS) (1 mile = 1.61 km).

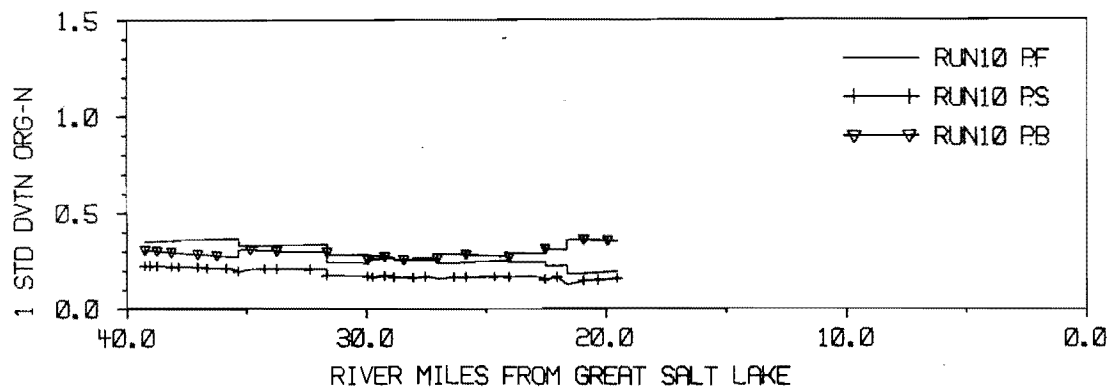


(a) Estimation and measurement errors

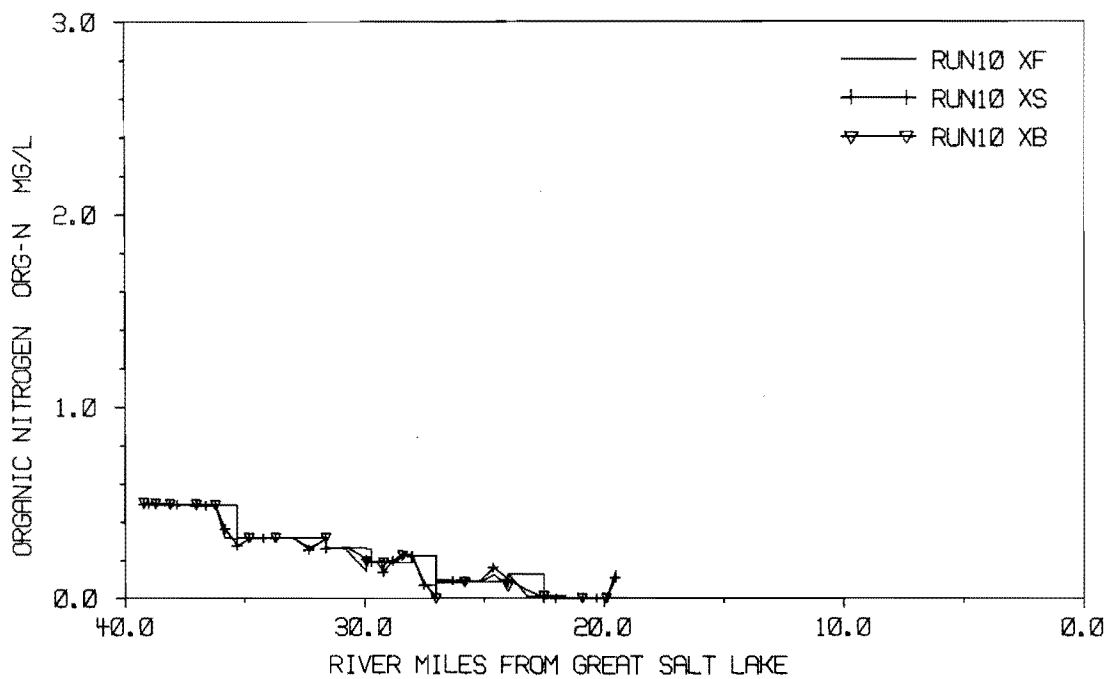


(b) Filter estimates and measured values

Figure 5.21. Smoothing algorithm results for ALG-N (XS and PS) (1 mile = 1.61 km).



(a) Estimation and measurement errors



(b) Filter estimates and measured values

Figure 5.22. Smoothing algorithm results for ORG-N (XS and PS) (1 mile = 1.61 km)

When examining the results from the backward LKF it must be remembered that it proceeds in the upstream direction. Thus, the estimation error grows or decays in the upstream direction until a sampling location is reached. At sampling locations a measurement update step reduces the estimation error to below the measurement noise. Unlike the forward and backward values of  $P$ , the smoothed values are not characterized by discrete jumps at sampling points. Instead, the estimation error rises to a peak approximately midway between sampling locations. This characteristic indicates that when information from all measurements is used, the confidence in the estimates decreases with distance from the adjacent sampling points. Smoothed values of  $P^S$  are less than the forward values indicating that better estimates are obtained from the smoothing algorithm than from the forward EKF. Although  $P^b$  is not directly adjusted for the effects of the point load estimation error, these effects are included indirectly through relinearization of the backward filter about the forward values for  $P$ . A distinct example of this is at river mile 31.7 (51.0 km).

As with the backward estimation error, the effects of measurement updating on the backward estimates must be interpreted in the upstream direction. Values of the smoothed estimates generally lie between the forward and backward estimates. The use of information contained in measurements in both the up- and downstream directions is indicated by the absence of discrete jumps in the smoothed estimates at sampling points.

Values of MSE for both the forward EKF and the FIS are contained in Table 5.4 under run 10. Firstly, it is interesting to compare EKF values of MSE in run 10 with those obtained in run 8. The difference is due



entirely to the fact that run 10 was performed over only the upstream half of the river while run 8 included the entire study length.

For BOD,  $\text{NH}_3\text{-N}$ , and  $\text{NO}_3\text{-N}$  this comparison indicates that the forward EKF estimates are closer to the measurements in the lower half of the river. For (ALG-N + ORG-N) and DO the comparison indicates that the forward EKF estimates are further from the measurements in the lower half of the river. It is interesting to note that MSE for  $\text{NO}_3\text{-N}$  is slightly greater than the  $\text{NO}_3\text{-N}$  measurement noise variance for the forward EKF estimates in run 10 indicating that over-fitting does not occur in the upper half of the river.

Values of MSE calculated using the smoothed estimates are all significantly less than those calculated for the forward EKF over the same length of the river. With the exception of  $\text{NH}_3\text{-N}$ , MSE values for the smoothed estimates are less than the corresponding measurement noise variances. This characteristic indicates that the smoothed estimates obtained in run 10 are "over-fitted." To avoid over-fitting the process model noise variances in Q should be reduced. However, in this study computer funds were limited, and so a new Q matrix was not determined from the FIS.

#### Sensitivity Studies

To assist in gaining familiarity with the filtering technique, several sensitivity studies are performed. The sensitivity of filter estimates to changes in the following statistics is investigated: the process model noise variance, the measurement noise variance, the initial estimation error variance, and the point load estimation error variance. Table 5.5 contains the values of the statistics used in the sensitivity runs.

Table 5.5. Values of the statistics used in the sensitivity runs.

Statistic		$Q$ (mg/l-day) <sup>2</sup>	$R$ (mg/l) <sup>2</sup>	$P(\xi_0)$ (mg/l) <sup>2</sup>	$Y$ (mg/l) <sup>2</sup>	
Water Quality parameter		NH <sub>3</sub> -N	NH <sub>3</sub> -N	ALG-N + ORG-N	NO <sub>3</sub> -N	All parameter
	Run	8	14	13	8	8
Low value	Statistic value	0.4	0.00001	0.01	0.04	See Table 5.6
	Run	--	--	--	--	19
Intermediate value	Statistic value	--	--	--	--	See Table 5.6
	Run	11	8	8	12	20
High value	Statistic value	4.0	0.01	0.25	2.25	See Table 5.6

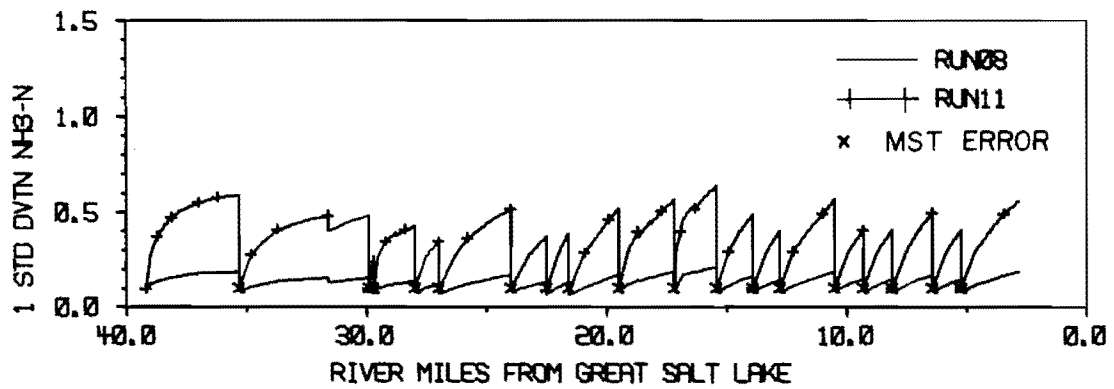
### Sensitivity study on process model noise variance

The significance of the process model noise covariance matrix (Q) is discussed earlier in this chapter in the section describing the method used for determining values for Q. In this sensitivity study the filter model was run for two different values of NH<sub>3</sub>-N process model noise variance. In run 8 the NH<sub>3</sub>-N process model noise variance is 0.4 (mg/l-day)<sup>2</sup> and in run 11 it is 4.0 (mg/l-day)<sup>2</sup>.

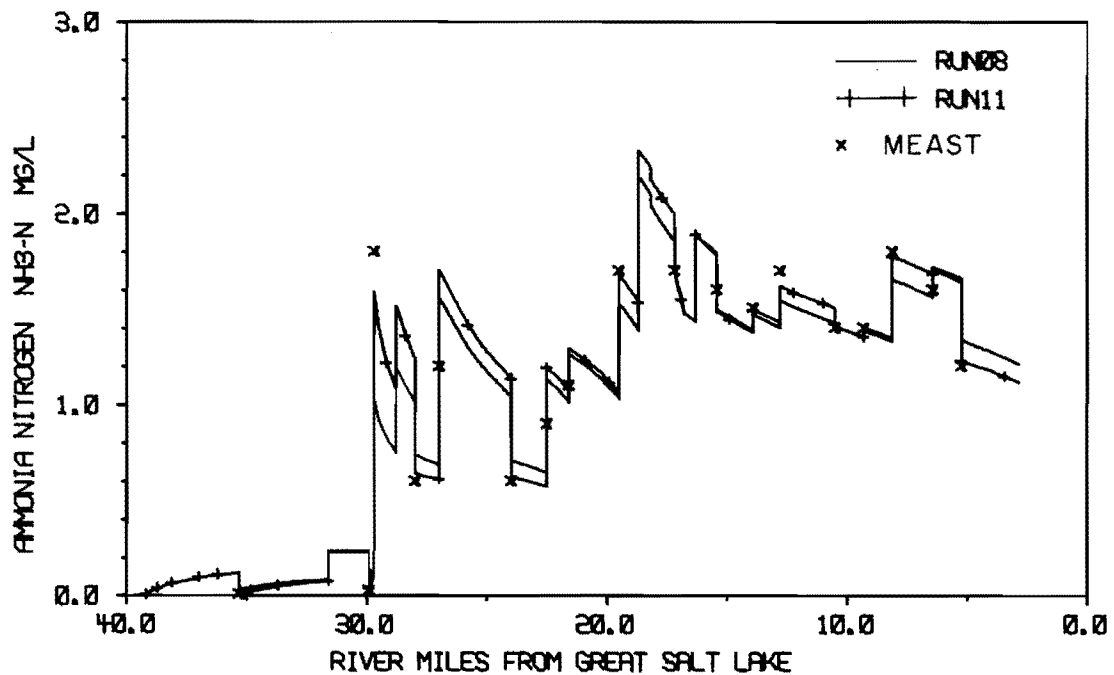
Figure 5.23 contains profiles of filter estimates and estimation errors for NH<sub>3</sub>-N obtained from runs 8 and 11. Estimation errors grow much faster with the larger value of Q used in run 11. However, measurement update always reduces the estimation error to less than the measurement noise variance for NH<sub>3</sub>-N. The higher value of Q used in run 11 signifies less confidence in the process model for NH<sub>3</sub>-N than in run 8. Therefore, filter estimates from run 11 follow the NH<sub>3</sub>-N measurement more closely than filter estimates from run 8. The MSE for NH<sub>3</sub>-N is reduced from 0.045 (mg/l)<sup>2</sup> to 0.003 (mg/l)<sup>2</sup> by changing Q from 0.04 (mg/l-day)<sup>2</sup> to 4.0 (mg/l-day)<sup>2</sup>. In addition, the reduced confidence in the NH<sub>3</sub>-N process model affects the MSE of linked parameters, notably (ALG-N + ORG-N) for which MSE is reduced from 0.258 (mg/l)<sup>2</sup> to 0.222 (mg/l)<sup>2</sup>.

### Sensitivity study on measurement noise variance

The significance of the measurement noise covariance matrix (R) is also discussed earlier in the section describing the method used for determining values for Q. Sensitivity studies were performed on the measurement noise variance for NH<sub>3</sub>-N and for (ALG-N + ORG-N).



(a) Estimation and measurement errors



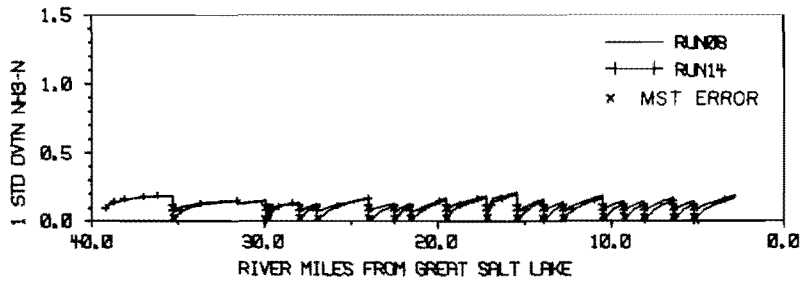
(b) Filter estimates and measured values

Figure 5.23 Sensitivity study on process model noise variance for NH<sub>3</sub>-N (1 mile = 1.61 km)

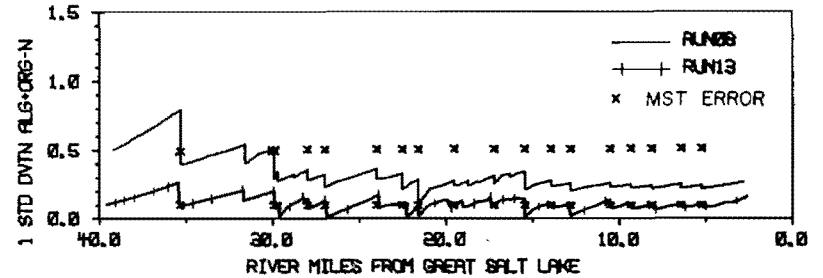
NH<sub>3</sub>-N Two different values of NH<sub>3</sub>-N measurement noise variance were used, namely,  $0.01 \text{ (mg/l)}^2$  in run 8 and  $0.00001 \text{ (mg/l)}^2$  in run 14. From Figure 5.24(a) it can be seen that the estimation errors are identical for both runs until the first sampling point is reached. At this and each subsequent sampling point the estimation error is reduced to below the new measurement noise variance indicated by the lower series of "χ" symbols. When the distance between successive sampling points is greater than about three miles the estimation errors converge for both values of R.

The effect of the lower value for R is similar to the effect of the higher value for Q in run 11. That is, because the smaller value of R signifies higher confidence in the measurement, it therefore, implies in relative terms, less confidence in the process model. Thus, the profiles of filter estimates for runs 11 and 14 are quite similar (compare Figures 2.23(a) and 2.24(a)). In run 14 the measurement update steps result in filter estimates that follow the measured values even closer than in run 11. This is because although the weighting is "tipped" in the same direction for runs 11 and 14, the degree of weighting is different for each run. The MSE for NH<sub>3</sub>-N in run 14 is reduced to almost zero and the MSE for (ALG-N + ORG-N) is reduced from  $0.258 \text{ (mg/l)}^2$  in run 8 to  $0.189 \text{ (mg/l)}^2$  in run 11.

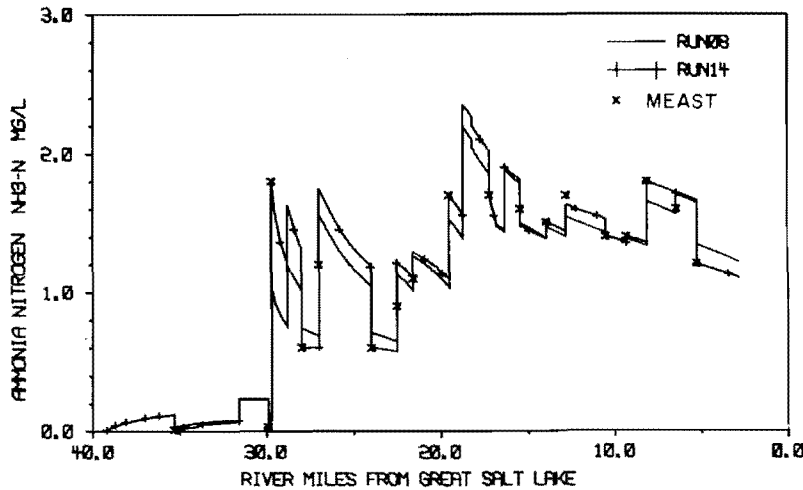
ALG-N + ORG-N The measurement noise variance in run 8 is  $0.25 \text{ (mg/l)}^2$  and in run 13 it is  $0.01 \text{ (mg/l)}^2$ . The initial value of  $P(\xi_0)$  is equal to R for (ALG-N + ORG-N) in both runs. Hence the profiles in Figures 5.25(a) start at different values. Measurement updates for each run reduce P below the value of R for that run. In fact, values of the



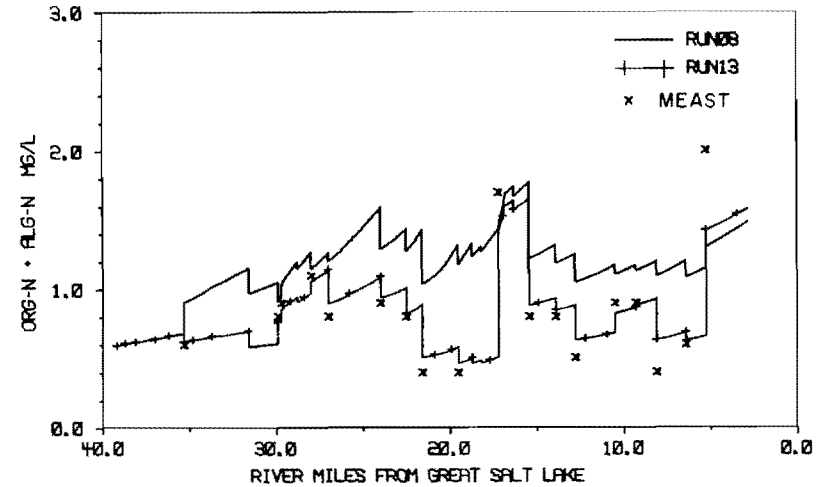
(a) Estimation and measurement errors



(a) Estimation and measurement errors



(b) Filter estimates and measured values



(b) Filter estimates and measured values

Figure 5.24. Sensitivity study on measurement noise variance for NH<sub>3</sub>-N - NH<sub>3</sub>-N results (1 mile = 1.61 km)

Figure 5.25. Sensitivity study on measurement noise variance for (ALG-N + ORG-N) - (ALG-N + ORG-N) results (1 mile = 1.61 km)

estimation error variance calculated using Equation 5.2 are negative after the measurement update at several of the sampling points. It is emphasized that the variances in the P matrix remained positive throughout run 13 for each state variable taken separately. It is the variance of the combination of ALG-N and ORG-N that becomes negative when calculated using Equation 5.2. These negative variances were set equal to zero for the purpose of plotting Figure 5.25(a). Estimation errors for runs 8 and 13 do not appear to be converging downstream at river mile 10.0 (16.1 km). For run 13, in which confidence in the measurements is higher than in run 8, the estimates are closer to the measurements than in run 8. MSE for (ALG-N + ORG-N) in run 13 is reduced to  $0.038 \text{ (mg/l)}^2$  which is greater than the corresponding R value of  $0.01 \text{ (mg/l)}^2$ . The filter estimates for (ALG-N + ORG-N) are more appealing for the viewpoint of obtaining predictions as close to the data as possible. However, acceptance of the results in run 13 as "better" than those in run 8 implies acceptance of the lower value for R which is not supported in the literature.

#### Sensitivity study on the initial estimation error variance

In the basic filter run the initial estimation error variance is equal to the measurement variance on the basis that a measurement vector is used to establish the initial state vector  $\left[ \bar{\mathbf{X}}(\xi_0) \right]$ . Thus, for run 8 the initial estimation error variance for  $\text{NO}_3\text{-N}$  is  $0.04 \text{ (mg/l)}^2$ . If no measurements are available at the upstream boundary we would probably place less confidence in the initial condition for the process model. This is done in run 12 for which the initial estimation error variance

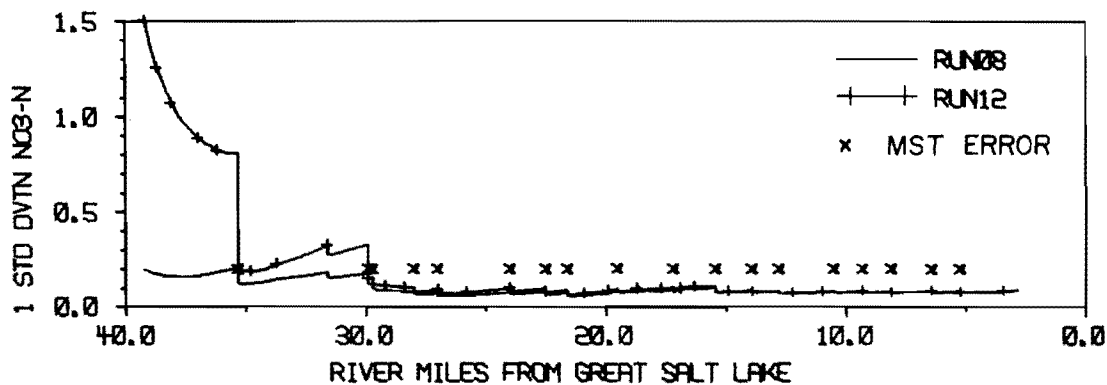
on  $\text{NO}_3\text{-N}$  was set equal to  $2.25 \text{ (mg/l)}^2$ . By doing this greater weighting is given to the first few measurements (Figure 5.26(b)). As more measurements are processed the confidence in the process model grows and hence,  $P$  declines (Figure 5.26(a)). After river mile 15.0 (24.2 km) there are no discernable differences in either the filter estimates or the estimation error variances for the two runs in which different values of  $P(\xi_0)$  were used.

Sensitivity study on point load estimation error variance

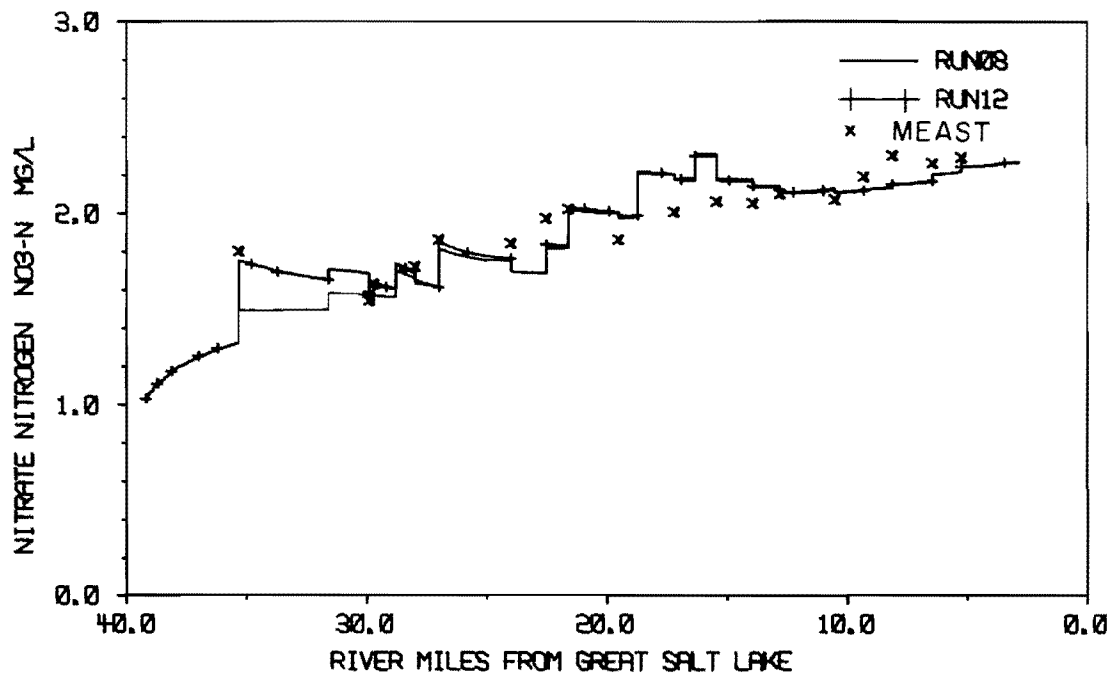
In this sensitivity study three different values were used for the estimation error variance ( $Y$ ) associated with the point load located at river mile 31.7 (51.0 km). The values used for  $Y$  are listed in Table 5.6. In run 8  $Y$  is equal to zero. The variances for  $Y$  in run 20 are double the arbitrary values used in run 19. Sensitivity results for  $\text{NO}_3\text{-N}$  are shown as they are typical of the results obtained for the other parameters. Figure 5.27 shows that in run 8 the estimation error ( $P$ ) is decreased when  $Y$  is zero, and increased by differing magnitudes for runs 19 and 20. However, the effect on  $P$  is negligible after the next measurement update. The filter estimates of  $\text{NO}_3\text{-N}$  are very slightly weighted towards the measurements at this sampling point for runs 19 and 20. However, the difference in estimates between run 8 and run 20, which results in the larger  $P$  value, is only 0.007 mg/l. Therefore, for practical purposes, the effect on the  $\text{NO}_3\text{-N}$  estimates is negligible in this example.

In the case of  $\text{ALG-N}$ , filter estimates are affected by changes to the variances in  $Y$  (see Figure 5.28). The estimation error variance of  $\text{ALG-N}$  is not affected directly by changes in the point load estimation





(a) Estimation and measurement errors

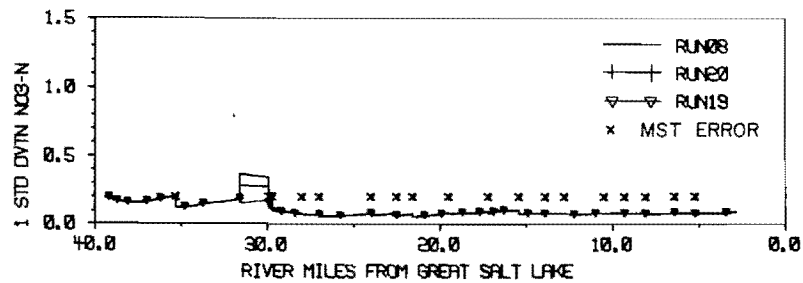


(b) Filter estimates and measured values

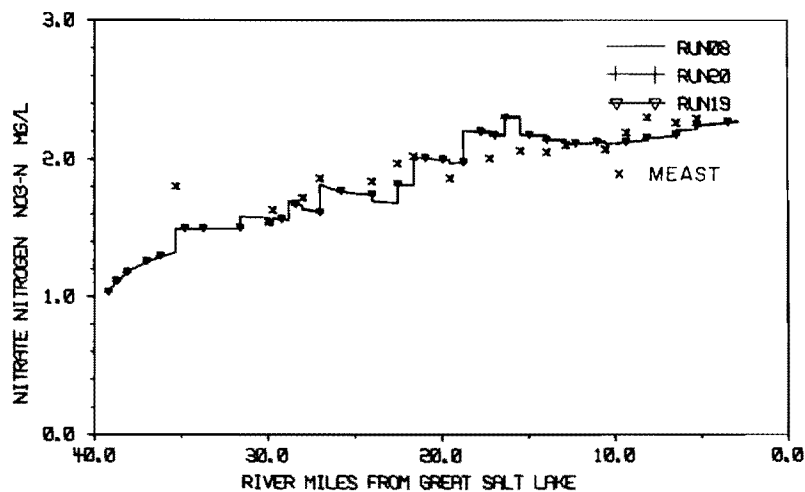
Figure 5.26 Sensitivity study on the initial estimation error variance for  $\text{NO}_3\text{-N}$  (1 mile = 1.61 km)

Table 5.6. Estimation error variances (Y) for the point load located at river mile 31.70 (51.0 km).

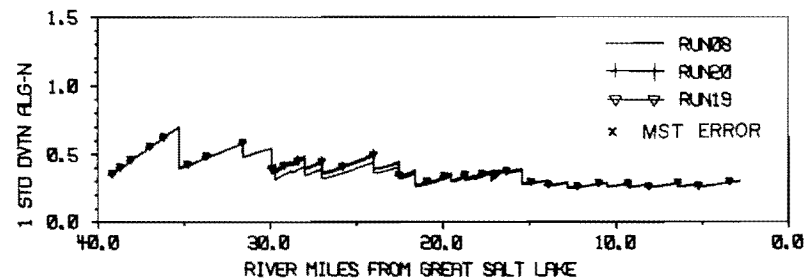
Parameter	Estimation error variance (mg/l) <sup>2</sup>		
	Run 19	Run 20	Other runs (including Run 8)
BOD	50.0	100.0	0.0
NH <sub>3</sub> -N	1.0	2.0	0.0
NO <sub>3</sub> -N	2.0	4.0	0.0
ALG-N	0.0	0.0	0.0
ORG-N	0.0	0.0	0.0
DO	16.0	32.0	0.0



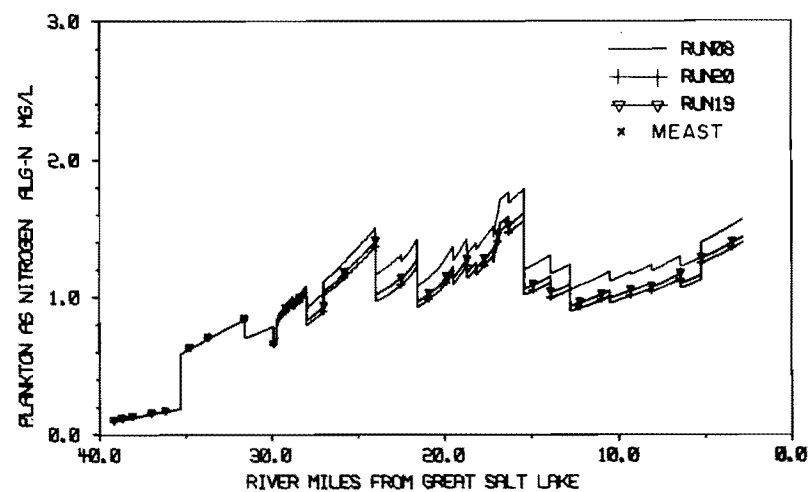
(a) Estimation and measurement errors



(b) Filter estimates and measured values



(a) Estimation and measurement errors



(b) Filter estimates and measured values

Figure 5.27. Sensitivity study on the estimation error variances associated with the point load at river mile 31.70 - NO<sub>3</sub>-N results (1 mile = 1.61 km).

Figure 5.28. Sensitivity study on the point load estimation error variances associated with the point load at river mile 31.70 - ALG-N results (1 mile = 1.61 km).

error variances of ALG-N since these remain zero for all three runs (see Table 5.6). However, the estimation error variance of ALG-N is indirectly affected through the measurement updating process. The increased uncertainty in the process model prediction of the other parameters causes an increase in the estimation error associated with ALG-N and similarly ORG-N which is not shown here. The reason for the estimation errors of ALG-N and ORG-N remaining changed, while the effect on the estimation error of other parameters dies out, is probably due to the relatively high measurement noise variance for (ALG-N + ORG-N). As a consequence of the increased estimation errors the estimates for ALG-N and ORG-N in runs 19 and 20 are weighted more toward the measurements than was the case in run 8. Thus, MSE for (ALG-N + ORG-N) was reduced in runs 19 and 20 compared with run 8 (see Table 5.4). This reduction of MSE resulting from changes in Y reinforces the suspicion that a simultaneous trial and error determination of Q and Y for each point load would be a much larger task than for Q alone.

#### Coefficient Estimation

The extended Kalman filter is a potentially useful tool for model calibration. Coefficients in the process model can be estimated at the same time as state variables are estimated. Although this method of parameter estimation is statistically less efficient compared with other techniques it does have the advantage of providing information on the variation of the coefficient with respect to the independent variable, in this case distance along the stream (Beck and Young, 1976). Coefficient estimation is achieved by augmenting the state vector with the

coefficients to be estimated. For each additional state variable this involves adding an additional equation to the process model, and an additional row and column to the process model noise covariance matrix. A process model of the following form is used for each of the coefficients estimated in this study:

$$\dot{X}_7 = 0 + \omega_7 \dots \dots \dots (5.3)$$

in which

$\dot{X}_7$  = first derivate with respect to travel time of  
 $X_7$  which is the coefficient to be estimated

This process model indicates that  $X_7$  does not change with travel time except in a manner that can be described by the white Gaussian noise process,  $\omega_7$ . Other process models for  $X_7$  may be used if appropriate.

$X_7$  is substituted into the other process model equations in place of the coefficient to be estimated. A result of treating some of the model coefficients as state variables is that a linear process model usually becomes non-linear. The initial state vector and the initial estimation error covariance matrix are augmented to accommodate the additional state variable. Since measurements are not available for model coefficients the measurement vector is unchanged, but a column of zeros is added to the right-hand side of the H matrix to keep Equation 4.22 consistent. The Jacobian matrix is also modified to reflect the changes to the process model.

The three coefficient estimation runs are described below.  $K_{23}$  is estimated by run 15, and  $K_{45}$  by run 16. In run 21 five of the coefficients ( $K_{23}$ ,  $K_{45}$ ,  $K_{52}$ ,  $\hat{\mu}$ ,  $K_{S3}$ ) in the equations describing the

cycling of nitrogen are estimated simultaneously with the six water quality parameters. In addition two runs for lateral inflow concentration estimation are also described. Lateral inflow concentration for  $\text{NO}_3\text{-N}$  is estimated by run 17 and for  $\text{NH}_3\text{-N}$  by run 18.

A fresh determination of the Q matrix was not undertaken for any of these runs. An arbitrary value for the process model variance associated with each coefficient estimated is assumed and the same value is used for the initial estimation error variance. These values are given in Table 5.7. The results from the coefficient estimation runs could be improved by refining the Q matrix.

#### $K_{23}$ estimation

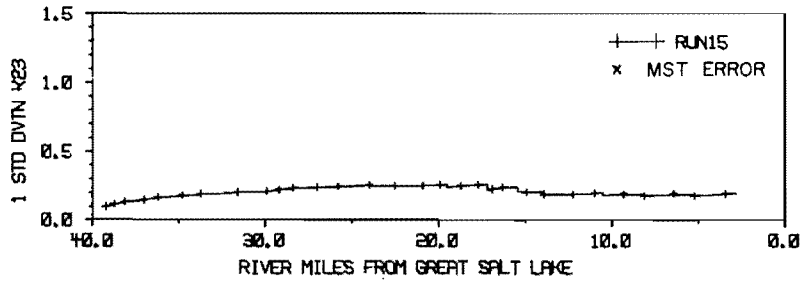
Filter estimates for  $K_{23}$ , the nitrification rate, are shown in Figure 5.29. Figures 5.30 through 5.33 contain results from some of the parameters using the filter estimates of  $K_{23}$ . Down to river mile 20.0 (32.2 km) the estimates of  $K_{23}$  are close to the calibration value of 0.3 per day. After river mile 20.0 (32.2 km),  $K_{23}$  estimates decline, become negative, and then rise to approximately 0.4 per day. A comparison of the MSE for run 15 and the MSE for run 8 indicates a substantial decline in the MSE for DO when  $K_{23}$  is estimated. Inspection of the DO profiles from run 15 (Figure 5.30) indicates a rise in DO below river mile 20.0 (32.2 km) compared to the estimates from run 8. It appears that the filter estimates of  $K_{23}$  may result largely from the reduction in MSE that can be obtained by changing the DO estimates.

In terms of the chemical processes a negative value for  $K_{23}$  implies denitrification. However, the near saturation levels of DO indicate that denitrification should not be taking place in the prototype system.

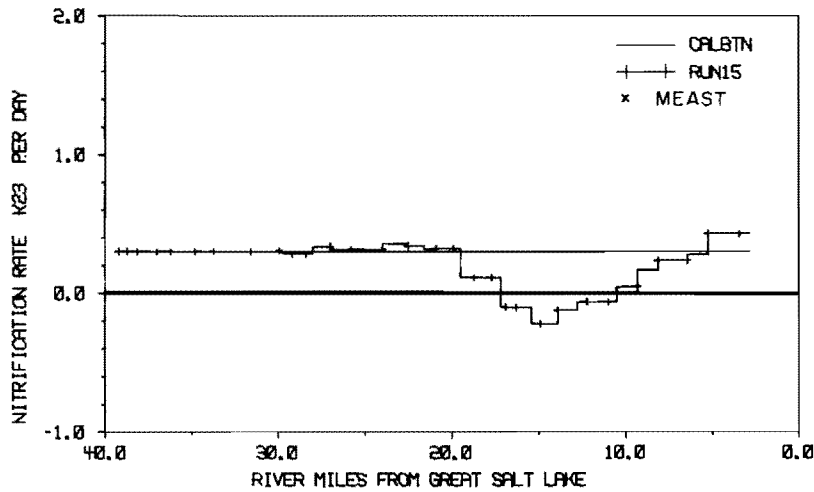
Table 5.7 Process model noise variances (Q) and initial estimation error variances (P( $\xi_0$ )) for the coefficients and lateral inflow concentrations estimated in runs 15 through 18 and 21.

Lateral Inflow Concentration or Model Coefficient		Units of P( $\xi_0$ ) Variances <sup>a</sup>	Variance	Run
U <sub>2</sub>	NH <sub>3</sub> -N concentration in lateral inflow	(mg/l) <sup>2</sup>	0.04	18
U <sub>3</sub>	NO <sub>3</sub> -N concentration in lateral inflow	(mg/l) <sup>2</sup>	2.25	17
K <sub>23</sub>	Nitrification rate	(per day) <sup>2</sup>	0.09	15 and 21
K <sub>45</sub>	Algal death rate	(per day) <sup>2</sup>	0.01	16 and 21
K <sub>52</sub>	Rate of decomposition of ORG-N to NH <sub>3</sub> -N	(per day) <sup>2</sup>	0.01	21
$\hat{\mu}$	Maximum specific growth rate of algae	(per day) <sup>2</sup>	3.00	21
K <sub>S3</sub>	Half-saturation coefficient for NO <sub>3</sub> -N	(mg/l) <sup>2</sup>	0.0002	21

<sup>a</sup>The units of process model noise variance are obtained by dividing the units of P( $\xi_0$ ) by (day)<sup>2</sup>. For example the units of process model noise variance for U<sub>2</sub> are (mg/l-day)<sup>2</sup>.

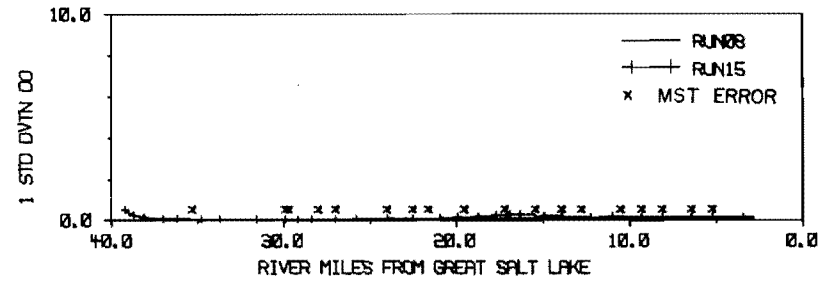


(a) Estimation and measurement errors

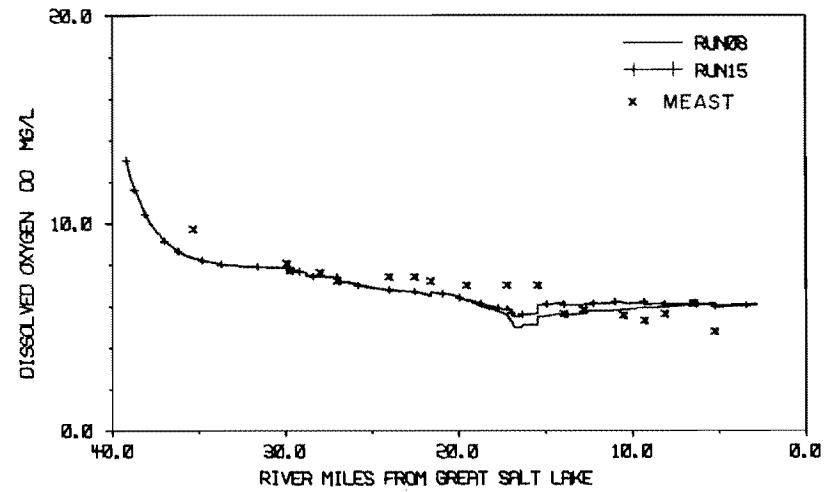


(b) Filter estimates and measured values

Figure 5.29. Coefficient estimation for  $K_{23}$  -  $K_{23}$  results (run 15) (1 mile = 1.61 km).



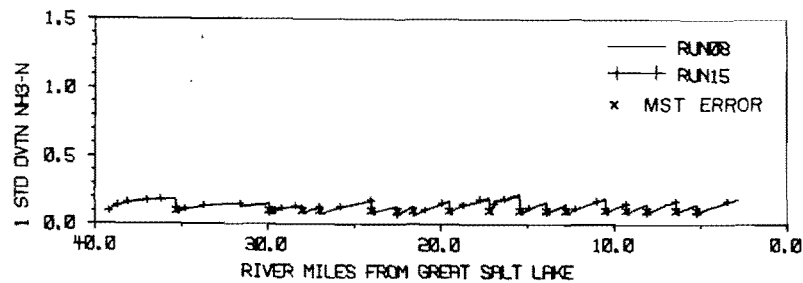
(a) Estimation and measurement errors



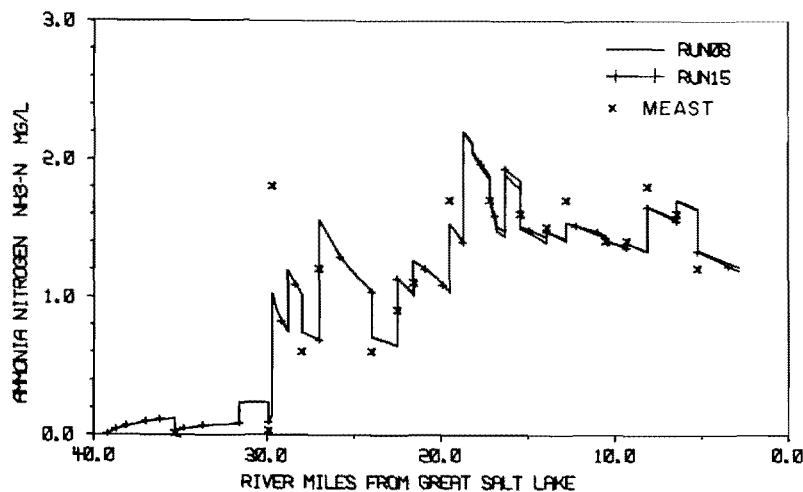
(b) Filter estimates and measured values

Figure 5.30. Coefficient estimation for  $K_{23}$  - DO results (run 15)(1 mile = 1.61 km).



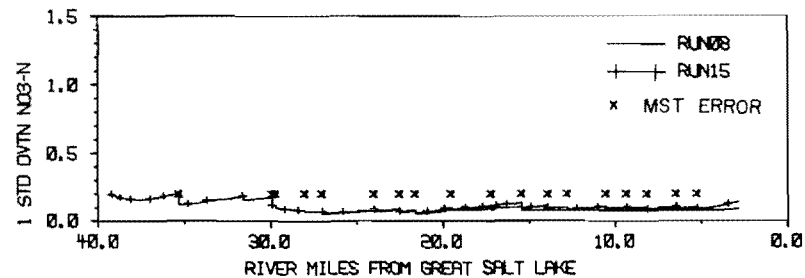


(a) Estimation and measurement errors

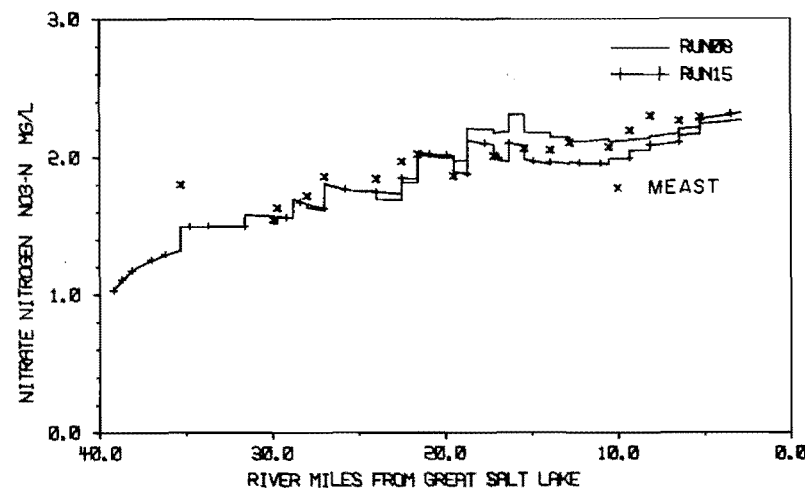


(b) Filter estimates and measured values

Figure 5.31. Coefficient estimation for  $K_{23}$  -  $\text{NH}_3\text{-N}$  results (run 15) (1 mile = 1.61 km).

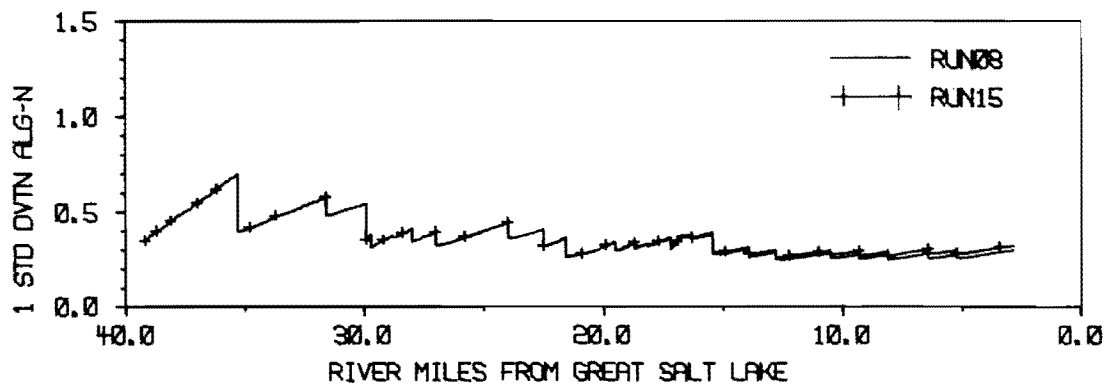


(a) Estimation and measurement errors

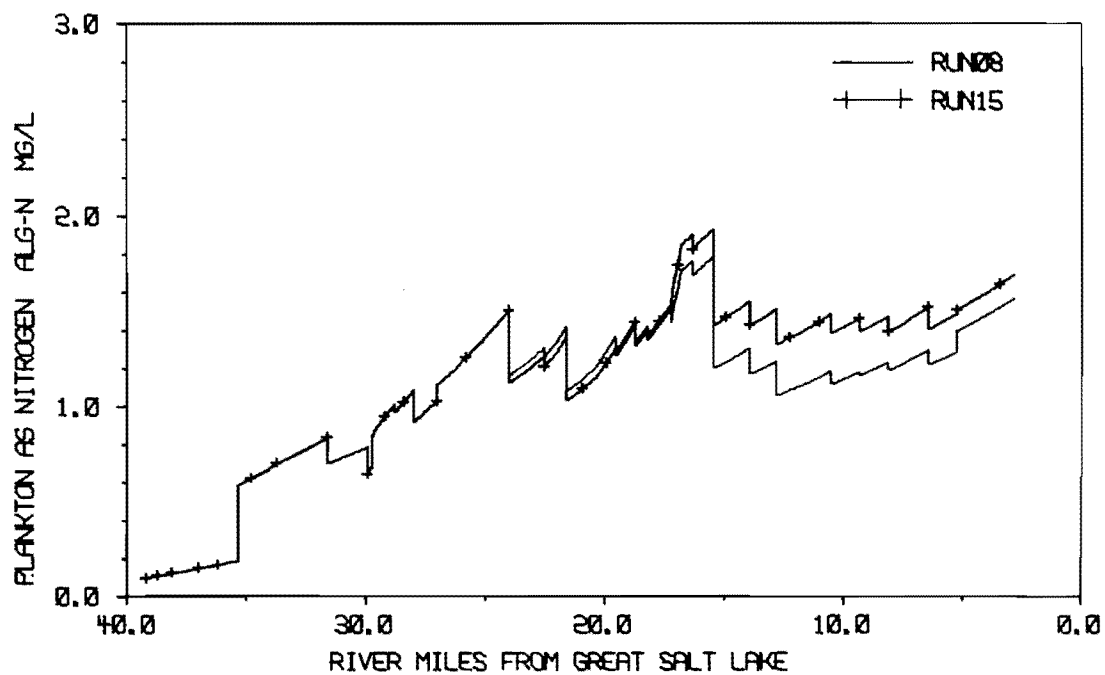


(b) Filter estimates and measured values

Figure 5.32. Coefficient estimation for  $K_{23}$  -  $\text{NO}_3\text{-N}$  results (run 15) (1 mile = 1.61 km).



(a) Estimation and measurement errors



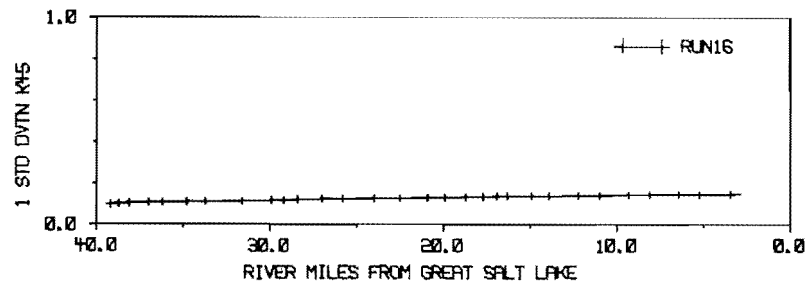
(b) Filter estimates and measured values

Figure 5.33. Coefficient estimation for  $K_{23}$   
 - ALG-N results (run 15)  
 (1 mile = 1.61 km).

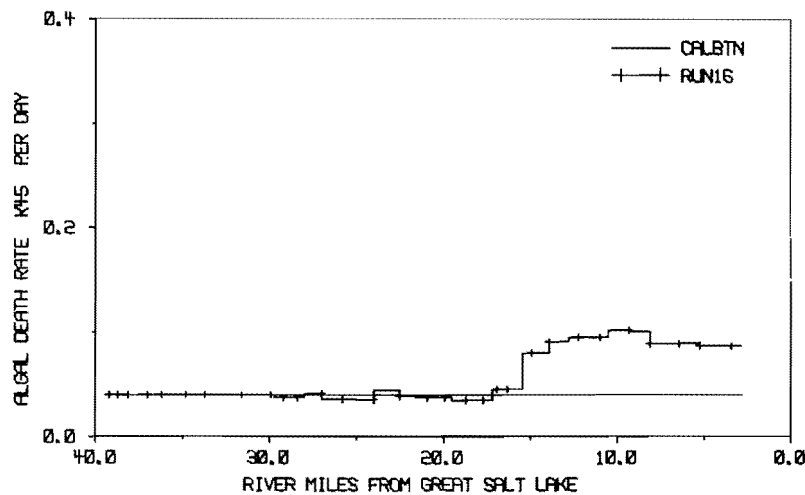
Therefore, from a chemical viewpoint the filter estimates of  $K_{23}$  are unacceptable. These results show the need for a technique for constraining state variables to a reasonable range of values. The effects of the filter estimates of  $K_{23}$ , on the estimates of  $\text{NH}_3\text{-N}$ ,  $\text{NO}_3\text{-N}$ , and  $\text{ALG-N}$ , are shown in Figures 5.31, 5.32, and 5.33 respectively. Slight increases in the estimation errors are caused by the introduction of estimation error associated with  $K_{23}$ , compared to run 8 in which  $K_{23}$  was treated as deterministic.

#### $K_{45}$ estimation

Figure 5.34 shows the filter estimates of the algal death rate,  $K_{45}$ , compared with the constant calibration value of 0.04 per day. Down to approximately river mile 16.0 (25.8 km) the filter estimates are very similar to the calibration value. Downstream of river mile 16.0 (25.8 km) the filter estimates jump to 0.08 - 0.10 per day. It is of interest to note that the calibration value of the maximum specific growth rate for algae below river mile 16.7 (26.9 km) is half of the upstream value. Perhaps the increase in filter estimates of the algal death rate is related to the change in the algal growth rate. Filter estimates for  $\text{ALG-N}$  and  $\text{ORG-N}$  based on the filter estimates of  $K_{45}$  are given in Figures 5.35 and 5.36, respectively. For example, the increased algal death rate just below river mile 16.0 (25.8 km) results in lower estimates of  $\text{ALG-N}$  and higher estimates of  $\text{ORG-N}$ . However, there is little change to the magnitude of  $(\text{ALG-N} + \text{ORG-N})$ . The effect of introducing uncertainty associated with  $K_{45}$  into the estimation error of  $\text{ALG-N}$  and  $\text{ORG-N}$  is shown by the increase in P values for both parameters.

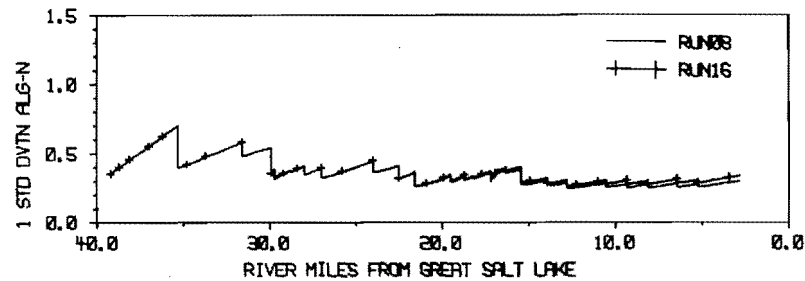


(a) Estimation and measurement errors

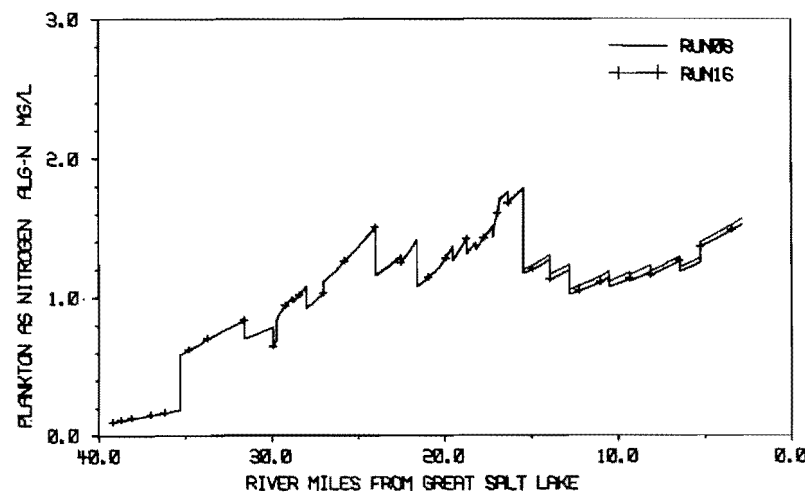


(b) Filter estimates and measured values

Figure 5.34. Coefficient estimation for  $K_{45}$   
 -  $K_{45}$  results (run 16)  
 (1 mile = 1.61 km).

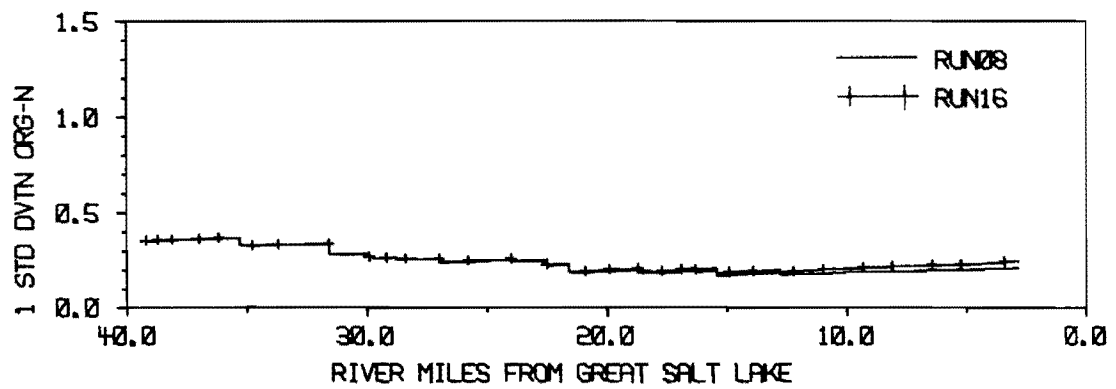


(a) Estimation and measurement errors

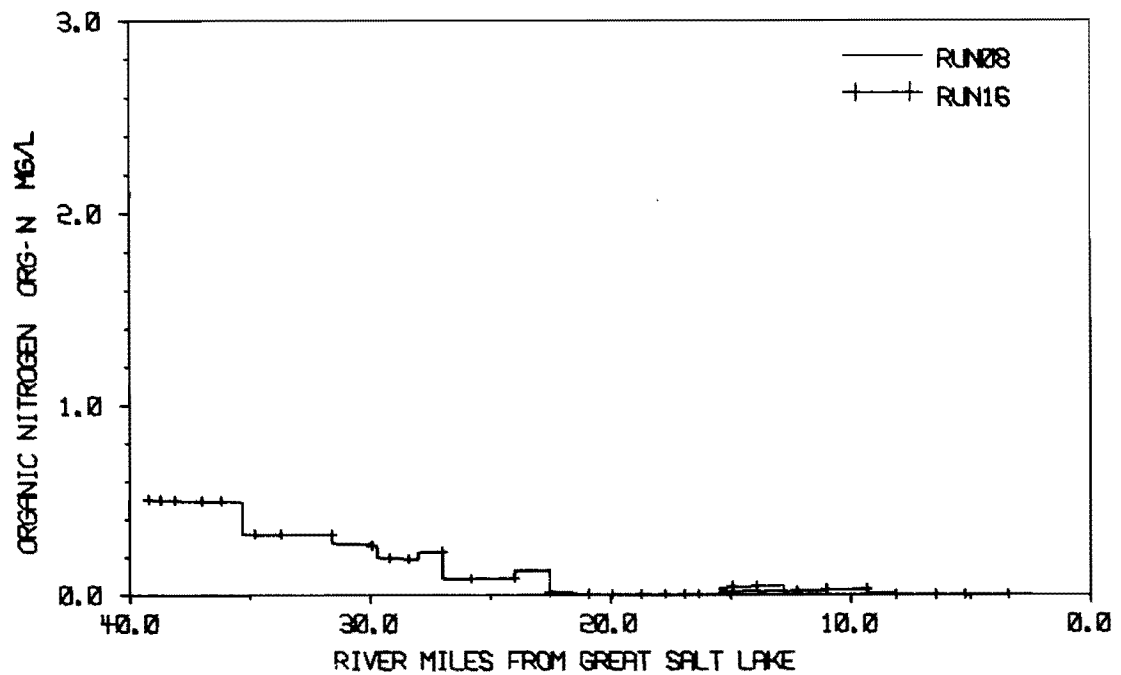


(b) Filter estimates and measured values

Figure 5.35. Coefficient estimation for  $K_{45}$   
 - ALG-N results (run 16)  
 (1 mile = 1.61 km).



(a) Estimation and measurement errors



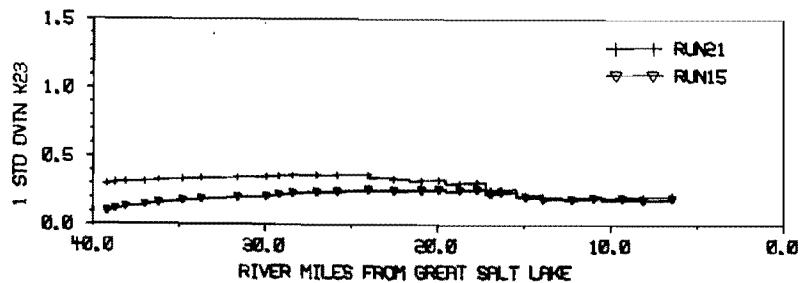
(b) Filter estimates and measured values

Figure 5.36. Coefficient estimation for  $K_{45}$   
 - ORG-N results (run 16)  
 (1 mile = 1.61 km).

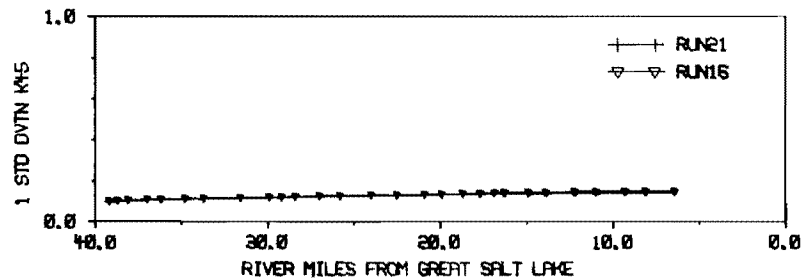
Estimation of the nitrogen  
cycle coefficients

In run 21 five coefficients pertaining to the nitrogen cycle part of the process model are estimated. Filter estimates for the coefficients, namely,  $K_{23}$ ,  $K_{45}$ ,  $K_{52}$ ,  $\hat{\mu}$ , and  $K_{S3}$ , are contained in Figures 5.37 through 5.41. In each figure the calibration values of the coefficient are shown. For  $K_{23}$  and  $K_{45}$  the results of the previous coefficient runs are also shown to facilitate comparison. As with the other coefficient estimation runs, the values used for the Q matrix could be improved. In this run the need for improving Q is dramatically illustrated by the divergence of filter estimates (see Figures 5.42 through 5.47). At river mile 5.8 (9.3 km), the estimation error variance for  $\text{NH}_3\text{-N}$  becomes negative and hence the P matrix is no longer positive-definite. Rather than attempt to change Q in such a way that divergence is avoided, it was decided to stop the run immediately before loss of positive-definiteness in P and use the results as an illustration of divergence. Thus run 21 covers river miles 39.2 (63.1 km) to 6.4 (10.3 km).

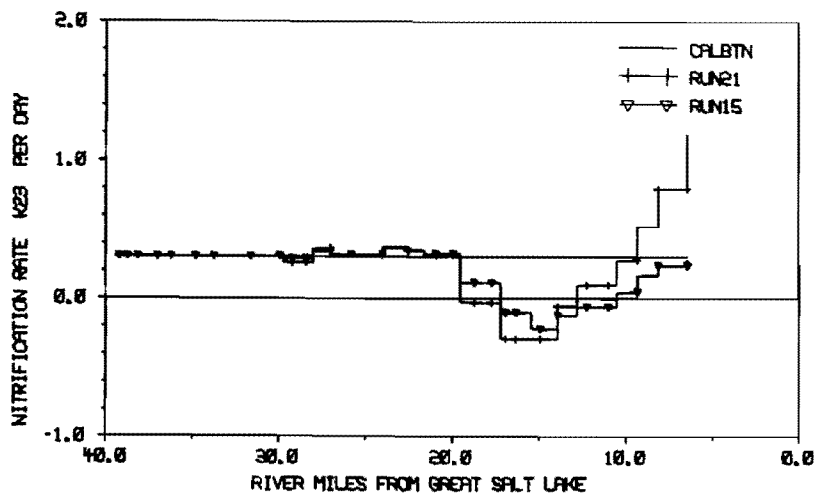
The onset of divergence is caused by the decay of P for  $\text{NH}_3\text{-N}$  (see Figure 5.44) which results in greater weighting for the process model predictions. Filter estimates for ammonia diverge from the measured values and also, presumably, from the true state for ammonia. Significant measurement updates are still taking place below river mile 10.0 (16.1 km) but these are not sufficient to overcome the divergence. To prevent divergence the Q matrix should be increased so that estimation errors are maintained at higher levels which are presumably close to the true values of P. The starting point in this example would be to increase



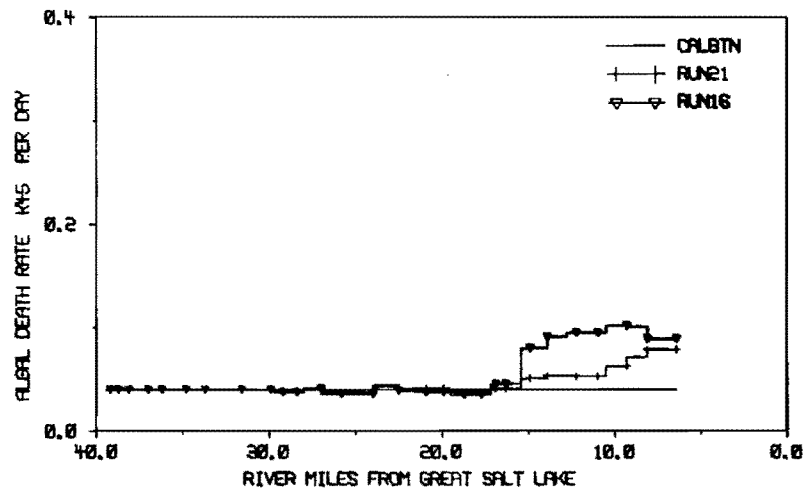
(a) Estimation and measurement errors



(a) Estimation and measurement errors



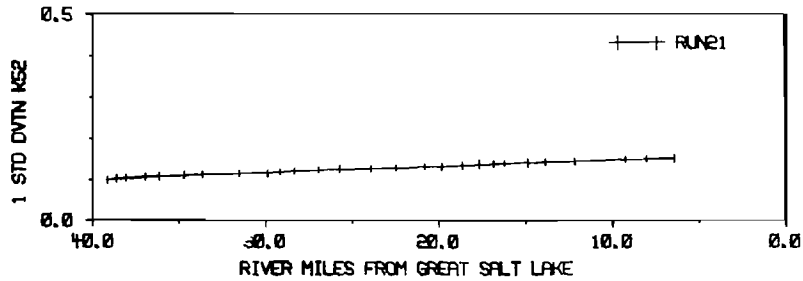
(b) Filter estimates and measured values



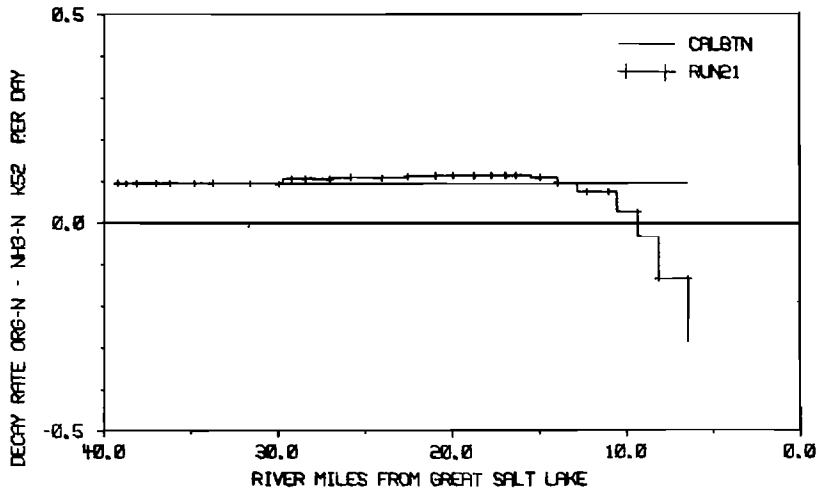
(b) Filter estimates and measured values

Figure 5.37. Estimation of the nitrogen cycle coefficients -  $K_{23}$  results (run 21) (1 mile = 1.61 km).

Figure 5.38. Estimation of the nitrogen cycle coefficients -  $K_{45}$  results (run 21) (1 mile = 1.61 km).

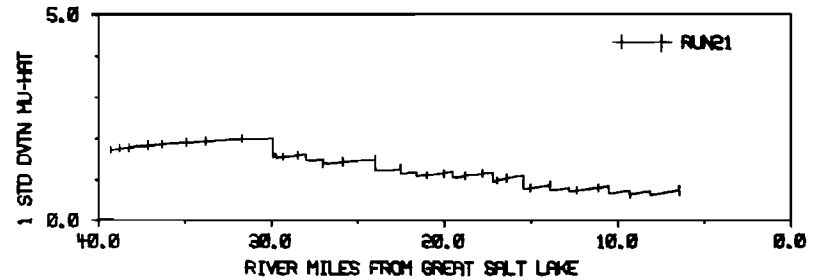


(a) Estimation and measurement errors

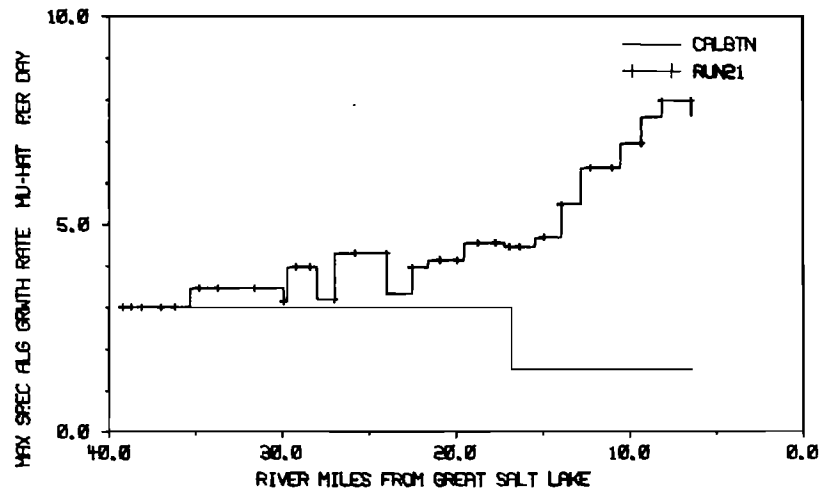


(b) Filter estimates and measured values

Figure 5.39. Estimation of the nitrogen cycle coefficients -  $K_{52}$  results (run 21) (1 mile = 1.61 km).



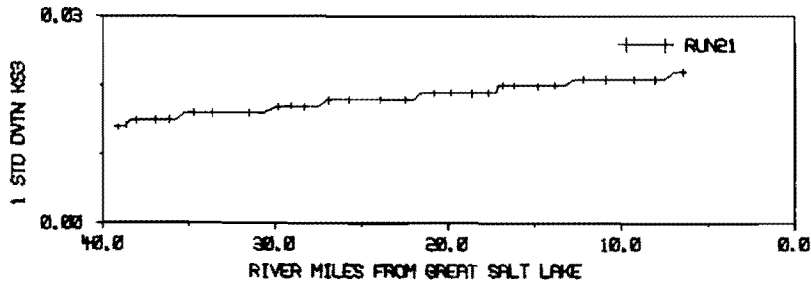
(a) Estimation and measurement errors



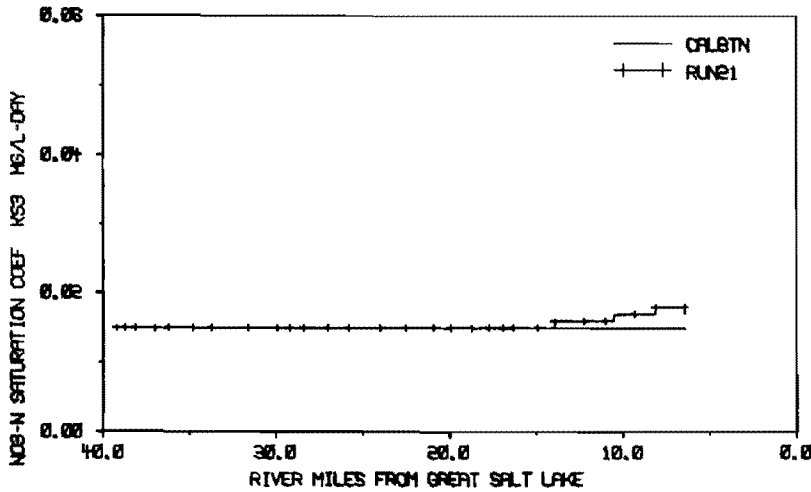
(b) Filter estimates and measured values

Figure 5.40. Estimation of the nitrogen cycle coefficients -  $\hat{\mu}$  results (run 21) (1 mile = 1.61 km).



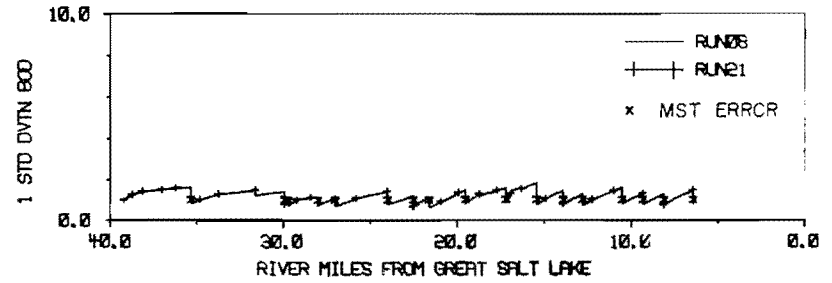


(a) Estimation and measurement errors

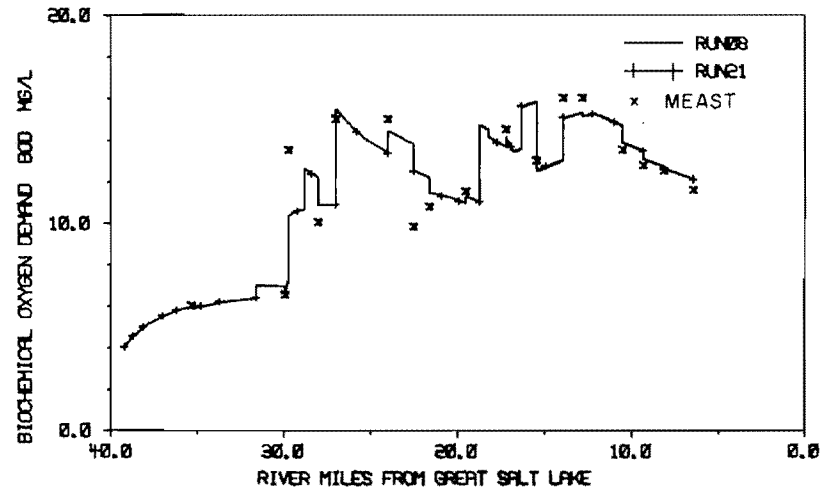


(b) Filter estimates and measured values

Figure 5.41. Estimation of the nitrogen cycle coefficients -  $K_{S3}$  results (run 21) (1 mile = 1.61 km).

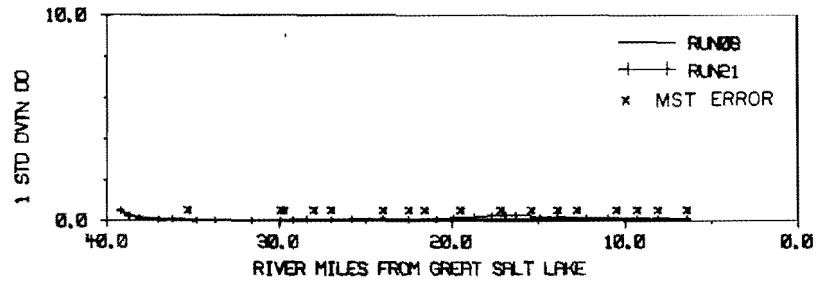


(a) Estimation and measurement errors

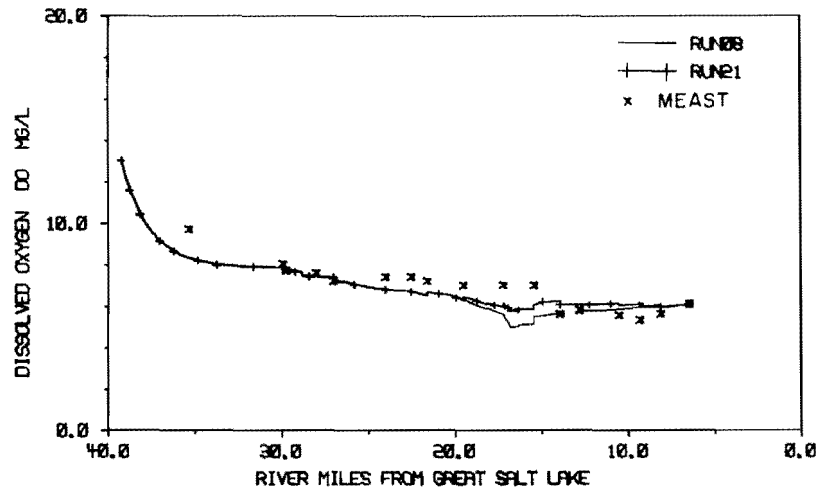


(b) Filter estimates and measured values

Figure 5.42. Estimation of the nitrogen cycle coefficients - BOD results (run 21) (1 mile = 1.61 km).

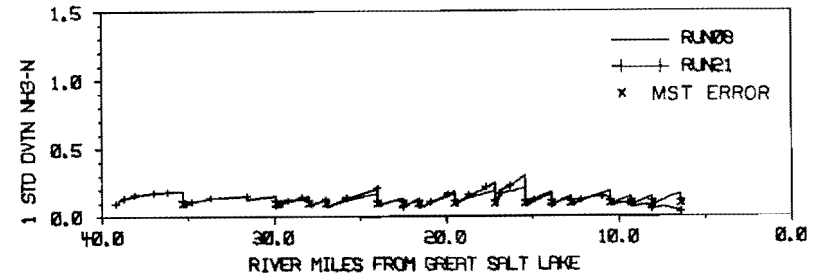


(a) Estimation and measurement errors

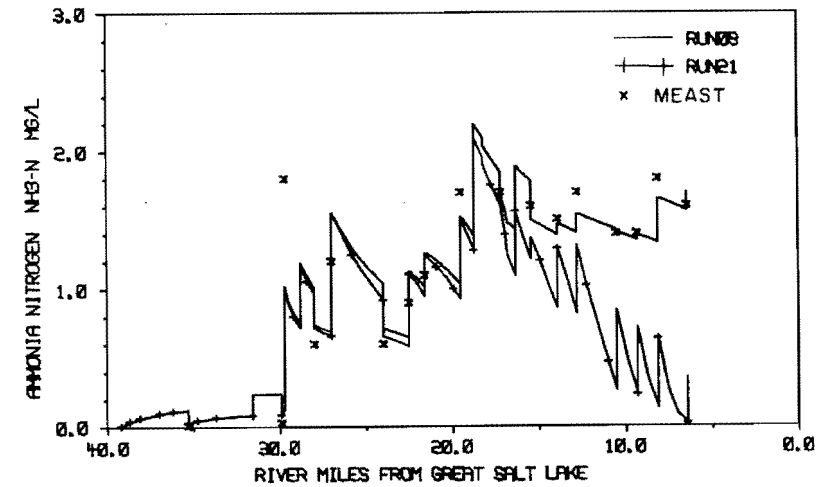


(b) Filter estimates and measured values

Figure 5.43. Estimation of the nitrogen cycle coefficients - DO results (run 21) (1 mile = 1.61 km).

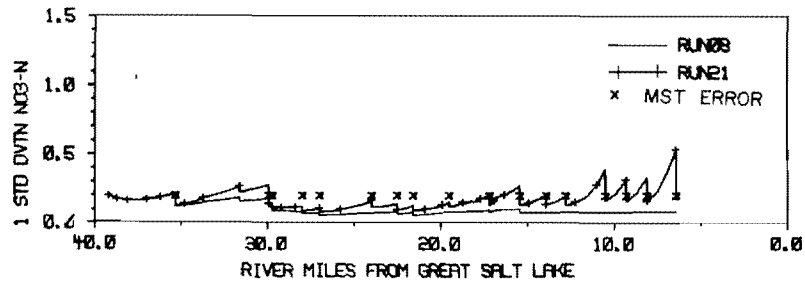


(a) Estimation and measurement errors

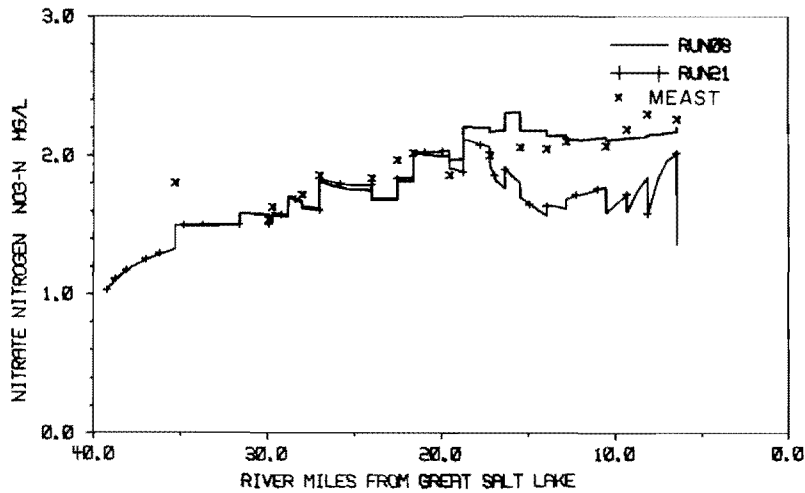


(b) Filter estimates and measured values

Figure 5.44. Estimation of the nitrogen cycle coefficients -  $\text{NH}_3\text{-N}$  results (run 21) (1 mile = 1.61 km).

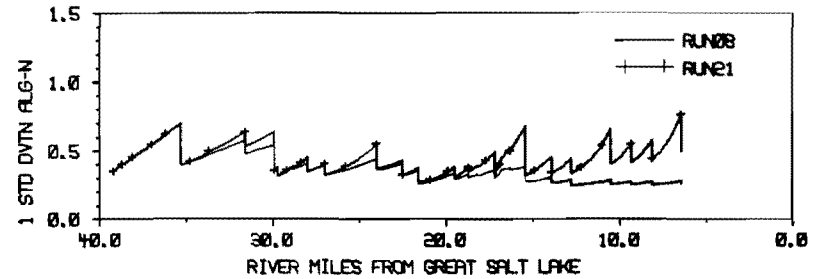


(a) Estimation and measurement errors

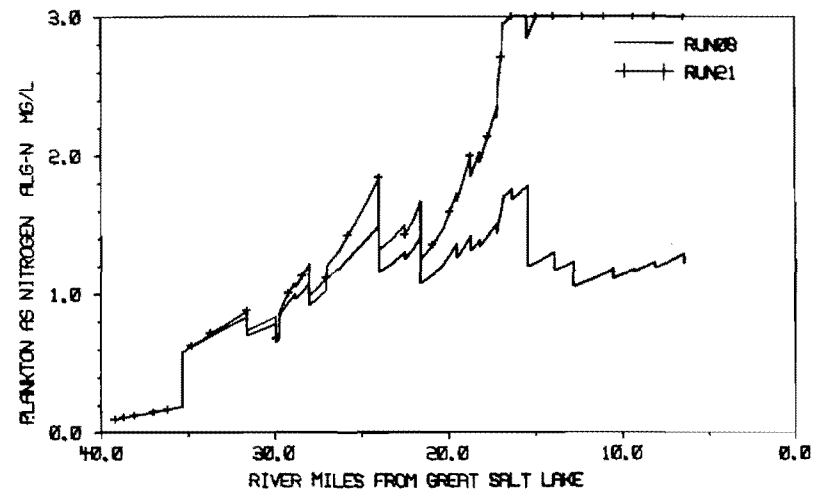


(b) Filter estimates and measured values

Figure 5.45. Estimation of the nitrogen cycle coefficients - NO<sub>3</sub>-N results (run 21) (1 mile = 1.61 km).

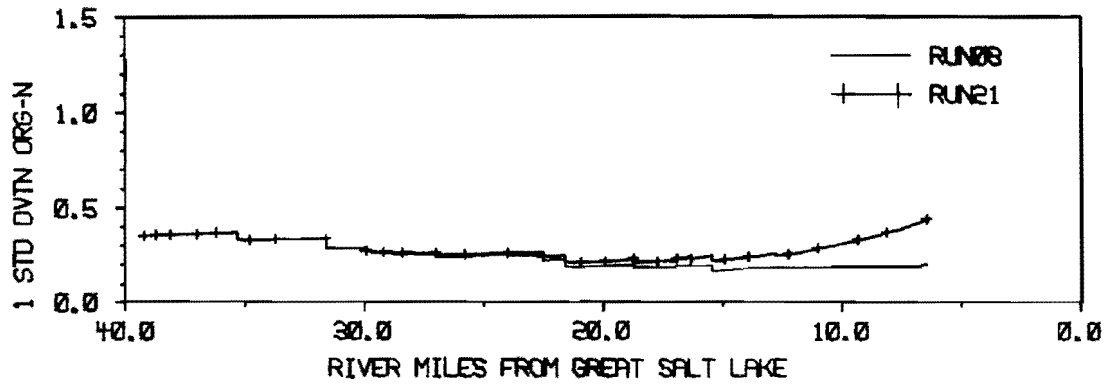


(a) Estimation and measurement errors

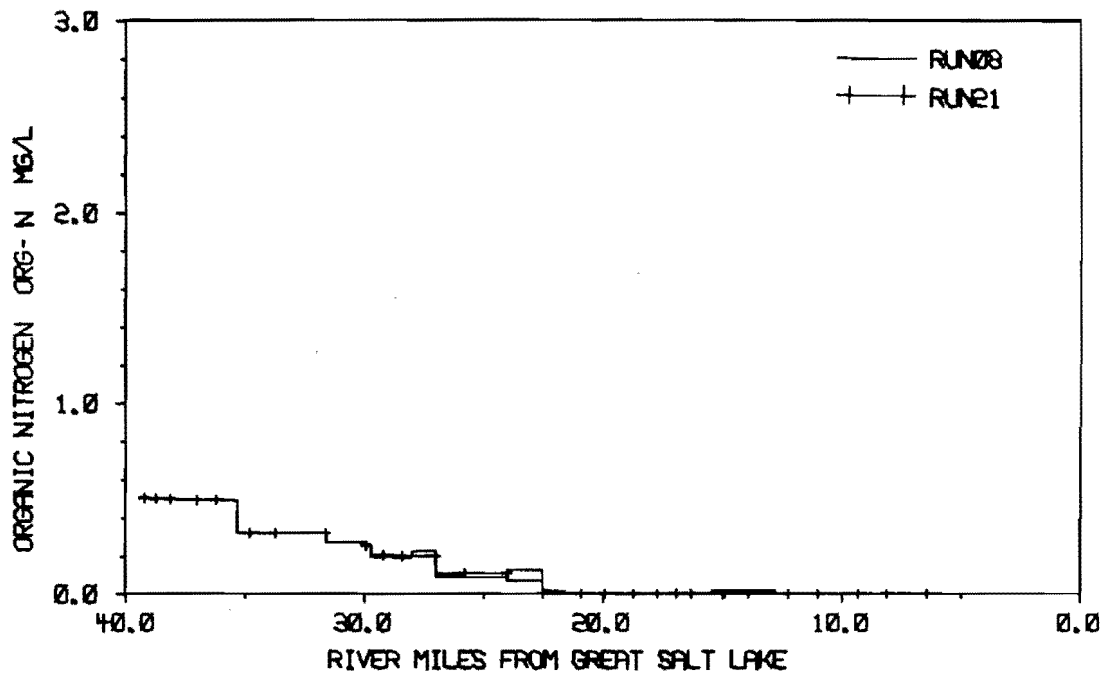


(b) Filter estimates and measured values

Figure 5.46. Estimation of the nitrogen cycle coefficients - ALG-N results (run 21) (1 mile = 1.61 km).



(a) Estimation and measurement errors



(b) Filter estimates and measured values

Figure 5.47. Estimation of the nitrogen cycle coefficients - ORG-N results (run 21) (1 mile = 1.61 km).

the process model variances associated with the coefficients. This would raise the estimation error of  $\text{NH}_3\text{-N}$  and hence reduce the weighting on the process model predictions.

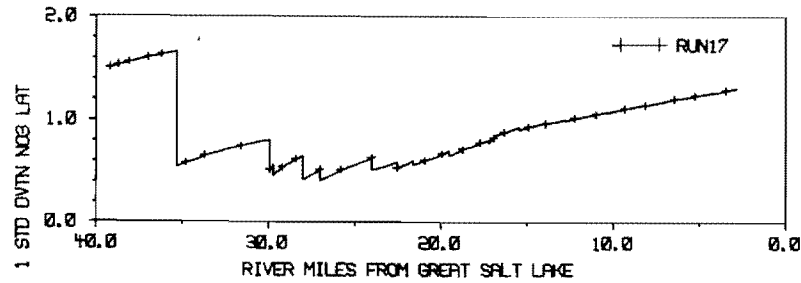
Divergence in the other water quality parameters appears to be strongly related to the divergence of  $\text{NH}_3\text{-N}$ . It is interesting to note that the filter estimates for BOD are unchanged. This is the case because in the process model BOD is independent of all the other water quality parameters and also independent of each of the five coefficients estimated in run 21.

In the presence of divergence it is not possible to draw conclusions about the values estimated for the five coefficients. It is noted however, that before divergence becomes severe, the estimates of  $K_{23}$  and  $K_{45}$  from run 21 are similar to those in runs 15 and 16, respectively (see Figures 5.37 and 5.38, respectively).

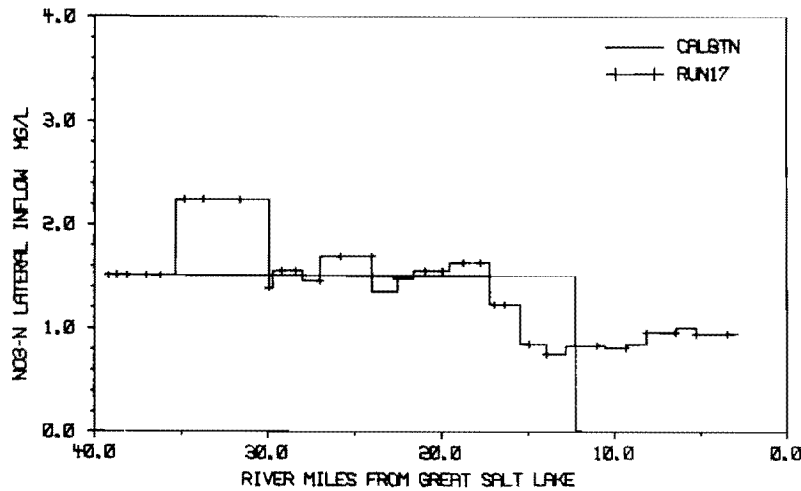
#### $\text{NO}_3\text{-N}$ lateral inflow estimation

Non-point sources of pollution are diverse and difficult, if not impossible, to measure. In conventional river water quality modeling the assignment of concentrations to various parameters in lateral inflow is an art which at best requires the exercise of engineering judgment, and which at worst is arbitrary in nature. Therefore, any light is welcome that can be thrown on the levels of the concentrations through the coefficient estimation procedures of the EKF.

The filter estimates for  $U_3$ , the lateral inflow concentration of  $\text{NO}_3\text{-N}$ , show the general trend of higher levels upstream, and lower levels downstream. The trend was observed in other studies on the Jordan River, and is used for the calibration in this study (see Figure 5.48).

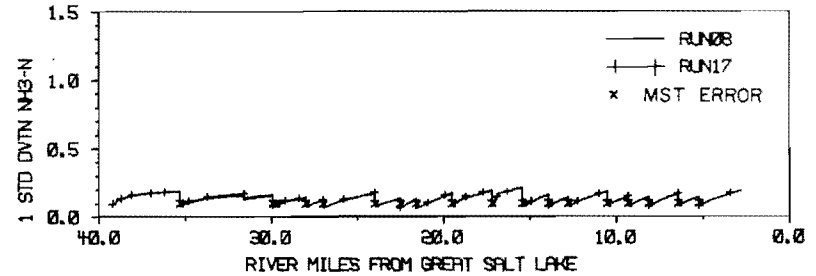


(a) Estimation and measurement errors

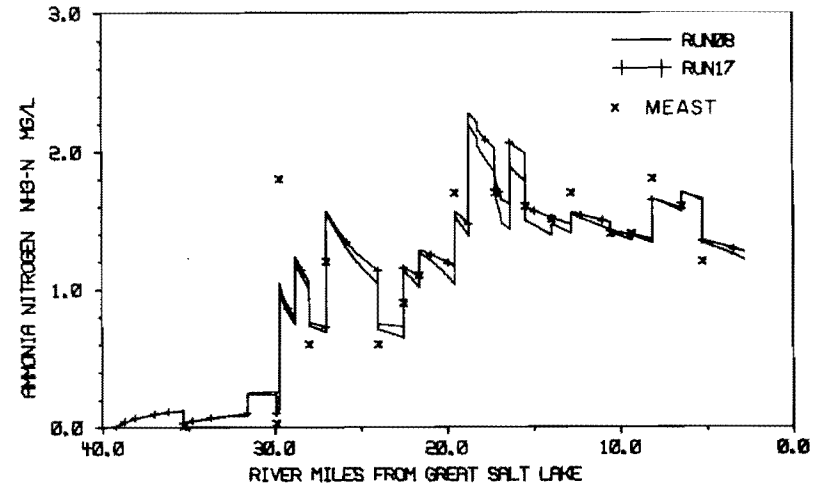


(b) Filter estimates and measured values

Figure 5.48. Lateral inflow concentration estimation for  $\text{NO}_3\text{-N}$  -  $\text{NO}_3\text{-N}$  lateral inflow results (run 17) (1 mile = 1.61 km).



(a) Estimation and measurement errors



(b) Filter estimates and measured values

Figure 5.49. Lateral inflow concentration estimation for  $\text{NO}_3\text{-N}$  -  $\text{NH}_3\text{-N}$  results (run 17) (1 mile = 1.61 km).

Results for the other water quality parameters affected by the estimation of  $U_3$  are shown in Figures 5.49 through 5.52. The estimation errors from  $\text{NO}_3\text{-N}$ ,  $\text{ALG-N}$  and  $\text{ORG-N}$  are increased by the introduction of  $U_3$  uncertainty and consequently filter estimates for the parameters are closer to the measurements.

#### $\text{NH}_3\text{-N}$ lateral inflow estimation

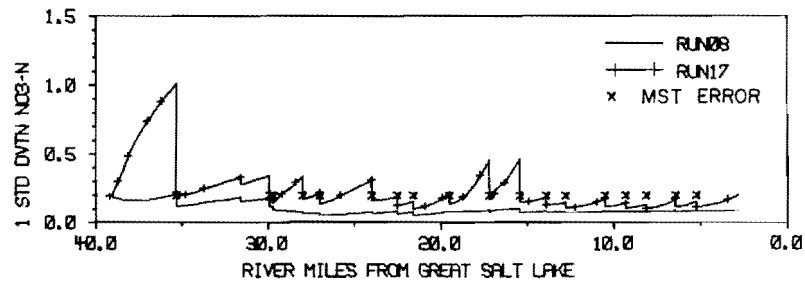
The filter estimates for  $U_2$ , the lateral inflow concentration of  $\text{NH}_3\text{-N}$ , are in quite good agreement with calibration values except below river mile 12.0 (19.3 km) (see Figure 5.53). It is interesting to note that the 0.8 mg/l level estimated by the filter below river mile 12.0 (19.3 km) is similar to the 0.9 mg/l level found by Dixon et al. (1975) for these reaches. However, in the calibration of the deterministic process model other available evidence pointed to a negligible concentration of  $\text{NH}_3\text{-N}$  in the lateral inflow of this downstream stretch of the Jordan River. The results of other water quality parameters affected by the estimation of  $U_2$  are shown in Figures 5.54 through 5.57.

#### Computational Requirements

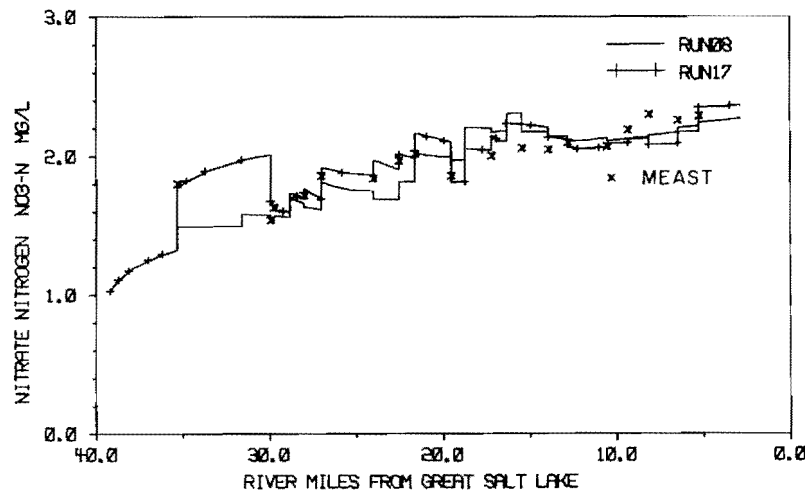
Figure 5.58 provides a comparison of the computational requirements for the techniques applied in this study. The comparison is in terms of the cost of the computer runs, adjusted to account for the different lengths of the river represented in some runs. The basic filter run costs almost double the cost of the deterministic process model run. The smoothing run costs approximately four times the cost of the deterministic process model run.

Some researchers have reported that computer costs for filter techniques are proportional to the cube of the order of the state vector. However, the three different size state vectors used in this study point to a relationship between the order of the state vector and computer costs that involves an index of less than 2.



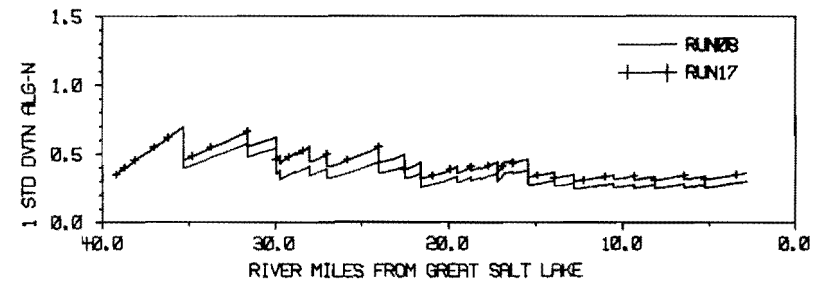


(a) Estimation and measurement errors

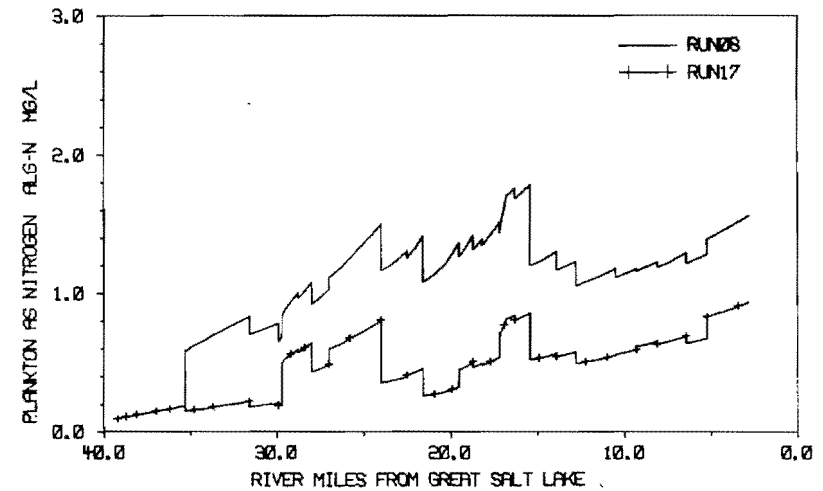


(b) Filter estimates and measured values

Figure 5.50. Lateral inflow concentration estimation for  $\text{NO}_3\text{-N} - \text{NO}_3\text{-N}$  results (run 17) (1 mile = 1.61 km).

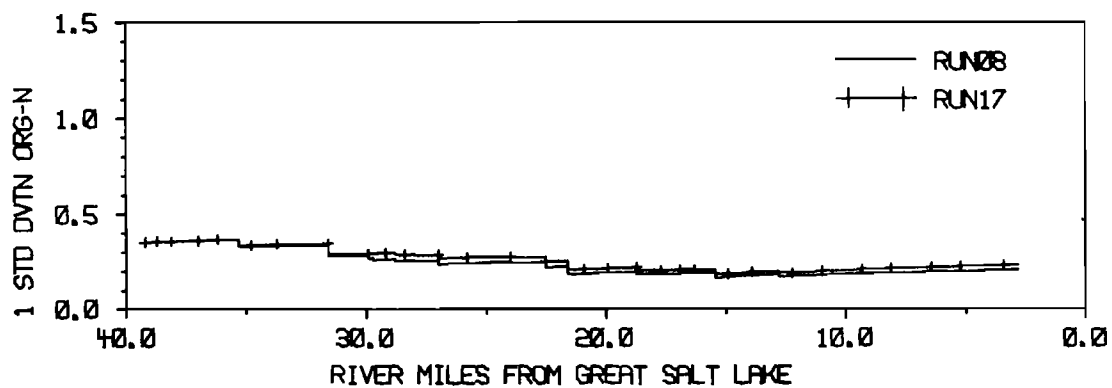


(a) Estimation and measurement errors

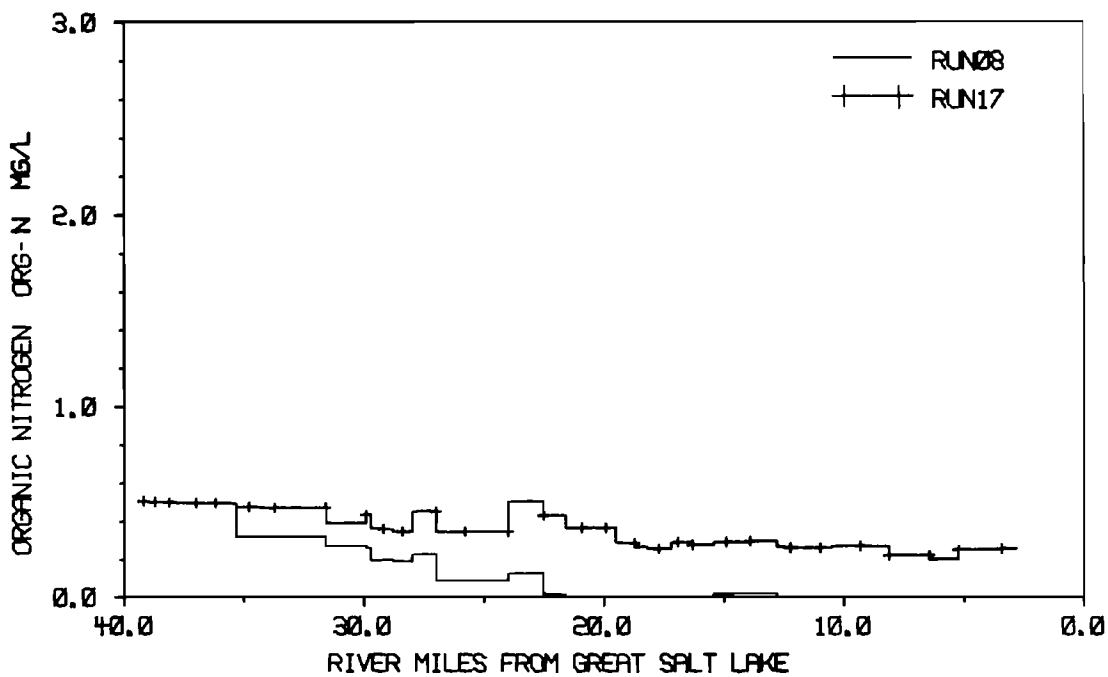


(b) Filter estimates and measured values

Figure 5.51. Lateral inflow concentration estimation for  $\text{NO}_3\text{-N} - \text{ALG-N}$  results (run 17) (1 mile = 1.61 km).

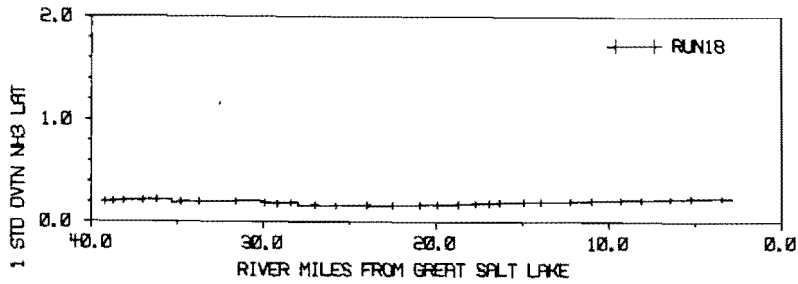


(a) Estimation and measurement errors

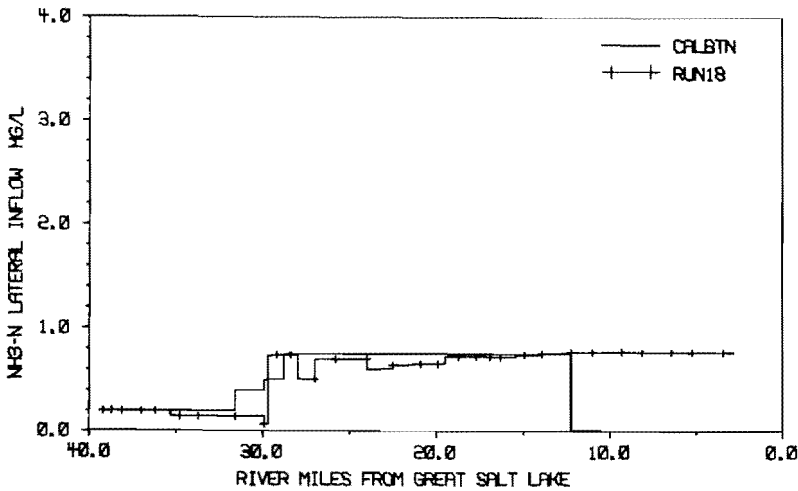


(b) Filter estimates and measured values

Figure 5.52. Lateral inflow concentration estimation for  $\text{NO}_3\text{-N} - \text{ORG-N}$  results (run 17) (1 mile = 1.61 km).

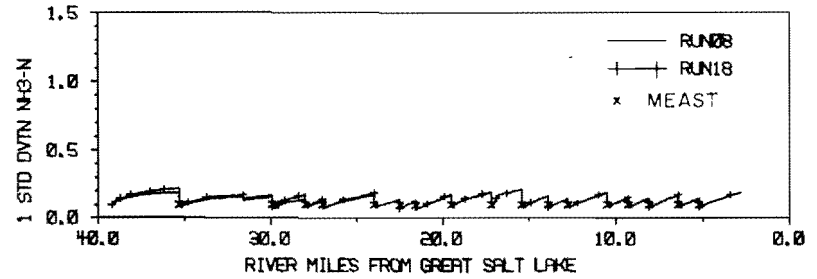


(a) Estimation and measurement errors

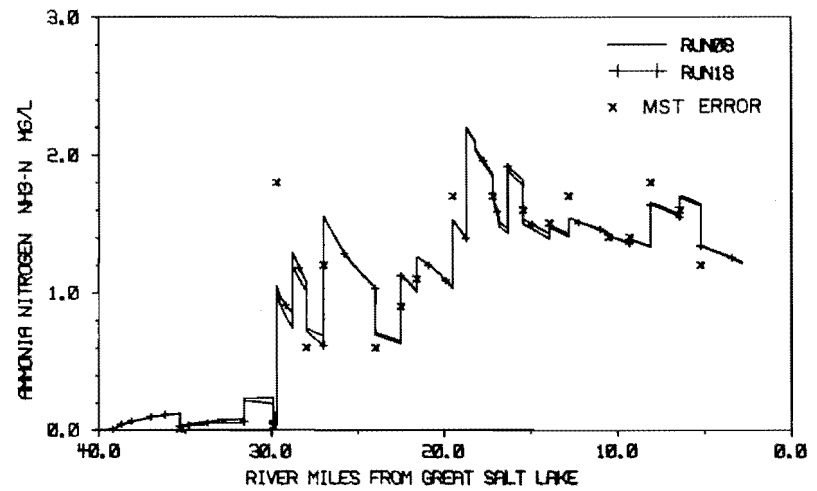


(b) Filter estimates and measured values

Figure 5.53. Lateral inflow concentration estimation for  $\text{NH}_3\text{-N} - \text{NH}_3\text{-N}$  lateral inflow results (run 8) (1 mile = 1.61 km).

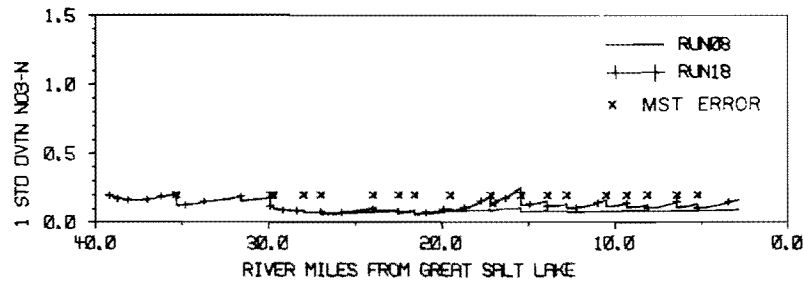


(a) Estimation and measurement errors

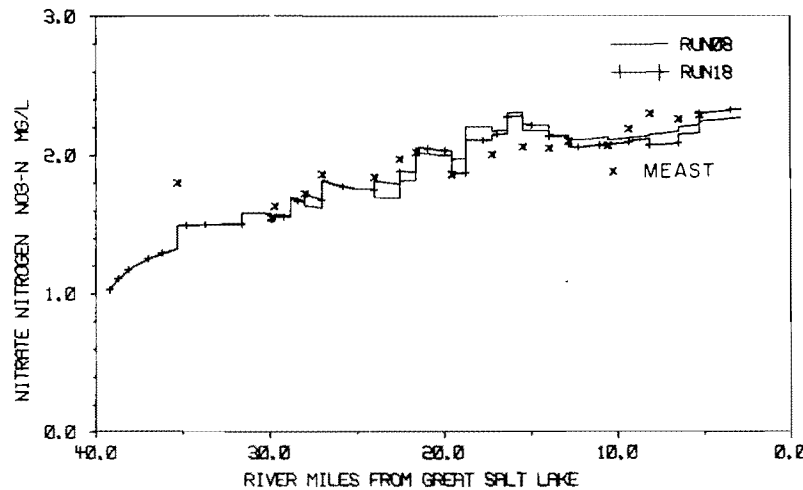


(b) Filter estimates and measured values

Figure 5.54. Lateral inflow concentration estimation for  $\text{NH}_3\text{-N} - \text{NH}_3\text{-N}$  results (run 18) (1 mile = 1.61 km).

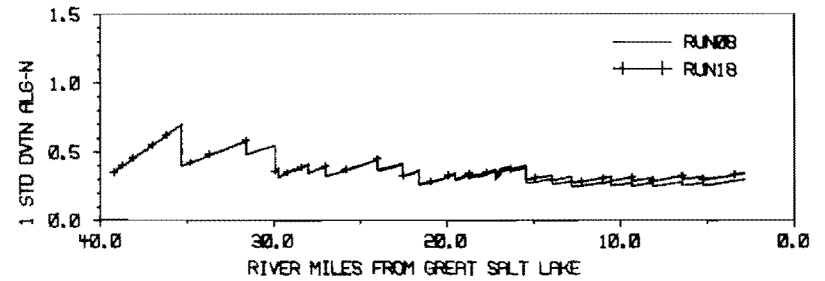


(a) Estimation and measurement errors

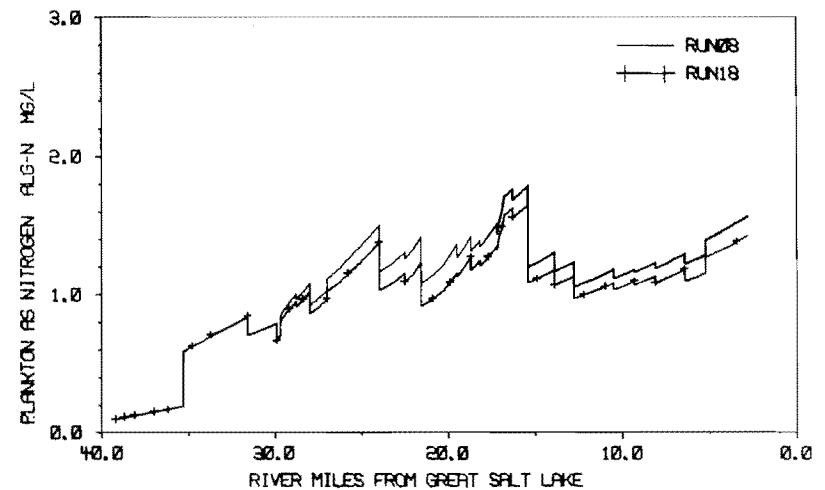


(b) Filter estimates and measured values

Figure 5.55. Lateral inflow concentration estimation for  $\text{NH}_3\text{-N} - \text{NO}_3\text{-N}$  results (run 18) (1 mile = 1.61 km).

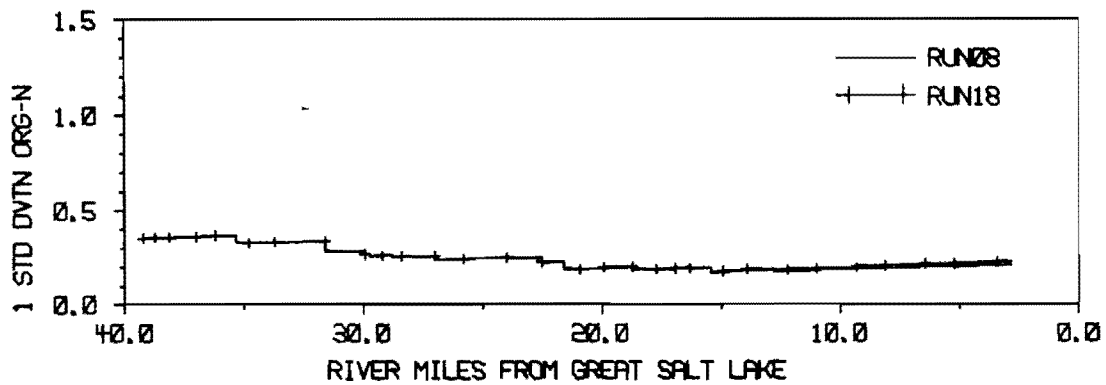


(a) Estimation and measurement errors

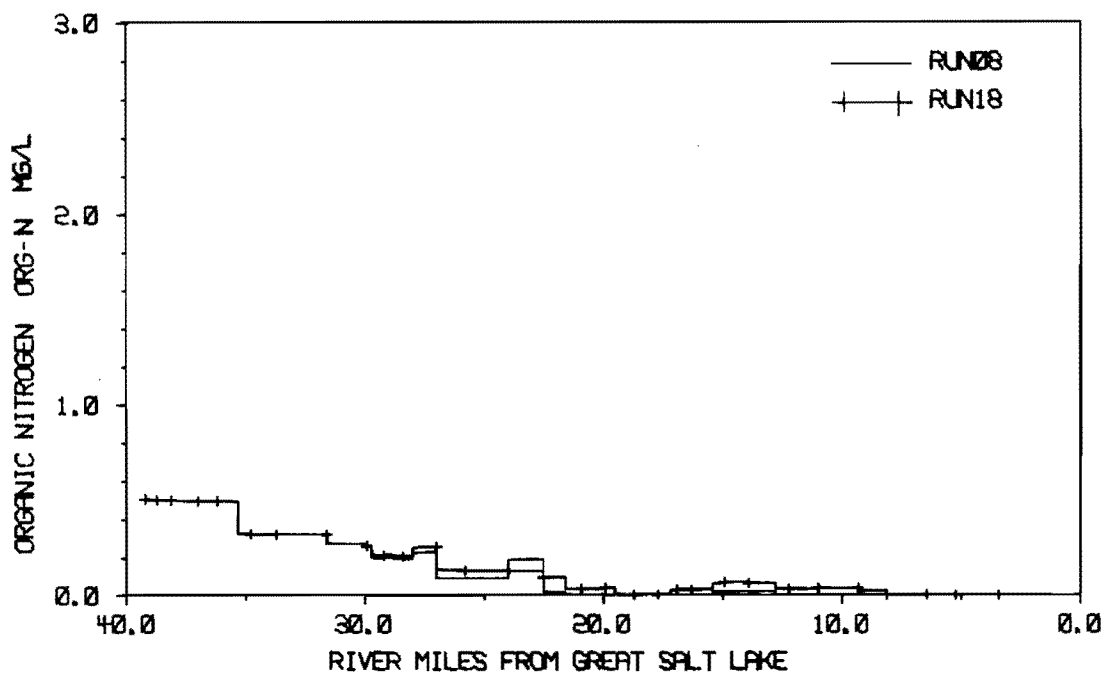


(b) Filter estimates and measured values

Figure 5.56. Lateral inflow concentration estimation for  $\text{NH}_3\text{-N} - \text{ALG-N}$  results (run 18) (1 mile = 1.61 km).



(a) Estimation and measurement errors



(b) Filter estimates and measured values

Figure 5.57. Lateral inflow concentration estimation for  $\text{NH}_3\text{-N}$  - ORG-N results (run 18) (1 mile = 1.61 km).

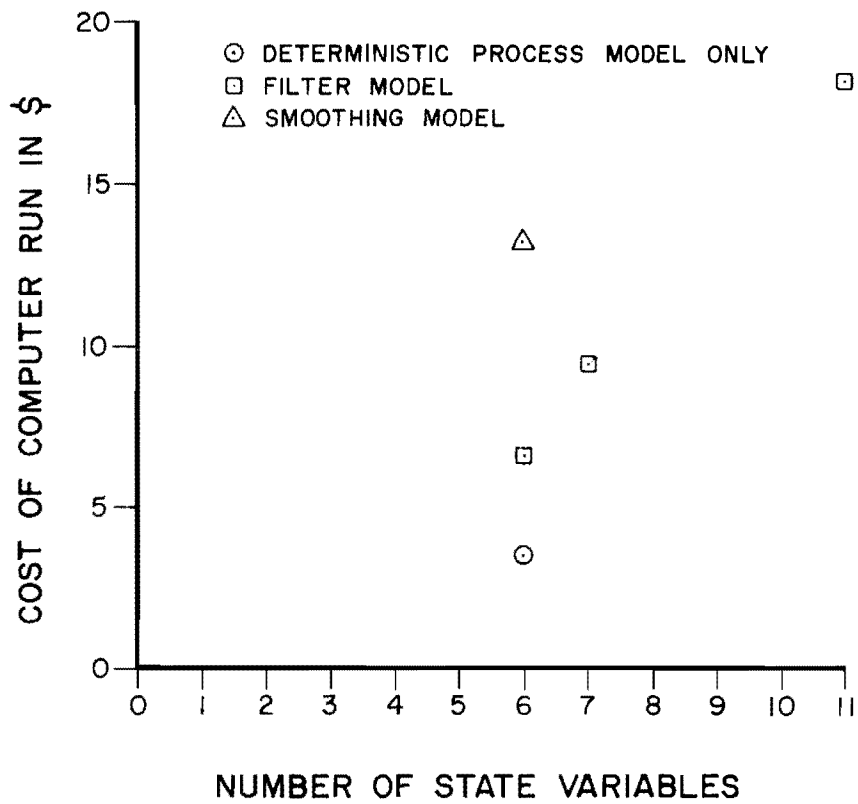


Figure 5.58. Comparison of the costs of computer runs.

## CHAPTER 6

## SUMMARY, CONCLUSIONS, AND RECOMMENDATIONS

Summary

The extended Kalman filter (EKF) is used to represent BOD, DO, and nitrogen cycling in a 36.4 mile (58.6 km) stretch in the Jordan River, Utah, under the assumption of steady-state conditions. Approximate minimum variance estimates of the water quality parameters are provided by the EKF filter. These estimates are obtained through a combination of two independent estimates of the state of the river water quality system: (1) predictions of the system state from a "phenomenologically meaningful" process model of the biochemical and stream transport processes; and (2) measurements of the water quality parameters. These two estimates are combined by a weighting procedure based on the uncertainties associated with the process model predictions and the measurements. The EKF also yields an estimation error covariance matrix from which confidence limits for the accuracy of the parameter estimates are obtained.

A sequential arrangement of extended Kalman filters is utilized. Each EKF in the sequence represents a river reach for which hydraulic and water quality characteristics are fairly uniform. Initial conditions for each EKF are based on the final conditions of the previous EKF adjusted to represent the effect of point loads or tributaries discharging into the main river between the two reaches.

A trial-and-error calibration procedure is used to obtain values for the model coefficients in the process model operated as a deterministic model independent of the filter. Determination of values for the Q matrix by a trial-and-error procedure is described. The approach is based on the

requirement that the mean square error of the differences between the filter estimates and the measurements be not less than the measurement noise variance.

A property of the EKF is that information contained in the measurements is used only in subsequent estimates of the system state. Therefore, information in the measurements is used only downstream of the sampling point at which the measurement was taken. To make use of the measurements in both the up- and downstream directions a fixed-interval smoothing algorithm (FIS) is implemented. This technique combines state estimates from filter passes in the up- and downstream directions. Sequential linearized Kalman filters are used for the pass in the upstream, or backward direction. Unlike the forward and backward estimates of the estimation error ( $P$ ), the smoothed values are not characterized by discrete jumps at sampling points. Instead, the estimation error rises to a peak approximately midway between sampling locations. This characteristic indicates that when information from all the measurements is used confidence in the estimates decreases with distance from the adjacent sampling points. Smoothed values of  $P$  are less than the values obtained from applying the forward EKF alone; thus indicating that the estimates obtained from the FIS are better, in a minimum variance sense, than the estimates obtained from the forward EKF.

To assist in gaining familiarity with the filtering technique, several sensitivity studies are performed. The sensitivity of filter estimates to changes in the following statistics was investigated: the process model noise variance, the measurement noise variance, the initial estimation error variance, and the point load estimation error variance. A large value for the process model noise variance has the effect of: (1) increasing the rate of growth of the estimation error, and (2) placing additional weighting on the measurements because the larger estimation error implies less confidence



in the process model predictions. At sampling points the measurement update procedure always results in an estimation error less than the measurement noise regardless of the values used for the process model noise variances. Changing the values of the measurement noise affects (1) the level of the estimation error after measurement updates, and (2) the weighting given to measurements. A larger initial estimation error variance gives relatively more weighting to the measurements but this effect decreases with distance from the upstream boundary. The sensitivity study on the point load estimation error variances indicates a small, but noticeable, effect on the estimation errors, and therefore, a slight effect on the state estimates via the weighting procedure.

The capability of estimating model coefficients and lateral inflow concentrations simultaneously with the water quality parameters is demonstrated. In one run five coefficients in the equations describing nitrogen cycling are estimated. This run also provides an example of filter divergence.

### Conclusions

The following conclusions have been developed from the results and experience gained during this study:

1. A steady-state filter model has been developed which is capable of immediate application to any stream for which the process model described in Chapter 4 is suitable, and for which the appropriate measurements are available.
2. In general, the filter estimates were quite similar to the deterministic process model estimates with the exception of ALG-N and ORG-N. The differences for these parameters are due to information contained in the measurement vector  $\underline{Z}$ , and the relatively low confidence placed in the

measurements of (ALG-N + ORG-N). This illustrates two important reasons for using estimation theory, namely: (a) to make use of the information content of the measurements, and (b) to allow for an explicit treatment of the uncertainties associated with the system, the model, the data, and the model responses.

3. Estimation theory provides values for the estimation-error associated with filter estimates. Values of the estimation error covariances matrix (P) varied from a coefficient of variation of almost zero for DO to a coefficient of variation in excess of 1.0 for ALG-N and ORG-N (see Figures 5.9 through 5.15). These values are potentially useful for establishing tolerances on stream quality standards which are reasonable in terms of our ability to estimate the true state of stream water quality using available measurements and current understanding of the stream processes expressed in the form of a mathematical process model.

4. Apart from the determination of approximate minimum variance estimates of the true state of a river water quality system, the current model could be used to design a stream sampling program. Under the assumption of steady-state conditions the location of sampling points and the parameters to be measured could be determined. This could be achieved by formulating constraints defining the maximum acceptable estimation errors associated with each parameter, and by locating sampling points such that these constraints are met. The estimation errors depend on the spacing of sampling points and are independent of the actual measurement values. Therefore, no data are required to design the stream sampling program. However, a trade-off relationship exists between the spacing of sampling points and the adequacy of the process model. If a poor process model is used, then estimation errors grow rapidly, and more frequent samples are required to meet the estimation

error constraint. In contrast less frequent samples are needed to meet the constraint if a precise process model is used because in this case, estimation errors grow at a slower rate.

5. The estimation theory techniques applied herein are not suitable for long-term forecasting or for predicting the effects of management changes on the river water quality system. The reason for this is simply that measurements, needed for updating, do not exist in either of these situations. However, indirect benefits may be gained through using the EKF for model identification, or for estimating coefficients and lateral inflow concentrations prior to long-term forecasting or management runs using the deterministic process model alone.

6. Application of the fixed-interval smoothing algorithm reduced the estimation error variances but smoothed estimates are not significantly different from the filtered estimates. However, an advantage of applying the smoothing algorithm to the steady-state problem is that the abrupt changes in both  $P$  and  $\underline{X}$  are smoothed out as a result of using the information contained in the measurements in both the up- and downstream directions.

7. The determination of suitable variances for the Q matrix appears to be a significant and complex step in applying the EKF. Experience does not seem to help in establishing a Q matrix a priori. The problem becomes more complicated if an estimation error covariance matrix for each point load also is estimated. Whenever the model structure is changed, a new Q matrix should be determined. Also, the Q matrix that worked satisfactorily for the filter run was found to be unsuitable for a smoother run on the entire study section of the Jordan River.

8. Use of the EKF for coefficient estimation requires a fresh determination of the Q matrix. This is partly because process model noise variances for the new state variables must be estimated and also because the

process noise variances of the original state variables may be reduced to offset the introduction of process model noise via some of the model coefficients. In addition, initial values for the estimation error covariance matrix must be estimated when coefficients are estimated. A trial-and-error determination of  $P(\xi_0)$  and  $Q$  may require several computer runs. Filter estimation for a single model coefficient may be largely determined by the previous calibration values for the coefficient. This conclusion is based on the results for  $K_{45}$ . Estimates of state variables are unconstrained and unrealistic values of model coefficients may result. An example of this, is the negative values obtained for the nitrification rate,  $K_{23}$ .

9. The sensitivity study on the point load estimation error variances showed that the impact on both filter estimates and estimation errors can be noticeable. Hence, the need for considering the accuracy with which the concentrations of point load constituents are known, is demonstrated. This approach could be used to assist in establishing tolerances on effluent standards.

10. Computer costs associated with estimation theory techniques are higher than the costs of running the corresponding process model as a purely deterministic model. Costs rise as the number of state variables are increased. In addition, the trial-and-error determination of suitable values for the  $Q$  matrix can be a very expensive task. However, the additional computer costs should be weighed against the utility that can be derived from the estimation error covariance matrix and the improved estimates of state (coefficients and lateral inflow concentrations).

#### Recommendations

The following recommendations for further work are based on the experience gained during this study:

1. During filter runs estimates for ORG-N,  $K_{23}$ , and  $K_{52}$  became negative. In each case, these negative values did not have a valid physical interpretation. Therefore, it is recommended that a modification to the EKF should be explored, in which state variables can be constrained to lie within a reasonable range of values.

2. Determination of suitable values for the Q matrix was found to be a costly and complex process. The trial-and-error technique adopted in this study could be developed into an automatic search procedure to satisfy an objective function based on the closeness of MSE to the corresponding variances in R while satisfying the constraint that  $MSE_i \geq R_{ii}$  for all measured variables. However, this procedure would lead to a single value for Q to be used throughout the filter run. If more data are available than was the case in this study, it is recommended that adaptive filtering techniques be explored as an approach for simultaneously estimating Q and the state vector. A decision-directed adaptive filtering algorithm such as that by Nahi and Schaeffer (1972) is recommended.

3. The applicability of the current filter model should be extended to allow for the simulation of river systems that include tributaries. Also, streamflow should be added as a state variable if computer funds are sufficient to run the filter with the expanded state vector. In this way uncertainties in streamflow will be incorporated into the estimation errors of the water quality parameters.

4. Consideration should be given to adding other water quality parameters to the state vector. Computer costs may be reduced by breaking the state vector into independent components and running each component as a separate model (Lettenmaier, 1975). For example, a state vector containing streamflow, stream temperature, BOD, DO,  $NH_3-N$ ,  $NO_3-N$ , ALG-N, ORG-N and

coliform, could be divided into: (a) streamflow-stream temperature, (b) streamflow-BOD- DO-nitrogen cycling, and (c) streamflow-coliform.

5. To extend the EKF technique to situations in which dispersion is an important stream transport process two possibilities exist: (a) a filter capable of modeling the second-order advection-diffusion equation could be developed; and (b) a mathematical procedure suitable for transforming the second-order advection-dispersion equation into first-order differential equations could be developed. Pimentel and Brewer (1975) have developed such a transformation for dispersion alone but their procedure does not cover the combined advection-dispersion situation.

6. The application of estimation theory to other types of water resources problems should continue. In particular, the problems of real time, short-term river flow forecasting, and reservoir operation appear to be promising possibilities.

7. The model for algal uptake of nitrogen in the ammonia and nitrate forms (Equations 4.11 and 4.14) should be tested using laboratory experiments.

## LITERATURE CITED

- Barnham, P.M., and D.E. Humphries. 1970. Further comments on the derivation of Kalman filters - Section I. Derivation of the Kalman filtering equations from elementary statistical principles. In: C.T. Leondes (Ed.). Theory and application of Kalman filtering. North Atlantic Treaty Organization, Advisory Group for Aerospace Research. pp.43-49.
- Beck, B., and P. Young. 1976. Systematic identification of DO-BOD model structure. Journal of the Environmental Engineering Division, Proceedings of the American Society of Civil Engineers, 102(EE5): 909-927.
- Beck, M.B. 1973. Control and systems theory applied to problems of river pollution. Ph.D. dissertation, University of Cambridge, Cambridge, England. (Original not seen).
- Beck, M.B. 1975. The identification of algal population dynamics in a freshwater stream. In: G.C. Vansteenkiste (Ed.). Modeling and simulation of water resources systems. North-Holland Publishing Company. pp.483-496.
- Bennett, J.P., and R.E. Rathbun. 1972. Reaeration in open-channel flow. Professional Paper 737, U.S. Geological Survey. p.56.
- Bowles, D.S., and W.J. Grenney. 1976a. River water quality modeling: A combined deterministic-stochastic approach. Proceedings of the Second International Association for Hydraulic Research Symposium on Stochastic Hydraulics, Lund, Sweden. pp.42.1-25.
- Bowles, D.S. and W.J. Grenney. 1976b. Steady-state river quality modeling by sequential extended Kalman filters. Paper presented at the American Geophysical Union Fall Annual Meeting, San Francisco, California. 25 p.
- Box, G.E.P., and D.M. Jenkins. 1970. Time series analysis forecasting and control. Holden-Day. 553 p.
- Bras, R.L., and I. Rodriguez-Iturbe. 1975. Rainfall-runoff as spatial stochastic processes: Data collection and synthesis. Report No.196, Ralph M. Parsons Laboratory, Massachusetts Institute of Technology, Cambridge, Massachusetts. 382 p.
- Brewer, J.W., and S.F. Moore. 1974. Monitoring: An environmental state estimation problem. Journal of Dynamic Systems, Measurement, and Control, Transactions of the American Society of Mechanical Engineers, 96(3):363-365.

- Caperon, J., and J. Meyer. 1972. Nitrogen-limited growth of marine phytoplankton - II. Uptake kinetics and their role in nutrient limited growth of phytoplankton. *Deep-Sea Research*, 19:618-632.
- Gauss, K.F. 1821. *Wenke, Gottingen*, 4. (Original not seen).
- Dixon, L.S., M.C. Teuscher, and W.J. Grenney. 1975. Assessment of proposed river management and planning alternatives by water quality simulation modeling. Report No. PRWA20-3, Utah Water Research Laboratory, College of Engineering, Utah State University, Logan, Utah. 77 p.
- Gelb, A. (Ed.) 1974. *Applied optimal estimation*. The Massachusetts Institute of Technology Press. 374 p.
- Graupe, D., D. Isailovic, and V. Yevjevich. 1975. Prediction model for runoff from karstified catchments. *Proceedings of the Bilateral United States-Yugoslavian Seminar in Karst Hydrology and Water Resources*, Dubrovnik, Yugoslavia. 17 p. (Draft copy seen).
- Harr, S.L., A.G. Hely, and R.W. Mower. 1971. *Water resources of Salt Lake County, Utah*. Technical Publication No.31, Department of Natural Resources, State of Utah. 243 p.
- Helweg, O.J. 1975. *A salinity management strategy for stream-aquifer systems*. Ph.D. dissertation, Colorado State University, Fort Collins, Colorado. 122 p.
- Hogg, R.V., and A.T. Craig. 1970. *Introduction to mathematical statistics*. Third Edition. The Macmillan Company, London. p. 168.
- Hydrologic Research Laboratory. 1976. Appendix A-Priority Research Subjects, Solicitation No. 6-35229. Department of Commerce, National Oceanic and Atmospheric Administration, National Weather Service, Office of Hydrology, Hydrologic Research Laboratory, Silver Springs, Maryland. 3 p.
- Hydroscience, Inc. 1976. Task 310 Report, Evaluation of Jordan River water quality. Report to Salt Lake County, Utah. (Draft copy seen).
- Jazwinski, A.H. 1969. Adaptive filtering. *Automatica*, 5:475-485.
- Jazwinski, A.H. 1970. *Stochastic processes and filtering theory*. Academic Press, New York. 376 p.
- Kalman, R.E. 1960. A new approach to linear filtering and prediction problems. *Transactions of the American Society of Mechanical Engineers, Journal of Basic Engineering*, 82(2):35-45.
- Kalman, R.E. 1963. New methods in Weiner filtering theory. Chapter 9, *Proceedings of the First National Symposium on Applications of Random Function Theory and Probability*. Wiley. pp. 270-389. (Original not seen).



- Kalman, R. E., and R. S. Bucy. 1961. New results in linear filtering theory. Transaction of American Society of Mechanical Engineers, Journal of Basic Engineering, 83(2):95-107.
- Koivo, A. J., and G. Phillips. 1976. Optimal estimation of DO, BOD, and stream parameters using a dynamic discrete-time model. Water Resources Research, 12(4):705-711.
- Kreider, D. L., R. G. Kuller, D. R. Ostberg, and F. W. Perkins. 1966. An introduction to linear analysis. Addison-Wesley Publishing Company, Inc. p. 290.
- Lee, E. A. 1972. Analysis, modeling, and forecasting of stochastic water quality systems. Contribution No. 110, Kansas Water Resources Research Institute, Manhattan, Kansas. 496 p.
- Lee, E. S., and I. K. Hwang. 1971. Dynamic modeling of stream quality by invariant imbedding. Water Resources Bulletin, 7(1):102-114.
- Legendre, A. M. 1806. Nouvelles methods pour la determination des orbits des cometes. Paris. (Original not seen).
- Leondes, C. T. (Ed.) 1970. Theory and applications of Kalman filtering. North Atlantic Treaty Organization, Advisory Group for Aerospace Research and Development. Available from National Technical Information Service, U. S. Department of Commerce, Springfield, Virginia. 537 p.
- Lettenmaier, D. P. 1975. Design of monitoring systems for detection of trends in stream quality, Technical report No. 39, Charles W. Harris Hydraulics Laboratory, Department of Civil Engineering, University of Washington, Seattle, Washington. 203 p.
- Lettenmaier, D. P., and S. J. Burges. 1976. Use of state estimation techniques in water resource system modeling. Water Resources Bulletin, 12(1):83-99.
- Moore, S. F. 1971. The application of linear filter theory to the design and improvement of measurement systems for aquatic environments. Ph.D. dissertation, University of California, Davis, California. 133 p.
- Moore, S. F. 1973. Estimation theory applications to design of water quality monitoring systems. Journal of the Hydraulics Division, Proceedings of the American Society of Civil Engineers, 99(HY5): 815-831.
- Moore, S. F., and J. W. Brewer. 1972. Environmental control systems: Treatment of uncertainty in models and data. Proceedings of the International Symposium on Uncertainties in Hydrologic and Water Resource Systems, Tucson, Arizona. pp. 16-28.

- Moore, S.F., G.C. Dandy, and R.J. deLucia. 1976. Describing variance with a simple water quality model and hypothetical sampling programs. *Water Resources Research*, 12(4):795-804.
- Nahi, N.E., and B.M. Schaeffer. 1972. Decision-directed adaptive recursive estimations: divergence prevention. *Institution of Electrical and Electronics Engineers, Transactions on Automatic Control*, AC-17(1):61-68.
- Özgören, M.K., R.W. Longman, and C.A. Cooper. 1974. Stochastic optimal control of artificial river aeration. *Proceedings of 1974 Joint Automatic Control Conference, American Institute of Chemical Engineers*. pp. 235-245.
- Pearce, B.R., R.N. DeGuida, G.C. Dandy, and S.F. Moore. 1975. Sampling network design for dispersion verification. *Proceedings of the Symposium on Modeling Techniques, San Francisco, California*. pp. 368-379.
- Perlis, H.J., and B. Okunseinde. 1974. Multiple Kalman filters in a distributed stream monitoring system. *Proceedings of 1974 Joint Automatic Control Conference, American Institute of Chemical Engineers*. pp. 615-623.
- Pimental, K.D., and J.W. Brewer. 1975. Toward a mathematical theory of environmental monitoring. Paper presented at the Winter Annual Meeting of the Automatic Control Division of the American Society of Mechanical Engineers, Houston, Texas. 15 p.
- Prasad, R. 1967. A nonlinear hydrologic system response model. *Journal of the Hydraulics Division, Proceedings of the American Society of Civil Engineers*, 93(HY4):201-221.
- Riley, J.P. 1970. Computer simulation of water resource systems. *Proceedings of the Second International Seminar for Hydrology Professors, Logan, Utah*. pp. 249-274.
- Schmidt, G.T. 1976. Linear and nonlinear filtering techniques. In: C.T. Leondes (Ed.). *Control and Dynamic Systems*, Academic Press. 12:63-98.
- Schwartz, L., and E.B. Stear. 1968. A computational comparison of several nonlinear filters. *Institute of Electrical and Electronics Engineers, Transactions on Automatic Control*, AC-13(1):83-86.
- Schweppe, F.C. 1973. *Uncertain dynamic systems*. Prentice-Hall Electrical Engineering Series. 563 p.
- Stone, H.L., and P.L.T. Brian. 1963. Numerical solution of convective transport problems. *Journal of the American Institute of Chemical Engineers*. 9(5).

- Unny, T.E. 1976. Transient and non-stationary random processes. A general lecture presented at the Second International Association for Hydraulic Research Symposium on Stochastic Hydraulics, Lund, Sweden. 41 p.
- Whitehead, P., and P. Young. 1975. A dynamic-stochastic model for water quality in part of the Bedford-Ouse River System. In: G.C. Vansteenkiste (Ed.). Modeling and Simulation of Water Resources Systems. North-Holland Publishing Company. pp. 417-438.
- Wiener, N. 1949. The extrapolation, interpolation, and smoothing of stationary time series. Wiley. 163 p.
- Yevjevich, V. 1971. Stochasticity in geophysical and hydrologic time series. Nordic Hydrology, II:217-242.
- Yevjevich, V. 1974. Determinism and stochasticity in hydrology. Journal of Hydrology. 22:225-238.
- Young, P. 1974. Recursive approaches to time series analysis. The Institute of Mathematics and its Applications. May/June. pp.209-224.
- Young, P., S.M. Shellswell, and C.G. Neethling. 1971. A recursive approach to time series analysis. Report TR 16, Control and Systems Division, University of Cambridge, Cambridge, England. 69 p.
- Young, P., and P. Whitehead. 1975. A recursive approach to time-series analysis for multivariable systems. In: G.C. Vansteenkiste (Ed.) Modeling and Simulation of Water Resources Systems. North-Holland Publishing Company. pp. 39-57.

APPENDIX A

## APPENDIX A

## USERS MANUAL FOR COMPUTER PROGRAMS

Three computer programs were developed for this study. The relationships between the programs are illustrated by Figure 3.4. EKFLKF is the filter model including the extended Kalman filter (EKF), linearized Kalman filter (LKF), and fixed interval smoothing algorithm (FIS). Results from filter runs are written onto a computer disk storage device, sorted by the data sorting program (PRSORT), and dumped onto punched cards. These punched cards are subsequently read by the plotting program (P) which produces continuous plots of the filter results. This appendix is divided into three parts:

	Page
I. Filter model (EKFLKF)	149
II. Data sorting program (PRSORT)	187
III. Plotting program (P)	193

I. Filter Model (EKFLKF)

	Page
1. Overall flow diagram of filter model (Figure A-1)	150
2. Input data and decision parameters for filter model (Table A-1).	154
3. Definition of state vector, measurement vector, input vector, and model coefficient vector in this study (Table A-2)	162
4. Program listing of filter model	164
5. Sample input for filter model	179
6. Sample output from filter model	181

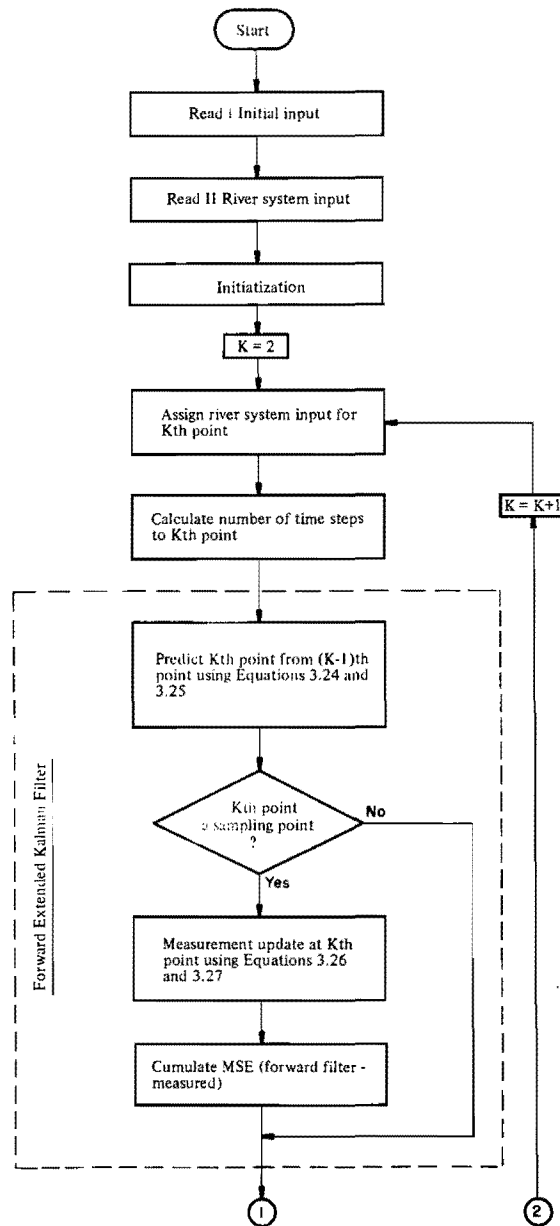
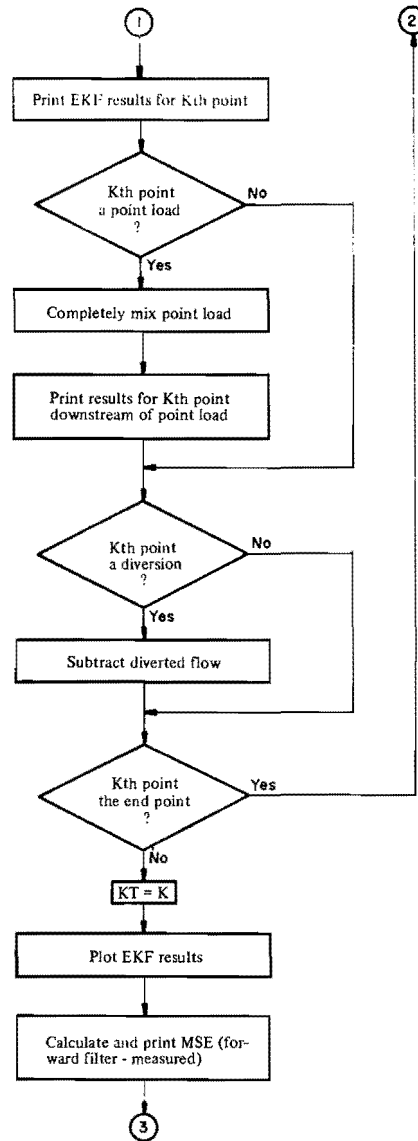
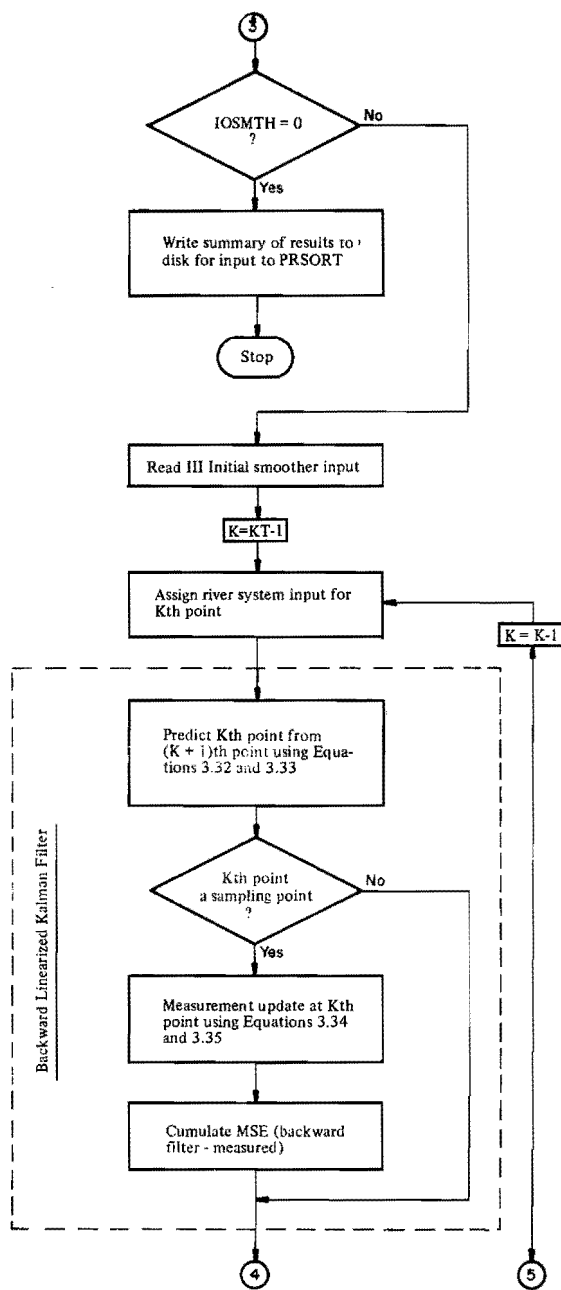


Figure A-1. Overall flow diagram of filter model.







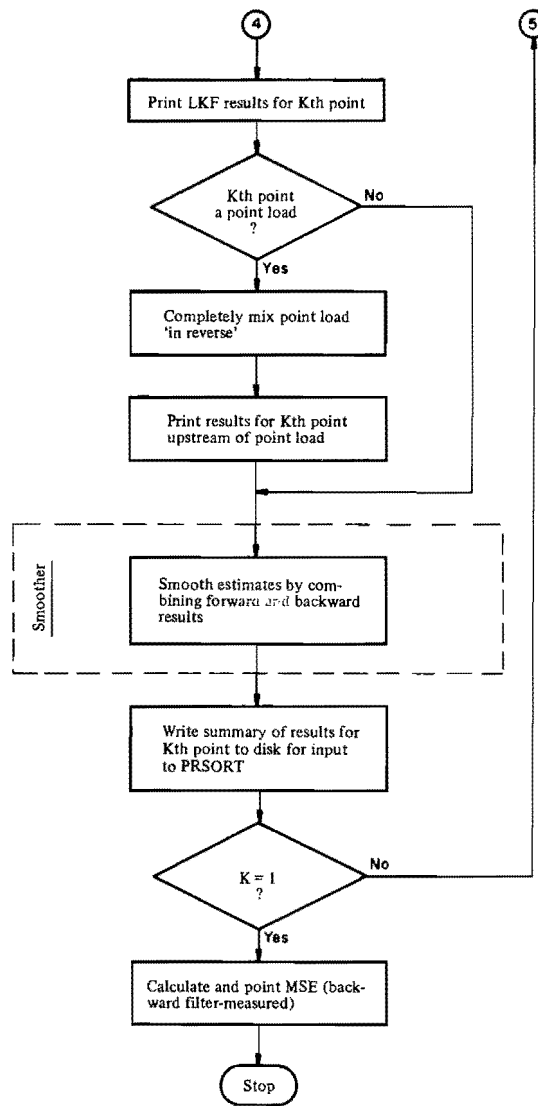


Table A-1. Input data and decision parameters for filter model (EKFLKF).

I. Initial input

1. (HDG(I), I = 1, 12) - Format (12A6)

1-72 HDG(I) Run heading

2. (XLABEL(I), I = 1, 12) - Format (12A6)

1-72 XLABEL(I) Label for x-axis of plotted output

3. N, L, IPI, IOUT, IC, NNN, IJK - Format (4I10, 10X, 3I10)

1-10 N Order of state vector

11-20 L Order of measurement vector

21-30 IPI Frequency of time steps to be plotted

31-40 IOUT Frequency of time steps to be printed

51-60 IC Number of model coefficients

61-70 NNN Number of state variables plus number of dependent variables

71-80 IJK = 0 Filter option

= 1 Deterministic process model option

4. NPLT, IU, IQ, NXNK, IOSMTH, IODPLT, IPS - Format (7I10)

1-10 NPLT Number of state variables to be plotted

11-20 IU Number of input variables

21-30	IQ	= 0 Print hydraulic variables = 1 Do not print hydraulic variables
31-40	NXNK	Numbers of state variables that are water quality parameters and not model coefficients augmenting the state vector
41-50	IOSMTH	= 0 Forward EKF only = 1 Smoothing option using end conditions of forward EKF for initial conditions of backward LKF = 2 Smoothing option and read initial conditions for backward LKF
		= 0 Do not plot results = 1 Plot results
51-60	IODPLT	= 0 Do not print results
61-70	IPS	= 1 Print Results

5. NMSTS2 - Format (I10)

1-10	NMSTS2	Number of the measurement at which alternative estimate of mean square error should commence
------	--------	--

6. T1, RMI, DT, QSTM - Format (4F10.0)

1-10	T1	Initial time (days)
11-20	RMI	River mile at upstream boundary
21-30	DT	Time step (days)
31-40	QSTM	Streamflow at upstream boundary (cfs)

7. (IOPT(I), I = 1,4), IOPTQ, IOPTR, IOPTPL - Format (7I10)

1-10	IOPT(1)	= 0 Entire H matrix input = 1 Only diagonal of H matrix input
11-20	IOPT(2)	= 0 Entire Q matrix input = 1 Only diagonal of Q matrix input
21-30	IOPT(3)	= 0 Entire R matrix input = 1 Only diagonal of R matrix input
31-40	IOPT(4)	= 0 Entire initial P matrix input = 1 Only diagonal of initial P matrix input
41-50	IOPTQ	= 0 Only one Q matrix input = 1 A different Q matrix input for each reach
51-60	IOPTR	= 0 Only one R matrix input = 1 A different R matrix input for each sampling point
61-70	IOPTPL	= 0 Y matrices not input (assumed identically zero) = 1 Y matrices input for each point load

(Card 8 is repeated for (NPLT+1) labels varying I)

8. (YYLABE(I,J), J = 1,9) - Format (9A6)

1-54	YYLABE(I,J)	Label for y-axis of plotted output
------	-------------	------------------------------------

9. (XHDG(I), I = 1, (NPLT+1)) - Format (10A8)

1-8	XHDG(1)	Brief heading for 1st state variable
9-16	XHDG(2)	Brief heading for 2nd state variable

etc.

10. (ZH DG(I), I = 1,L) - Format (10A8)

1-8 ZH DG(1) Brief heading for 1st measurement variable

9-16 ZH DG(2) Brief heading for 2nd measurement variable

etc.

11. (YMIN1(I), I = 1, (NPLT+1)) - Format (8F10.0)

1-10 YMIN1(1) Minimum y-value for plot of 1st state variable

11-20 YMIN1(2) Minimum y-value for plot of 2nd state variable

etc.

12. (YMAX1(I), I = 1, (NPLT+1)) - Format (8F10.0)

1-10 YMAX1(1) Maximum y-value for plot of 1st state variable

11-20 YMAX1(2) Maximum y-value for plot of 2nd state variable

etc.

13. (CH DG(I), I = 1, IC) - Format (10A8)

1-10 CH DG(1) Brief heading for 1st model coefficient

11-20 CH DG(2) Brief heading for 2nd model coefficient

etc.

14. (UHDG(I), I = 1, IU) - Format (10A8)

1-10 UHDG(1) Brief heading for 1st input variable

11-20 UHDG(2) Brief heading for 2nd input variable

etc.

(IOPT(1) = 0 Card 15 is repeated for L rows of HH varying I

IOPT(1) = 1 Card 15 contains the diagonal elements of HH)

15. (HH(I,J), J = 1, N) - Format (8F10.0)

HH(I,J) Measurement coefficient matrix

(Omit card 16 if IOPTQ = 1

IOPT(2) = 0 Card 16 is repeated for N rows of Q varying I

IOPT(2) = 1 Card 16 contains the diagonal elements of Q)

16. (Q(I,J), J = 1, N) - Format (8F10.0)

Q(I,J) Process model noise covariance matrix (mg/l - day)<sup>2</sup>

(Omit card 17 if IOPTR = 1

IOPT(3) = 0 Card 17 is repeated for L rows of R varying I

IOPT(3) = 1 Card 17 contains the diagonal element of R)

17. (R(I,J), J = 1, L) - Format (8F10.0)

R(I,J) Measurement noise covariance matrix (mg/l)<sup>2</sup>

18. (XX(I,1), I = 1, N) - Format (8F10.0)

1-10 XX(1,1) Initial mean value for the 1st state variable at upstream boundary (forward EKF run) (mg/l)<sup>2</sup>

11-20 XX(2,1) Initial mean value for the 2nd state variable at upstream boundary (forward EKF run) (mg/l)<sup>2</sup>

etc.

(IOPT(4) = 0          Card 19 is repeated for N rows of P varying I  
 IOPT(4) = 1          Card 19 contains the diagonal elements of P)  
 19. (P(I,J), J = 1, N) - Format (8F10.0)

                                P(I,J)                          Initial estimation error covariance matrix at upstream  
 boundary (forward EKF run)  $(\sigma_{ij}^2)$

## II. River system input

Cards in subsections A through E contain the input data necessary to describe the different types of points on the river system. The cards must be arranged in the order in which the points occur in the real river. A point load must precede each new reach. A zero flowrate should be assigned to this point load if it does not exist in the real river.

### A. Beginning of reach

20. "R", RM2, (C(I,1), I = 1, IC) - Format (A1, F9.0, 7F10.0/(8F10.0))

1	"R"	Card identifier for reach
2-10	RM2	River mile at upstream boundary of reach
11-20	C(1,1)	Value of 1st model coefficient for reach beginning at RM2
21-30	C(2,1)	Value of 2nd model coefficient for reach beginning at RM2

etc.

21. (U(I,1), I = 1, IU) - Format (8F10.0)

1-10	U(1,1)	Value of 1st input for reach beginning at RM2
11-20	U(2,1)	Value of 2nd input for reach beginning at RM2

etc.



(Omit card 22 if IOPTQ = 0)

22. Same as card 16

B. Sampling point

23. "M", RM2, (Z(I,1), I = 1, L) - Format (A1, F9.0, 7F10.0/(8F10.0))

1	"M"	Card identifier for sampling point
2-10	RM2	River mile at sampling point
11-20	Z(1,1)	Value of 1st measurement variable at RM2
21-30	Z(2,1)	Value of 2nd measurement variable at RM2

etc.

(Omit card 24 if IOPTR = 0)

24. Same as card 17

C. Point load

25. "P", RM2, QPL, (PL(I,1), I = 1, NXNK) - Format (A1, F9.0, 7F10.0/(8F10.0))

1	"P"	Card identifier for point load
2-10	RM2	River mile at point load
11-20	QPL	Flowrate of point load (cfs)
21-30	PL(1,1)	Concentration of 1st water quality parameter in point load (mg/l)
31-40	PL(2,1)	Concentration of 2nd water quality parameter in point load (mg/l)

etc.

(Omit card 26 if IOPTPL = 0)

26. (YPL(I,I), I = 1, NXNK) - Format (8F10.0)

YPL(I,I) Diagonal elements of estimation error covariance matrix  
of water quality parameter concentration in point load (mg/l)

D. Diversion

27. "D", RM2, QDIV, - Format (A1, F9.0, F10.0)

1	"D"	Card identifier for diversion
2-10	RM2	River mile at diversion
11-20	QDIV	Flowrate of diversion (cfs)

E. End point

28. "E", RM2 - Format (A1, F9.0)

1	"E"	Card identifier for end point
2-10	RM2	River mile at end point

III. Initial smoother input

(Omit cards 29 and 30 if IOSMTH not equal to 2)

29. (XB(I,1), I = 1,N) - Format (8F10.0)

1-10	XB(1,1)	Initial mean value for the 1st state variable at downstream boundary (backward LKF run) (mg/l)
11-20	XB(2,1)	Initial mean value for the 2nd state variable at downstream boundary (backward LKF run) (mg/l)

etc.

30. (PB(I,I), I = 1, N) - Format (8F10.0)

PB(I,I) Diagonal elements of initial estimation error covariance matrix  
at downstream boundary (backward LKF run) (mg/l)<sup>2</sup>

Table A-2. Definition of state vector, measurement vector, input vector, and model coefficient vector.

Vector	Computer mnemonic	Text Symbol	Definition	Units
State	X(1,1)	$X_1$	Estimated concentration of BOD in the stream	mg/l
	X(2,1)	$X_2$	Estimated concentration of $\text{NH}_3\text{-N}$ in the stream	mg/l
	X(3,1)	$X_3$	Estimated concentration of $\text{NO}_3\text{-N}$ in the stream	mg/l
	X(4,1)	$X_4$	Estimated concentration of ALG-N in the stream	mg/l
	X(5,1)	$X_5$	Estimated concentration of ORG-N in the stream	mg/l
	X(6,1)	$X_6$	Estimated concentration of DO in the stream	mg/l
Measurement	Z(1,1)	$Z_1$	Measured concentration of BOD in the stream	mg/l
	Z(2,1)	$Z_2$	Measured concentration of $\text{NH}_3\text{-N}$ in the stream	mg/l
	Z(3,1)	$Z_3$	Measured concentration of $\text{NO}_3\text{-N}$ in the stream	mg/l
	Z(4,1)	$Z_4$	Measured concentration of (ALG-N + ORG-N) in the stream	mg/l
	Z(5,1)	$Z_5$	Measured concentration of DO in the stream	mg/l
Input	U(1,1)	$U_1$	Concentration of BOD in lateral inflow	mg/l
	U(2,1)	$U_2$	Concentration of $\text{NH}_3\text{-N}$ in lateral inflow	mg/l
	U(3,1)	$U_3$	Concentration of $\text{NO}_3\text{-N}$ in lateral inflow	mg/l
	U(4,1)	$B_6$	Uptake of DO by stream bottom	mg/ft <sup>2</sup> -day
	U(5,1)	q	Lateral inflow rate	cfs/mile
	U(6,1)	$\lambda$	Stream temperature	deg. C
	U(7,1)	A	Cross sectional area of stream	ft <sup>2</sup>
	U(8,1)	h	Stream depth averaged over cross section	ft
	U(9,1)	$U_6$	Concentration of DO in lateral inflow	mg/l

Table A-2. continued.

Vector	Computer mneumonic	Text Symbol	Definition	Units
Model Coefficient	C(1,1)	$K_d$	BOD decay rate	base e, per day
	C(2,1)	$K_{52}$	Rate of decomposition of ORG-N to $\text{NH}_3\text{-N}$	base e, per day
	C(3,1)	$K_{23}$	Nitrification rate ( $\text{NH}_3\text{-N}$ to $\text{NO}_3\text{-N}$ )	base e, per day
	C(4,1)	$K_{45}$	Algal death rate (ALG-N to ORG-N)	base e, per day
	C(5,1)	--	Blank	
	C(6,1)	$K_{S3}$	Half-saturation coefficient for $\text{NO}_3\text{-N}$	mg/l
	C(7,1)	$\hat{\mu}$	Maximum specific growth rate of algae	base e, per day
	C(8,1)	$\beta$	Ratio of half-saturation coefficient for $\text{NO}_3\text{-N}$ to half-saturation coefficient for $\text{NH}_3\text{-N}$	dimensionless
	C(9,1)	$X_{6\text{sat}}$	Saturation concentration of DO	mg/l
	C(10,1)	4.57	mg $\text{O}_2$ /mg N	dimensionless
	C(11,1)	--	Blank	
	C(12,1)	$\gamma$	Weighting coefficient to indicate the preference of algae for $\text{NH}_3\text{-N}$ over $\text{NO}_3\text{-N}$	dimensionless

#### 4. Program listing of filter model.

```

C**** TO IMPLEMENT CONTINUOUS-DISCRETE EXTENDED KALMAN FILTER
C ON RIVER WATER QUALITY PROBLEM
C WITH A) FIRST ORDER NONLINEAR PROCESS DYNAMICS
C B) LINEAR MEASUREMENT DYNAMICS

REAL ID,KK,KKT
DOUBLE PRECISION XHDG,ZHDE,CHEG,UHOG

COMMON/B1/G(20,20),Q(20,20),H(20,20),R(20,20),XX(20,1),P(20,20),
. X1(20,1),IO(20,20),THT(20,20),PHOD(20,20),P1(20,20),
. FF(20,20),FFT(20,20),DUM1(20,20),PPMOD(400,1),H(20,20),
. UHOG(20),DUMINI(20,70),UC(20,1),
. DUM2(20,20),DUM3(20,20),KK(20,20),KKT(20,20),
. Z(20,1),RHS(400,1),PP(400,1),HDG(12),XLABEL(12),
. YLABEL(9),A(104,5),YP(100),YM(100),YU(100),YL(100)
COMMON/B2/X(100),F(20,1),RK(4,400),COOLST(6),PL(20,1),
. XHDG(20),ZHOG(20),YYP(20,100),YYM(20,100),YYU(20,100),
. YTL(20,100),YYMAX(20),YYMIN(20),YLABE(20,9),YMINI(20),
. YMAX1(20),C(20,1),ICPT(4),CHOG(20),CODE(70),RMIN(70),
. JDUT,JPLT,JY,NH,T,MC,N,L,DT,RNI,NN,IPI,IOUT,NTS,JI,
. JT2,K,RM1,RM2,YEL,RP,T1,T2,IJK,NPLT,QSTM,KRH,NPLT1,IQ
COMMON/B3/DM(20,70),RIN(20,70),DUMIN(20,70),KRCH(70),IX
COMMON/B4/PDI(20,20),QSTMST(30),X1ST(12,650),VELST(300),
. XKS(12,300),PPBI(400,1),KW,RHS(20,1),
. PDG(20),PDG(20),IPS,AXNK,FMSE2(20,1),NMSTS2,
. ICSMTH,YPL(20,20),YIN(20,70),FMSE(20,1),NMSTS,
. PBIHOD(20,20),RK1(4,20),XS(20,1),PBMOD(20,20),
. PBI(20,20),RINV(20,20),PS1(20,20),PS(20,20),XS1(20,1),
. XB(20,1),XB1(20,1),FMST(300),XPHOD(20,1),ATST(70),IT,KT
COMMON/B5/PST(12,12,300)
COMMON/B6/P1ST(12,12,300)

DATA COOLST/'R','M','P','E','C','' /
DATA A/1045+' ' /

500 FORMAT(12A6)
501 FORMAT(8I10)
502 FORMAT(1H1,12A6/
. 1H0,35HORDER OF SYSTEM/NUMBER OF STATES N=>I8/
. 1H 35HNUMBER OF OBSERVABLE OUTPUTS L=>I8/
. 1H 35HPLOT INTERVAL IPI=>I8/
. 1H 35HPRINT INTERVAL IOUT=>I8/
. 1H 35HINITIAL TIME (DAYS) T1=>F8.2/
. 1H 35HINITIAL RIVER MILES RMI=>F8.2/
. 1H 35HINITIAL STREAMFLOW (CFS) QSTM=>F8.2/
. 1H 35HCOMPUTATIONAL TIME STEP (DAYS) CT=>F3.4//

505 FORMAT(1H0,20HCoefficient VECTOR C/)
507 FORMAT(1HC,22HV-C OF PROCESS NOISE Q/)
508 FORMAT(1H0,21HOBSERVATION MATRIX HH/)
509 FORMAT(1HC,26HV-C OF OBSERVATION NOISE R/)
511 FORMAT(1H0,32HC FOR ERROR COVARIANCE MATRIX P/)
515 FORMAT(8F10.0)
517 FORMAT(1H1,27HINITIAL CONDITIONS TIME=>F8.4,7H RM=>F8.3/
. 1H 50(1H*))
518 FORMAT(10A8)
519 FORMAT(1H0,27HC FOR ESTIMATE OF STATE XX/)
522 FORMAT(1HC,5HYMINI/)
523 FORMAT(1H0,5HYMAX/)
529 FORMAT(A1,F9.0,7F10.0)
530 FORMAT(1H0,19HCODE NOT RECOGNISED)
531 FORMAT(1H ,A1,F9.2,10F10.3/1H ,10X,10F10.3)

```

```

532 FORMAT(1H0,10HRIVER MILE,10(2),A8)/1H ,10X,10(2X,A8))
533 FORMAT(1H0,70HESTIMATE OF STATE AFTER POINT LOAD IS INSTANTANEOUSL
. Y COMPLETELY MIXED/)
534 FORMAT(1H1,48HRIVER SYSTEM LAYOUT, HYDRAULICS AND LOADING DATA/
. 1H ,48(1H*))
535 FORMAT(1H0,76HERROR COVARIANCE MATRIX AFTER POINT LOAD IS INSTANTAN
. EOUSLY COMPLETELY MIXED/)
536 FORMAT(1H0,2X,8HV-VECTOR,10(2),A8)/1H ,10X,10(2X,A8))
537 FORMAT(1H ,9X,1HU,10F10.3/1H ,10X,10F10.3)
538 FORMAT(1H0,10HMEAS VECTOR,10(2),A8)/1H ,10X,10(2X,A8))
539 FORMAT(1H0,10HPTLD & DIV,7X,3+CFS,9(2X,A8)/1H ,10X,10(2X,A8))
540 FORMAT(1H0,13HSINGULAR RINV/)
540 FORMAT(2H02,3HIT=>I4,3HRM=>F1(.5,4HVEL=>F10.5,2HQ=>F10.5,2HK=>
. I5,6HCODE=>A1)
541 FORMAT(1H1,2I4,F10.5,I4,A1)
542 FORMAT(1H ,I2,I3,I2,4F9.5,2(2),4F9.5))
543 FORMAT(3I4,6F10.3)
544 FORMAT(1H ,6HMEASTS,10F10.5)
545 FORMAT(15,8F9.4)
570 FORMAT(1H1,119H K IX I XI P1 XX P
. XB PB XB1 PB1 XS1 PS1 XS
. PS//)
571 FORMAT(1H1,69HMEAN SQUARE ERROR (OBSERVED - FILTER) PSE(NMSTS),
. SEC(NMSTS/2), R, Q//)

C *** INPUT-INITIAL

READ 500,(XHDG(I),I=1,12)
READ 501,(XLABEL(I),I=1,12)
READ 501,(N,L,IPI,IOUT,KR,IC,NAH,IJK,NPLT,IU,IQ,AXNK,ICSMTH,IOPTPL,
. KW,1PS,NMSTS2
READ 515,Y1,RMI,IOT,QSTM
PRINT 502,(XHDG(I),I=1,12),N,L,IPI,IOUT,T1,RMI,QSTM,DT
READ 501,(IOPT(I),I=1,4),IDPTG,IDPTR,IOPTPL
NPLT1=NPLT+1
DO 15 I=1,NPLT1
READ 500,(YLABE(I),J=1,9)
15 CONTINUE
READ 518,(XHDG(I),I=1,NPLT1)
READ 518,(ZHOG(I),I=1,L)
READ 515,(YMINI(I),I=1,NPLT1)
PRINT 522
CALL MOUT(YMINI,NPLT1,1,2,XHDG,XHDG)
READ 515,(YMAX1(I),I=1,NPLT1)
PRINT 523
CALL MOUT(YMAX1,NPLT1,1,2,XHDG,XHDG)
READ 518,(CHOG(I),I=1,IC)
READ 518,(UHOG(I),I=1,IU)
PRINT 508
CALL MIN(HH,L,N,IOPT(1),3,2+O,XHDG)
IF(IOPT(1).NE.0)GOTO 20
PRINT 507
CALL MIN(Q,N,N,IOPT(2),3,XHDG,XHDG)
IF(IOPT(2).NE.0)GOTO 25
PRINT 509
CALL MIN(R,L,L,IOPT(3),3,ZHOG,ZHOG)
DO 23 I=1,L
DO 22 J=1,L
RINV(I,J)=R(I,J)
22 CONTINUE
23 CONTINUE

```

```

CALL MINVSR(RINV,L,3)
IF(CABS(C).LT.1.E-4)PRINT 54C
25 READ 515,(XX(I,1),I=1,N)
CALL MIN(P,N,N,IOPT(4),X,XHDG,XHDG)
C *** INPUT-RIVER SYSTEM
PRINT 534
PRINT 532,(CHDG(I),I=1,IC)
PRINT 536,(UHOG(I),I=1,IU)
PRINT 537,(XHDG(I),I=1,N)
PRINT 538,(ZHOG(I),I=1,L)
K=0
K1=0
65 K1=K+1
READ 529,CODE(K),RMIN(K),(DUMIN(I,K),I=1,7)
IF(CODE(K).EQ.CODLST(1))GOTO 70
IF(CODE(K).EQ.CODLST(2))GOTO 80
IF(CODE(K).EQ.CODLST(3))GOTO 90
IF(CODE(K).EQ.CODLST(4))GOTO 100
IF(CODE(K).EQ.CODLST(5))GOTO 55
PRINT 530
STOP
C * REACH
70 IF(IC.GT.7)READ 515,(DUMIN(I,K),I=8,IC)
PRINT 531,CODE(K),RMIN(K),(DUMIN(I,K),I=1,IC)
READ 515,(DUMINI(I,K),I=1,IU)
PRINT 537,(DUMINI(I,K),I=1,IU)
IF(IOPT(4).NE.1)GOTO 77
PRINT 507
CALL MIN(Q,N,N,IOPT(2),3,XHDG,XHDG)
DO 79 I=1,N
DO 78 J=1,N
QIN(I,J,K)=Q(I,J)
78 CONTINUE
79 CONTINUE
K1=K1+1
KRCHK1)=K
GOTO 65
C * MEASUREMENT
80 IF(L.GT.7)READ 515,(DUMIN(I,K),I=8,L)
PRINT 531,CODE(K),RMIN(K),(DUMIN(I,K),I=1,L)
IF(IOPT(4).NE.1)GOTO 87
PRINT 509
CALL MIN(R,L,L,IOPT(3),3,ZHDG,ZHDG)
DO 89 I=1,N
DO 88 J=1,N
RIN(I,J,K)=R(I,J)
88 CONTINUE
89 CONTINUE
GOTO 65
C * POINT LOAD
90 IF(NPLT.GT.7)READ 515,(COUPL(I,K),I=8,(NXNK+1))
PRINT 531,CODE(K),RMIN(K),EDUMIN(I,K),I=1,(NXNK+1))
IF(IOPT(4).EQ.0)GOTO 65
CALL MIN(YPL,NXNK,NXNK+1,3,XHDG,XHDG)
DO 93 I=1,NXNK
YIN(I,K)=YPL(I,I)
93 CONTINUE
GOTO 65
C * DIVERSION

```

```

95 PRINT 531,CODE(K),RMIN(K),DUMIN(I,K)
GOTO 65
C * END POINT
100 KT=K
K1T=K1
PRINT 531,CODE(K),RMIN(K)
C *** INITIALISATION
C * IDENTITY MATRIX
DO 140 I=1,N
ID(I,I)=1.
140 CONTINUE
C * TRANSPOSE MH
CALL MTRANS(MH,MHT,L,N)
ND=MN-N
T=T1
JT=1
NM=N*N
NMSTS=0
C * STORAGE ARRAYS
MST(1)=1
RMST(1)=RMI
QSTMST(1)=QSTM
VELST(1)=QSTM*86400./(DUMIN(I,7)+5280.)
X45=XX(4,1)*XX(5,1)
X1ST(NPLT,1)=X45
XXST(NPLT,1)=X45
PST(NPLT,1,NPLT,1)=P(4,4)+P(5,5)+2*P(4,5)
P1ST(NPLT,1,NPLT,1)=P(4,4)+P(5,5)+2*P(4,5)
DO 150 I=1,N
X1ST(I,1)=XX(I,1)
XXSI(I,1)=XX(I,1)
DO 145 J=1,N
PST(I,J,1)=P(I,J)
P1ST(I,J,1)=P(I,J)
145 CONTINUE
150 CONTINUE
C *** EXECUTE C-D ENF OVER RM1 TO RP2
C * ASSIGN INPUT-RIVER SYSTEM READY FOR EXECUTION
K=0
K1=0
JT2=1
RM2=RMI
RM=RMI
165 RM1=RM
T1=T
K=K+1
IF(CODE(K).EQ.CODLST(1))GOTO 170
RM2=RMIN(K)
IF(CODE(K).EQ.CODLST(2))GOTO 180
IF(CODE(K).EQ.CODLST(3))GOTO 190
GOTO 215
C * REACH
170 DO 172 I=1,IC
C(I,1)=DUMIN(I,K)
172 CONTINUE
DO 173 I=1,IU
U(I,1)=DUMINI(I,K)

```

```

173 CONTINUE
IF(IQ.EQ.1)WRITE(6,/)CODE(K),JT2,T,RM,QSTM,UC(5),VEL
IF(K.EQ.1)GOTO 174
NTST(K)=NTST(K-1)
174 K1=K1+1
IF(K1.EQ.N1)GOTO 165
C * KRRH IS K VALUE FOR REACH CHARACTERISTICS
KRRH=KRRH(K1+1)
IF(K.NE.1)GOTO 165
C * INITIALISE DEPENDENT VARIABLES & PRINT INITIAL CONDITIONS
IF(ND.GT.0)CALL EQNDEP(XX,P,C,DT)
PRINT 517,T,1,RMI
PRINT 519
CALL MOUT(XX,MNN,1,2,XHDG,XHDG)
PRINT 511
CALL MOUT(P,MNN,MNN,3,XHDG,XHDG)
C * INITIALISE PLOTTING VARIABLES
175 IF(ND.GT.0)CALL EQNDEP(XX,P,C,DT)
X(1)=0.
X45=XX(4,1)+XX(5,1)
XX(NPLT1,1)=X45
P(NPLT1,NPLT1)=P(4,4)+P(5,5)+2*P(4,5)
DO 178 I=1,NPLT1
YYM(I,1)=XX(I,1)
YYP(I,1)=XX(I,1)
YYU(I,1)=XX(I,1)+SQRT(P(I,1))
YYL(I,1)=XX(I,1)-SQRT(P(I,1))
IF(YYM(I,1).GT.YYMAX(I))YYMAX(I)=YYM(I,1)
IF(YYU(I,1).GT.YYMAX(I))YYMAX(I)=YYU(I,1)
IF(YYM(I,1).LT.YYMIN(I))YYMIN(I)=YYM(I,1)
IF(YYL(I,1).LT.YYMIN(I))YYMIN(I)=YYL(I,1)
178 CONTINUE
GOTO 165
C * MEASUREMENT
180 DO 185 I=1,L
Z(I,1)=DUMIN(I,K)
185 CONTINUE
GOTO 215
C * POINT LOAD
190 DO 195 I=2,(NXNK+1)
I1=I-1
PL(I1,1)=DUMIN(I,K)
195 CONTINUE
QPL=DUMIN(1,K)
IF(IOPPL.EQ.0)GOTO 215
DO 205 I=1,NXNK
YPL(I,1)=YIN(I,K)
205 CONTINUE
C * NUMBER OF TIME STEPS
215 VEL=QSTM*06400./(UC(7,1)+5200.)
T2=T1+(RM1-RM2)/VEL
NTS=FIXX(T2-T1)/DT)
217 IF(NTS.GT.0)GOTO 220
NTST(K)=NTST(K-1)
IF(CODE(K).EQ.CDDLST(2))GOTO 225
IF(CODE(K).EQ.CDDLST(3))GOTO 240
IF(CODE(K).EQ.CDDLST(4))GOTO 400
IF(CODE(K).EQ.CDDLST(5))GOTO 160
220 JT1=JT2+1
GOTO 230
225 JT1=JT2

```

```

230 CALL SCDEF
NTST(K)=JT2
IF(CODE(K).EQ.CDDLST(3))GOTO 240
IF(CODE(K).EQ.CDDLST(5))GOTO 160
IF(K.EQ.KT)GOTO 400
GOTO 165
C * COMPLETELY MIX POINT LOAD
240 QSTM1=QSTM+QPL
DO 250 I=1,NXNK
XX(I,1)=(QSTM*XX(I,1)+PL(I,1)+QPL)/QSTM1
P(I,1)=P(I,1)+(QSTM/QSTM1)+2*YPL(I,1)+(QPL/QSTM1)+2
DO 245 J=1,NXNK
IF(I.EQ.J)GOTO 245
P(I,J)=P(I,J)+(QSTM/QSTM1)+2
245 CONTINUE
250 CONTINUE
QSTM=QSTM1
QSTMST(IT)=QSTM
IF(IQ.EQ.1)WRITE(6,/)CODE(K),JT2,T,RM,QSTM,QPL
X45=XX(4,1)+XX(5,1)
XX(NPLT1,1)=X45
P(NPLT1,NPLT1)=P(4,4)+P(5,5)+2*P(4,5)
IF(IPS.EQ.0)GOTO 270
PRINT 533
CALL MOUT(XX,N,1,2,XHDG,XHDG)
IF(IJK.EQ.1)GOTO 270
PRINT 535
CALL MOUT(P,N,N,3,XHDG,XHDG)
270 JT=JT+1
JPLT=JPLT+1
X(JT)=RMI-RM
X45=XX(4,1)+XX(5,1)
XX(NPLT1,1)=X45
P(NPLT1,NPLT1)=P(4,4)+P(5,5)+2*P(4,5)
DO 350 I=1,NPLT1
XXST(I,IT)=XX(I,1)
PST(I,IT)=P(I,1)
YYP(I,JT)=XX(I,1)
YYU(I,JT)=XX(I,1)+SQRT(P(I,1))
YYL(I,JT)=XX(I,1)-SQRT(P(I,1))
YYM(I,JT)=XX(I,1)
IF(YYU(I,JT).GT.YYMAX(I))YYMAX(I)=YYU(I,JT)
IF(YYL(I,JT).LT.YYMIN(I))YYMIN(I)=YYL(I,JT)
350 CONTINUE
GOTO 165
C * SUBTRACT DIVERTED FLOW
360 QSTM=QSTM+DUMIN(1,K)
IF(IQ.EQ.1)WRITE(6,/)CODE(K),JT2,T,RM,QSTM,DUMIN(1,K)
GOTO 165
C *** PLOT RESULTS
400 IF(IOPPL.EQ.0)GOTO 400
DO 450 I=1,NPLT1
DO 410 J=1,JT
Y(J)=YYM(I,J)
Y(J)=YYP(I,J)
Y(J)=YYU(I,J)
Y(J)=YYL(I,J)
410 CONTINUE
YMAX=YMAX(I)

```

```

      YMIN=YMIN(I)
      IF(YMAX(I).GT.YMAX)YMAX=YMAX(I)
      IF(YMIN(I).LT.YMIN)YMIN=YMIN(I)
      DO 420 J=1,9
      YLABEL(J)=YLABE(I,J)
420  CONTINUE
      IF(IJK.EQ.1)GOTO 425
C * PLOT PREDICTED VALUES + STANDARD DEVIATION - C
      CALL PL36(C,JT,A,X,X(I),X(JT),XLABEL,YU,YMIN,YMAX,YLABEL,HOG,-195)
C * PLOT PREDICTED VALUES - STANDARD DEVIATION - C
      CALL PL36(C,JT,A,X,X(I),X(JT),XLABEL,YL,YMIN,YMAX,YLABEL,HOG,-195)
C * PLOT MEASURED VALUES - M
425  CALL PL36(C,JT,A,X,X(I),X(JT),XLABEL,YM,YMIN,YMAX,YLABEL,HOG,-212)
C * PLOT UPDATED STATE ESTIMATES - E
430  CALL PL36(C,JT,A,X,X(I),X(JT),XLABEL,YP,YMIN,YMAX,YLABEL,HOG,197)
450  CONTINUE

C *** MEAN SQUARE ERROR (OBSERVED - FILTER)

460  IF(IJK.EQ.1)GOTO 480
      NMS=NMS1-NMS12
      DO 470 I=1,L
      FMSE(I,1)=FMSE(I,1)/(NMS1-1)
      FMSE2(I,1)=FMSE2(I,1)/NMS
470  CONTINUE
      PRINT 571
      CALL MOUT(FMSE,L,1,2,ZHOG,ZHOG)
      CALL MOUT(FMSE2,L,1,2,ZHOG,ZHOG)
      PRINT 569
      CALL MOUT(L,L,3,ZHOG,ZHOG)
      PRINT 507
      CALL MOUT(Q,M,N,3,XHOG,XHOG)

C *** SMOOTH ESTIMATES

480  PRINT 570
      IF(IOSMTH.EQ.0)GOTO 490
      CALL SMOOTH
      GOTO 499

C *** PRINT SUMMARY OF OUTPUT TO LINE PRINTER AND DISK IF ESTIMATES NOT
C SMOOTHED

490  KI=KT
      KII=KT
      DO 497 IIT=1,JT2
      IT=JT2-IIT+1
      COD=CODLST(6)
491  IF(NST(KI).LT.IT)GOTO 492
      COD=CODE(KI)
      KII=KI
      KI=KI-1
      GOTO 491
492  IX=4+IIT-3
      PRINT 560,IT,RMST(IIT),VELST(IT),OSTNST(IT),KII,COD
      WRITE(KW,561)IX,IT,RMST(IIT),KII,COD
      IF(COD.NE.CODLST(2))GOTO 493
      PRINT 564,(DUMIN(I,KII),I=1,L)
      WRITE(KW,565)KII,(DUMIN(I,KII),I=1,L)
493  DO 495 I=1,N
      PRINT 562,KII,IX,I,XIST(I,IX),SQRT(P1ST(I,IX)),XXST(I,IT),

```

```

      SQRT(PST(I,IT))
      WRITE(KW,563)KII,IX,I,XIST(I,IX),SQRT(P1ST(I,IX)),PST(I,IT),
      SQRT(PST(I,IT))
495  CONTINUE
      I=N+1
      PRINT 562,KII,IX,I,P1ST(4,5,IT),PST(4,5,IT)
      WRITE(KW,563)KII,IX,I,P1ST(4,5,IT),PST(4,5,IT)
497  CONTINUE
499  LOCK KW

      STOP
      END

```



```

COMPUTING ZSEKI
C*** CONTINUOUS-DISCRETE EXTENDED KALMAN FILTER
REAL I3,KK,KFT
DOUBLE P,FC,ISFN,XHOG,ZHOG,CHCG,UMDG
COMMON/B1/G(20,20),G(20,20),H(20,20),R(20,20),XX(20,1),P(20,20),
- X1(20,1),IQ(20,20),HHT(20,20),PMOD(20,20),P1(20,20),
- FF(20,20),FFT(20,20),DUM1(20,20),PPMOD(400,1),H(20,20),
- UMG(20),DUMI1(20,70),I(20,1),
- DUM2(20,20),DUM3(20,20),KK(20,20),KKT(20,20),
- Z(20,1),RHS(400,1),FP(400,1),HDGL(2),XL,BFL(12),
- YLABEL(9),A(1045),YPL(100),YM(100),YH(100),YL(100)
COMMON/B2/X(100),F(20,1),RK(4,400),CODLST(6),PL(20,1),
- XHOG(20),ZHOG(20),YYP(20,100),YYH(20,100),YYU(20,100),
- YYL(20,100),YYMAX(20),YYMIN(20),YLABE(20,9),YMINI(20),
- YMAX1(20),C(20,1),ICPT(4),CHOG(20),CODE(70),RMIN(70),
- JOUT,JPLT,JT,NN,1,NC,N,L,DT,RM1,NNN,1P1,IOUT,NTS,JT1,
- JT2,K,RM1,RM2,VEL,RM,T1,T2,IJK,NPLT,QSTM,KRH,NPLT1,IQ
COMMON/B3/QIN(20,20,70),RIN(20,20,70),DUMIN(20,70),KRCH(70),IX
COMMON/B4/PBI(20,20),QSTMST(300),X1ST(12,650),VELST(300),
- X1ST(12,300),PPBI(400,1),MW,RHS1(20,1),
- PIDG(20),PDG(20),IPS,AKXK,FHSE2(20,1),NMSIS2,
- IOSMTH,YPL(20,20),YIN(20,70),FMSE(20,1),NPSTIS,
- PBIHQD(20,20),RK1(4,20),XS(20,1),PPMOD(20,20),
- PBI(20,20),RINX(20,20),PS1(20,20),PS(20,20),XS1(20,1),
- XRI(20,1),XB1(20,1),FMST(300),XPMOD(20,1),NTST(70),IT,KT
COMMON/B5/PST(12,12,300)
COMMON/B6/P1ST(12,12,300)
503 FORMAT(1H0,20OBSERVATION VECTOR Z/)
504 FORMAT(1H0,12HTIME STEP NC,15,9H TTME,F8.4,7H RM,F8.3/1+ ,
- .49(1H*))
516 FORMAT(1H0,23HHH*P1+HHT+R IS SINGULAR/)
520 FORMAT(1H0,35HUPDATED ERROR COVARIANCE MATRIX P/)
521 FORMAT(1H0,28HUPDATED ESTIMATE OF STATE XX/)
527 FORMAT(1H0,36HPREDICTED ERROR COVARIANCE MATRIX P1/)
528 FORMAT(1H0,30HPREDICTED ESTIMATE OF STATE X1/)

```

C \*\*\* TIME LOOP

```

IP=0
JOUT=0
JPLT=0
IT=JT1-1
50 IT=IT+1
IF(NTS.NE.0)GOTO 60
IF(IJK.EQ.0)GOTO 300
GOTO 260
60 TI=T
T=T+DT
QSTM=QSTM+U(S,1)*VEL+DT
RM=RM-VEL*DT
IF(IQ.EQ.1)WRITE(6,/)CODE(K),IT,T,RM,QSTM,U(S,1),VEL
RMST(IT)=RM
QSTMST(IT)=QSTM
VELST(IT)=VEL
JOUT=JOUT+1
JPLT=JPLT+1

```

```

C ** STATE ESTIMATE PROPAGATION X1
C X1=XX+INTEGRAL(TI TO T) OF F
IF(IJK.NE.1)GOTO 145
THOD=TI
DO 120 I=1,N
XPMOD(I,1)=XX(I,1)
120 CONTINUE
DO 130 KSEL=1,4
IX=4*IT+KSEL-7
CALL EQN1(XPMOD,U,C,F,N,VEL)
CALL RUNGE(KSEL,N,DT,F,XPMOD,THOD,TI,XX,RK1)
DO 125 I=1,N
X1ST(I,IX)=XPMOD(I,1)
X1ST(I,1T)=XPMOD(I,1)
125 CONTINUE
130 CONTINUE
DO 140 I=1,N
X1(I,1)=XPMOD(I,1)
140 CONTINUE
DO 143 I=1,N
XX(I,1)=X1(I,1)
143 CONTINUE
GOTO 300

C ** ERROR COVARIANCE PROPAGATION P1
C P1=P+INTEGRAL(TI TO T) CF (FF*P+P*FFT+Q)
145 THOD=TI
DO 160 I=1,N
XPMOD(I,1)=XX(I,1)
DO 150 J=1,N
IJ=(I-1)*N+J
PP(I,J)=P(I,J)
PMOD(I,J)=P(I,J)
150 CONTINUE
160 CONTINUE
DO 210 KSEL=1,4
IX=4*IT+KSEL-7
CALL EQN2(XPMOD,U,C,FF,N,VEL)
C * FF*P
CALL MMULT(FF,PMOD,DUM1,N,N,N)
C * P*FFT
CALL MTRANS(FF,FFT,N,N)
CALL MMULT(PMOD,FFT,DUM2,N,N,N)
C * DUM3=FF*P+P*FFT+Q
DO 180 I=1,N
DO 170 J=1,N
DUM3(I,J)=DUM1(I,J)+DUM2(I,J)+C(I,J)
IJ=(I-1)*N+J
RHS(I,J)=DUM3(I,J)
170 CONTINUE
180 CONTINUE
CALL EQN1(XPMOD,U,C,F,N,VEL)
CALL RUNGE(KSEL,N,DT,F,XPMOD,THOD,TI,XX,RK1)
CALL RUNGE(KSEL,N,DT,RHS,PPM(D,THOD,TI,PP,RK)
DO 200 I=1,N
X1ST(I,IX)=XPMOD(I,1)
X1ST(I,1T)=XPMOD(I,1)
DO 190 J=1,N
IJ=(I-1)*N+J
PMOD(I,J)=PPMOD(I,J)
P1ST(I,J,IT)=PMOD(I,J)

```

```

PST(I,J,IT)=PMD(I,J)
190 CONTINUE
200 CONTINUE
210 CONTINUE
    DO 230 I=1,N
        XI(I,1)=XPMO(I,1)
        DO 220 J=1,N
            PI(I,J)=PMD(I,J)
220 CONTINUE
230 CONTINUE

C ** SKIP UPDATE IF NO OBSERVATION AVAILABLE
DO 250 I=1,N
    XX(I,1)=XI(I,1)
    DO 240 J=1,N
        P(I,J)=PI(I,J)
240 CONTINUE
250 CONTINUE
    GOTD 300

C ** KALMAN GAIN MATRIX KK
C KK=P1*HMT*(HH*P1+HMT*R)**-1
260 IF(IJK.EQ.1)GOTO 305
    CALL MMULT(HH*P1,DUM1,L,N,N)
    CALL MMULT(DUM1,HMT,DUM1,L,N,L)
    CALL MADSUB(DUM1,R,DUM1,L,N,1)
    CALL MINVSR(DUM1,L,N)
    IF(ABS(CO).LT.1.E-45)PRINT 516
    CALL MMULT(HMT,DUM1,DUM1,N,L,L)
    CALL MMULT(P1,DUM1,KN,N,N,L)

C ** STATE ESTIMATE UPDATE XX
C XX=XI+KK*(Z-H), H=HH*XI
    CALL MMULT(HH*XI,H,L,N,1)
    CALL MADSUB(Z,H,DUM1,L,1,-1)
    CALL MMULT(KK,DUM1,DUM1,N,L,1)
    CALL MADSUB(XI,DUM1,XX,N,1,1)

C ** ERROR COVARIANCE UPDATE P
C P=(I0-KK*HH)*P1+(I0-KK*HH)*T+KK*R*KKT
C * KK*R*KKT
    CALL MTRANS(KK,KN,L)
    CALL MMULT(R,KN,T,DUM1,L,N,N)
    CALL MMULT(KK,DUM1,DUM1,N,L,N)
C * (I0-KK*HH)*T
    CALL MMULT(KK*HH,DUM2,N,L,N)
    CALL MADSUB(I0,DUM2,DUM2,N,N,-1)
    CALL MTRANS(DUM2,DUM3,N,N)
    CALL MMULT(P1,DUM3,DUM3,N,N,N)
    CALL MMULT(DUM2,DUM3,P,N,N,N)
    CALL MADSUB(P,DUM1,P,N,N,1)
    DO 290 I=1,N
        XXST(I,IT)=XX(I,1)
        DO 260 J=1,N
            PST(I,J,IT)=P(I,J)
280 CONTINUE
290 CONTINUE

C *** CALCULATE MEAN SQUARE ERROR (OBSERVED - FILTER)
C FMSE=FMSE+(Z-HH*XX)**2

```

```

    CALL MMULT(HH*XX,DUM1,L,N,1)
    CALL MADSUB(Z,DUM1,DUM1,L,1,-1)
    DO 295 I=1,L
        FMSE(I,1)=FMSE(I,1)+DUM1(I,1)**2
295 CONTINUE
    NMSTS=NMSTS+1
    IF(NMSTS.LT.NMSTS2)GOTO 300
    DO 298 I=1,L
        FMSE2(I,1)=FMSE2(I,1)+DUM1(I,1)**2
298 CONTINUE

C *** CALCULATE DEPENDENT VARIABLES & THEIR MEAN SQUARE ERRORS
300 IF(ND.GT.0)CALL EQNOEP(XX,P,C,DT)

C *** PRINT RESULTS
305 IF(IPS.EQ.0)GOTO 307
    IF(NTS.NE.0)GOTO 310
    IF(IJK.EQ.0)GOTO 336
    IF(IPS.EQ.0)GOTO 330
    GOTD 325
310 IF(IT.EQ.JT2)GOTO 315
    IF(JOUT.LT.IOUT)GOTO 330
315 PRINT 504,IT,T,RM
    JOUT=0
    IF(IJK.EQ.1)GOTO 318
    IF(CODE(K).EQ.COOLST(2).AND.IT.EQ.JT2)GOTO 320
    PRINT 527
    CALL MOUT(P,NNN,NNN,3,XHOG,XHCG)
318 PRINT 528
    CALL MOUT(XX,NNN,1,2,XHOG,XHOC)
    GOTD 330
320 PRINT 527
    CALL MOUT(P1,N,N,3,XHOG,XHCG)
    PRINT 528
    CALL MOUT(XI,N,1,2,XHOG,XHOG)
    PRINT 503
325 CALL MOUT(Z,L,1,2,XHOG,XHOG)
    PRINT 520
    CALL MOUT(P,NNN,NNN,3,XHOG,XHCG)
    PRINT 521
    CALL MOUT(XX,NNN,1,2,XHOC,XHOC)

C *** STORE RESULTS FOR PLOTTING
330 IF(IP.EQ.1)GOTO 336
    IF(NTS.EQ.0)GOTO 336
    IF(IT.EQ.JT2)GOTO 335
    IF(JPLT.LT.IPI)GOTO 400
335 JT=JT+1
336 X(JT)=RMI-RM
    JPLT=0
    X45=XX(4,1)+XX(5,1)
    XX(NPLT,1)=X45
    P(NPLT1,NPLT1)=P(4,4)+(XX(4,1)/X45)**2+P(5,5)+(XX(5,1)/X45)**2
    DO 350 I=1,NPLT1
        YP(I,JT)=XX(I,1)
        YU(I,JT)=XX(I,1)+SQRT(P(I,1))
        YL(I,JT)=XX(I,1)-SQRT(P(I,1))
        YN(I,JT)=XX(I,1)

```

```

IF(CODE(K),NE,CODLST(2),OR,IT,NE,JT)GOTO 340
IF(1.EQ.4-OR,1.EQ.5)GOTO 34C
IF(1.EQ.NPLT)GOTO 337
I1=1
IF(1.EQ.6)I1=-1
YYM(I,JT)=2(I,1)
GOTO 339
337 YYM(NPLT,I,JT)=(I,1)
339 IF(YYM(I,JT).GT.YYMAX(I))YYMAX(I)=YYM(I,JT)
IF(YYM(I,JT).LT.YYMIN(I))YYMIN(I)=YYM(I,JT)
340 IF(YYJ(I,JT).GT.YYMAX(I))YYMAX(I)=YYJ(I,JT)
IF(YYJ(I,JT).LT.YYMIN(I))YYMIN(I)=YYJ(I,JT)
350 CONTINUE
400 IF(NIS.EQ.0)GOTO 480
VEL=QSTM*86400./U(7,1)+5280.
C * PERFORM A FURTHER TIME STEP IF RM WILL BE CLOSER TO RM2 AFTER
TIME STEP THAN BEFORE
IF(RM.LT.RM2)GOTO 450
RMRM2=RM-RM2
IF(RMRM2.GT.VEL*DT-RMRM2)GOTO 5C
450 IF(IT.EQ.JT)GOTO 480
JT2=IT
IF(JPLT.EQ.C)IP=1
IF(CODE(K),EQ,CODLST(2))GOTO 260
IF(JPLT.EQ.0)GOTO 480
GOTO 315
C END OF TIME LOOP
480 RETURN
END

```

```

SUBROUTINE SMOOTH
C*** SMOOTHING WITH EITHER FORWARD AND BACKWARD ESTIMATES
C FORWARD = 1 EXTENDED KALMAN FILTER
C BACKWARD = 0 6-D LINEARISED KALMAN FILTER

REAL D,K*,KKT
DOUBLE PRECISION XHGG,ZHGG,CHGG,UHGG

COMMON/B1/G(20,20),Q(20,20),R(20,20),R(20,20),XX(20,1),P(20,20),
X1(20,1),ID(20,20),FHC(20,20),PMDD(20,20),X(20,20),
F(20,20),FFI(20,1),CUMI(20,20),PPMDD(400,1),M(20,20),
UHGG(20),DUMINI(20,10),UC(20,1),
QUH2(20,20),RGM3(20,20),RN(20,20),KKT(20,20),
Z(20,1),S(40,1),FP(400,1),PDG(12),XLAB(12),
YLAB(12),S(1045),YP(100),YMC(100),YU(100),YL(100)
COMMON/B2/X(100),F(20,1),RK(4,400),CODLST(6),PL(20,1),
XHGG(20),ZHGG(20),YYP(20,100),YYM(20,100),YYU(20,100),
YYL(20,100),YYMAX(20),YYMIN(20),YLABE(20,9),YMINI(20),
YMAXI(20),G(20,1),I(PT(4),CHGG(20),CODE(70),RMI(70),
JOUT,JPLT,JT,NN,T,NC,N,L,CT,RMI,NN,IPI,IOUT,NIS,JT1,
JT2,K,RMI,RM2,VEL,R,IT2,TJK,NPLT,QSTM,KRH,NPLT1,TQ
COMMON/B3/QIN(20,20,70),RIN(20,20,70),DUMIN(20,70),KRH(70),IX
COMMON/B4/PB1(20,20),GSTMST(30),X1ST(12,650),VELST(300),
XXST(12,300),PPB1(400,1),KWRHMS1(20,1),
PIDG(20),PDG(20),IPS,KXNK,FMSE2(20,1),NMSTS2,
IOSMTH,YPL(20,20),YIN(20,70),FMSE(20,1),NMSTS,
PBIMDD(20,20),PK1(4,20),XS(20,1),PBIMDD(20,20),
PB1(20,20),RIN(20,20),PS1(20,20),PS(20,20),XS1(20,1),
XB(20,1),XB1(20,1),FMST(300),XPMDD(20,1),ATST(70),TT,KT
COMMON/B5/PST(12,12,300)
COMMON/B6/P1ST(12,12,300)

507 FORMAT(1H0,22HV-C OF PROCESS NOISE Q/)
509 FORMAT(1H0,26HV-C OF OBSERVATION NOISE R/)
511 FORMAT(1H0,33HC FOR ERROR COVARIANCE MATRIX PB/)
515 FORMAT(8F10.0)
517 FORMAT(1H0,27HINITIAL CONDITIONS TIME=F8.4,7H RM=F8.3/
.1H,50(1H*))
519 FORMAT(1H0,27HC FOR ESTIMATE OF STATE XB/)
533 FORMAT(1H0,70HESTIMATE OF STATE AFTER POINT LOAD IS INSTANTANEOUSL
.Y COMPLETELY MIXED/)
535 FORMAT(1H0,76HERROR COVARIANCE MATRIX AFTER POINT LOAD IS INSTANTA
.NEOUSLY COMPLETELY MIXED/)
546 FORMAT(1H0,23HSINGULAR P1 AT '260'+10/)
547 FORMAT(1H0,21HSINGULAR P AT '280'+1/)
548 FORMAT(1H0,24HSINGULAR PS1 AT '280'+10/)
549 FORMAT(1H0,23HSINGULAR PS AT '260'+13/)
550 FORMAT(1H0,22HSINGULAR PS AT '360'+2/)
552 FORMAT(1H0,23HSINGULAR FB1 AT '280'+3/)
553 FORMAT(1H0,25HSINGULAR PB11 AT '280'+18/)
560 FORMAT(2H02,3HIT=,I4,3HRM=,F10.5,2HQ=,F10.5,2HX=,
.I5,6HCODE=,A1)
561 FORMAT(1H2,214,F10.5,[4,A1])
562 FORMAT(1H,12,13,12,4F9.5,2(2),4F9.5)
563 FORMAT(1I4,6F10.3)
564 FORMAT(1H,6HMEASTS,10F10.5)
565 FORMAT(15,8F9.4)
571 FORMAT(1H1,71HMEAN SQUARE ERROR (OBSERVED - SMOOTH)ER) MSE(NMSTS),
.MSECNMSTS/2),R,Q/)

```

```

C *** INITIALISATION
      ICI=0
      IT=JT2
      IX=4*IT-3
      NMSYS=0
      DO 20 I=1,L
      FMSE(I,1)=0.
      FMSE2(I,1)=0.
20    CONTINUE
      IF(IOSMTH.EQ.2)GOTO 50
      DO 40 I=1,M
      XB(I,1)=XXST(I,IT)
      XB1(I,1)=X1ST(I,IX)
      DO 30 J=1,N
      PBI(I,J)=PST(I,J,IT)
      PBI1(I,J)=P1ST(I,J,IT)
30    CONTINUE
40    CONTINUE
      GOTO 80
50    READ 519,(XB(I,1),I=1,M)
      CALL MIN(PBI,N,N,1,0,XHDG,XHDC)
      DO 70 I=1,M
      XB1(I,1)=XB(I,1)
      DO 60 J=1,N
      PBI1(I,J)=PBI(I,J)
60    CONTINUE
70    CONTINUE

C *** ASSIGN INPUT-RIVER SYSTEM READY FOR EXECUTION
80    K=KT
      KRH=K
      VEL=VELST(IT)
      T=DT*(IT-1)
      PRINT 517,T,HMST(IT)
      PRINT 519
      CALL MDUT(XB,N,N,1,2,XHDG,XHDC)
      PRINT 511
      CALL MDUT(PBI,N,N,N,3,XHDG,XHDC)
      GOTO 260
90    ICI=1
      KP=K
100   KP=KP-1
      IF(CODE(KP).NE.CODLST(1))GOTO 100
C * REACH
      KRH=KP
      DO 175 I=1,IC
      C(I,1)=DUMIN(I,KRH)
175   CONTINUE
      DO 176 I=1,IU
      U(I,1)=DUMIN(I,KRH)
176   CONTINUE
      GOTO 179
178   IF(K.EQ.KRH)GOTO 90
179   K=K-1
      IF(CODE(K).EQ.CODLST(2))GOTO 180
      IF(CODE(K).EQ.CODLST(3))GOTO 199
      GOTO 215
C * MEASUREMENT
180   DO 195 I=1,L

```

```

      Z(I,1)=DUMIN(I,K)
185   CONTINUE
      GOTO 215
C * POINT LOAD
190   DO 195 I=2,NPLT1
      I1=I-1
      PL(I,1)=DUMIN(I,K)
195   CONTINUE
      QPL=DUMIN(1,K)
C *** EXECUTE BACKWARD C-D LINEARISED KALMAN FILTER
C * NUMBER OF TIME STEPS
215   NTS=NTST(K+1)-NTST(K)
      ITT=NTS
      IF(NTS.LE.0)GOTO 220
      ITT=0
218   ITT=ITT+1
      CALL LDFK1
      IF(ITT.NE.NTS)GOTO 260
220   IF(CODE(K).EQ.CODLST(2)) GOTO 225
      IF(CODE(K).EQ.CODLST(3)) GOTO 240
      GOTO 260
225   CALL LDKF2
      GOTO 260
C * COMPLETELY MIX POINT LOAD 'IN REVERSE'
240   QSTM=QSTMST(IT)
      QSTM1=QSTM-QPL
      DO 250 I=1,NKN
      XB(I,1)=(QSTM*XB(I,1)-PL(I,1)+QPL)/QSTM1
      DO 245 J=1,NKN
      PBI(I,J)=PBI(I,J)+(QSTM/QSTM1)*2
245   CONTINUE
250   CONTINUE
      IF(CPS.EQ.0)GOTO 260
      PRINT 533
      CALL MDUT(XB,N,1,2,XHDG,XHDC)
      PRINT 535
      CALL MDUT(PBI,N,N,3,XHDG,XHDC)
C *** SMOOTH - COMBINE FORWARD AND BACKWARD ESTIMATES
260   DO 260 I=1,M
      X1(I,1)=X1ST(I,IX)
      XX(I,1)=XXST(I,IT)
      DO 270 J=1,N
      P1(I,J)=P1ST(I,J,IT)
      P2(I,J)=P2ST(I,J,IT)
      PBI1(I,J)=PBI1(I,J)
      PBI2(I,J)=PBI2(I,J)
270   CONTINUE
      P1UG(I)=P1(I,1)
      P2UG(I)=P2(I,1)
280   CONTINUE
      P145=P1(4,5)
      P245=P2(4,5)
      CALL MINVSR(P,N,0)
      IF(ABS(D).LT.1.E-45)PRINT 544
      CALL MINVSR(P,M,0,4,0)
      IF(ABS(D).LT.1.E-45)PRINT 552
      IF(ITT.NE.NTS)GOTO 185

```

```

IF(COD.EQ.1)MADSUB(C)GOTO 260
IF(COD.EQ.2)GOTO 360

C ** 1 PRINT QUANT
C
PSINV=PINV+PBINV
CALL MINVSP(P,N,D)
IF(ABS(CD).LT.1.E-45)PRINT 546
CALL MADSUB(P,PBMOD,PS1,N,N,1)
CALL MINVSR(PS,N,D)
IF(ABS(CD).LT.1.E-45)PRINT 547
P=INV=PINV+PBINV
CALL MINVSP(P,N,D)
IF(ABS(CD).LT.1.E-45)PRINT 551
CALL MADSUB(P,PBMOD,PS,N,N,1)
CALL MINVSR(PS,N,D)
IF(ABS(CD).LT.1.E-45)PRINT 545
XS=PS+(PINV*XX+PBINV*XB1)
CALL MMULT(P,XX,DUM1,N,N,1)
CALL MMULT(PBMOD,XB1,DUM2,N,N,1)
CALL MADSUB(DUM1,DUM2,DUM1,N,N,1)
CALL MMULT(PS,DUM1,XS,N,N,1)
XS1=PS1+(PINV*X1+PBINV*XB)
CALL MMULT(P1,X1,DUM1,N,N,1)
CALL MMULT(PBMOD,XB,DUM2,N,N,1)
CALL MADSUB(DUM1,DUM2,DUM1,N,N,1)
CALL MMULT(PS1,DUM1,XS1,N,N,1)
GOTO 400

C ** 2 OTHER
C
PSINV=PINV+PBINV
360 CALL MADSUB(P,PBMOD,PS,N,N,1)
CALL MINVSR(PS,N,D)
IF(ABS(CD).LT.1.E-45)PRINT 551
XS=PS+(PINV*XX+PBINV*XB)
CALL MMULT(P,XX,DUM1,N,N,1)
CALL MMULT(PBMOD,XB,DUM2,N,N,1)
CALL MADSUB(DUM1,DUM2,DUM1,N,N,1)
CALL MMULT(PS,DUM1,XS,N,N,1)
C
XS1=XS, PS1=PS
DO 380 I=1,N
XS1(I)=XS(I)
DO 370 J=1,N
PS1(I,J)=PS(I,J)
370 CONTINUE
380 CONTINUE

C *** PRINT SUMMARY OF OUTPUT TO LINE PRINTER AND DISK
400 COD=CODLST(6)
IF(NTST(K).EQ.IT)COD=CODE(K)
PRINT 560,IT,RMST(IT),VEL,QSTMST(IT),K,COD
WRITE(KM,561)IX,IT,RMST(IT),K,COD
IF(COD.NE.CODLST(2))GOTO 410
PRINT 564,(Z(I),I=1,L)
WRITE(KM,565)K,(Z(I),I=1,L)
410 DO 420 I=1,N
PRINT 562,K,IX,I,X1(I),SQRT(P1DG(I)),XX(I),SQRT(P0G(I)),
XB(I),SQRT(PB1(I)),XB1(I),SQRT(PB1I(I)),XS1(I),
SQRT(PS1(I)),XS(I),SQRT(PS(I))
WRITE(KM,563)K,IX,I,X1(I),SQRT(P1DG(I)),XX(I),SQRT(P0G(I)),
XB(I),SQRT(PB1(I)),K,IX,I,XB1(I),

```

```

SQRT(PB1I(I)),XS1(I),SQRT(PS1(I)),XS(I),
SQRT(PS(I))
420 CONTINUE
I=N+1
PRINT 562,K,IX,I,F145,P45,PE1(4,5),PB11(4,5),FS(4,5),PS(4,5)
WRITE(KM,563)K,IX,I,P145,P45,FE1(4,5),PB1I(4,5),PS(4,5),
IF(CEI.EQ.0)GOTO 90
IF(ITI.LT.NTS)GOTO 218
IF(K.GT.1)GOTO 178
C *** MEAN SQUARE ERROR (OBSERVED - SMOOTHER)
450 NMS=NMST5-NMST52-1
DC 470 T=L,L
FMSE(I)=FMSE(I)/(NMST5-1)
FMSE2(I)=FMSE2(I)/NMS
470 CONTINUE
PRINT 571
CALL MOUT(FMSE,L+1,2,ZHOG,ZHOG)
CALL MOUT(FMSE2,L+1,2,ZHOG,ZHOG)
PRINT 509
CALL MOUT(R,L+3,ZHOG,ZHOG)
PRINT 507
CALL MOUT(O,N,N+3,ZHOG,ZHOG)

RETURN
END

```

```

SUBROUTINE LDEKFP
C*** CONTINUOUS-DISCRETE BACKWARD LINEARISED KALMAN FILTER - PREDICTION
REAL ID,KK,KKT
DOUBLE PRECISION XHOG,ZHOG,CHOG,UHOG
COMMON/B1/G(20,20),Q(20,20),H(20,20),R(20,20),XX(20,1),P(20,20),
X1(20,1),ID(20,20),HT(20,20),PMOD(20,20),P1(20,20),
FF(20,20),FFT(20,20),DUM1(20,20),PPMOD(400,1),H(20,20),
UHOG(20),DUMIN1(20,70),U(20,1),
DUM2(20,20),DUM3(20,20),KK(20,20),KKT(20,20),
Z(20,1),RHS(400,1),PP(400,1),HOG(12),XLABEL(12),
YLABEL(9),A(104,1),YP(100),YM(100),YU(100),YL(100)
COMMON/B2/X(100),F(20,1),RK(4,400),CDDLST(6),PL(20,1),
XHOG(20),ZHOG(20),YYP(20,100),YIM(20,100),YYU(20,100),
YLL(20,100),YMAX(20),YMIN(20),YLABE(20,9),YMINI(20),
YMAXI(20),C(20,1),ICPT(4),CHOG(20),CODE(70),RMIN(70),
JOUT,JPLT,JT,NN,I,NC,N,L,DT,RMI,NNN,IPI,IOUT,NTS,JT1,
JT2,K,RM1,RM2,VEL,RP,T1,T2,IJK,NPLT,QSTM,KRH,NPLT1,IQ
COMMON/B3/QIN(20,20,70),RIN(20,20,70),DUMIN(20,70),KRCH(70),IX
COMMON/B4/PBI(20,20),QSTMST(30),X1ST(12,650),VELST(300),
XXST(12,300),PPBI(40,1),KW,RHS1(20,1),
PIDG(20),PDG(20),IPS,NXAK,FMSE2(20,1),NMSST2,
IOSMTH,YPL(20,20),YIN(20,70),FMSE(20,1),NMSST,
PBIMOD(20,20),RK1(4,20),XSC(20,1),PBMOD(20,20),
PBI1(20,20),RINVC(20,20),PS1(20,20),PS(20,20),XS1(20,1),
XB(20,1),XB1(20,1),RMST(300),XPMOD(20,1),NTST(70),IT,KT
COMMON/B5/PST(12,12,300)
COMMON/B6/P1ST(12,12,300)
504 FORMAT(1H0,12HTIME STEP NC,15,9H TIME,F8.4,7H RM,F8.3/1+ ,
.49(1H*))
527 FORMAT(1H0,37HPREDICTED ERROR COVARIANCE MATRIX PBI/)
528 FORMAT(1H0,31HPREDICTED ESTIMATE OF STATE XB1/)
C ** STATE ESTIMATE PROPAGATION S1
C XB1=XB+INTEGRAL(TI TO T) CF (-F-FF*(XB-X))
C ** ERROR COVARIANCE PROPAGATION PBII
C PBI1=PB1+INTEGRAL(TI TO T) CF (-FF*PB-PB*FFT+Q)
TMOO=TI
IT=IT-1
DO 160 I=1,N
XPMOD(I,1)=XX(I,1)
DO 150 J=1,N
IJ=(I-1)*N+J
PPBI(I,J,1)=PB(I,J)
PBIMOD(I,J)=PBI(I,J)
150 CONTINUE
160 CONTINUE
DO 210 KSEL=1,4
IX=4-IT-KSEL+2
IF(KSEL.GT.1)GOTO 162
IF(CODE(K+1).EQ.CDDLST(2))GOTO 164
DO 163 I=1,N
X1(I,1)=X1ST(I,IX)
163 CONTINUE
GOTO 168
164 DO 165 I=1,N
X1(I,1)=XXST(1,IT+1)
165 CONTINUE

```

```

168 VEL=VELST(IT)
CALL EQN1(X1,U,C,F,N,VEL)
CALL EQN2(X1,U,C,FF,N,VEL)
C * FF*(XB-X)
CALL MAOSUB(XPMOD,X1,DUM1,N,1,-1)
CALL MMULT(FF,DUM1,DUM1,N,N,1)
C * RHS1=(-F-FF*(XB-X))
DO 170 I=1,N
RHS1(I,1)=-F(T,1)-DUM1(I,1)
170 CONTINUE
C * FF*PB
CALL MMULT(FF,PBIMOD,DUM1,N,N,N)
C * PB*FFT
CALL MTRANS(FF,FFT,N,N)
CALL MMULT(PBIMOD,FFT,DUM2,N,N,N)
C * RHS=(-FF*PB-PB*FFT+Q)
DO 180 I=1,N
DO 175 J=1,N
DUM3(I,J)=-DUM1(I,J)-DUM2(I,J)+Q(I,J)
IJ=(I-1)*N+J
RHS(I,J)=DUM3(I,J)
175 CONTINUE
180 CONTINUE
CALL RUNGE(KSEL,N,DT,RHS1,XPMOD,TMOD,TI,XX,RK1)
CALL RUNGE(KSEL,NN,DT,RHS,PPMOD,TMOD,TI,PPBI,RK1)
DO 200 I=1,N
DO 190 J=1,N
IJ=(I-1)*N+J
PBIMOD(I,J)=PPMOD(I,J,1)
190 CONTINUE
200 CONTINUE
210 CONTINUE
DO 230 I=1,N
XB1(I,1)=XPMOD(I,1)
XB(I,1)=XB1(I,1)
DO 220 J=1,N
PBI1(I,J)=PBIMOD(I,J)
PBI(I,J)=PBI1(I,J)
220 CONTINUE
230 CONTINUE
IX=IX-1
C ** PRINT RESULTS
IF(IPS.EQ.0)GOTO 400
T=OT+(IT-1)
PRINT 504,IT,T,RMST(IT)
PRINT 527
CALL MOUT(PBI1,NNN,NNN,1: XHOG,XHD6)
PRINT 528
CALL MOUT(XB1,NNN,1,2,XHOG,XHOG)
400 RETURN
END

```

```

SUBROUTINE LOEKFU
C**** CONTINUOUS-DISCRETE BACKWARD LINEARISED KALMAN FILTER - UPDATE
REAL ID,KK,KKT
DOUBLE PRECISION XHOG,ZHOG,CHOG,UHOG

COMMON/B1/G(20,20),Q(20,20),H(20,20),R(20,20),XX(20,1),F(20,20),
* X1(20,1),ID(20,20),HHT(20,20),FMDD(20,20),P1(20,20),
* FF(20,20),FFI(20,20),DUM1(20,20),PPMDD(400,1),H(20,20),
* UHOG(20),DUMTN1(20,70),U(20,1),
* DM2(20,20),DUM3(20,20),KK(20,20),KKT(20,20),
* Z(20,1),RHS(400,1),PP(400,1),HOG(12),XLABEL(12),
* YLABEL(9),A(104,4),YF(100),YMC(100),YU(100),YL(100)
COMMON/B2/X(100),F(20,1),RK(4,400),CODLST(6),PL(20,1),
* XHOG(20),ZHOG(20),YYP(20,100),YYM(20,100),YYU(20,100),
* YYL(20,100),YYMAX(20),YYMIN(20),YLABEC(20,9),YMIN1(20),
* YMAX1(20),C(20,1),IDPT(4),CHOG(20),CODE(70),RM1N(70),
* JOUT,JPLT,JT,NN-T,NC,4,L,DT,RM1,NNN,1PT,1OUT,NTS,JT1,
* JT2,K,RM1,RM2,VEL,R1,T1,T2,IJK,NPLT,QSTM,KRM,APL1,10
COMMON/B3/QIN(20,20,70),RIN(20,20,70),DUMTN(20,70),KRCH(70),IX
COMMON/B4/PBI(20,20),QSTNST(30),X1ST(12,65),VELST(300),
* XXST(12,300),PPBI(400,1),KW,RHS1(20,1),
* P1OG(20),POG(20),IPS,NXNK,FMSE2(20,1),NMSTS2,
* IGSMT,YP1(20,20),YIN(20,70),FMSE(20,1),NMSTS,
* PBIHOG(20,20),RK1(4,20),XS(20,1),PBHOG(20,20),
* PBI(20,20),RIN(20,20),PS1(20,20),PS(20,20),XS1(20,1),
* XB(20,1),XB1(20,1),FMST(300),XPMDD(20,1),NTST(70),IT,KT
COMMON/B5/PST(12,12,300)
COMMON/B6/P1ST(12,12,300)

503 FORMAT(1H0,20OBSERVATION VECTOR Z/)
520 FORMAT(1H0,34UPDATED ERROR COVARIANCE MATRIX PB/)
521 FORMAT(1H0,28UPDATED ESTIMATE OF STATE X8/)
552 FORMAT(1H0,21HSINGULAR PBI AT *0*46/)

C ** KALMAN GAIN MATRIX
KK=PB1*HHT*(HH+PB1*HHT*R)**-1
CALL MMULT(HHT,PB1,DUM1,L,N,N)
CALL MMULT(DUM1,HHT,DUM1,L,N,L)
CALL MADSUB(DUM1,R,DUM1,L,L,1)
CALL MINVSR(DUM1,L,0)
IF(ABS(D)-L.T.1.E-45)PRINT 552
CALL MMULT(HHT,DUM1,DUM1,N,L,L)
CALL MMULT(PB1,DUM1,KK,N,N,L)

C ** STATE ESTIMATE UPDATE XE
XB=XB1+KK*(Z-HH*XB1)
CALL MMULT(HH,XB1,N,L,N,1)
CALL MADSUB(Z,H,DUM1,L,1,-1)
CALL MMULT(KK,DUM1,DUM1,N,L,1)
CALL MADSUB(XB1,DUM1,XB,N,1,1)

C ** ERROR COVARIANCE UPDATE PB
P=(ID-KK*HH)+PB1*(ID-KK*PH)+KK*R*KKT
CALL TRANS(KK,KKT,N,L)
CALL MMULT(R,KKT,DUM1,L,L,N)
CALL MMULT(KK,DUM1,DUM1,N,L,N)
CALL MMULT(KK,HH,DUM2,N,L,N)
CALL MMULT(KK,HH,DUM2,N,L,N)

CALL MADSUB(ID,DUM2,DUM2,N,N,1)
CALL MMULT(KK,DUM2,DUM2,N,N,1)
CALL MMULT(PB1,DUM2,PBI,N,N,1)

C ** PRINT RESULTS
IF(CIPS.LO.G)STOP 100
PRINT 503
CALL MOUT(Z,L,1,2,ZHOG,ZHOG)
PRINT 520
CALL MOUT(PBI,NN,NAN,3,XHOG,XHOG)
PRINT 521
CALL MOUT(XB,NN,1,2,XHOG,XHOG)

C *** CALCULATE MEAN SQUARE ERROR (OBSERVED - SMOOTHER)
FMSE=FMSE+(Z-HH*XB)**2
CALL MMULT(HH,XB,DUM1,L,N,1)
CALL MADSUB(Z,DUM1,DUM1,L,1,-1)
DO 295 I=1,L
FMSE(I)=FMSE(I)+DUM1(I,1)**2
295 CONTINUE
NMSTS=NMSTS+1
IF(NMSTS.GT.NMSTS2)GO TO 300
DO 298 I=1,L
FMSE2(I-1)=FMSE2(I,1)+DUM1(I,1)**2
298 CONTINUE

300 RETURN
END

```

```

SUBROUTINE EQM1(X,U,C,F,A,VEL)
C**** EQUATIONS FOR ELEMENTS OF F VECTOR
DIMENSION X(20,1),C(20,1),F(20,1),U(20,1)
DO 20 I=1,N
  F(I,1)=C
20 CONTINUE
C**** NITROGEN CYCLING AND BOD-DO IN JORDAN RIVER, UTAH, USA
A=U(7,1)
H=U(8,1)
Q=U(5,1)*86400./5280.
QCA=Q/A
T=U(6,1)
C0=C(1,1)+1.08**(T-20.)
C52=C(2,1)+1.08**(T-20.)
C23=C(3,1)+1.08**(T-20.)
C45=C(4,1)+1.08**(T-20.)
C1=C(13,1)+1.08**(T-20.)
C2=C(14,1)+1.08**(T-20.)
C3=C(15,1)+1.08**(T-20.)
C4=C(16,1)+1.08**(T-20.)
C5=C(17,1)+1.08**(T-20.)
C6=C(18,1)+1.08**(T-20.)
VELFS=VEL*5280./86400.
CA=20.174+VELFS*.607/H**1.685*1.047**(T-20.)
AA=C(12,1)*X(2,1)+X(3,1)
BB=C(6,1)+C(8,1)*X(2,1)+X(3,1)
CC=C(8,1)*X(2,1)+X(3,1)
CCDAA=CC/AA
TH=C(17,1)*X(2,1)/AA
F(1,1)=-C0*X(1,1)-C1*X(1,1)+(L(1,1)-X(1,1))*Q0A
F(2,1)=-C52*X(5,1)-C23*X(2,1)-C2*X(2,1)-TH*C(7,1)*CCDAA*X(4,1)+
  (U(2,1)-X(2,1))*Q0A
F(3,1)=-C3*X(3,1)+C23*X(2,1)*(1.-TH)*C(7,1)*CCDAA*X(4,1)+
  (U(3,1)-X(3,1))*QCA
F(4,1)=-C4*X(4,1)+C(7,1)*CCDAA*X(4,1)-C45*X(4,1)-X(4,1)*Q0A
F(5,1)=-C45*X(4,1)-C52*X(5,1)-C5*X(5,1)-X(5,1)*Q0A
F(6,1)=-CA*(C(9,1)-X(6,1))-C0*X(1,1)-C(10,1)*C23*X(2,1)-
  C6*X(6,1)-U(4,1)/(28.317*H)-(U(9,1)-X(6,1))*Q0A
F(7,1)=0.
RETURN
END

SUBROUTINE EQM2P(X,P,C,CT)
C**** EQUATIONS FOR DEPENDENT VARIABLES CALCULATED FROM STATE VARIABLES
RETURN
END

```

```

SUBROUTINE EQN2(X,U,C,FF,A,VEL)
C**** EQUATIONS FOR ELEMENTS OF FF MATRIX
DIMENSION X(20,1),C(20,1),FF(20,20),U(20,1)
DO 50 I=1,N
  DO 40 J=1,N
    FF(I,J)=0.
40 CONTINUE
50 CONTINUE
C**** NITROGEN CYCLING AND BOD-DO IN JORDAN RIVER, UTAH, USA
A=U(7,1)
H=U(8,1)
Q=U(5,1)*86400./5280.
QCA=Q/A
T=U(6,1)
C0=C(1,1)+1.08**(T-20.)
C52=C(2,1)+1.08**(T-20.)
C23=C(3,1)+1.08**(T-20.)
C45=C(4,1)+1.08**(T-20.)
C1=C(13,1)+1.08**(T-20.)
C2=C(14,1)+1.08**(T-20.)
C3=C(15,1)+1.08**(T-20.)
C4=C(16,1)+1.08**(T-20.)
C5=C(17,1)+1.08**(T-20.)
C6=C(18,1)+1.08**(T-20.)
VELFS=VEL*5280./86400.
CA=20.174+VELFS*.607/H**1.685*1.047**(T-20.)
AA=C(12,1)*X(2,1)+X(3,1)
BB=C(6,1)+C(8,1)*X(2,1)+X(3,1)
CC=C(8,1)*X(2,1)+X(3,1)
CCDAA=CC/AA
BBCC=BB*CC
BB2=BB*BB
AA2BB2=AA*AA*BB2
TH=C(12,1)*X(2,1)/AA
FF(1,1)=-C0-C1-Q0A
FF(2,2)=-C23-C2-Q0A-(C(7,1)+C(12,1)*X(4,1)/AA2BB2)+
  (C(6,1)+C(8,1)*X(2,1)+AA*X(3,1))*BBCC)
FF(2,3)=-C(7,1)+C(12,1)*X(2,1)+X(4,1)/AA2BB2)+
  (C(6,1)+AA*BBCC)
FF(2,4)=TH+C(7,1)*CCDAA
FF(2,5)=C52
FF(3,2)=(C23-C(7,1)*X(4,1)/AA2BB2)+
  (C(6,1)+C(8,1)*X(3,1)+AA-C(12,1)*X(3,1))*BBCC)
FF(3,3)=-C3-Q0A-(C(7,1)+X(4,1)/AA2BB2)+
  (C(6,1)+X(3,1)+AA-C(12,1)*X(2,1))*BBCC)
FF(3,4)=(1.-TH)*C(7,1)*CCDAA
FF(4,2)=C(6,1)+C(7,1)+C(8,1)*X(4,1)/BB2
FF(4,3)=FF(4,2)/C(8,1)
FF(4,4)=-C45-Q0A-C4+C(7,1)*CCCAA
FF(5,4)=C45
FF(5,5)=-C52-C5-Q0A
FF(6,1)=-C0
FF(6,2)=-C(10,1)+C23
FF(6,6)=-CA-C6-Q0A
RETURN
END

```



```

SUBROUTINE MEN(AA,LL,MM,ICDIAG,ICUT,RHDG,CHDG)
C**** TO READ MATRIX AA(LL*MM)
C IF ICDIAG=1 ONLY DIAGONAL ELEMENTS ARE READ
C IF ICUT=1 PRINT MATRIX
DOUBLE PRECISION RHDG,CHDG
DIMENSION AA(20,20),RHDG(20),CHDG(20)
9001 FORMAT(8F10.0)
IF(ICDIAG-1)IO=10,10
10 DO 20 I=1,LL
READ 9001,(AA(I,J),J=1,MM)
20 CONTINUE
GOTO 60
30 DO 50 I=1,LL
DO 40 J=1,MM
AA(I,J)=0.
40 CONTINUE
50 CONTINUE
READ 9001,(AA(I,I),I=1,LL)
60 IF(ICUT-1)IO=70,70
70 CALL MDUT(AA,LL,MM,ICUT,RHDG,CHDG)
80 RETURN
END

```

```

SUBROUTINE MDUT(AA,LL,MM,ICUT,RHDG,CHDG)
C**** TO PRINT MATRIX AA(LL*MM)
C IF ICUT=2 PRINT ROW HEADINGS
C IF ICUT=3 PRINT ROW & COLUMN HEADINGS
DOUBLE PRECISION RHDG,CHDG
DIMENSION AA(20,20),RHDG(20),CHDG(20)
9000 FORMAT(1H,12F10.5/)
9002 FORMAT(1H,10X,11(2X,A8))
9003 FORMAT(1H,A8,2X,11F10.5/1H,1(X,11F10.5/)
IF(ICUT-1)GOTO 2)
10 DO 10 I=1,LL
PRINT 9000,(AA(I,J),J=1,MM)
CONTINUE
RETURN
20 IF(ICUT-2)GOTO 25
PRINT 9002,(CHDG(J),J=1,MM)
25 DO 30 I=1,LL
PRINT 9003,RHDG(I),(AA(I,J),J=1,MM)
30 CONTINUE
RETURN
END

```

```

SUBROUTINE MDSUB(AA,EB,CC,LL,MM,NAAS)
C**** TO ADD OR SUBTRACT MATRICES CC(LL*MM)=AA(LL*MM)+NAAS*(EB(LL*MM)
DIMENSION AA(20,20),EB(20,20),CC(20,20)
IF(NAAS)SO=50,50,10
C**** ADDITION
10 DO 30 I=1,LL
DO 20 J=1,MM
CC(I,J)=AA(I,J)+EB(I,J)
20 CONTINUE
30 CONTINUE
RETURN
C**** SUBTRACTION
50 DO 70 I=1,LL
DO 60 J=1,MM
CC(I,J)=AA(I,J)-EB(I,J)
60 CONTINUE
70 CONTINUE
RETURN
END

```

```

SUBROUTINE MMULT(AA,BB,CC,LL,MM,NN)
C**** TO FORM MATRIX PRODUCT CC(LL*NN)=AA(LL*MM)*BB(MM*NN)
DIMENSION AA(20,20),BB(20,20),CC(20,20),A1(20,20),B1(20,20),
C1(20,20)
10 DO 30 J=1,MM
DO 20 I=1,LL
A1(I,J)=AA(I,J)
20 CONTINUE
DO 30 K=1,NN
B1(J,K)=BB(J,K)
30 CONTINUE
DO 40 I=1,LL
DO 40 J=1,NN
C1(I,J)=0.
DO 40 K=1,MM
C1(I,J)=C1(I,J)+A1(I,K)*B1(K,J)
40 CONTINUE
DO 50 I=1,LL
DO 50 J=1,NN
CC(I,J)=C1(I,J)
50 CONTINUE
RETURN
END

```

```

C**** SUBROUTINE MTRANS(AA,AT,LL,MM)
      TO TRANSPOSE MATRIX AA(20,20) AND THUS OBTAIN AT(MM*LL)
      DIMENSION AA(20,20),AT(20,20)
      DO 20 I=1,LL
      DO 10 J=1,MM
      AT(J,I)=AA(I,J)
10 CONTINUE
20 CONTINUE
      RETURN
      END

C**** SUBROUTINE RUNGE(KSEL,NCYS,DT,FYT,YMOD,IMOD,TD,YO,RK)
      FOURTH ORDER RUNGE-KUTTA ALGORITHM FOR INTEGRATION OF VECTOR FYT
      DIMENSION FYT(400,1),YMOD(400,1),YO(400,1),RK(4,400)
      GOTO(10,20,30,40),KSEL
10 DTA=DT/3.
      TMO=TO+DTA
      DO 15 I=1,NOYS
      RK(I,1)=FYT(I,1)
      YMOD(I,1)=YO(I,1)+DTA*RK(I,1)
15 CONTINUE
      RETURN
20 DTA=DT/3.
      TMO=TO+2.*DTA
      DO 25 I=1,NOYS
      RK(2,I)=FYT(I,1)
      YMOD(I,1)=YO(I,1)+DTA*RK(1,I)+DTA*RK(2,I)
25 CONTINUE
      RETURN
30 TMO=TO+DT
      DO 35 I=1,NOYS
      RK(3,I)=FYT(I,1)
      YMOD(I,1)=YO(I,1)+DT*(RK(1,I)-RK(2,I)+RK(3,I))
35 CONTINUE
      RETURN
40 TMO=TO+DT
      DTA=DT/8.
      DO 45 I=1,NOYS
      RK(4,I)=FYT(I,1)
      YMOD(I,1)=YO(I,1)+DTA*(RK(1,I)+3.*RK(2,I)+3.*RK(3,I)+RK(4,I))
45 CONTINUE
      RETURN
      END

```

```

C SUBROUTINE MINV
C PURPOSE
C INVERT A MATRIX
C USAGE
C CALL MINVSP(A,N,D,L,M)
C DESCRIPTION OF PARAMETERS
C A - INPUT MATRIX, DESTROYED IN COMPUTATION AND REPLACES BY
C RESULTANT INVERSE.
C N - ORDER OF MATRIX A
C D - RESULTANT DETERMINANT
C L - WORK VECTOR OF LENGTH N
C M - WORK VECTOR OF LENGTH N
C REMARKS
C MATRIX A MUST BE A GENERAL MATRIX
C SUBROUTINES AND FUNCTION SUBPROGRAMS REQUIRED
C NONE
C METHOD
C THE STANDARD GAUSS-JORDAN METHOD IS USED. THE DETERMINANT
C IS ALSO CALCULATED. A DETERMINANT OF ZERO INDICATES THAT
C THE MATRIX IS SINGULAR.
C .....
C SUBROUTINE MINV(A,N,D,L,M)
C DIMENSION A(L),L(L),M(L)
C .....
C SEARCH FOR LARGEST ELEMENT
C
D=1.0
NK=-N
DO 80 K=1,N
NK=NK+K
L(K)=K
M(K)=K
KK=NK+K
BIGA=A(KK)
DO 20 J=K,N
IZ=N+(J-1)
DO 20 I=K,M
IJ=IZ+I
10 IF(ABS(BIGA)-ABS(A(IJ))) 15,20,20
15 BIGA=A(IJ)
L(K)=I
M(K)=J
20 CONTINUE
C INTERCHANGE ROWS
C
J=L(K)
IF (J-K) 35,35,25
KI=K-N
DO 30 I=1,N
KI=KI+N

```

```

HOLD=-A(KI)
JI=KI-K+J
A(KI)=A(JI)
A(JI)=HOLD
30
C
C INTERCHANGE COLUMNS
C
35 I=M(K)
IF(I-K) 45,45,58
38 JP=N*(I-1)
DO 40 J=1,N
JK=NK+J
JI=JP+J
HOLD=-A(JK)
A(JK)=A(JI)
A(JI)=HOLD
40
C
C DIVIDE COLUMN BY MINUS PIVOT (VALUE OF PIVOT ELEMENT IS
C CONTAINED IN BIGA)
C
45 IF(BIGA) 48,46,48
46 D=0.0
RETURN
48 DO 55 I=1,N
IF(I-K) 50,55,50
50 IK=NK+I
A(IK)=A(IK)/(-BIGA)
55 CONTINUE
C
C REDUCE MATRIX
C
DO 65 I=1,N
IK=NK+I
HOLD=A(IK)
IJ=I-N
DO 65 J=1,N
IJ=IJ+N
IF(I-K) 60,65,60
60 IF(J-K) 62,65,62
62 KJ=J-I+K
A(IJ)=HOLD+A(KJ)+A(IJ)
65 CONTINUE
C
C DIVIDE ROW BY PIVOT
C
KJ=K-N
DO 75 J=1,N
KJ=KJ+N
IF(J-K) 70,75,70
70 A(KJ)=A(KJ)/BIGA
75 CONTINUE
C
C PRODUCT OF PIVOTS
C
D=D*BIGA
C
C REPLACE PIVOT BY RECIPROCAL
C
A(KK)=1.0/BIGA
80 CONTINUE
C

```

```

C FINAL ROW AND COLUMN INTERCHANGE
C

```

```

K=N
100 K=(K-1)
IF(K) 150,150,105
105 I=L(K)
IF(I-K) 120,120,108
108 JQ=N*(K-1)
JR=N*(I-1)
DO 110 J=1,N
JK=JQ+J
HOLD=A(JK)
JI=JR+J
A(JK)=-A(JI)
110 A(JI)=HOLD
120 J=M(K)
IF(J-K) 100,100,125
125 KI=K-N
DO 130 I=1,N
KI=KI+N
HOLD=A(KI)
JI=KI-K+J
A(KI)=-A(JI)
130 A(JI)=HOLD
GO TO 100
150 RETURN
END

```

```

SUBROUTINE MINVSR(A,L,D)
C*** TO CONVERT MATRIX A TO VECTOR AA, INVERT AA IN SUBROUTINE MINV,
C & CONVERT INVERSE BACK TO MATRIX A
DIMENSION A(20,20),LL(20),MP(20),AA(400)
DO 20 I=1,L
DO 10 J=1,L
IJ=(J-1)*L+I
AA(IJ)=A(I,J)
10 CONTINUE
20 CONTINUE
CALL MINV(AA,L,D,LL,MM)
DO 40 I=1,L
DO 30 J=1,L
IJ=(J-1)*L+I
A(I,J)=AA(IJ)
30 CONTINUE
40 CONTINUE
RETURN
END

```

5. Sample input for filter model.

NITROGEN CYCLING AND BOD-DO IN JORDAN RIVER, UTAH, USA: EXTENDED KALMAN FILTER										R	28.0	.7	.1	.30	.04		.015	3
(M=MEASURED, E=ESTIMATED, C=CONSTANT, STD DEVIN & E-STD DEVIN)											2	7.9	4.57		2	C	0	0
39.2-RIVER MILES											0	0	0					
											12	.75	1.5	0	30	20	70	1.5
											7.27							
										M	26.7	15	1.7	1.86	.8	7.2		
										P	26.5	7		17	5			3.95
										R	26.5	.7	.1		.04		.015	3
BIOCHEMICAL OXYGEN DEMAND BOD MG/L											2	7.9	4.57		2	0	0	0
AMMONIA NITROGEN NH3-N MG/L											0	0	0					
NITRATE NITROGEN NOS-N MG/L											12	.75	1.5	0	30	20	70	1.5
PLANKTON AS NITROGEN ALG-N MG/L											7.27							
ORGANIC NITROGEN MG/L										P	26	0						
DISSOLVED OXYGEN DO MG/L										R	26.0	.7	.1	0	.04		.015	3
ORG-N + ALG-N MG/L											2	7.9	4.57		2	0	0	0
BOD NH3-N NOS-N ALG-N (RG-N DOALG+DRGN											0	0	0					
BOD NH3-N NOS-NALG+DRGN DO											12	.75	1.5	0	30	20	100	2.0
K0 K52 K23 K45 ELANK RS(NG3) MU-HAT BETA DO SATMG02/MGN										P	25.5	0						
DLANK GAMMA K1 K2 K3 K4 K5 K6										R	25.0	.7	.1	.30	.04		.015	3
LAT BODLAT NH3LAT NOSLAT ALGLAT DOALG+DRGLAT											2	7.9	4.57		2	0	0	0
1											0	0	0					
											12	.75	1.5	0	20	20	100	2.0
											7.58							
										M	23.7	15	.6	1.84	.9	7.4		
										M	22.8	9.8	.9	1.97	.8	7.4		
										P	22.6	12	5	.5	2			7
										R	22.6	.7	.1	.30	.04		.015	3
											2	7.9	4.57		2	0	0	0
											0	0	0					
											12	.75	1.5	0	20	20	100	2.0
											7.58							
										D	22.2	-50						
										P	22.2	7	60	17	5			3.95
										R	22.0	.7	.1	.30	.04		.015	3
											2	7.9	4.57		2	0	0	0
											0	0	0					
											12	.75	1.5	0	20	20	165	2.0
											7.58							
										M	21.4	10.8	1.1	2.07	.6	7.2		
										P	21.4	94	12.0	2.20	6			7.3
										R	21.4	.7	.1	.30	.04		.015	3
											2	7.9	4.57		2	0	0	0
											0	0	0					
											12	.75	1.5	0	20	20	165	2.0
											7.58							
										P	20.0	0						
										R	20.0	.7	.1	.30	.04		.015	3
											2	7.9	4.57		2	0	0	0
											0	0	0					
											12	.75	1.5	0	20	20	75	3.6
											7.58							
										M	19.4	11.5	1.7	1.86	.8	7.2		
										P	18.7	10	60	17	5			
										R	18.7	.7	.1	.30	.04		.015	3
											2	7.9	4.57		2	0	0	0
											0	0	0					
											12	.75	1.5	0	20	20	275	3.6
											7.58							
										P	18.5	20	0	17	5			
										R	18.5	.7	.1	.30	.04		.015	3

	2	7.9	4.57		2	0	0	0
	0	0	0					
	12	.75	1.5	0	20	20	275	3.6
	7.58							
P	18.1	15	5	.5	2			7.9
R	18.1	.7	.1	.30	.04		.015	3
	2	7.9	4.57		2	0	0	0
	0	0	0					
	12	.75	1.5		20	20	275	3.6
	7.58							
M	17.2	14.5	1.70	2.00	1.7	7		
U	16.7	-317						
P	16.7	0						
R	16.7	.7	.1	.30	.04		.015	1.5
	2	7.9	4.57		2	0	0	0
	0	0	0					
	50	.75	1.5	121	3	20	100	2.2
	7.5							
P	16.2	6	60	12	5			6
R	16.2	.7	.1	.30	.04		.015	1.5
	2	7.9	4.57		2	0	0	0
	0	0	0					
	50	.75	1.5	121	3	20	100	2.2
	7.5							
M	15.5	13	1.6	2.06	.8	7		
P	15	18	5	.5	2			7
R	15.0	.7	.1	.30	.04		.015	1.5
	2	7.9	4.57		2	0	0	0
	0	0	0					
	50	.75	1.5	121	3	20	100	2.2
	7.5							
M	14.	16	1.5	2.05	.8	5.6		
M	12.6	16	1.7	2.10	.5	5.8		
P	12.4	10	5	.5	2			7.9
R	12.4	.7	.1	.30	.04		.015	1.5
	2	7.9	4.57		2	0	0	0
	0	0	0					
	50	.75	1.5	121	3	20	100	2.2
	7.5							
P	12	0						
R	12.0	.7	.1	.30	.04		.015	1.5
	2	7.9	4.57		2	0	0	0
	0	0	0					
	0	0	0	121	0	20	100	2.2
	7.5							
M	10.5	13.5	1.4	2.07	.9	5.5		
M	9.2	12.8	1.4	2.19	.9	5.3		
M	8.3	12.5	1.8	2.30	.4	5.6		
M	6.2	11.6	1.6	2.26	.6	6.1		
P	5.9	2	60	12	5			3.95
R	5.9	.7	.1	.30	.04		.015	1.5
	2	7.9	4.57		2	0	0	0
	0	0	0					
	0	0	0	121	0	20	100	2.2
	7.5							
M	5.1	14	1.2	2.29	2.	4.7		
E	2.8							
	14.2	1.3	2.28	1.3	.1	5.4		
	1.	.01	.04	.125	.125	.25		

## 6. Sample output from filter model.

NITROGEN CYCLING AND BCD-DC IN JEROME RIVER, UTAH, USA: EXTENDED KALMAN

```

ORDER OF SYSTEM/NUMBER OF STATES N=      6
NUMBER OF OBSERVABLE OUTPUTS      L=      5
PLOT INTERVAL                      IFI=      1
PRINT INTERVAL                     ICLI=      1
INITIAL TIME (DAYS)                T1=      0.00
INITIAL FIVER PILES                FPI=     29.20
INITIAL STREAMFLOW (CFS)           RSTM=     29.00
COMPUTATIONAL TIME STEP (DAYS)     DT=     0.0200
    
```

YMIN1

```

BCC      0.00000
NF3-A    0.00000
AC3-A    0.00000
ALG-A    0.00000
ERF-A    0.00000
EC        0.00000
ALG+ERF  0.00000
    
```

YMAX1

```

BCC      20.00000
NF3-A    3.00000
AC3-A    3.00000
ALG-A    3.00000
ERF-A    3.00000
EC       14.00000
ALG+ERF  3.00000
    
```

OBSERVATION MATRIX FF

	BCC	NF3-A	AC3-A	ALG-A	ERF-A	EC
BCC	1.00000	0.00000	0.00000	0.00000	0.00000	0.00000
NF3-A	0.00000	1.00000	0.00000	0.00000	0.00000	0.00000
AC3-A	0.00000	0.00000	1.00000	0.00000	0.00000	0.00000
ALG+ERF	0.00000	0.00000	0.00000	1.00000	1.00000	0.00000
EC	0.00000	0.00000	0.00000	0.00000	0.00000	1.00000

V-C OF PROCESS NOISE Q

	BCC	NF3-A	AC3-A	ALG-A	ERF-A	EC
BCC	20.00000	0.00000	0.00000	0.00000	0.00000	0.00000
NF3-A	0.00000	0.40000	0.00000	0.00000	0.00000	0.00000
AC3-A	0.00000	0.00000	0.01000	0.00000	0.00000	0.00000
ALG-A	0.00000	0.00000	0.00000	0.00000	0.00000	0.00000
ERF-A	0.00000	0.00000	0.00000	0.00000	0.00000	0.00000
EC	0.00000	0.00000	0.00000	0.00000	0.00000	0.10000

V-C OF OBSERVATION NOISE R

	BCC	NF3-A	AC3-A	ALG+ERF	EC
BCC	1.00000	0.00000	0.00000	0.00000	0.00000
NF3-A	0.00000	0.01000	0.00000	0.00000	0.00000
AC3-A	0.00000	0.00000	0.04000	0.00000	0.00000
ALG+ERF	0.00000	0.00000	0.00000	0.25000	0.00000
EC	0.00000	0.00000	0.00000	0.00000	0.25000

RIVER SYSTEM LAYOUT, HYDRAULICS AND LOADING DATA

RIVER FILE	K1 ELANF	K2 GAPPA	K23 K1	K45 K2	K46 K3	K5(KNO3) K4	MU-TA1 K5	EE1A P6	EC SAT	PGC2/P6A
L-VECTOR	LAT BCC	LAT NH3A	LAT NO3A	BCTE2EMD	LAT IAF	N TEMP	XS-AFEA	N LF1F	LAT CC	
PTLD 8 CIV	CFS	ECD	NH3-A	NO3-A	ALC-A	CRG-A	CC			
MEAS VE(DF	ECC	NH3-F	NO3-A	ALC+CFCA	CC					
R 35.20	0.700	0.100	0.300	0.040	5.000	0.015	3.000	2.000	7.900	4.570
	0.000	2.000	0.000	0.000	0.000	0.000	0.000	0.000		
L	8.000	0.200	1.500	0.000	11.000	20.000	40.000	1.200	7.270	
D 37.20	-8.000									
M 35.10	8.000	0.010	1.800	0.000	5.700					
D 34.20	-4.000									
P 31.70	20.000	10.000	1.000	2.000	0.000	0.000	7.900			
R 21.70	0.700	0.100	0.300	0.040	5.000	0.015	3.000	2.000	7.900	4.570
	0.000	2.000	0.000	0.000	0.000	0.000	0.000	0.000		
L	8.000	0.400	1.500	0.000	11.000	20.000	50.000	1.200	7.270	
M 30.00	6.500	0.030	1.540	0.000	8.000					
D 30.00	-100.000									
P 30.00	0.000	0.000	0.000	0.000	0.000	0.000	0.000			
R 30.00	0.700	0.100	0.300	0.040	5.000	0.015	3.000	2.000	7.900	4.570
	0.000	2.000	0.000	0.000	0.000	0.000	0.000	0.000		
L	12.000	0.500	1.500	0.000	30.000	20.000	60.000	1.200	7.270	
M 25.00	13.500	1.800	1.630	0.500	7.700					
P 28.50	3.000	60.000	12.000	5.000	0.000	0.000	3.950			
R 28.50	0.700	0.100	0.300	0.040	5.000	0.015	3.000	2.000	7.900	4.570
	0.000	2.000	0.000	0.000	0.000	0.000	0.000	0.000		
L	12.000	0.750	1.500	0.000	30.000	20.000	60.000	1.200	7.270	
M 28.20	10.000	0.600	1.720	1.100	7.600					
P 28.00	0.000	0.000	0.000	0.000	0.000	0.000	0.000			
R 28.00	0.700	0.100	0.300	0.040	5.000	0.015	3.000	2.000	7.900	4.570
	0.000	2.000	0.000	0.000	0.000	0.000	0.000	0.000		
L	12.000	0.750	1.500	0.000	30.000	20.000	70.000	1.500	7.270	
M 28.70	15.000	1.200	1.860	0.800	7.200					
P 28.50	7.000	60.000	12.000	5.000	0.000	0.000	3.950			
R 28.50	0.700	0.100	0.300	0.040	5.000	0.015	3.000	2.000	7.900	4.570
	0.000	2.000	0.000	0.000	0.000	0.000	0.000	0.000		
L	12.000	0.750	1.500	0.000	30.000	20.000	70.000	1.500	7.270	
P 28.00	0.000	0.000	0.000	0.000	0.000	0.000	0.000			
R 28.00	0.700	0.100	0.300	0.040	5.000	0.015	3.000	2.000	7.900	4.570
	0.000	2.000	0.000	0.000	0.000	0.000	0.000	0.000		
L	12.000	0.750	1.500	0.000	30.000	20.000	100.000	2.000	7.270	
P 25.00	0.000	0.000	0.000	0.000	0.000	0.000	0.000			
R 25.00	0.700	0.100	0.300	0.040	5.000	0.015	3.000	2.000	7.900	4.570
	0.000	2.000	0.000	0.000	0.000	0.000	0.000	0.000		
L	12.000	0.750	1.500	0.000	30.000	20.000	100.000	2.000	7.500	
M 23.70	15.000	0.600	1.840	0.900	7.400					
P 22.00	9.800	0.500	1.970	0.800	7.400					
R 22.00	12.000	5.000	0.500	2.000	0.000	0.000	7.000			
	0.700	0.100	0.300	0.040	5.000	0.015	3.000	2.000	7.900	4.570
	0.000	2.000	0.000	0.000	0.000	0.000	0.000	0.000		
L	12.000	0.750	1.500	0.000	30.000	20.000	100.000	2.000	7.500	
D 22.20	-30.000									
P 22.00	7.000	60.000	12.000	5.000	0.000	0.000	3.950			
R 22.00	0.700	0.100	0.300	0.040	5.000	0.015	3.000	2.000	7.900	4.570
	0.000	2.000	0.000	0.000	0.000	0.000	0.000	0.000		
L	12.000	0.750	1.500	0.000	30.000	20.000	165.000	2.500	7.500	
M 21.40	10.800	1.100	2.020	0.400	7.200					
P 21.40	54.000	12.200	2.200	3.000	0.000	0.000	7.300			

R	21.40	0.700	0.100	0.300	0.040	5.000	0.015	3.000	2.000	7.900	4.570
		0.000	2.000	0.000	0.000	0.000	0.000	0.000	0.000	0.000	
	L	12.000	0.700	1.500	0.000	20.000	20.000	165.000	2.500	7.500	
P	20.00	0.000	0.000	0.000	0.000	0.000	0.000	0.000	0.000		
R	20.00	0.700	0.100	0.300	0.040	5.000	0.015	3.000	2.000	7.900	4.570
		0.000	2.000	0.000	0.000	0.000	0.000	0.000	0.000		
	L	12.000	0.750	1.500	0.000	20.000	20.000	275.000	3.600	7.500	
M	15.40	11.500	1.700	1.800	0.400	7.000					
P	18.70	10.000	0.000	12.000	5.000	0.000	0.000	6.000			
R	18.70	0.700	0.100	0.300	0.040	5.000	0.015	3.000	2.000	7.900	4.570
		0.000	2.000	0.000	0.000	0.000	0.000	0.000	0.000		
	L	12.000	0.700	1.500	0.000	20.000	20.000	275.000	3.600	7.500	
P	18.30	20.000	0.000	12.000	5.000	0.000	0.000	6.000			
R	18.30	0.700	0.100	0.300	0.040	5.000	0.015	3.000	2.000	7.900	4.570
		0.000	2.000	0.000	0.000	0.000	0.000	0.000	0.000		
	L	12.000	0.750	1.500	0.000	20.000	20.000	275.000	3.600	7.500	
P	18.10	15.000	5.000	0.500	2.000	0.000	0.000	7.900			
R	18.10	0.700	0.100	0.300	0.040	5.000	0.015	3.000	2.000	7.900	4.570
		0.000	2.000	0.000	0.000	0.000	0.000	0.000	0.000		
	L	12.000	0.700	1.500	0.000	20.000	20.000	275.000	3.600	7.500	
M	17.20	14.500	1.700	2.000	1.700	7.000					
D	18.70	17.000									
P	18.70	0.000	0.000	0.000	0.000	0.000	0.000	0.000			
R	18.70	0.700	0.100	0.300	0.040	2.500	0.015	1.500	2.000	7.900	4.570
		0.000	2.000	0.000	0.000	0.000	0.000	0.000	0.000		
	L	50.000	0.700	1.500	121.000	3.000	20.000	100.000	2.200	7.500	
P	18.20	0.000	0.000	12.000	5.000	0.000	0.000	6.000			
R	18.20	0.700	0.100	0.300	0.040	2.500	0.015	1.500	2.000	7.900	4.570
		0.000	2.000	0.000	0.000	0.000	0.000	0.000	0.000		
	L	50.000	0.750	1.500	121.000	3.000	20.000	100.000	2.200	7.500	
M	15.50	13.000	1.600	2.000	0.800	7.000					
P	15.00	18.000	5.000	0.500	2.000	0.000	0.000	7.000			
R	15.00	0.700	0.100	0.300	0.040	2.500	0.015	1.500	2.000	7.900	4.570
		0.000	2.000	0.000	0.000	0.000	0.000	0.000	0.000		
	L	50.000	0.750	1.500	121.000	3.000	20.000	100.000	2.200	7.500	
M	14.00	16.000	1.500	2.050	0.800	5.000					
M	12.60	16.000	1.700	2.100	0.500	5.800					
P	12.40	10.000	5.000	0.500	2.000	0.000	0.000	7.500			
R	12.40	0.700	0.100	0.300	0.040	2.500	0.015	1.500	2.000	7.900	4.570
		0.000	2.000	0.000	0.000	0.000	0.000	0.000	0.000		
	L	50.000	0.750	1.500	121.000	3.000	20.000	100.000	2.200	7.500	
P	12.40	0.000	0.000	0.000	0.000	0.000	0.000	0.000			
R	12.00	0.700	0.100	0.300	0.040	2.500	0.015	1.500	2.000	7.900	4.570
		0.000	2.000	0.000	0.000	0.000	0.000	0.000	0.000		
	L	0.000	0.000	0.000	121.000	0.000	20.000	100.000	2.200	7.500	
M	10.50	13.500	1.400	2.070	0.500	5.500					
M	9.20	12.800	1.400	2.150	0.500	5.300					
M	6.20	12.500	1.600	2.300	0.400	5.600					
M	6.20	11.600	1.600	2.200	0.600	6.100					
P	5.50	2.000	0.000	12.000	5.000	0.000	0.000	3.500			
R	5.50	0.700	0.100	0.300	0.040	2.500	0.015	1.500	2.000	7.900	4.570
		0.000	2.000	0.000	0.000	0.000	0.000	0.000	0.000		
	L	0.000	0.000	0.000	121.000	0.000	20.000	100.000	2.200	7.500	
M	5.10	14.000	1.200	2.290	2.000	4.700					
E	2.60										



INITIAL COEFFICIENTS    TIME 0.0000    RM 39.200  
 .....

IC FOR ESTIMATE OF STATE XX

BCC	4.00000
NF3-N	0.01000
NC2-N	1.00000
ALG-N	0.10000
CFG-N	0.50000
CC	17.00000

IC FOR EFFECT COVARIANCE MATRIX P

	BCC	NF3-N	NC2-N	ALG-N	CFG-N	CC
BCC	1.00000	0.00000	0.00000	0.00000	0.00000	0.00000
NF3-N	0.00000	0.01000	0.00000	0.00000	0.00000	0.00000
NC2-N	0.00000	0.00000	0.04000	0.00000	0.00000	0.00000
ALG-N	0.00000	0.00000	0.00000	0.12500	0.00000	0.00000
CFG-N	0.00000	0.00000	0.00000	0.00000	0.12500	0.00000
CC	0.00000	0.00000	0.00000	0.00000	0.00000	0.25000

MEAN SQUARE ERROR (OBSERVED - FILTER) PSE(NPSTS), PSE(NPSTS/2), R, G

BCC 1.10276  
 NF3-N 0.04455  
 NG3-N 0.02350  
 ALG+ERF 0.25827  
 EC 0.65867  
 ECC 0.21689  
 PF3-P 0.00851  
 NC3-A 0.01219  
 ALG+ERF 0.31456  
 EC 0.86942

V-C OF OBSERVATION ACISE R

	BCC	NF3-N	NG3-N	ALG+ERF	EC
ECC	1.00000	0.00000	0.00000	0.00000	0.00000
NF3-N	0.00000	0.01000	0.00000	0.00000	0.00000
NG3-N	0.00000	0.00000	0.04000	0.00000	0.00000
ALG+ERF	0.00000	0.00000	0.00000	0.25000	0.00000
EC	0.00000	0.00000	0.00000	0.00000	0.25000

V-C OF PROCESS ACISE Q

	BCC	NF3-N	NG3-N	ALG-N	ERF-N	EC
ECC	20.00000	0.00000	0.00000	0.00000	0.00000	0.00000
NF3-N	0.00000	0.40000	0.00000	0.00000	0.00000	0.00000
NG3-N	0.00000	0.00000	0.01000	0.00000	0.00000	0.00000
ALG-N	0.00000	0.00000	0.00000	0.00000	0.00000	0.00000
ERF-N	0.00000	0.00000	0.00000	0.00000	0.00000	0.00000
EC	0.00000	0.00000	0.00000	0.00000	0.00000	0.10000

K	IX	I	XI	F1	XX	F	XB	FB	XB1	FE1	XS1	FS1	XS	FS
211=	74FP=	2.84243VEL=	25.46187G=	18C.04476K=	65000E=	E								
65293	1	12.62166	1.60693	12.62166	1.60693									
65293	2	1.20498	0.19424	1.20850	0.15424									
65293	3	2.27428	0.09273	2.27428	0.09273									
65293	4	1.56959	0.30307	1.56959	0.30307									
65293	5	-0.06129	0.21303	-0.06129	0.21303									
65293	6	6.11546	0.10051	6.11546	0.10051									
65293	7	-0.02212	-0.03212											
211=	73FP=	3.43167VEL=	25.46187G=	18C.04476K=	65000E=									
65289	1	12.75560	1.52251	12.75560	1.52251									
65289	2	1.24057	0.17388	1.24057	0.17388									
65289	3	2.26408	0.08559	2.26408	0.08559									
65289	4	1.52442	0.29170	1.52442	0.29170									
65289	5	-0.06269	0.20975	-0.06269	0.20975									
65289	6	6.09709	0.09471	6.09709	0.09471									
65289	7	-0.02133	-0.03133											
211=	72FP=	4.02090VEL=	29.46187G=	18C.04476K=	65000E=									
65285	1	12.98006	1.33244	12.98006	1.33244									
65285	2	1.27200	0.15035	1.27200	0.15035									
65285	3	2.25803	0.08464	2.25803	0.08464									
65285	4	1.48055	0.28054	1.48055	0.28054									
65285	5	-0.06406	0.20648	-0.06406	0.20648									
65285	6	6.07469	0.09037	6.07469	0.09037									
65285	7	-0.02055	-0.03055											
211=	71FP=	4.61014VEL=	25.46187G=	18C.04476K=	65000E=									
65281	1	13.16306	1.10332	13.16306	1.10332									
65281	2	1.30323	0.12188	1.30323	0.12188									
65281	3	2.25014	0.08085	2.25014	0.08085									
65281	4	1.42795	0.26960	1.42795	0.26960									
65281	5	-0.06540	0.20310	-0.06540	0.20310									
65281	6	6.05227	0.08760	6.05227	0.08760									
65281	7	-0.02579	-0.02579											
211=	70FP=	5.19520VEL=	25.46187G=	18C.04476K=	64000E=	P								
MEASIS	14.00000	1.20000	2.25000	2.00000	4.70000									
64277	1	11.94026	1.34592	11.94026	0.80212									
64277	2	1.61047	0.15223	1.33428	0.06357									
64277	3	2.22071	0.08464	2.24240	0.07722									
64277	4	1.26505	0.28036	1.39657	0.25888									
64277	5	-0.12853	0.20331	-0.06670	0.19965									
64277	6	6.10707	0.09118	6.02988	0.08820									
64277	7	-0.02899	-0.02505											
211=	69FP=	5.78662VEL=	25.46187G=	18C.04476K=	64000E=									
64273	1	12.16860	1.12003	12.16860	1.12003									
64273	2	1.67148	0.12368	1.67148	0.12368									
64273	3	2.21312	0.08138	2.21312	0.08138									
64273	4	1.25199	0.26942	1.25199	0.26942									
64273	5	-0.12980	0.19986	-0.12980	0.19986									
64273	6	6.07521	0.08824	6.07521	0.08824									
64273	7	-0.02828	-0.02828											
211=	68FP=	6.37785VEL=	25.13460G=	18C.04476K=	61000E=	P								
MEASIS	11.60000	1.60000	2.26000	0.60000	6.10000									

II. Data Sorting Program (PRSORT)

	Page
1. Overall flow diagram of data sorting program (Figure A-2)	188
2. Input data and decision parameters for data sorting program (Table A-3)	190
3. Program listing of data sorting program	191

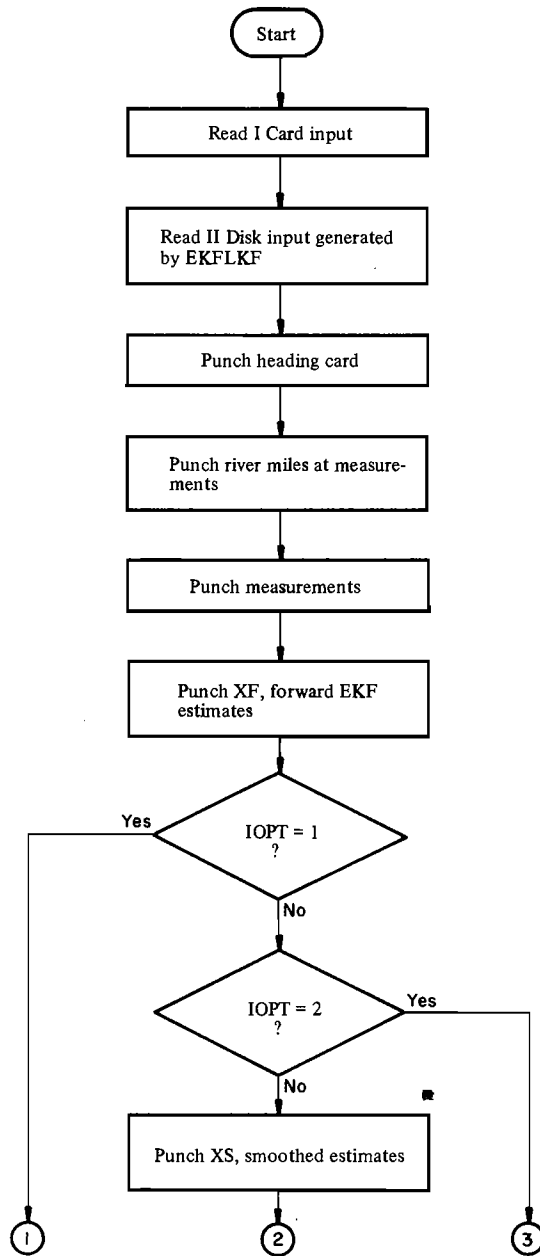


Figure A-2. Overall flow diagram of data sorting program.

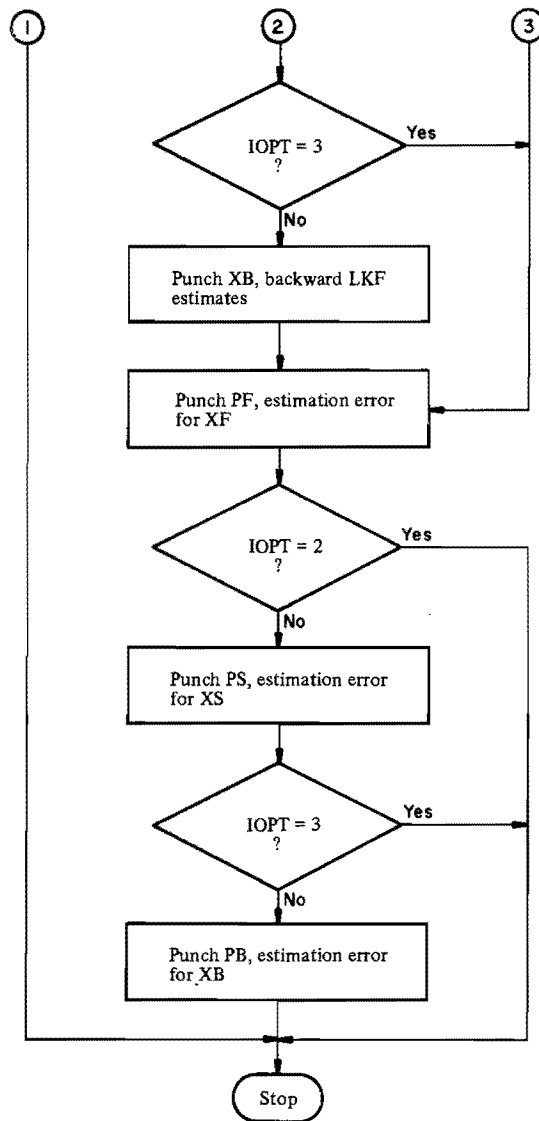


Table A-3. Input data and decision parameters for data sorting program (PRSORT).

I. Card input

1. IRUN, N, L, KW, IOPT - Format (8X, A2, 4I10)

9,10	IRUN	Run number identification
11-20	N	Order of state vector
21-30	L	Order of measurement vector
31-40	KW	Number of computer output unit to which sorted data is to be written for subsequent input to plotting program (P).
41-50	IOPT	= 1 Deterministic process model results only (XF) = 2 Forward filter results only (XF, PF) = 3 Forward filter and smoother results only (XF, PF, XS, PS) = 4 Forward filter, smoother, and backward filter results (XF, PF, XS, PS, XB, PB)

II. Disk input

These data and decision parameters are generated by the filter model (EKFLKF).

### 3. Program listing of data sorting program.

```

C*** PROGRAM TO SORT DISK STORED OUTPUT FROM FILTER MODEL IN
C PREPARATION FOR PLOTTING ON UNRL COMPUTER

      DIMENSION RM(300),RNM(50),Z(1,50),XF(20,300),PF(20,300),
      . XSC(20,300),PS(20,300),XB(20,300),PB(20,300),
      . RHM(150),Z1(10,50),PF45(300),PS45(300),PB45(300)

      DATA CODEM/'M'

900 FORMAT(I1,4X,I4,F10.5,4X,A1)
901 FORMAT(5X,8F9.4)
902 FORMAT(12X,6F10.3)
903 FORMAT(5X,I4,F10.5,4X,A1)
904 FORMAT(8X,A2,5I10)
950 FORMAT(3HRUN,A2,5HRM ,17F4.1)
951 FORMAT(3HRUN,A2,1HI,I2,2HZ ,1(F7.3)
952 FORMAT(3HRUN,A2,5HRM ,17F4.1)
953 FORMAT(3HRUN,A2,1HI,I2,2HXF,1(F7.3)
954 FORMAT(3HRUN,A2,1HI,I2,2HXP,1(F7.3)
955 FORMAT(3HRUN,A2,1HI,I2,2HXS,1(F7.3)
956 FORMAT(3HRUN,A2,1HI,I2,2HPS,1(F7.3)
957 FORMAT(3HRUN,A2,1HI,I2,2HXB,1(F7.3)
958 FORMAT(3HRUN,A2,1HI,I2,2HPB,1(F7.3)
959 FORMAT(17H PROGRAM COMPLETE)
960 FORMAT(3HRUN,5X,A2,4HIOPT,I6,3HITM,I7,3HNT2,I7,6HKROTYP,I4)

C *** INPUT
C ** FROM CARDS
      READ(5,904)IRUN,N,L,KW,IOPT
      N1=N+1

C ** FROM DISC STORAGE
      READ(8,900)KRDTYP,NT,RH(NT),CCOE
      IT1=NT
      NT1=NT-1
      NT2=2*NT
      NT3=NT2-1
      ITM=0
      IF(CODE.NE.CODEM)GOTO 20
      ITM=ITM+1
      RHM(ITM)=RH(NT)
      READ(8,901)(Z(I,ITM),I=1,L)
20 IF(KRDTYP.EQ.2)GOTO 100
C * CARD TYPE 1
      DO 30 I=1,N
      READ(8,902)XF(I,NT21),PF(I,NT21),XF(I,NT2),PF(I,NT2)
30 CONTINUE
      READ(8,902)PF45(NT21),PF45(NT2)
      DO 50 J=1,NT1
      IT=NT-J
      IT2=2*IT
      IT3=IT2-1
32 READ(8,903)IT1,RH(IT),CCOE
      IF(CODE.NE.CODEM)GOTO 35
      ITM=ITM+1
      RHM(ITM)=RH(IT)
      READ(8,901)(Z(I,ITM),I=1,L)
35 DO 40 I=1,N
      READ(8,902)XF(I,IT21),PF(I,IT21),XF(I,IT2),PF(I,IT2)
40 CONTINUE

      READ(8,902)PF45(IT21),PF45(IT2),PB45(IT21),PB45(IT2),PS45(IT21),
      . PS45(IT2)
      IF(IT1.EQ.IT1)GOTO 32
      IT1=IT1
      CCNTINUE
50 CONTINUE
C * CARD TYPE 2
100 DO 130 I=1,N
      READ(8,902)XF(I,NT21),PF(I,NT21),XF(I,NT2),PF(I,NT2),
      . XB(I,NT21),PB(I,NT21),XB(I,NT2),PB(I,NT2),
      . XS(I,NT21),PS(I,NT21),XS(I,NT2),PS(I,NT2)
130 CONTINUE
      READ(8,902)PF45(NT21),PF45(NT2),PB45(NT21),PB45(NT2),PS45(NT21),
      . PS45(NT2)
      DO 150 J=1,NT1
      IT=NT-J
      IT2=2*IT
      IT3=IT2-1
132 READ(8,903)IT1,RH(IT),CCOE
      IF(CODE.NE.CODEM)GOTO 135
      ITM=ITM+1
      RHM(ITM)=RH(IT)
      READ(8,901)(Z(I,ITM),I=1,L)
135 DO 140 I=1,N
      READ(8,902)XF(I,IT21),PF(I,IT21),XF(I,IT2),PF(I,IT2),
      . XB(I,IT21),PB(I,IT21),XB(I,IT2),PB(I,IT2),
      . XS(I,IT21),PS(I,IT21),XS(I,IT2),PS(I,IT2)
140 CONTINUE
      READ(8,902)PF45(IT21),PF45(IT2),PB45(IT21),PB45(IT2),PS45(IT21),
      . PS45(IT2)
      IF(IT1.EQ.IT1)GOTO 132
      IT1=IT1
      CCNTINUE
150 CONTINUE

C ** REVERSE ORDER OF RHM AND Z ARRAYS
200 DO 203 IT=1,ITM
      ITR=ITM-IT+1
      RHM(IT)=RHM(ITR)
      DO 202 I=1,L
      Z1(I,IT)=Z(I,ITR)
202 CONTINUE
203 CONTINUE
C *** CALCULATE ALG=N * ORG=N VALUES AND PUNCH SORTED DATA ONTO CARDS
204 WRITE(KW,960)IRUN,IOPT,IT3,NT2,KRDTYP

C ** RM AT MEASUREMENTS
      IT2=0
205 IT1=IT2+1
      IT2=IT1+16
      IF(ITM-IT2)210,220,220
210 IT2=ITM
220 WRITE(KW,950)IRUN,(RHM(I1),I1=IT1,IT2)
      IF(IT2.NE.ITM)GOTO 205

C ** MEASUREMENTS
      DO 260 I=1,L
      IT2=0
235 IT1=IT2+1
      IT2=IT1+9
      IF(ITM-IT2)240,250,250
245 IT2=ITM

```



```

250 WRITE(KW,951)IRUN,I,(Z1(I,IT),IT=IT1,IT2)
    IF(IT2.NE.ITN)GOTO 235
260 CONTINUE
C ** RM
    IT2=0
270 IT1=IT2+1
    IT2=IT1+16
    IF(NT-IT2)280,290,290
280 IT2=NT
290 WRITE(KW,952)IRUN,(RM(IT),IT=IT1,IT2)
    IF(IT2.NE.NT)GOTO 270
C ** XF
    DO 300 J=1,NT2
    XF(N1,J)=XF(4,J)+XF(5,J)
300 CONTINUE
    DO 340 I=1,N1
    IT2=0
310 IT1=IT2+1
    IT2=IT1+9
    IF(NT-IT2)320,330,330
320 IT2=NT2
330 WRITE(KW,953)IRUN,I,(XF(I,IT),IT=IT1,IT2)
    IF(IT2.NE.NT2)GOTO 310
340 CONTINUE
    IF(IOPT.EQ.1)GOTO 700
    IF(IOPT.EQ.2)GOTO 600
C ** XS
    DO 400 J=1,NT2
    XS(N1,J)=XS(4,J)+XS(5,J)
400 CONTINUE
    DO 440 I=1,N1
    IT2=0
410 IT1=IT2+1
    IT2=IT1+9
    IF(NT-IT2)420,430,430
420 IT2=NT2
430 WRITE(KW,955)IRUN,I,(XS(I,IT),IT=IT1,IT2)
    IF(IT2.NE.NT2)GOTO 410
440 CONTINUE
    IF(IOPT.EQ.3)GOTO 600
C ** XB
    DO 490 J=1,NT2
    XB(N1,J)=XB(4,J)+XB(5,J)
490 CONTINUE
    DO 530 I=1,N1
    IT2=0
500 IT1=IT2+1
    IT2=IT1+9
    IF(NT-IT2)510,520,520
510 IT2=NT2
520 WRITE(KW,957)IRUN,I,(XB(I,IT),IT=IT1,IT2)
    IF(IT2.NE.NT2)GOTO 500
530 CONTINUE
C ** PF
    DO 600 J=1,NT2
    PF(N1,J)=SQRT(PF(4,J)**2+PF(5,J)**2+PF(6,J))

```

```

350 CONTINUE
    DO 390 I=1,N1
    IT2=0
360 IT1=IT2+1
    IT2=IT1+9
    IF(NT-IT2)370,380,380
370 IT2=NT2
380 WRITE(KW,954)IRUN,I,(PF(I,IT),IT=IT1,IT2)
    IF(IT2.NE.NT2)GOTO 360
390 CONTINUE
    IF(IOPT.EQ.2)GOTO 700
C ** PS
    DO 445 J=1,NT2
    PS(N1,J)=SQRT(PS(4,J)**2+PS(5,J)**2+PS(6,J))
445 CONTINUE
    DO 480 I=1,N1
    IT2=0
450 IT1=IT2+1
    IT2=IT1+9
    IF(NT-IT2)460,470,470
460 IT2=NT2
470 WRITE(KW,956)IRUN,I,(PS(I,IT),IT=IT1,IT2)
    IF(IT2.NE.NT2)GOTO 450
480 CONTINUE
    IF(IOPT.EQ.3)GOTO 700
C ** PB
    DO 535 J=1,NT2
    PB(N1,J)=SQRT(PB(4,J)**2+PB(5,J)**2+PB(6,J))
535 CONTINUE
    DO 570 I=1,N1
    IT2=0
540 IT1=IT2+1
    IT2=IT1+9
    IF(NT-IT2)550,560,560
550 IT2=NT2
560 WRITE(KW,958)IRUN,I,(PB(I,IT),IT=IT1,IT2)
    IF(IT2.NE.NT2)GOTO 540
570 CONTINUE
    IF(KW.EQ.6)GOTO 750
    KW=6
    GOTO 204
750 PRINT 959

    STOP
    END

```

III. Plotting Program (P)

	Page
1. Overall flow diagram of plotting program (Figure A-3).	194
2. Input data and decision parameters for plotting program (Table A-4).	195
3. Program listing of plotting program.	200

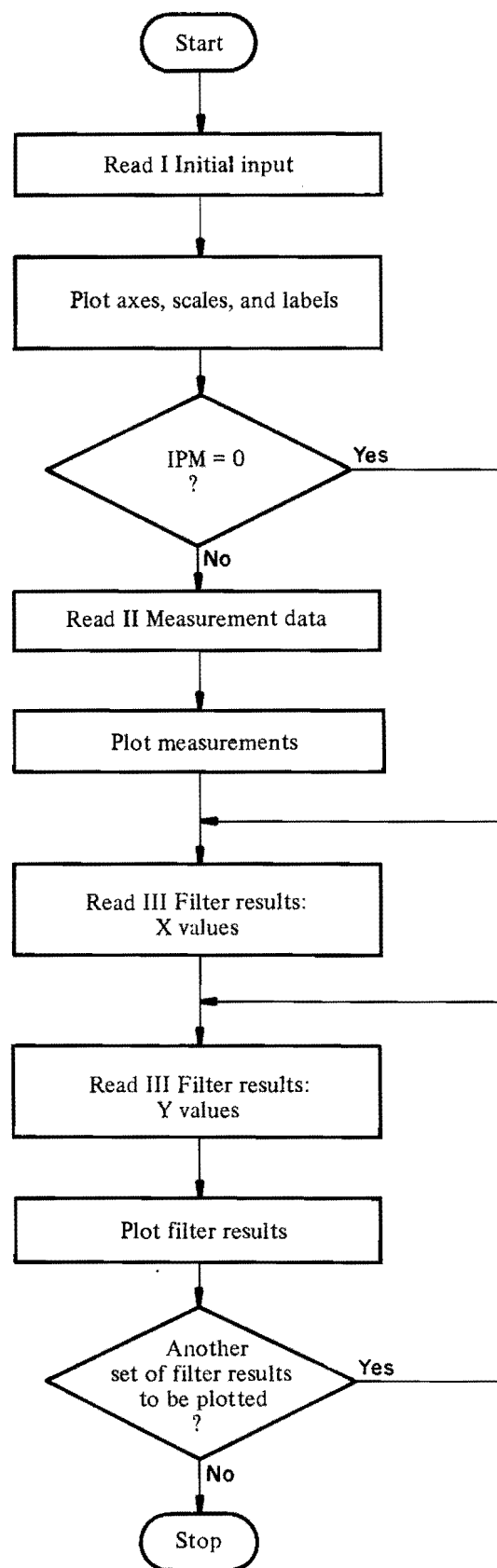


Figure A-3. Overall flow diagram of plotting program.

Table A-4. Input data and decision parameters for plotting program (P).

\* Cards 4, 7, 8, 9, and 11 are generated by the data sorting program (PRSORT) from results obtained from the filter model (EKFLKF).

I. Initial input

1. IPM, NVX, NVY, PUY, XL, YL, XMAX, XP, YP, YMAX, XVAL1, XMIN, YMIN - Format (3I5, 10F5.0)

1-5	IPM	= 0 No measurements to be plotted = 1 Measurements to be plotted
6-10	NVX	Number of A4 fields required to read x-axis heading on card 5
11-15	NVY	Number of A4 fields required to read y-axis heading on card 6
16-20	PUY	Number of data units between major ticks on y-axis
21-25	XL	Length of x-axis in inches
26-30	YL	Length of y-axis in inches
31-35	XMAX	Maximum value of river miles on x-axis
36-40	XP	Plotting window in x-direction in inches
41-45	YP	Plotting window in y-direction in inches
46-50	YMAX	Maximum value of y-axis
51-55	XVAL1	Maximum value of x-axis
56-60	XMIN	Minimum value of x-axis
61-65	YMIN	Minimum value of y-axis

2. NDX, NDY, XT, H2T, CHT, HTL, XVAL, YVAL - Format (2I5, 6F5.0)

1-5	NDX	Number of decimal places in x-axis labels
6-10	NDY	Number of decimal places in y-axis labels
11-15	XT	Title location in inches from left-hand edge of plotting window
16-20	H2T	Size of characters in axis label
21-25	CHT	Size of characters in title
26-30	HTL	Size of characters in axis labels
31-35	XVAL	Data units between left-hand edge of plotting window and origin of graph
36-40	YVAL	Data units between bottom edge of plotting window and origin of graph

3. NGX, NGY, NSKX, NSKY, NSMBL, ISZ - Format (6I5)

1-5	NGX	Number of minor ticks between major ticks on x-axis
6-10	NGY	Number of minor ticks between major ticks on y-axis
11-15	NSKX	Label every NSKXth major tick on x-axis
16-20	NSKY	Label every NSKYth major tick on y-axis
21-25	NSMBL	= 0 No symbol plotted = 1 '+' symbol plotted = 2 'x' symbol plotted = 3 'v' symbol plotted
26-30	ISZ	Size of symbol in the number of 2/100 inch units

4. \* ITM, NT2 - Format (25X, I5, 5X, I5)
- |       |     |  |
|-------|-----|--|
| 26-30 | ITM | Number of measurements to be plotted                       |
| 36-40 | NT2 | Number of calculated points (filter results) to be plotted |
5. (FMTX(I), I = 1, NVX) - Format (NVX\*A4)
- |  |         |  |
|--|---------|--|
|  | FMTX(I) | x-axis heading written as a format statement |
|--|---------|--|
6. (FMTY(I), I = 1, NVY) - Format (NVY\*A4)
- |  |         |  |
|--|---------|--|
|  | FMTY(I) | y-axis heading written as a format statement |
|--|---------|--|

## II. Measurement data

(Omit cards 7 and 8 if IPM = 0)

7. \* (X(I), I = 1, ITM) - Format (10X, 17F4.1)
- |       |      |                                  |
|-------|------|----------------------------------|
| 11-14 | X(1) | River mile at 1st sampling point |
| 15-18 | X(2) | River mile at 2nd sampling point |
|       |      | etc.                             |
8. \* (Y(I), I = 1, ITM) - Format (10X, 10F7.2)
- |       |      |                                      |
|-------|------|--------------------------------------|
| 11-17 | Y(1) | Measured value at 1st sampling point |
| 18-24 | Y(2) | Measured value at 2nd sampling point |
|       |      | etc.                                 |

III. Filter results

9.\* (X(I), I = 2, NT2, 2) - Format (10X, 17F4.1)

11-14 X(2) River mile at first and second points to be plotted

15-18 X(4) River mile at third and fourth points to be plotted

etc.

(Cards 10 through 12 are repeated for each set of results to be plotted)

10. NTITLE, NVT, NSMBL, ISZ, NSK, YT, XS, YS - Format (5I5, 3F5.0)

1-5 NTITLE = 0 No title to be plotted  
= 1 Title to be plotted

6-10 NVT Number of A4 fields required to read title on card 12

11-15 NSMBL Symbol to be plotted (see card 3)

16-20 ISZ Size of symbol in the number of 2/100 inch units

21-25 NSK Plot symbol at every NSKth calculated point

26-30 YT Title location in inches from bottom edge of plotting window

31-35 XS Standby position for pen in inches from left-hand edge of plotting window

36-40 YS Standby position for pen in inches from bottom edge of plotting window

11.\* (Y(I), I = 1, NT2) - Format (10X, 10F7.2)

11-20 Y(1) Calculated value at first point

21-30 Y(2) Calculated value at second point

etc.

(Omit card 12 if NTITLE = 0)

12. (FMTT(I), I = 1, NVT) - Format (20A4)

FMTT(I) Title written as a format statement



### 3. Program listing of plotting program.

```

PAGE 1      C**** PROGRAM TO PLOT RESULTS FROM FILTER MODEL

          X(F5,1),Y(F5,2)

900  FORMAT(1X,1F5,1)
901  FORMAT(1X,1F5,2)
902  FORMAT(2X,1F5,1)
903  FORMAT(15,1F5,1)
904  FORMAT(25X,1F5,1)
906  FORMAT(31X,1F5,1)
907  FORMAT(161X)
908  FORMAT(515,1F5,1)

C *** INITIAL INPUT
      TYPE 951
951  FORMAT(5#HC COMPLETELY NEW CARD DECK REQUIRED - SET UP PLOTTER/)
      READ(6,906)IPM,NVX,NVY,PUY,XL,YL,YMAX,XP,YP,YVAL1,XMIN,YMIN
      READ(6,902)NDX,NDY,XT,H2T,CHT,HTL,XVAL,YVAL
      READ(6,907)NGX,NGY,NSKX,NSKY,NSMBL,ISZ
      READ(6,904)ITM,NT2
      NT=NT/2
      INS=1

C *** PLOTTING
C ** SETUP AXES, SCALES, TITLE, ETC
      N=0
      JY=0
      NSK=1
      NLINE=0
      NAXIS=1
      NGRID=1
      NLABX=1
      NLABY=1
      NTITLE=0
      ANGT=0.0
      PUX=10.0
      XS=0.0
      YS=0.0
      XREF=0.0
      YREF=0.0
      XN=0.0
      YN=0.0
      END=1.0E30
      NI=1
      MIND=1
      CALL GRAPH(X,Y,N,JY,NSK,NLINE,NSMBL,NAXIS,NGRID,NLABX,NLABY,
      ,NTITLE,XT,YT,H2T,ANGT,NGX,NGY,NDX,NDY,ISZ,CHT,PUX,PUY,XL,YL,XS,YS,
      ,NVX,NVY,NVT,YMIN,XMAX,HTL,XREF,YREF,XVAL,YVAL,XP,YP,XN,YN,END,
      ,YMIN,YMAX,NI,MIND,NSKX,NSKY,XVAL1)
      JY=1
      NAXIS=0
      NGRID=0
      NLABX=0
      NLABY=0

```

```

PAGE 2      C**** PROGRAM TO PLOT RESULTS FROM FILTER MODEL

C ** MEASUREMENTS - DISCRETE PLOTS
      IF(IPM.EQ.0)GOTO 200
      READ(6,901)(Y(I),I=1,ITM)
      READ(6,901)(Y(I),I=1,ITM)
      DO 150 I=1,IT
          X(I)=XVAL1-X(I)
150  CONTINUE
      N=ITM
      NTITLE=0
      CALL GRAPH(X,Y,N,JY,NSK,NLINE,NSMBL,NAXIS,NGRID,NLABX,NLABY,
      ,NTITLE,XT,YT,H2T,ANGT,NGX,NGY,NDX,NDY,ISZ,CHT,PUX,PUY,XL,YL,XS,YS,
      ,NVX,NVY,NVT,YMIN,XMAX,HTL,XREF,YREF,XVAL,YVAL,XP,YP,XN,YN,END,
      ,YMIN,YMAX,NI,MIND,NSKX,NSKY,XVAL1)

C ** LINE PLOTS
200  READ(6,900)(Y(I),I=2,NT2,2)
      DO 205 I=2,NT2,2
          I1=I-1
          X(I1)=X(I)
205  CONTINUE
      DO 210 I=1,NT2
          X(I)=YVAL1-X(I)
210  CONTINUE
220  TYPE 954
954  FORMAT(45#CARD DECK FOR NEW Y REQUIRED - SET UP PLOTTER/)
      PAUSE 10
      READ(6,906)NTITLE,NVT,NSMBL,ISZ,NSK,XT,XS,YS
      READ(6,901)(Y(I),I=1,NT2)
      N=NT2
      NLINE=1
      CALL GRAPH(X,Y,N,JY,NSK,NLINE,NSMBL,NAXIS,NGRID,NLABX,NLABY,
      ,NTITLE,XT,YT,H2T,ANGT,NGX,NGY,NDX,NDY,ISZ,CHT,PUX,PUY,XL,YL,XS,YS,
      ,NVX,NVY,NVT,YMIN,XMAX,HTL,XREF,YREF,XVAL,YVAL,XP,YP,XN,YN,END,
      ,YMIN,YMAX,NI,MIND,NSKX,NSKY,XVAL1)
      IF(INS.EQ.0)GOTO 220

300  STOP
      END

```

```

C** SUBROUTINE GRAPH
SUBROUTINE GRAPH(X,Y,N,JY,NSK,NLINE,NSMBL,NAXIS,NGRID,NLABX,NLABY,
1NTITLE,XT,YT,H2T,ANGT,NGX,NGY,NDX,NVY,ISZ,CMT,PUX,PY,XL,YL,XS,YS,
2NVX,NVY,NVT,XP,IN,XYMAX,NL,XPER,YREF,XVAL,YVAL,XP,YP,YN,END)
3SYM,XYMAX,CI,MINO,NSKX,NSKY,XVAL)
C** DIMENSION X(1),Y(1),FMTX(25),FMTY(25),FMTT(25),FXLB(42),NSMBL(1)
DIMENSION X(1),Y(1),FMTX(25),FMTY(25),FMTT(25),FXLB(42)
C X AND Y ARE THE DATA TO BE PLOTTED. N IS THE NUMBER OF DATA PTS
C JY IS THE NO OF THE Y VAR BEING PLOTTED WHEN MORE THAN 1 PLOTTED
C IF NLINE = 1 POINT PLOT NSYMBL = SYMBOL CODE (0 TO 12)
C   1 LINE PLOT
C NAXIS = 0 DO NOT DRAW AXIS
C   1 DRAW AXIS WITH TICK MARKS PNT EVERY XINC AND YINC
C NGRID = 0 DO NOT DRAW GRID
C   1 DRAW GRID - USE SAME INCREMENTS ON X AND Y AXIS AS TICKS
C   -1 ENCLOSE PLOT AREA DO NOT DRAW GRID
C NLABX = -1 JUST PLOT VALUES WITH TICK MARKS IF NAXIS = 1
C   0 DO NOT LABEL ARSCISSA
C   1 LABEL ARSCISSA AND IF TICKED PLOT VALUES
C   2 LABEL ARSCISSA AND PUT 3 CHAR LABELS BETWEEN TICKS
C   INSTEAD OF VALUES
C NLABY = -1 JUST PLOT VALUES WITH TICK MARKS IF CALLED FOR
C   0 DO NOT LABEL Y AXIS
C   1 LABEL Y AXIS AND IF TICKED PLOT VALUES
C NTITLE = 0 DO NOT PLOT GRAPH TITLE
C   1 PLOT GRAPH TITLE
C   -1 PLOT SYMBOL BEFORE PLOTTING TITLE
C (XT,YT) STARTING POSITION FOR PLOTTING TITLE IN INCHES
C H2T AND ANGT ARE CHARACTER HT AND ANGLE FOR PLOTTING TITLE
C NGX IS NO OF TICKS TO SKIP BEFORE WRITING VALUES ON ARSCISSA
C NGY IS NO OF TICKS TO SKIP BEFORE WRITING VALUES ON Y AXIS
C NDX = NO OF PLACES TO RIGHT OF DECIMAL PT FOR PLOTTING X VALUES
C NDY = NO OF PLACES TO RIGHT OF DECIMAL PT FOR PLOTTING Y VALUES
C ISZ = SIZE ARGUMENT FOR PLOTTING VALUES AND SYMBOL IN UNITS OF .05
C XINC = INCREMENT ON X AXIS FOR TICKS AND GRID IN INCHES
C YINC = INCREMENT ON Y AXIS FOR TICKS AND GRID IN INCHES
C PUX IS PLOTTING UNITS PER MAJOR GRID FOR LABELLING X
C PUY IS PLOTTING UNITS PER MAJOR GRID FOR LABELLING Y
C XL AND YL ARE LENGTH OF X AND Y AXIS IN INCHES
C (XS,YS) IS LOCATION OF NEXT STANDBY FROM CURRENT REF IN INCHES
C FMTX IS FORMAT OF X LABEL AND MUST BE LESS THAN 99 CHARACTERS
C FMTY IS FORMAT OF Y LABEL AND MUST BE LESS THAN 99 CHARACTERS
C FMTT IS FORMAT OF TITLE AND MUST BE LESS THAN 99 CHARACTERS
C NVX IS NO OF VARIABLES IN FORMAT FOR XLABEL LE 25
C NVY IS NO OF VARIABLES IN FORMAT FOR YLABEL LE 25
C NVT IS NO OF VARIABLES IN FORMAT FOR TITLE LE 25
C YSCALE = SCALE FACTOR IN X = PROBLEM UNITS/INCH
C YSCALE = SCALE FACTOR IN Y = PROBLEM UNITS/INCH
C (XREF,YREF) IS REFERENCE POSITION IN INCHES FROM STANDBY
C CMT = 1/2 HT OF CHARACTERS TO BE PLOTTED WITH PTEXT
C (XVAL,YVAL) PROBLEM UNITS AT (XREF,YREF)
C XP = PLOT SIZE (POSITIVE INCHES IN X DIRECTION FROM REFERENCE)
C YP = PLOT SIZE (POSITIVE INCHES IN Y DIRECTION FROM REFERENCE)
C XN = PLOT SIZE (NEGATIVE INCHES IN X DIRECTION FROM REFERENCE)
C YN = PLOT SIZE (NEGATIVE INCHES IN Y DIRECTION FROM REFERENCE)
C END IS MISSING DATA ON Y CHARACTER TEST. IF Y VAL GE END THEN

```

```

C   0TES NOT PLOT THAT VALUE
C   NTL IS CHARACT FOR XVAL AND LABEL OF AXES
C   XMIN AND XMAX ARE MIN AND MAX OF X DATA
C   YMIN AND YMAX ARE MIN AND MAX OF Y DATA
C   1 IS STARTING ELEMENT TO BEGIN PLOTTING --IF NLINE 0 SET NIK1
C   NIK1 IS OPTION FOR ADJUSTING XVAL TO BE LESS THAN XMIN IN THE
C   SCALE ROUTINE - IF GE 1 THEN ADJUST OTHERWISE DO NOT ADJUST
C** NSK IS NO OF PTS TO PLOT BEFORE PLOTTING A SYMBOL
NSKXX=NSKX
NSKYY=NSKY
IF(CI,LE,MIN) NI=1
NIIRNI=1
C** IF(JY,GT,1) GO TO 170
C CALCULATE YSCALE, XSCALE, XINC, AND YINC
CALL SCAL(YSCALE,XINC,NGX,XYMAX,XMIN,XVAL,XL,PUX,MINO)
CALL SCAL(XSCALE,YINC,NGY,XYMAX,YMIN,YVAL,YL,PUY,MINO)
C IF SKN B OF SKIP WRITING READY PLOTTER, ETC
1 OCT 25500
J = 2
J = 3
2 TYPE 500
500 FORMAT(39HREADY PLOTTER AT STANDBY POSITION = RSP/)
OCT 25000
3 CALL SBYSET
CALL PLTSET(YSCALE,YSCALE,XREF,YREF,XVAL,YVAL,XP,YP,YN,XY)
C CHECK TO SEE IF NEED TO READ TITLES
200 FORMAT(21A4)
C IF(JY,GT,1) GO TO 11
4 IF(NTITLE,NE,0,AND,JY,EQ,1) READ(5,200)(FMTT(I),I=1,NVT)
IF(NLABX,GE,1) READ(6,200)(FMTX(I),I=1,NVX)
IF(NLABY,EQ,2,AND,JY,EQ,1) READ(6,200)(FXLB(I),I=1,40)
11 IF(NLABY,EQ,1)READ(6,200)(FMTY(I),I=1,NVY)
C DRAW AXIS IF NAXIS GT 0
CALL PENUP
IF(NAXIS)76,75,5
5 CALL INPLOT(0.,0.)
NX=XL/XINC+.5
IF(NSKX,LT,0)NSKXX=NX
NY=YL/YINC+.5
IF(NSKY,LT,0)NSKYY=NY
IF(NX,EQ,0)NY=1
IF(NY,EQ,0)NX=1
IXM=ISZ*2
RISZ=ISZ
CALL GSIZE(ISZ)
CALL CHSIZE(CMT,0.)
C DRAW X AXIS
CALL PENUP
IF(NLABX)15,10,15
10 CALL INPLOT(XL,0.)
GO TO 40
15 Y1=0.-RISZ+.05-2.*CMT
16 CALL GSIZE(IXM)
CALL YMARK
CALL GSIZE(ISZ)
CALL PENUP
VAL=XVAL1-XVAL
XDX=NGX

```

PAGE 3 C GRAPH OF Y VS X ON ARITHMETIC PAPER

```

DXCL=1.0*CHT+.5*XINC+XDX
IF(NLABX.GT.1) GO TO 1R
XX=2.
CALL CHECK(YSCALE,VAL,XX,VAL,RNCOL,NDX)
Y1=XX-CHT+(PNCOL-1.)+.R
17 CALL INPLOT(X1,Y1)
CALL PLTVAL(VAL,NDX)
CALL INPLOT(P.,0.)
18 CALL PENUP
DO 3R I=1,NX
RI=1
XX=XINC+RI
CALL INPLOT(XX,P.)
CALL XMARK
IF(NLABX)2R,31,2R
C CHECK TO SEE IF NEED TO PLOT VAL
2R IF(MOD(I,NGX).NE.0) GO TO 3R
CALL GSIZE(IX)
CALL XMARK
CALL GSIZE(ISZ)
IF(NLABY.LF.1) GO TO 25
CALL PENUP
X1=XX-DXCL
CALL INPLOT(X1,Y1)
LI=(2+I)/NRX-1
IF(LI.GT.3R) GO TO 2R
XLBX1=FXLR(LI)
XLBX2=FXLR(LI+1)
CALL PLTEXT
ADR XLBX1
GO TO 2R
25 IF(MOD(I,NSKXX).NE.0)GO TO 3R
CALL CHECK(YSCALE,YVAL,XX,VAL,RNCOL,NDX)
X1=XX-CHT+(PNCOL-1.)+.R
CALL PENUP
CALL INPLOT(X1,Y1)
CALL PLTVAL(VAL,NDX)
2R CALL INPLOT(XX,P.)
CALL PENUP
3R CONTINUE
4R CALL PENUP
CALL INPLOT(P.,P.)
DO Y AXIS
CALL PFADN
IF(NLABY)5R,4S,5R
45 CALL INPLOT(P.,YL)
GO TO 75
5R CALL GSIZE(IX)
CALL YMARK
CALL GSIZE(ISZ)
CALL PENUP
VAL=YVAL
YY=P.
CALL CHECK(YSCALE,YVAL,YY,VAL,RNCOL,NDY)
X1=P.-1.5+RNCOL+CHT-CHT-RISZ+.25
X1MAX=X1
CALL INPLOT(X1,P.)
CALL PLTVAL(VAL,NDY)

```

PAGE 4 C GRAPH OF Y VS X ON ARITHMETIC PAPER

```

CALL INPLOT(P.,P.)
CALL PENUP
DO 65 I=1,NY
RI=1
YY=YINC+RI
CALL INPLOT(P.,YY)
CALL YMARK
IF(NLABY)55,45,55
C CHECK TO SEE IF NEED TO PLOT VAL
55 IF(MOD(I,NGY).NE.0) GOTO 65
CALL GSIZE(IX)
CALL YMARK
CALL GSIZE(ISZ)
IF(MOD(I,NSKYY).NE.0)GO TO 65
CALL CHECK(YSCALE,YVAL,YY,VAL,RNCOL,NDY)
Y1=P.-1.5+RNCOL+CHT-CHT-RISZ+.25
IF(ABS(X1).GT.ABS(X1MAX)) X1MAX=X1
CALL PENUP
CALL INPLOT(X1,YY)
CALL PLTVAL(VAL,NDY)
CALL INPLOT(P.,YY)
CALL PENUP
65 CONTINUE
75 CALL PENUP
SEE IF GRID CALLED FOR
7R IF(NSGRID) 94,10R,9R
8R NX=NX/NGX
IF(NX.LE.0) NY=1
NY=NY/NGY
IF(NY.LE.0) NY=1
DO 85 I=1,NX,2
RI=XINC
X1=XINC+RI
CALL INPLOT(X1,P.)
CALL PENUP
CALL INPLOT(X1,YL)
CALL PENUP
82 L=I+1
IF(L.GT.NX) GO TO 8R
RL=L+NRX
X1=XINC+RL
CALL INPLOT(X1,YL)
CALL PENUP
CALL INPLOT(X1,P.)
CALL PENUP
85 CONTINUE
DO 9R I=1,NY,2
PI=YINC
Y1=YINC+PI
CALL INPLOT(P.,Y1)
CALL PENUP
CALL INPLOT(YL,Y1)
CALL PENUP
92 L=I+1
IF(L.GT.NY) GO TO 9R
PL=L+NGY
Y1=YINC+PI
CALL INPLOT(PL,Y1)

```

PAGE 5 C GRAPH OF Y VS X ON ARITHMETIC PAPER

```
CALL PENON
CALL INPLOT(P.,Y1)
CALL PENUP
98 CONTINUE
94 IF(NAXIS)95,95,96
95 CALL INPLOT(XL,P.)
CALL PENON
CALL INPLOT(P.,0.)
96 CALL INPLOT(P.,YL)
CALL PENON
CALL INPLOT(XL,YL)
CALL INPLOT(XL,0.)
C PLOT X AND Y DATA
100 CALL PENUP
IF(JY,LE,0)GOTO 121
XX=X(NI)
YY=Y(NI)
C** IF(YY,LE,0.) GO TO 98
IF(YY,GE,END) GO TO 98
101 CALL PLOT(XX,YY)
CALL OSIZE(ISZ)
C** NSM=NSMBL(NI)
C** CALL SYMBOL(NSM)
C** CALL SYMBOL(NSMBL)
CALL SYMBL(NSMBL)
CALL PENON
98 DO 120 I=NI,N
IF(NLINE,EC,P) CALL PENUP
XX=X(I)
YY=Y(I)
C** IF(YY,LE,0.) GO TO 122
IF(YY,GE,END) GO TO 122
102 CALL PLOT(XX,YY)
IF(NLINE,GT,P) CALL PENON
C** NSM=NSMBL(I)
C** CALL SYMBOL(NSM)
C** IF(MOD(I,NSK),EQ,0) CALL SYMBOL(NSMBL)
IF(MOD(I,NSK),EQ,0) CALL SYMBL(NSMBL)
120 CONTINUE
CALL PENUP
C** IF(JY,GT,1) GO TO 150
121 IF(NAXIS)140,140,122
C LABEL ABSCISSA
122 IF(NLABX)130,130,125
125 RL=4*NVX-5
CHL=1.6*RL+HTL
IF(CHL,GT,(XL-XN))PAUSE 1
X1=(XL-CHL)+.5
Y1=P.-.05*PISZ-5.*CHT-HTL
CALL CHSIZE(HTL,P.)
CALL INPLOT(X1,Y1)
CALL PLTEXT
ADR FMTX
C LABEL Y AXIS
130 IF(NLABY)140,140,135
135 CALL CHSIZE(HTL,P.)
RL=4*NVY-5
CHL=1.6*RL+HTL
```

PAGE 6 C GRAPH OF Y VS X ON ARITHMETIC PAPER

```
C IF(CHL,GT,(YL-YN)) PAUSE 2
Y1=(YL-CHL)+.5
X1=XIMAX-3.*CHT-HTL
CALL INPLOT(X1,Y1)
CALL PLTEXT
ADR FMTY
C TEST TO SEE IF NEED GRAPH TITLE
140 IF(NTITLE)145,150,145
C PLOT TITLE
145 CALL INPLOT(XT,YT)
IF(JY,GT,1)GO TO 150
IF(NTITLE,GT,0) GO TO 147
CALL OSIZE(ISZ)
C** CALL SYMBOL(NSMBL)
CALL SYMBL(NSMBL)
CALL PENUP
X1=XT+.1*RI SZ
CALL INPLOT(X1,YT)
147 CALL CHSIZE(H2T,ANGT)
CALL PLTEXT
ADR FHTT
150 CALL INPLOT(XS,YS)
C WRITEOUT SCALE FACTORS
WRITE(6,400) YMIN,YMAX,PUY,YSSCALE
400 FORMAT(1X$HMIN =F10.2,$X$HMAX =F10.2,$X$HPUY =F10.2,$X7=SCALE =
F10.3)
RETURN
END
```

```

C SUBROUTINE TO CHECK VALUE AND GET NO OF COLUMNS
SUBROUTINE SCAL(ZSCALE,ZINC,NGZ,ZMAX,ZMIN,ZVAL,ZL,PUZ,MINO)
VAL=ZVAL*ZSCALE,Z2
PUZ=Z
IF (Z2.LE.PUZ GO TO 20
CORR=Z+17.+(=N7Z)
20 IF (ABS(VAL).LE.CORR) GO TO 23
IF (VAL)21,23,Z2
21 VAL=VAL-CORR
GO TO 24
22 VAL=VAL+CORR
GO TO 24
23 NCOL=2
VAL=Z
GO TO 30
24 NCOL=ALOSIZ(ABS(VAL))
IF (NCOL)25,25,30
25 NCOL=2
GO TO 35
30 NCOL=NCOL*2
35 IF (VAL.LT.P.1 NCOL=NCOL+1
50 NCOL=NCOL+NOZ
RETURN
END

```

```

C SUBPROGRAM TO CALC SCALE FACTORS
SUBROUTINE SCAL(ZSCALE,ZINC,NGZ,ZMAX,ZMIN,ZVAL,ZL,PUZ,MINO)
IF (MINO.LT.1) GO TO 15
IF ZMIN IS BELOW ZVAL THEN ADJUST ZVAL DOWNWARD TO EVENTUALLY
INCLUDE ZMIN IF MINO GE 1
5 NRVL=ZMIN/PUZ
RVL=NRVL
ZVAL=RVL+PUZ
8 IF (ZMIN-ZVAL)10,15,15
10 ZVAL=ZVAL-PUZ
GO TO 8
15 RNG=ZMAX-ZVAL
NDIV=RNG/PUZ
PDIV=NDIV
ZMX1=RDIV+PUZ+ZVAL
IF (ZMX1.LT.ZMAX)NDIV=NDIV+1
RNGZ=RNGZ
RDIV=NDIV
ZSCALE=PUZ*RDIV/ZL
ZINC=ZL/(RDIV*RNGZ)
RETURN
END

```

C SUBROUTINE TO MAKE MULTIPLE SMBL PLOTS IF NSMBL .GT. 10

```

SUBROUTINE SYMBOL(NSMBL)
IF (NSMBL.LT.10)GO TO 10
K=NSMBL/10
L=MOD(NSMBL,10)
CALL SYMBOL(K)
CALL SYMBOL(L)
GO TO 20
10 CALL SYMBOL(NSMBL)
20 RETURN
END

```

## VITA

David S. Bowles  
Candidate for the Degree of  
Doctor of Philosophy

Dissertation: Estimation Theory Applied to River Water Quality Modeling

Major Field: Civil and Environmental Engineering

Biographical Information:

Personal Data: Born at Romford, Essex, England, June 30, 1949, son of Stanley W. and Elsie C. M. Bowles; married Valerie R. Curd, April 29, 1972; one child: Penny-Anne.

Education: Attended Branfil Primary and Junior Schools, Gaynes Secondary Modern School, and Hornchurch Grammar School, all in Essex, England; received the Bachelor of Science degree in Civil Engineering with First Class Honours from the City University, London, England, in 1972; completed the requirements for the Doctor of Philosophy degree in Civil and Environmental Engineering, specializing in Water Resources and Hydrology, at Utah State University, Logan, Utah, in 1976.

Professional Experience: 1976 to present, Research Engineer, Utah Water Research Laboratory, Logan, Utah; 1972-1976, Graduate Research Assistant, Utah Water Research Laboratory, Logan, Utah; 1974-75, Consultant to E. P. Fisk, SIYANCO, Riyadh, Saudia Arabia; 1967-72 (aggregate of 3 years), Indentured Civil Engineer, George Wimpey & Co., Ltd., Hammersmith, London, England.

Professional Societies: Institution of Civil Engineers, London; American Society of Civil Engineers; American Geophysical Union; and American Water Resources Association.

Publications: 15 publications and 10 technical reports.